

National Center for Intermodal Transportation for Economic Competitiveness

# NCITEC

## Project 2012 – 25

### Disaster Protection of Transport Infrastructure and Mobility Using Flood Risk Modeling and Geospatial Visualization

## Final Report: NCITEC Project 2012 - 25

### The University of Mississippi

Principal Investigator: **Dr. Waheed Uddin**, Director CAIT

Co-Principal Investigator: **Dr. Mustafa Altinakar**, Director NCCHE

**REPORT: UM-CAIT/2015-01**

May 2015



**Center for Advanced Infrastructure Technology**

**The University of Mississippi**

University, MS 38677-1848, USA

Voice: 662-915-5363 Fax: 662-915-5523

<http://www.olemiss.edu/projects/cait/>

[cait@olemiss.edu](mailto:cait@olemiss.edu) [cvuddin@gmail.com](mailto:cvuddin@gmail.com)

U.S. Department of Transportation

Research and Innovative Technology Administration

Federal Grant or Other Identifying Number Assigned by Agency: DTRT12-G-UTC14

# DISASTER PROTECTION OF TRANSPORT INFRASTRUCTURE AND MOBILITY USING FLOOD RISK MODELING AND GEOSPATIAL VISUALIZATION

Final Report: NCITEC Project 2012 - 25

## ABSTRACT

Transportation infrastructure networks are essential to sustain our economy, society and quality of life. Natural disasters cost lives, infrastructure destruction, and economic losses. In 2013 over 28 million people were displaced worldwide by natural disasters with 90 % in Asia and about half million in North America. During 1980 to 2011, the overall loss from weather related catastrophes was US\$ 1,060 Billion (in 2011 values) in North America. Floods and hurricanes are the most common and damaging among all weather related natural disasters. Additionally, floods adversely impact the environment and biodiversity. Worldwide floods claimed millions of lives and resulted in billion-dollar economic costs. In the United States, billions of dollars in repair and replacement costs of bridge assets were needed after the disaster of 2005 Hurricane Katrina on the Gulf Coast. Higher frequency and ferocity of rainfall and coastal hurricanes in recent years have increased the risk of flood disasters. The NCITEC project “Disaster Protection of Transport Infrastructure and Mobility Using Flood Risk Modeling and Geospatial Visualization” addresses the goal of using flood simulations to assess the flood risk and impacts on the built infrastructure. The primary objectives of this project are to: select a test site in Mississippi on the downstream of a river, extract river centerline and infrastructure features on a geospatial map, simulate extreme flood scenarios, and evaluate the structural integrity of bridges.

Traditionally, flood simulation and risk mapping relied on one-dimensional flood models. In this project, two-dimensional flood propagation modeling is simulated over large areas using the DSS-WISE software, developed by the National Center for Computational Hydroscience and Engineering. It combines a state-of-the-art two-dimensional numerical model, CCHE2D-FLOOD, with a digital elevation model (DEM) of the study area and geospatial visualization. The numerical model solves full dynamic shallow water equations over the DEM of natural topography that can handle mixed flow regimes, wetting/drying, and disconnected flow domains. The extreme flood simulation results for the pilot study Sardis site considering 10-m square computation cells of the bare ground indicate a total area of 31 mi<sup>2</sup> (80 km<sup>2</sup>) inundated. The floodwater reached up to 39 ft (12 m) above the ground level and 13–16 ft (4 – 4.9 m) over the top of the two highways and rail infrastructure bridges. The local scour around the 10 ft-diameter bridge piers in the main channel is estimated as 17.30 ft (5.3 m), which is severe. A detailed structural integrity analysis of the US-51 bridge model shows the most critical condition as the factor of safety approaches 1.0. This happens when the floodwater level is at the top of the concrete girders, which destabilizes the girder-bearing areas. Field evidence and failure analysis of post-flood images show the washing away and destruction of bridges over streams and other bodies of water when the floodwater reaches the deck level, as observed for bridge destruction cases during both 2005 Katrina and 2011 Irene hurricane disasters. This important finding of optimum clearance of bridge superstructure above the channel bed is recommended to implement in state bridge management systems for flagging such vulnerable bridges and prioritizing for mitigation.

## **ACKNOWLEDGEMENTS**

This research project was funded by U.S. Department of Transportation / Research and Innovative Technology Administration through the National Center for Intermodal Transportation for Economic Competitiveness (NCITEC). Research described in this paper was conducted at the University of Mississippi Center for Advanced Infrastructure Technology (CAIT) and the National Center for Computational Hydroscience and Engineering (NCCHE). Thanks are due to the Mississippi DOT Bridge Engineering Division who provided copies of bridge drawings, photos, and related information on bridge design and construction.

This report is authored by Waheed Uddin, the Principal Investigator (PI) of NCITEC Project 2012-25, with major contributions from Co-PI Mustafa Altinakar who guided the NCCHE flood simulation studies. Thanks are due to the doctoral students Alper Durmus, Quang Nguyen and Marcus McGrath, as well as other CAIT research assistants for their contributions to the project.

## **DISCLAIMER**

The University of Mississippi, Mississippi State University, and the U.S. Department of Transportation do not endorse service providers, products, or manufacturers. Trade names or software or manufacturer's names appear herein solely because they are considered essential to the purpose of this report.

The contents of this report do not necessarily reflect the views and policies of the sponsor agency.

## TABLE OF CONTENTS

TITLE PAGE	Page
ABSTRACT .....	1
ACKNOWLEDGEMENT .....	2
DISCLAIMER .....	2
TABLE OF CONTENTS .....	3
1. BACKGROUND .....	4
1.1 Introduction .....	4
1.2 Objectives .....	6
1.3 Research Methodology .....	6
1.4 Overview of Project Accomplishments .....	7
2. FLOOD SIMULATION METHODOLOGY AND RESEARCH RESULTS .....	18
2.1 Review of Flood Simulation Methodologies .....	18
2.2 Computational Modeling and Simulations of Extreme Flood Scenarios .....	19
2.3 Geospatial Mapping and Summary Results of Extreme Flood Simulations .....	24
2.4 Flood Inundation Impacts of Extreme Flood Simulations .....	28
3. ASSESSING FLOOD IMPACTS ON PAVEMENT AND BRIDGES .....	33
3.1 Extreme Flood Inundation Impact Assessment for the Pilot Study Site .....	33
3.2 Evaluation of Highway Embankment Stability Subjected to Floodwater .....	35
3.3 Evaluation of Scouring Potential Around Bridge Piers .....	36
3.4 Extreme Flood Impacts on Bridge Superstructure .....	37
4. IMPLEMENTATION OF RESEARCH RESULTS .....	48
4.1 Expected Results .....	48
4.2 Sustainable Bridge Management System .....	49
4.3 Overall Benefit to Transportation Infrastructure and Society .....	50
4.4 Recommendations and Future Work .....	50
5. REFERENCES .....	51
APPENDIX .....	

# 1. BACKGROUND

## 1.1 Introduction

Weather-related natural disasters include flooding, hurricanes, severe storms, tornadoes etc. These disasters also have significant socio-economic impacts on lifeline infrastructure, public services, people's lives, and their livelihoods. Over 28 million people were displaced due to natural disasters worldwide in 2013 with 90 % in Asia and about half million in North America (EM-DAT 2012). About 60% of all disasters costing one billion dollars or more in the United States were related to weather causing more than 300 billion dollars cost in damages in the past decade in the United States alone (NOAA 2010). Floods and other weather related hazards are the most common and damaging natural disasters (Figure 1) and most occurred in the Southeastern states. Center for American Progress (CAP) reported that extreme weather events caused \$208 billion of economic cost in the United States with more than 1,200 deaths between 2011 and 2013 (Weiss and Manning 2013). Other key statistics of flood and weather related natural disasters worldwide and in the United States follow:

- There have been more than 4,000 occurrences of floods reported globally since 1900. As a result, around seven million people were killed, millions more were displaced, and more than 3.4 billion were affected (EM-DAT 2012).
- Historically, being the most destructive among all natural disaster types, floods caused around \$ 90 billion of damage cost in the United States between 1955 and 2000 (Durmus 2012). Iowa suffered the highest flood damage cost (\$7.7 Billion) followed by California (\$7.0 Billion), Louisiana (\$6.6 Billion), and Texas (\$6.0 Billion).
- NOAA (2015) reported for the United States:
  - Total 80 U.S. weather and climate events that each had losses exceeding \$1 billion from 2004 to 2013, compared with only 46 events in the previous decade.
  - Additionally, Hurricane Katrina disaster on the Louisiana and Mississippi Gulf Coast resulted in 1,836 deaths, 770,00 people displaced, and more than \$100 billion in infrastructure and economic costs. The storm landed on August 29, 2005 with 155 mph wind, 10 inch rainfall, and 20ft coastal wave surge. More than 90% structures destroyed including the Bay Bridge and Biloxi-Ocean Springs bridges on Mississippi Coast.
  - Similarly, huge losses were estimated after 2012 Hurricane Irene and 2012 Hurricane Sandy on the East Coast.
  - Figure 2 shows a spatial distribution map of billion dollar weather related disasters during 2005-2014, which resulted in total 3,816 deaths and total economic cost of \$545 billion.
- During 1980 to 2011 worldwide, the overall loss from weather catastrophes was US\$ 1,060 billion (in 2011 values), the insured losses amounted to US\$ 510 billion, and some 30,000 people lost their lives according to a report by Munich Re (Munich Re 2012). The report further shows that over the past three decades, the number of weather-related loss

events in North America grew by a factor of five. This compares with a four-fold increase in Asia, 2.5 in Africa, 2 in Europe, and 1.5 in South America (Munich Re 2012).

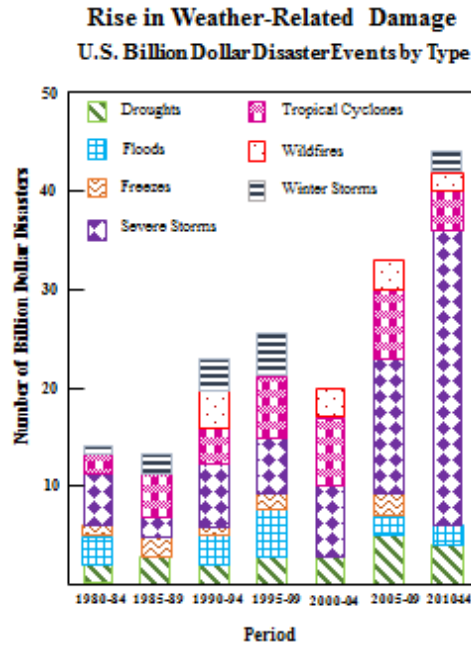


Figure 1. Billion dollars weather related disaster types in the United States, 1980-2014

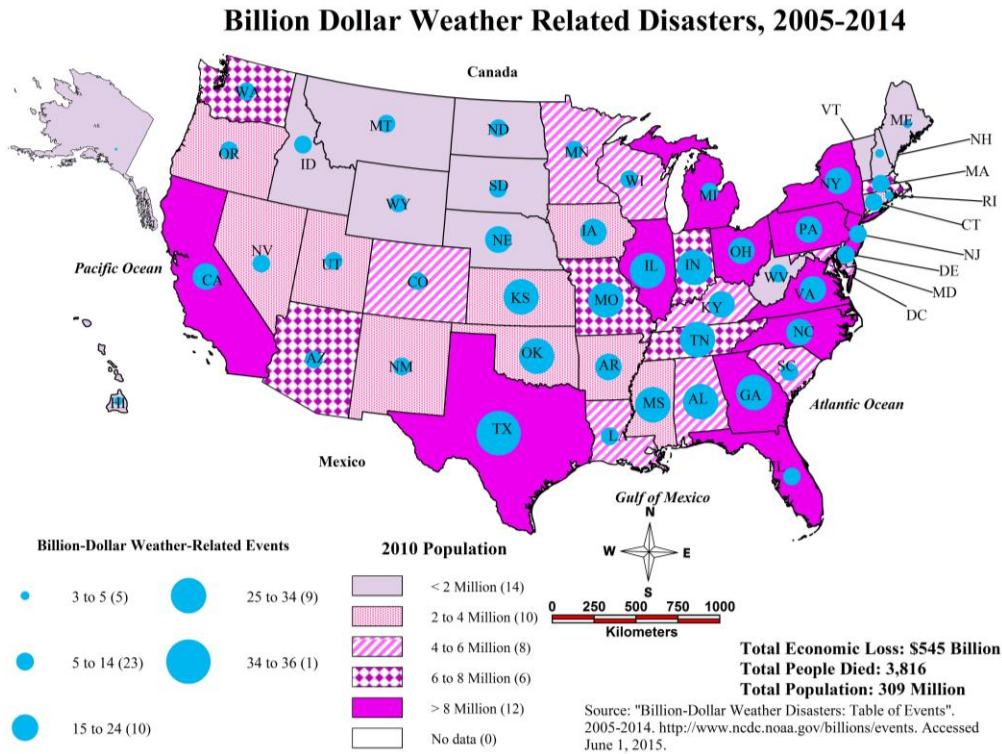


Figure 2. Spatial distribution of extreme weather related disasters in the U.S., 2005-2014

The critical lifeline infrastructure assets include roads, bridges, rail lines, levees and dams. Critical transportation infrastructure assets are under a continuous risk of flood hazards and subject to significant damage, such as washing away of pavements and bridges. Washing away of bridges and highway segments disrupt public mobility, freight traffic and supply chain, emergency management, and even disaster evacuation routes. Each year millions of dollars are devoted to emergency funds and mitigation of damaged transport infrastructure. Flood protective design and the safeguard of infrastructure are important issues under current and future climate impact scenarios. Last year, The White House launched its Climate Action Plan to prepare U.S. citizens and communities for climate change adaptation (White House 2014).

This project addresses the NCITEC theme of efficient, safe, secure, and sustainable national intermodal transportation network that can be made resilient to disasters. Major goals of this project are to develop geospatial visualization models of flood disasters and evaluate their impacts on road infrastructure.

## **1.2 Objective**

The primary objective is to identify and implement computational and geospatial visualization technologies to enhance decision support systems for transport infrastructure protection from extreme weather related natural disasters such as floods.

The project objective is accomplished by using airborne remote sensing and geospatial technologies for modeling and visualization of terrain and built infrastructure, adapting computational modeling and simulation of flood scenarios, flood risk mapping, and simulating extreme flood events for estimating flood disaster impacts on transport infrastructure network assets.

## **1.3 Research Methodology**

The project research teams of the Center for Advanced Infrastructure Technology (CAIT) and the National Center for Computational Hydroscience and Engineering (NCCHE) collaborated closely in the study by first identifying potential study sites in Mississippi (CAIT 2014, NCCHE 2014). The planimetrics features of the selected infrastructure and river centerline on the pilot study site were first developed by CAIT researchers. Traditional one-dimensional (1-D) flood simulation models are inadequate due to often discontinuous flood plains, do not provide detailed floodwater velocity and discharge profiles, and do not handle mixed flow regimes. In this study, a (2-D) numerical flood modeling software CCHE2D-FLOOD developed by NCCHE was adopted. The following key steps of the research methodology were implemented:

1. Select study sites in Mississippi.
2. Acquire high-resolution 2 ft (61 cm) imagery for 2-D feature extraction using GeoMedia Pro and ArcGIS geospatial software packages.
3. Create planimetrics and coordinates of river centerline (CL), cross-sections, highways, rail lines and other built infrastructure assets.

4. Setup a geospatial domain for NCCHE’s flood simulation software CCHE2D-FLOOD and DSS-WISE.
5. Run extreme flood simulations for high-resolution bare ground digital elevation model (DEM).
6. Analyze flood simulation outputs for floodwater vectors and hydrodynamic forces at river CL and cross-sections.
7. Run extreme flood simulations for DEM modified with built infrastructure elevations.
8. Analyze flood simulation outputs for floodwater vectors and hydrodynamic forces at river CL and cross-sections.
9. Compare the flood depths and inundations in Steps 6 and 8.
10. Use floodwater simulation results for the structural integrity assessment of transportation infrastructure by calculating the factor of safety against sliding (for highway embankment) and overturning (for highway bridge superstructure).

The research approach presented here can be implemented with any off-the-shelf geospatial software and with flood computational modeling software available through NCCHE. Figure 3 shows the research workflow from selecting study site to using the extreme flood simulation results. Figure 4 shows the project pilot study “Sardis” site in northern Mississippi.

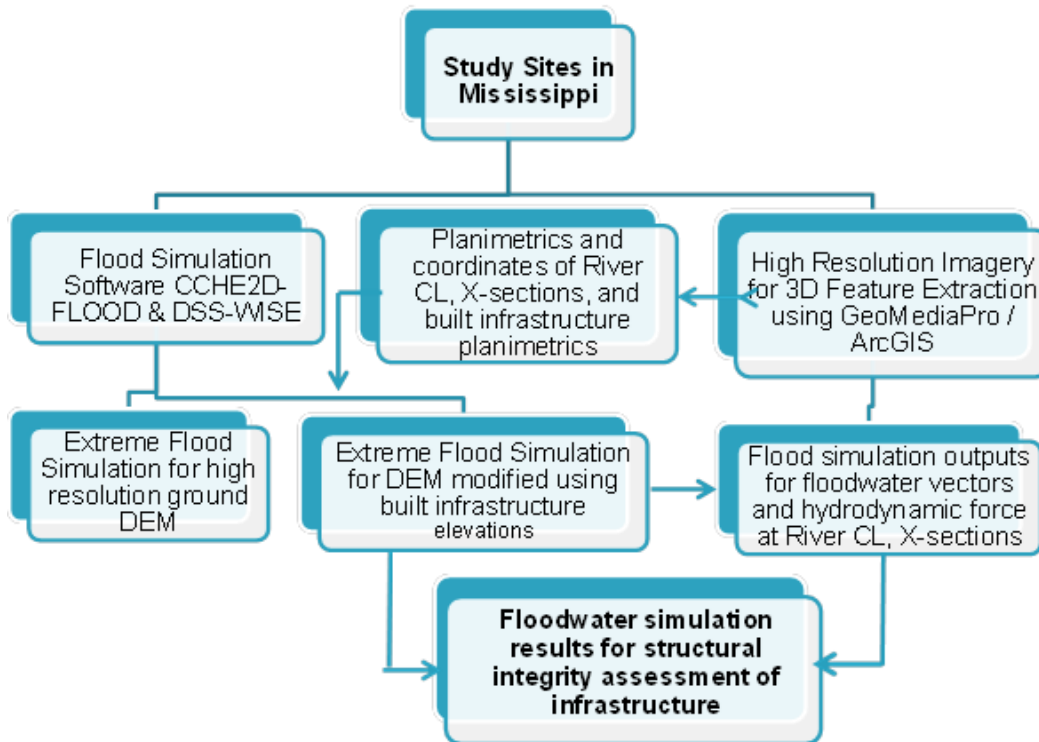


Figure 3. Schematic of research workflow

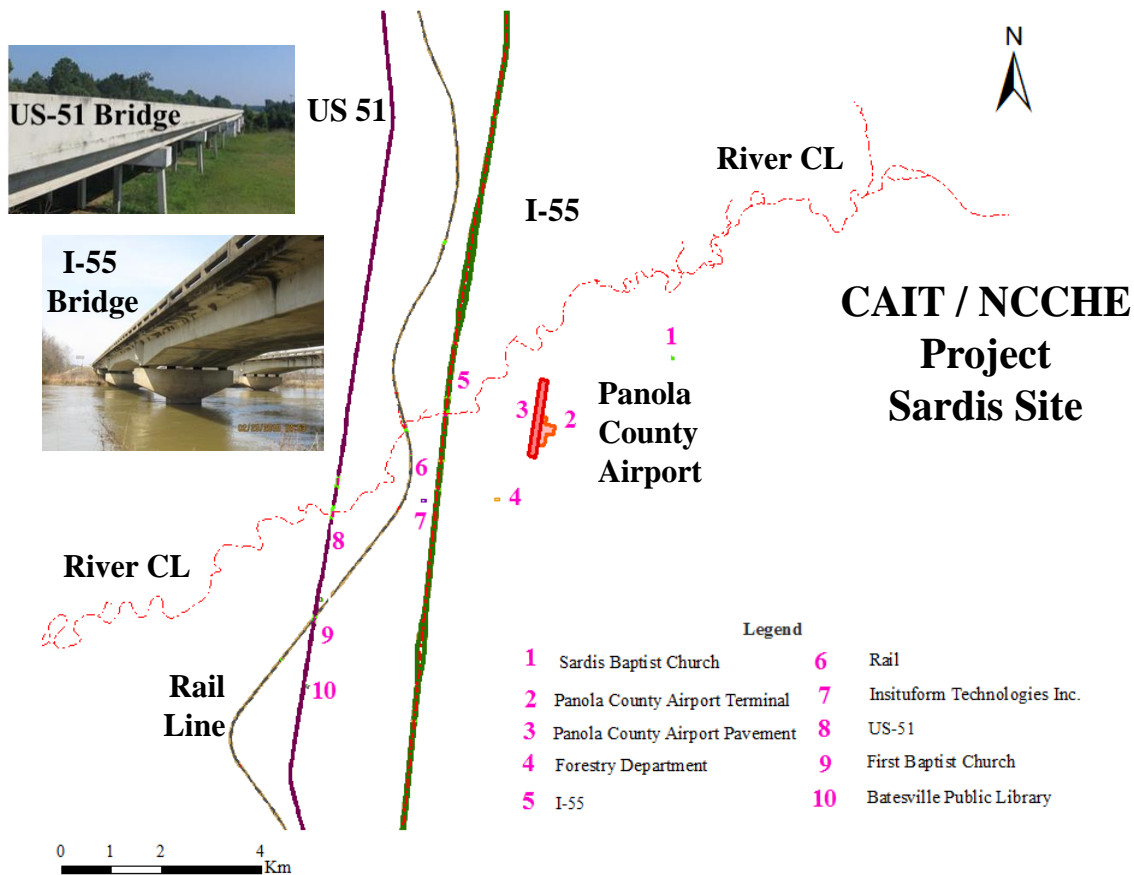


Figure 4. Tallahatchie River CL downstream at Sardis Dam pilot study site and planimetrics visualization of transportation assets (Bridge Photo credits: Mike Cresap, Justin Walker and Scott Westerfield of the Mississippi DOT)

#### 1.4 Overview of Project Accomplishments

Key project results are.

1. This project developed a framework of geospatial decision support system for flood risk assessment and impacts on infrastructure including roads, bridges, and buildings. The methodology was implemented for a pilot case study of Sardis site in Northern Mississippi.
2. Computer simulations for flood risk mapping and vulnerability assessment of highway and bridge assets were evaluated.
3. The pilot case study shows the importance of this approach disaster resilience for saving lives and billions of dollars in flood damages that can be avoided.
4. The developed approach is able to assess flood related vulnerabilities of traditional urbanization processes and infrastructure systems, which create negative impacts on the environment and the natural cycle of the ecosystem.
5. Training of under graduate and graduate students for geospatial workforce development and enhancing infrastructure asset management are additional benefits.

The project results have been presented at regional and national meetings and published, as summarized in the following list, and disseminated through social media.

*Book Published*

Uddin, W., W.R. Hudson, and Ralph Haas (2013). *Public Infrastructure Asset Management*. McGraw-Hill, ISBN 0071820116. (Book published, July 2013) This second revised and expanded edition of our 1997 *Infrastructure Management* book includes several new sections on flood disaster examples, rapid flood impact assessment using remote sensing imagery and geospatial technologies, and examples of life cycle benefit cost analysis for flood disaster mitigation and protection of built infrastructure. Other new topics include supply chain management, use of remote sensing imagery and geospatial technologies, asset management practice for transportation and other lifeline public infrastructure, and value engineering applications for investment decision making.

The highlights of the book are discussed in the following blog post.

<http://infrastructureglobal.com/dr-robert-khayat-ole-miss-chancellor-emeritus-infrastructure-improvement-cannot-be-delayed-if-we-are-to-continue-as-a-vital-nation/>

YouTube video: <http://youtu.be/LiHqJInrFy0>

*Book In Progress*

Uddin, W. (2016). *Disaster Resilience Management of Infrastructure Systems*. Taylor and Francis, UK. In progress. (Book contract signed June 2015 and manuscript to be submitted in January 2016) This book addresses natural disaster vulnerability assessment and protection of lifeline infrastructure from natural disasters. The motivation of this book is largely based on this NCITEC flood simulation project research and worldwide infrastructure damages and related adverse economic impacts of 2011 and 2012 extreme tsunami, hurricane, and flood disasters.

*Book Chapter*

Uddin, W. (2014). Chapter 23 “Mobile and Area Sources of Greenhouse Gases and Abatement Strategies,” in *Handbook of Climate Change Mitigation and Adaptation*, edited by Wei-Yin Chen, John M. Seiner, Toshio Suzuki and Maximilian Lackner, Springer. (Updated Chapter 23 of the 2012 Handbook in December 2014. The reference book will be available in early 2016).

<http://www.springer.com/energy/renewable+and+green+energy/book/978-3-319-14408-5>

Hossain, A. K. M. Azad, Yafei Jia, Xiaobo Chao, Mustafa Altinakar. (2014). Advances in Application of Remote Sensing Techniques to Enhance the Capability of Hydrodynamic Modeling in Estuary. Chapter in *Remote Sensing and Modeling: Advances in Coastal and Marine Resources*, Coastal Research Library (CRL) series, vol. 9, First edited by Charles W. Finkl, Christopher Makowski, 06/2014: chapter 12: pages 295-313; Springer International Publishing., ISBN: 9780123847034

Ding, Yan, Elgohry, Moustafa, Altinakar, Mustafa S. and Wang, Sam S. Y. (2013). Simulation of Morphological Changes due to Dam Removal – Chapter 7, In *Sediment Transport: Monitoring,*

*Modeling and Management*, Abdul Khan et al. eds., Nova Science Publishers, New York, pp213-238. (ISBN: 978-1-62618-683-5)

#### *Journal*

Uddin, W., M.S. Altinakar, and A. Durmus. (2015). Extreme flood simulations to assess inundation impacts and structural integrity of transportation infrastructure assets. *International Journal of Critical Infrastructure Protection*, April 2015. (submitted for publication review)

Singh, J., Altinakar, M.S., and Ding, Y. (2014). Numerical Modeling of Rainfall-Generated Overland Flow Using Nonlinear Shallow-Water Equations. *J. Hydrol. Eng.*, 10.1061/(ASCE)HE.1943-5584.0001124 , 04014089.

Uddin, W. (2013). Value Engineering Applications for Managing Sustainable Intermodal Transportation Infrastructure Assets. *Production Engineering Review*, Vol. 4, No. 1, March 2013, pp. 74–84.

Ding, Y., Kuiry, S.N., Elgohry M., Jia, Y., Altinakar, M.S., and Yeh, K.-C. (2013). Impact assessment of sea-level rise and hazardous storms on coasts and estuaries using integrated processes model. *Ocean Engineering*, Accepted, In Press. <http://dx.doi.org/10.1016/j.oceaneng.2013.01.015>

#### *Conference Proceedings and Presentations*

Durmus, A., Q. Nguyen, M.Z. McGrath, M.S. Altinakar, W. Uddin. (2015). Numerical Modeling and Simulation of Extreme Flood Inundation to Assess Vulnerability of Transportation Infrastructure Assets. 94<sup>th</sup> Annual Meeting of the Transportation Research Board (TRB), The National Academies, Washington DC. TRB Online Proceedings, January 10-14, 2015. (published and presented by Uddin, international conference)

Uddin, W., M.S. Altinakar, and A. Durmus. (2015). Extreme flood simulations to assess inundation impacts and structural integrity of transportation infrastructure assets. Presented by Uddin at The TISP 2015 Critical Infrastructure Symposium, Baltimore, Maryland, 20-22 April 2015, national conference)

Altinakar, M.S., M. McGrath, V.P. Ramalingam, and W. Uddin. (2015). Two-Dimensional Flood Modeling for the Assessment of Impacts on Critical Infrastructures. University Transportation Center (UTC) Conference for the Southeastern Region, University of Alabama at Birmingham. Birmingham, Alabama, March 26-27, 2015. (presented by Altinakar and Uddin, regional UTC conference)

Durmus, A., Q. Nguyen, M.Z. McGrath, M.S. Altinakar, and W. Uddin. (2015). Numerical Modeling and Simulation of Extreme Flood Inundation To Assess Vulnerability of Transportation Infrastructure Assets. University Transportation Center (UTC) Conference for the Southeastern Region, University of Alabama at Birmingham. Birmingham, Alabama, March 26-27, 2015. (presented by Durmus, regional UTC conference)

Uddin, W. (2015). Aircraft Safety on Airfield Pavements with Standing Water and Slush. Workshop 143- Influence of Airfield Surface Irregularity on Aircraft Life, Presented at the 94th Annual Meeting of The Transportation Research Board, Washington, DC, January 10-15, 2015.

Uddin, W. (2013). Geospatial Technologies for Highway Asset Management and Natural Disaster Risk Reduction Planning. keynote lecture, 2013 IJPC - First Internal Journal of Pavements Conference, São Paulo, Brazil, December 9-10, 2013. (This trip was at no cost to the project. Dr. Uddin was an invited guest of the conference organizer professors from Mackenzie University, São Paulo, Brazil, who co-chaired the 2013 IJPC conference.)

Uddin, W. and M.S. Altinakar. (2013). NCITEC Project 2012-25: Disaster Protection of Transport Infrastructure and Mobility Using Flood Risk Modeling and Geospatial Visualization—Overview and Progress to Date. Presentation of project overview, First NCITEC conference, Starkville, Mississippi, October 31-November 1, 2013. (Attended by the NCITEC consortium partners including UM project PIs, faculty, and students)

Altinakar, M.S., McGrath, M.Z., Ramalingam, V.P., Matheu, E.E., Matthews, M., Seda-Sanabria, and Thomas, B. Jr. (2013). Web-Based, Automated 2D Dam-Break Simulation and Mapping. Proceedings of MODSIM World 2013, 4/30-5/2, 2013, Hampton Roads Convention Center in Hampton, VA.

Ding, Y., Ding, T., Jia, Y., Altinakar, M.S. (2013). Prediction of Wind, Wave, and Storm Surge due to Hurricane ISAAC in the northern Gulf Coast, In: Proceeding of the World Environmental & Water Resources Congress 2013, ASCE, Cincinnati, Ohio, May 19-23, 2013 (15pp).

### *Workshop and Symposium*

*December 5, 2014 Workshop: “Extreme Flood Inundation Mapping and Risk Modeling of Transportation Infrastructure Assets”*

The workshop was opened to all by email invitations and CAIT web page posting. It was held in NCCHE Conference Room, Brevard 3rd Floor, University of Mississippi Oxford campus. Presentations were made by Dr. Uddin, Dr. Altinakar (jointly with NCCHE researchers Marcus McGrath and Vijay Ramalingam), Alper Durmus, Quang Nguyen, with closing remarks by Dr. Altinakar.

*February 7, 2013 Symposium: “NCITEC-Symposium at the University of Mississippi (UM)”*

This UM symposium featured welcome by UM administrators, NCITEC project overview by the NCITEC Director, announcement of new NCITEC/DOT grant opportunity to all UM faculty/researchers, and presentations by all current NCITEC project investigators about their research project accomplishments.

### *Web Site, Social Media and Online Postings*

UM CAIT web page: <http://www.olemiss.edu/projects/cait/ncitec/>

The NCITEC project tab on the University of Mississippi CAIT web site, linked to Mississippi State web site, provides useful background of NCITEC goals, university partners, and UM project summaries.

*Twitter:* <https://twitter.com/drwaheeduddin>

*Blog:* <http://infrastructureglobal.com/> Dr. Uddin’s blog about infrastructure and natural disasters around the globe.

*SlideShare:* Over 3,600 SlideShare views of 9 presentations. A recent SlideShare presentation, based on 2014 workshop presentations and 2015 TRB paper, was posted.

<http://slidesha.re/1CiiDn> Another slide presentation was posted on “NCITEC Intermodal Transportation and Disaster Safeguard Research Projects at CAIT.”

<https://www.slideshare.net/waheeduddin/uddin-caitncitecprojects11-oct2013slsh>

*Twitter:* <https://twitter.com/drwaheeduddin> Started in January 2012; several lists and “Global Infrastructure” timeline created; over 22,500 tweets to date.

*Twitter:* <https://twitter.com/disasterglobal> Started in 2012 on topics of protection from natural disasters and managing infrastructure assets; over 3,300 tweets to date.

*Twitter:* <https://twitter.com/InfrastructureG> Started in January 2014 to focus on built infrastructure and transportation assets; several lists on specific categories such as sustainable transportation; over 930 tweets to date.

*YouTube Videos:* Over 1,680 views of project related seven YouTube videos were reported to date. <http://youtu.be/8JjM2QEexFE>

The NCCHE’s initial flood simulation results for the Sardis pilot site in northern Mississippi (Figure 4) were used by Dr. Uddin to develop and post the following YouTube video on infrastructureglobal channel. [http://youtu.be/h\\_FRfj-i8IA](http://youtu.be/h_FRfj-i8IA)

### *Student of the Year Award*

NCCHE’s PhD student Marcus McGrath was announced as 2013 Student of the Year (SOY) awardee. This news was posted on the CAIT/NCITEC web page.

<http://www.olemiss.edu/projects/cait/ncitec/>

### *Presentations to External Organizations*

The PI and co-PI presented the project highlights and key results to the visiting professors of the following universities and other on-site presentations:

*October 29-30, 2014:* Acey Roberts, Mississippi DOT ITS Engineer and GRITS President, lectured both days about the video panel wall installed in CAIT Laboratory in collaboration with the MDOT. Visiting attendees of the winter workshop of the Gulf Region Intelligent Transportation Society (GRITS) toured the CAIT Transportation Lab on October 30. The workshop was held at the University of Mississippi Campus in Oxford, Oct 29-30, 2015. Dr. Uddin provided brief overview of the Lab facilities, the NCITEC projects, and history of the Lab evolution in cooperation with the Mississippi DOT Traffic Engineering Division as a part of the establishment of a model ITS Lab.

*October 24-25, 2014:* Dr. Uddin teaching and research profile was compiled and presented at the annual banquet on 24th October in Austin, Texas to honor 2014 inductees of the University of Texas CAEE Academy of Distinguished Alumni where he received the award.

*October 21, 2014:* Dr. Uddin attended the annual board meeting as 2014 appointed member and the conference of the Mississippi Transportation Institute (MTI), in Convention Center, Jackson, Mississippi. Briefly interacted with State Senator and Representative speakers, the Mississippi DOT Executive Director, as well as, Chief Engineer, Bridge Engineer, Aviation Engineer, and Research Division engineers.

*October 3, 2014:* Dr. Lucy P. Priddy visited the Lab. She is Research Civil Engineer with the ERDC Airfields and Pavements Branch in Vicksburg, Mississippi. After welcome remarks by Dr. Uddin, Dr. Lucy Priddy reflected on her experience during her University of Mississippi years as one of the first UG RAs who worked on CAIT research projects during 1999-2002.

*September 14-17, 2014:* Dr. Uddin attended the ITS3C regional conference and presented overview of NCITEC projects and Gulf Coast rail study results. The conference was organized by the Gulf Region Intelligent Transportation Society (GRITS), the Intelligent Transportation Society of Florida (ITSFL) and the Intelligent Transportation Society of Georgia (ITSGA). The joint conference was held September 14-17, 2014 at the Arthur R. Outlaw Convention Center in Mobile, Alabama.

*December 12, 2013:* Visit to Brazil's Dutra Concession Highway from Rio de Janeiro to São Paulo, Project Office. (This highway passes through a major river floodplain and a portion of the highway was washed away during the flood and landslide recently. Dr. Uddin made a presentation in collaboration with Dr. Rita Fortes to the highway concession operator staff on the approach of geospatial analysis and flood simulations being pursued in this NCITEC project to protect transport infrastructure from flood disasters.)

*October 28, 2013:* Visiting EITs from the Mississippi DOT, Ms. Jessica Headrick (Planning Division) and Ms. Catherine Colby Willis (Roadway Design Division) were presented project overview and on-going planimetrics examples of Sardis site. The visit was held at CAIT Transportation Modeling & Visualization Lab in UM Jackson Center. Both EITs worked with

CAIT on geospatial and airport laser survey projects before graduating from the University of Mississippi.

*February 28, 2013:* Project presentation to visiting Fulbright Fellow Dr. Raza Bhatti from St. Louis, Missouri. Dr. Bhatti was interested in UM floodplain modeling capability and this project scope because he was involved in biodiversity conservation program and voluntary aid effort in Sukkur-Khairpur area. This area near Sukkur Barrage over Indus River (the main flood breach site) was devastated during the 2010 superflood of Pakistan.

*November 16, 2012:* Visiting faculty of Mackenzie University (São Paulo, Brazil), Transportation Engineering Professors João Merighi and Rita Fortes, at CAIT Transportation Modeling Lab, Oxford, Mississippi. (Both visiting professors were Dr. Uddin's guests from Mackenzie University, São Paulo, Brazil, and our universities have a long standing cooperative agreement.)

*NCCHE's Presentations and Award:* Dr. Altinakar made several presentations to the NCCHE's flood research funding agencies, visiting delegations, and abroad. The DSS-WISE Software used for the NCITEC project is now being employed by several federal agencies and Mississippi state agencies. The agencies that use DSS-WISE include: (a) DHS Dams Sector Branch, (b) USACE HQ, (c) USACE MMC, (d) USACE-ERDC, (e) USACE Vicksburg District, (f) Mississippi Department of Environmental Quality, and Federal Emergency Management Agency (FEMA).

- On December 22, 2014, the Maine RRAP Team was awarded the Trailblazer Award by the Department of Homeland Security. (NCCHE is part of the Maine RRAP Team and carried out all the storm surge and flood simulations with different climate change and sea-level rise scenarios.)  
“...in recognition of their exceptional leadership and innovative thinking in performing the first RRAP to focus on the potential impacts of climate change. Their work has significantly furthered national climate change policy objectives as directed by the President and will serve as the model for other communities to better understand the risks and impacts of climate change and how to promote planning and resilience. Their leadership, teamwork, and initiative are a great credit to themselves and the Office of Infrastructure Protection.”
- On May 30, 2013, a one-day short course was taught at FEMA Region IV in Atlanta, GA, and the use of DSS-WISE Lite software for automated dam-break flood modeling and mapping. The short course was sponsored by the ASDSO (Association of State Dam Safety Officials). A new set of course materials with over 500 slides were prepared for this short course. The course was attended by 48 participants, which included FEMA Region IV and Region VIII personnel and State Dam Safety Officials from several states.
- On May 21, 2013, NCCHE worked with the Dam Safety Engineers in North Dakota to urgently simulate four critical dams and provided the inundation maps in only a couple of hours. The results were also shared with FEMA Region IV.
- On May 8, 2013, a one-day short course was taught in Seattle, WA, within the framework of ASDSO Western Regional Conference and sponsored by the ASDSO. A new set of

course materials with over 500 slides were prepared for this short course. The course was attended by 30 participants.

- On April 15-16, 2013, a two-day short course for teaching the use of the DSS-WISE-DSAT Link was organized, at the facilities of USACE Vicksburg District. The short course was organized in collaboration with (1) Critical Lifelines Branch, Sector Outreach and Programs Division, Office of Infrastructure Protection, National Protection and Programs Directorate, the DHS (represented by Yazmin Seda-Sanabria, National Program Manager) and (2) CIPR, USACE Headquarters, Office of Homeland Security (represented by Dr. Enrique Matheu, Chief). The course was attended by 19 engineers from USACE MMC.
- On March 14-15, 2013, NCCHE Organized the Sino-American Workshop on Computation, Uncertainty, and Risk Assessment in Hydrosience and Engineering at UM with the participation of researchers from top national universities in Taiwan as well as the representatives of the Taiwan Typhoon and Flood Research Institute (TTFRI). Flood hazard and protection of infrastructures against flood hazard was one of the topics covered by the workshop.

### *Students Support*

The project supported several graduate and undergraduate students, as follows:

6 PhD (4 CAIT, 2 NCCHE); 6 UG (CAIT)

One PhD student, Alper Durmus, is pursuing his doctoral research on project simulation data to enhance structural integrity analysis of a highway bridge and bridge asset management system for identifying and prioritization of flood vulnerable bridges on streams and rivers. He has been advanced to candidacy and expected to complete his doctoral research and defend his dissertation in the next 6-10 months.

### *Collaboration*

The PI and Co-PI contacted and collaborated with the following organization during this project:

As required by the NCCHE mission, the Co-PI kept close contacts with the following agencies:

- Department of Homeland Security (DHS) Science and Technology Directorate; FEMA
- USDA Agricultural Research Service (ARS)
- US Army Research Office (ARO)
- US Army Corps of Engineers (CoE)
- Mississippi Department of Marine Resources
- Mississippi Emergency Management Agency
- Association of State Dam Safety Officials (ASDSO)

The PI collaborated with the following organizations, who provided support to the project team:

- IAVO Research & Scientific, Durham, North Carolina: IAVO has provided licenses of the GeoSPHERIC package that embeds a new version of the GeoGenesis® geospatial software. The software has been installed on seven computer stations in CAIT Transportation Modeling and Geospatial Labs. The value of the software for each computer seat is being used as in-kind cost share for this project. Their help is also acknowledged for identifying imagery specifications and providing training data to CAIT students.
- Intergraph for continuing academic license of GeoMedia Pro at no cost to the University of Mississippi for use on CAIT projects (worth \$118,000 per year).
- As Intergraph Registered Research Lab, CAIT Remote Sensing and Geospatial Analysis Laboratory and CAIT Transportation Modeling and Visualization Laboratory is receiving geospatial industry support for education and training of students in geographical information system (GIS) applications through the project research tasks.

This Intergraph software grant is a cooperative feature of this project. Since January 2014 the statewide license has been provided by MARIS. This software and ArcGIS software, provided by Mississippi Mineral Resource Institute, were used to create planimetrics of roads, bridges, and buildings from high resolution aerial imagery.

The following organizations were as cooperative features of this project:

- 1) Mississippi Department of Transportation (MDOT): MDOT Roadway Design Division has been contacted for access to aerial imagery for candidate sites(s) in Mississippi. Follow up of initial contacts was made through an EIT who is Dr. Uddin's former student and CAIT staff.
- 2) MDOT Planning Division through contact with Dr. Uddin's former student and EIT for accessing overlapping aerial imagery scenes of the study sites.
- 3) MDOT Transportation Information Director (Mike Cresap) and MDOT Director of Structures -State Bridge Engineer (Justin Walker) have been especially helpful to provide drawings and photos for the I-55/US-51 highway bridges on the Sardis site and updated geospatial database of all state maintained highways and bridges of Mississippi. These were very important and useful contributions to this project.
- 4) Mississippi Automated Resource Information System (MARIS): This is a statewide resource agency in Mississippi for no-cost Landsat imagery and DEM data sources of selected counties in Mississippi. <http://www.maris.state.ms.us/>  
Project researchers downloaded bare ground 5 ft DEM/contour data and 2 ft aerial imagery scenes of Sardis site.

Additionally, Dr. Uddin contacted MARIS and requested 2 ft aerial imagery and DEM of other candidate sites. We received this data for Tunica site on a USB hard disk.

- 5) US Army ERDC Hydraulics Lab, Vicksburg, Mississippi (Dr. Kenneth Ned Mitchell)

### *Project Impacts*

The project is likely to make an impact beyond the bounds of science, engineering, and the academic world in the following areas:

- Enhancing public understanding of flood disaster, prevention, and mitigation through visualization products which are easy to understand and communicate with government stakeholders, businesses, media, and general public.
- Adapting the developed approach for flood disaster mitigation practices, decision support systems for disaster evacuation routing and emergency management, and landuse and flood control policies.
- Implementing disaster protection methodologies and web-based social networking tools to build disaster resilience infrastructure and communities, improve community preparedness and infrastructure defense against flood disasters, and protect social fabric, economic viability, civic facilities, and environmental conditions against flood disasters.

Detailed outcomes, accomplishments, recent presentations and publications, and impacts are presented in the final project progress report, which is included in Appendix.

## 2. FLOOD SIMULATION METHODOLOGY AND RESEARCH RESULTS

### 2.1 Review of Flood Simulation Methodologies

Higher frequency and ferocity of rainfall and coastal hurricanes due to extreme weather and climate change impacts have increased the risk of flood hazards in coastal and inland regions. Figure 5 shows several site photos of recent disastrous floods on the Gulf Coast and East Coast of the United States (Uddin et al. 2015). These disasters result in adverse impacts on transportation infrastructure, destruction of communities and businesses, and disruptions in recovery operations and mobility of goods and people. Catastrophic failures of built infrastructure and damages to roads and bridges due to extreme flood events require flood vulnerability assessment. This research is focused on using flood risk modeling and geospatial visualization for managing disaster resilience and protection of transport infrastructure.



Figure 5. Evidence of catastrophic failures of built infrastructure and damages to roads and bridges due to extreme flood events

Traditionally, flood simulation and risk mapping relied on one-dimensional (1D) flood models. The Hydrologic Engineering Center River Analysis System or HEC-RAS (HEC-RAS 2014) is a commonly used 1D flood modeling and simulation software. The 1D flood simulation approach is inadequate for flood propagation due to often discontinuous flood plains (Cook 2008). In

addition, one-dimensional flood modeling used in practice do not handle mixed flow regimes (EA 2009). The inherent limitations of 1D flood modeling are summarized as follows:

- Cannot correctly model non-channelized flows
- Do not provide correct information on the arrival time
- Cannot simulate mixed regime flows and or shock waves
- cannot provide information on flow direction when results are presented on two-dimensional flood maps

## 2.2 Computational Modeling and Simulations of Extreme Flood Scenarios

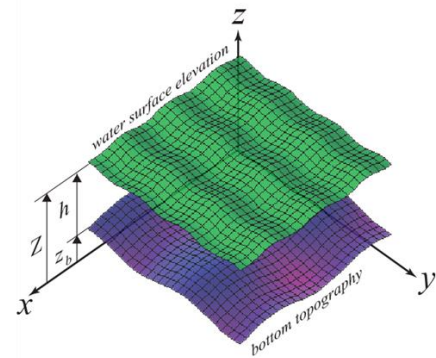
### DSS-WISE and CCHE2D-FLOOD Software Packages

In this study, two-dimensional (2D) flood propagation modeling is simulated over large areas using the DSS-WISE software, developed by the National Center for Computational Hydroscience and Engineering. It combines a state-of-the-art two-dimensional numerical model, CCHE2D-FLOOD, with a digital elevation model (DEM) of the study area and GIS visualization (Altinakar et al. 2009, Singh et al. 2011, Durmus et al. 2015). The numerical simulation analyzes full dynamic 2D shallow water equations in conservation form (Figure 6).

$$\frac{\partial h}{\partial t} + \frac{\partial hu}{\partial x} + \frac{\partial hv}{\partial y} = q_v$$

$$\frac{\partial hu}{\partial t} + \frac{\partial hu^2}{\partial x} + \frac{\partial huv}{\partial y} = -gh(\partial Z / \partial x) - g\left(u\sqrt{u^2 + v^2} / C^2\right)$$

$$\frac{\partial hv}{\partial t} + \frac{\partial huv}{\partial x} + \frac{\partial hv^2}{\partial y} = -gh(\partial Z / \partial y) - g\left(v\sqrt{u^2 + v^2} / C^2\right)$$



<p><math>h</math> = water depth</p> <p><math>u, v</math> = flow velocities in x and y</p> <p><math>z_b</math> = bed elevation</p> <p><math>Z = z_b + h</math> = water surface elevation</p> <p><math>C</math> = Chezy friction coefficient</p>	<p><math>g</math> = gravitational acceleration</p> <p><math>hu, hv</math> = unit discharges in x and y</p> <p><math>t</math> = time</p> <p><math>x, y, z</math> = coordinates</p> <p><math>S_{fx}, S_{fy}</math> = slopes of the energy grade line</p>
--	--

Figure 6. 2D Shallow water equations in conservation form (Altinakar et al. 2015a)

The numerical model solves full dynamic shallow water equations over the digital elevation model or DEM of natural topography that can handle mixed flow regimes, wetting/drying, and disconnected flow domains. The vector form of 2D equations, numerical modeling, and flood simulation and related details are further discussed in the NCCHE final project report (Altinakar et al. 2015a), which is included in Appendix. Figure 7 shows the features of DSS-WISE software package that uses the CCHE2D-FLOOD for numerical modeling of flood simulation.

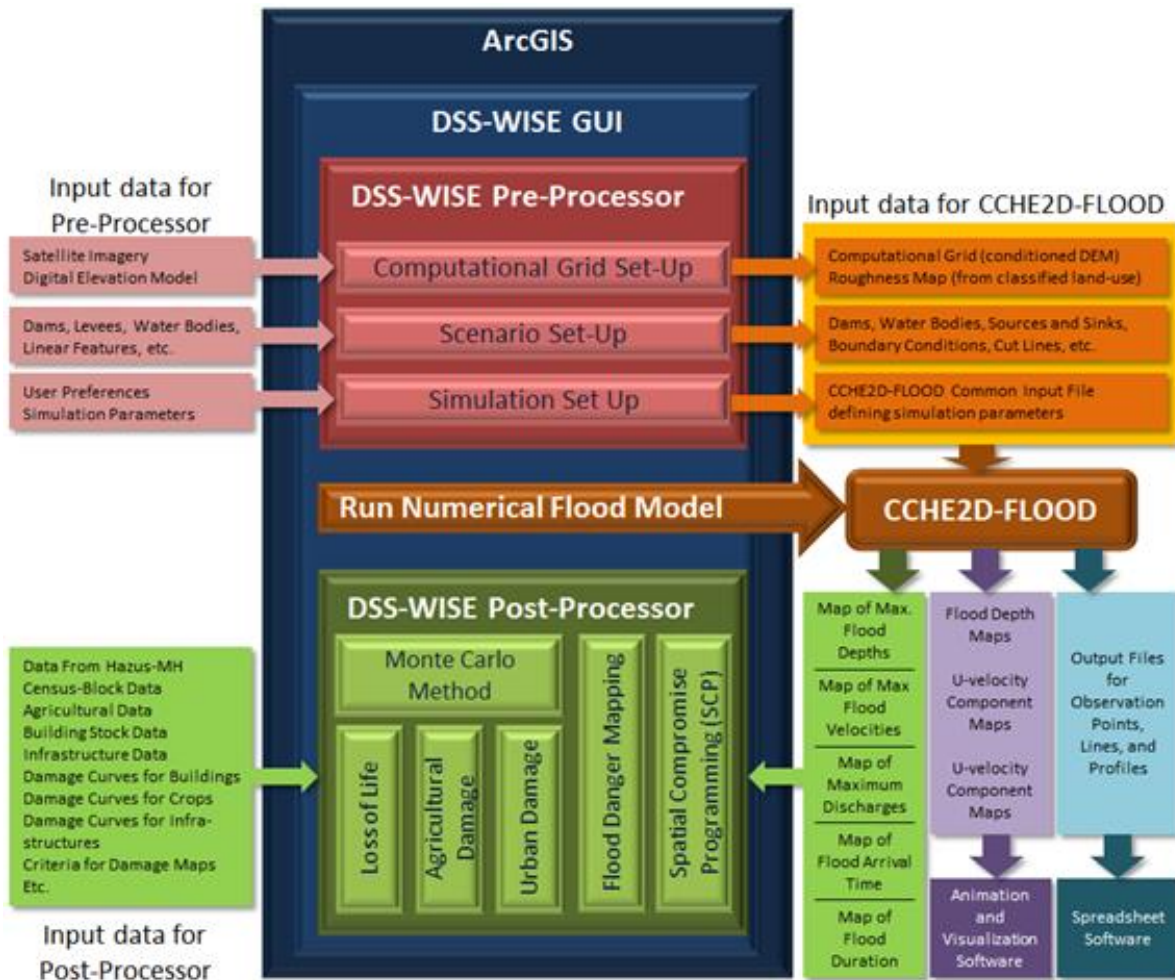


Figure 7. Features and capabilities of DSS-WISE (Altinakar et al. 2015a)

The key features of the NCCHE’s 2D flood modeling and simulations are (Altinakar et al. 2015b):

- Uses finite volume discretization to solve conservative form of full dynamic two-dimensional shallow water equations and handles disconnected flow domains.
- Fluxes are calculated using the shock capturing HLLC scheme.
- Analyzes wetting and drying areas of the simulation domain.
- Uses DEM as computational grid.

- Provides capabilities for realistic modeling for complex real-life engineering applications.
- Multi-core, multi-threaded parallel programming to increase computation speed.

The following results are provided after the flood simulations:

- Geo-referenced raster files and vector shp files (general risk mapping)
  - Extent of the flood
  - Map of maximum flood depths (maximum depth achieved during the simulation)
  - Map of flood arrival time (dry area becoming wet regardless of the depth of flow)
  - Map of maximum specific discharge (velocity times depth), which also gives an idea about the momentum
- Time series data (csv files) at selected locations (especially for evaluation of potential impacts to structures, transportation network, and buildings)
  - Time history of flow depth, velocity vector (x and y components) along specified longitudinal profile
  - Discharge hydrographs at selected cross sections
  - Time history of flow depth, flood water surface elevation, velocity components and magnitude and flow direction at selected observation locations
- Products for easy dissemination of information
  - KMZ file of the results for visualization on Google Earth (does not necessitate any special software).

Current users of DSS-WISE and CCHE2D-FLOOD include (Altinakar et al. 2015b):

- U.S. Department of Homeland Security Dams Sector
- U.S. Army Corps of Engineers (USACE) Headquarters, Washington DC
- USACE-ERDC (Engineer Research and Development Center), Vicksburg, MS, Military Hydrology Group
- USACE-MMC (Modeling Mapping and Consequence)
- USACE Vicksburg District
- Mississippi Department of Environmental Quality

### **Extreme Flood Simulation and Impact Assessment Approach**

The flood modeling and simulation approach can be implemented with any off-the-shelf geospatial software and with software available through NCCHE. For this project the following 10-step approach for flood simulation and impact assessment implemented in this study:

1. Select study sites in Mississippi. (Sardis site was used for the pilot study.)
2. Acquire high-resolution 2 ft (61 cm) imagery for 2-D feature extraction using GeoMedia Pro/ArcGIS geospatial software.

3. Create planimetrics and coordinates of river centerline or CL, cross-sections, highways, rail lines and other built infrastructure assets.
4. Setup a geospatial domain for flood simulation software CCHE2D-FLOOD and DSS-WISE.
5. Run extreme flood simulations for high-resolution bare ground DEM.
6. Analyze flood simulation outputs for floodwater vectors and hydrodynamic forces at river CL and cross-sections.
7. Run extreme flood simulations for DEM modified with built infrastructure elevations.
8. Analyze flood simulation outputs for floodwater vectors and hydrodynamic forces at river CL and cross-sections.
9. Compare the flood depths and inundations in Steps 6 and 8.
10. Use floodwater simulation results for the structural integrity assessment of transportation infrastructure by calculating the factor of safety against sliding (for highway embankment) and overturning (for highway bridges).

### Pilot Study Site and Simulation Domain

Figure 8 shows the four sites identified initially. Figure 9 shows the simulation domain details of the Sardis site in Northern Mississippi, which was selected as the pilot study site.

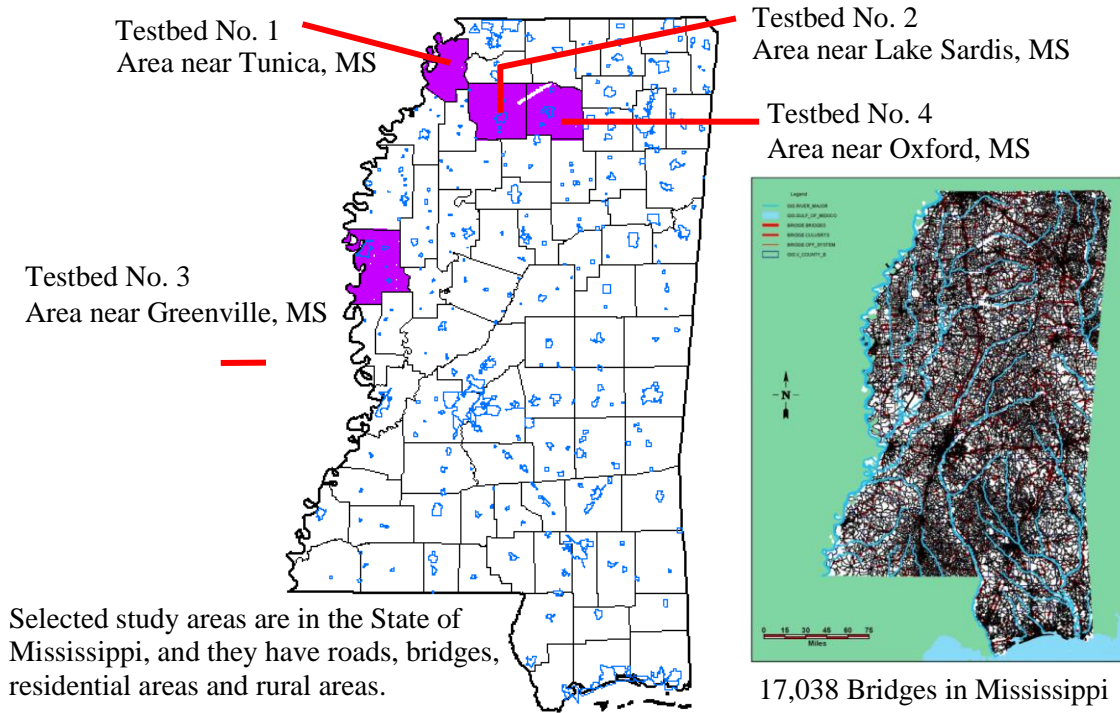
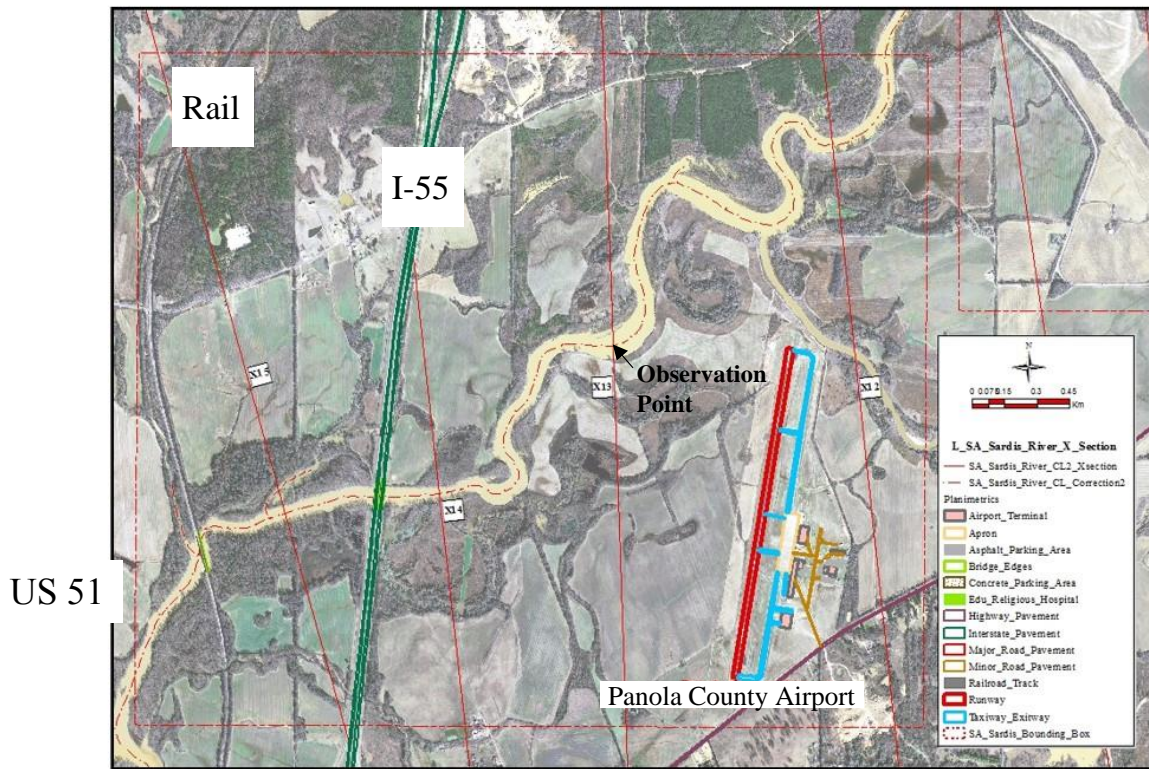


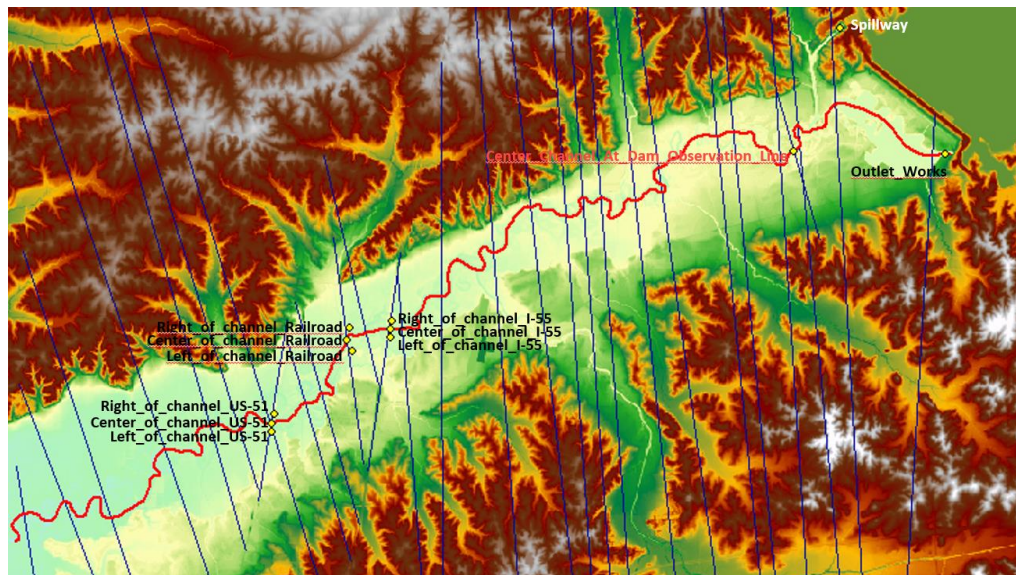
Figure 8. Identification of candidate study sites

River Downstream CL and Cross-Sections with Major Highways, Rail and Airport Features



Observation line (Cross-Sections)

Observation profile (River CL)



**Observation points:** 3 observation points (left, middle, right) are defined for each bridge

Figure 9. Pilot study site (Sardis) features, DEM and 10-m cell size of simulation domain

The 10m cell size domain of the Sardis pilot study site was used for the flood simulation conducted in January 2014 using high-resolution ground DEM data (of the bare ground and DSS-WISE software. The following details show the accuracy of DEM (USGS 2014) and domain used for flood inundation simulation

- Absolute accuracy of elevation of 1.55 m
- Relative accuracy of elevation of 0.81 m
- Based on LIDAR topographic data used by the U.S. Geological Survey (USGS) for the pilot study site
- 20,580 meters west-east by 17,260 meters north-south, corresponding to 2,058 columns and 1,726 rows of 10 m by 10 m size cells (which corresponds to a total of 3,552,108 cells)

### **2.3 Geospatial Mapping and Summary Results of Extreme Flood Simulations**

The research methodology (Figure 3) includes the following key steps, which are discussed in this section:

- Extract infrastructure features for highways, rail and some buildings including their height above the ground elevation.
- Run extreme flood simulations for high-resolution bare ground DEM on a geospatial map.
- Analyze flood simulation outputs for floodwater vectors and hydrodynamic forces at river CL and cross-sections.
- Run flood simulations again after incorporating 3D models of highways, rail, airport, and selected buildings considering the heights of selected infrastructure features.
- Compare the flood depths and inundations using simulation results for 10m, 5m, 3m cell size resolutions.
- Use floodwater simulation results for structural integrity assessment of bridges and pavements.

#### **Feature Extraction and DEM Used**

The flood simulation used site planimetrics, river CL and cross-sections, which were created from 2 ft (61 cm) high-resolution aerial imagery acquired through the cooperation of Mississippi Department of Transportation and Mississippi Automated Resource Information System. Figure 4 shows the entire site planimetrics and Figure 8 shows a partial view of the planimetrics of the infrastructure features, river CL, and cross-sections. The same remote sensing data of 2 ft (61 cm) high-resolution aerial imagery and DEM data were used to implement flood risk mapping models. Figure 9 shows the cross-section observation lines and observation points on the river CL. The cross-section observation lines were created based on a preliminary study and are perpendicular to the river CL (Durmus et al. 2015).

The pilot site includes the following major transportation corridors: 1) I-55 Bridge (double bridge), 2) Rail Bridge, and 3) US-51 Bridge. Figure 10 shows the three bridge crossings in these corridors in the pilot test site. At bridges, the bridge deck is not represented as elevation in the DEM. The flow is thus free to pass through the bridge openings. The 2D simulations cannot represent a pressure flow under the deck.

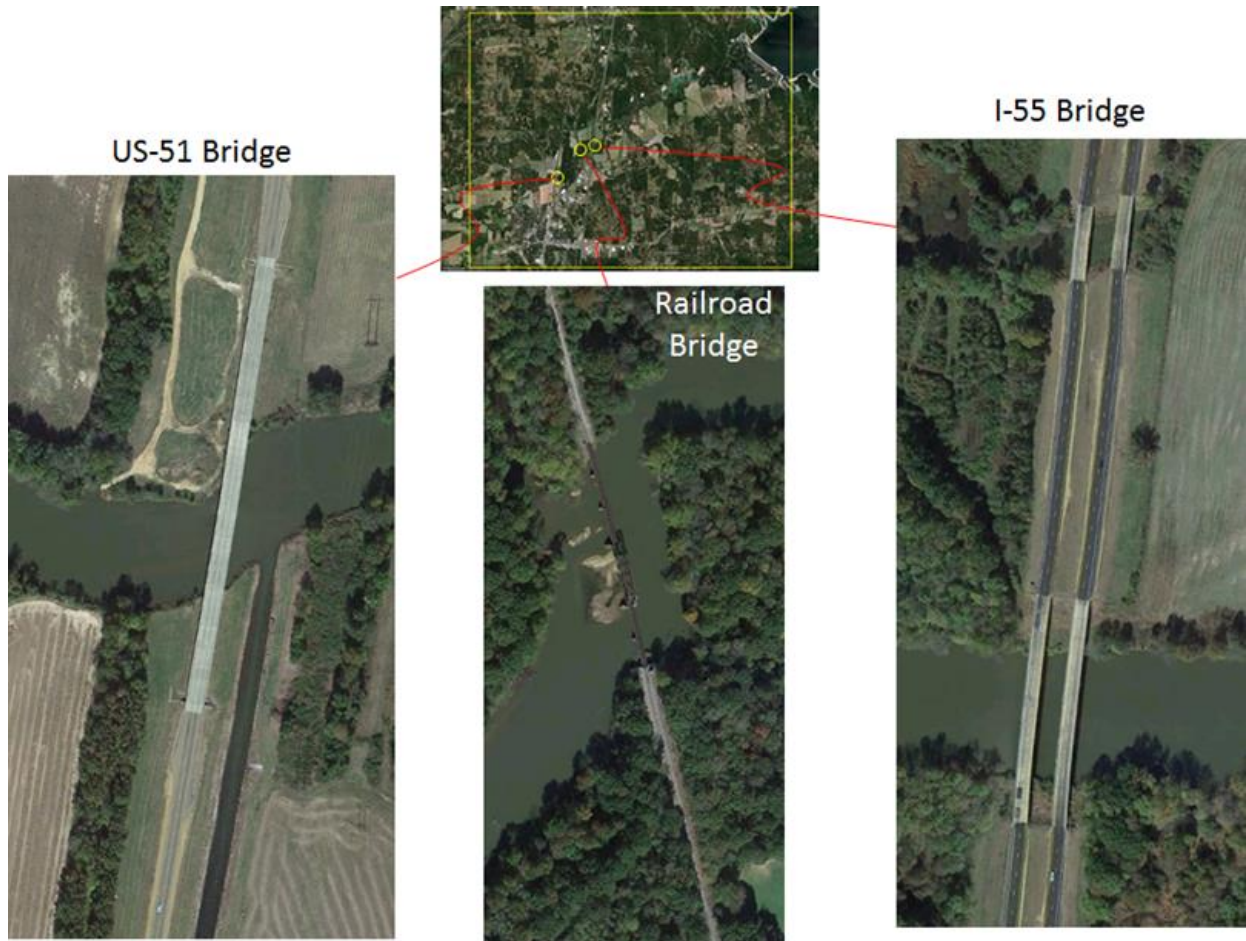


Figure 10. Major transportation corridors and bridge crossings at Sardis pilot study site

For simulations 5m and 3m cell size, the selected structures were burned into the DEM as elevations in order to model flow around them. Due to the use of a regular Cartesian grid as computational mesh, the structures cannot be burned into the DEM with their exact shape. As expected, the smaller the cell size, the better approximated the shape of the structure (Altinakar et al. 2015b). Figure 11 shows the representation of selected structures in the DEM. Representing the structures for coarser cell size was not practical.

The selected cell sizes for the simulation domain are shown in Figure 12.

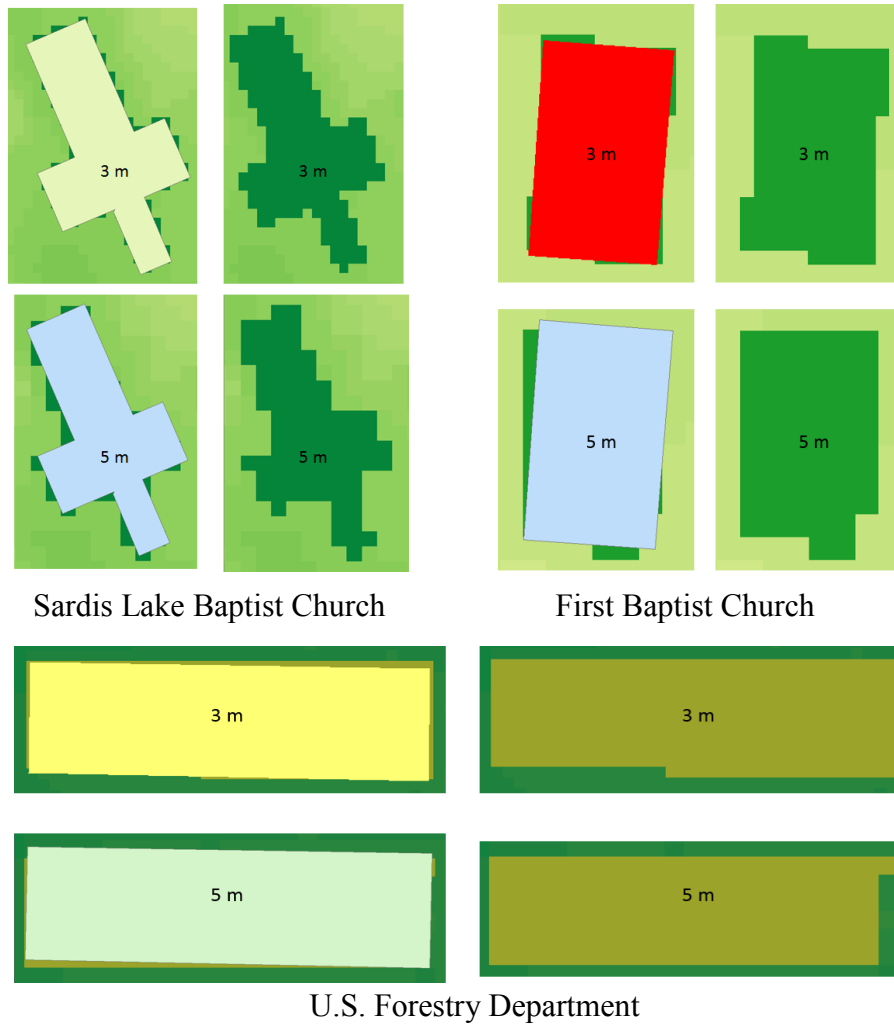


Figure 11. Representation of structures in the DEM

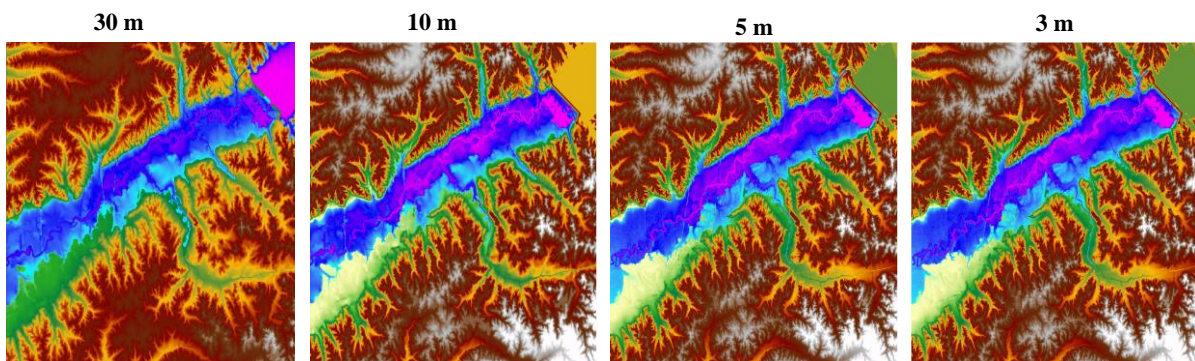


Figure 11. Different cell sizes for computational modeling, DEM, and resulting flood inundation

The computational domains for these simulations at different cell sizes are summarized in Table 1. The simulated scenario is based on a 218 m wide partial breach of levees in the study area. The simulation initiated when the water level was at the top of the levees as and it reached its final shape after 0.44 hours. Typical flood inundation simulation from the start point in the flood plain to the west end of the simulation domain was 48 hours.

Table 1. Extreme flood simulation scenarios

Computational Domain	Simulation for 30m DEM	Simulation for 10m DEM	Simulation for 5m DEM	Simulation for 3m DEM
<b>Cell size (m)</b>	<b>30</b>	<b>10</b>	<b>5</b>	<b>3</b>
Number of Columns	3085	2058	4116	6860
Number of Rows	2589	1726	3452	5753
Number of Cells	7,987,065	3,552,108	14,208,432	39,465,580
East-West Extent (km)	92.550	20.580	20.580	20.580
North-South Extent (km)	77.670	17.260	17.260	17.259
Spatial Reference	NAD_1983_UTM_Zone_16N			
Datum	D_North American_1983			
Min Elevation (m)	37.964	53.410	53.147	53.147
Max Elevation (m)	189.784	136.070	139.868	139.900
Structures Burned into the DEM	No	No	Yes	Yes
Bridge Openings	Cleared	Cleared	Cleared	Cleared
Manning's Roughness	Overall Manning's roughness of 0.035 m <sup>-1/3</sup> s			

Flood Scenarios were simulated based on cell sizes. Discharge hydrograph for 30m cell size was computed during the simulation by imposing a trapezoidal breach forming in 0.44 hours.

Discharge hydrographs for smaller cell sizes were obtained during the simulation with 30m DEM is directly imposed as a source at the downstream of the dam. Figure 12 shows a flood inundation map for 3m cell domain. Figure 13 shows a sample output of flood depth and flood velocity for 10m cell domain along the observation profile “channel CL”. Detailed discussion is provided in Appendix report (Altinakar et al. 2015a).

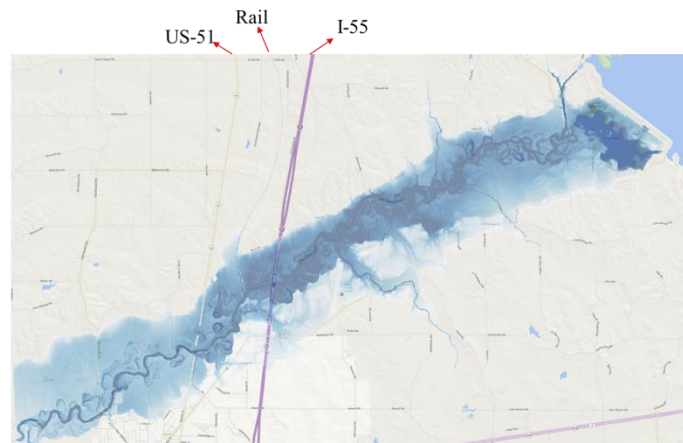
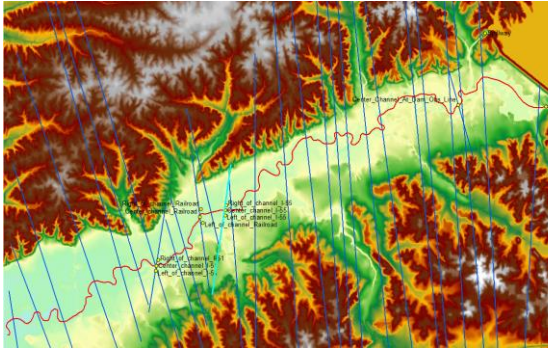


Figure 12. Map of maximum flow depth computed with 3-m cell size overlaid on a road map

Plot of Flood Depth and Flood Velocity along the Observation Profile “Channel CL”

2014 Study of Flood Risk Mapping, Mississippi



Flow depths up to 10m  
Flow velocities up to 6m/s

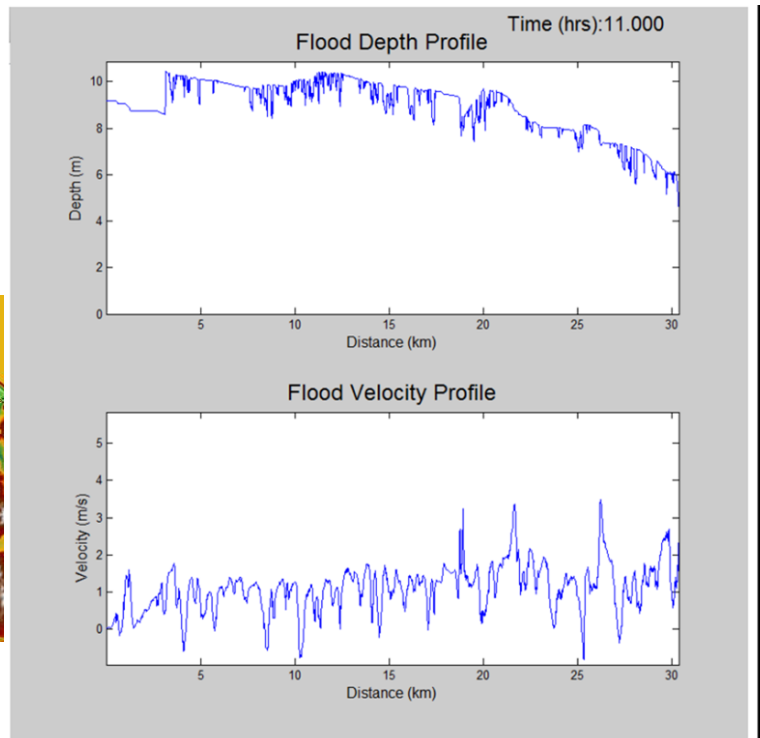


Figure 13. Flood depths and velocities along the downstream river channel

## 2.4 Flood Inundation Impacts of Extreme Flood Simulations on Infrastructure

### Floodwater Depth, Floodwater Velocity, and Inundation Map

Key features of extreme flood inundation simulation results for 10m computational cell size include propagation of floodwater with time, floodwater depth, and floodwater velocity from the start point on the profile. The CCHE-FLOOD simulation module provided 2D raster maps of flood propagation over 48 hours and data files of flood arrival times, flood depths, and floodwater velocities along the river CL and at given cross-section points. The following results of the flood inundation simulations were generated:

- 1 profile observation line (along the river CL)
- 29 cross section lines (observation lines perpendicular to the river CL)
- 12 observation points on cross section lines (at selected infrastructure assets)

Simulated floodwater depth along the river CL for the first 12 hours of the simulation is shown in Figure 14. Darker colors represent later time steps. As shown, floodwater depth increases

throughout the first 12 hours of the inundation simulation. Figure 15 shows depth and velocity of floodwater at the start of river profile and at selected transportation infrastructure assets.

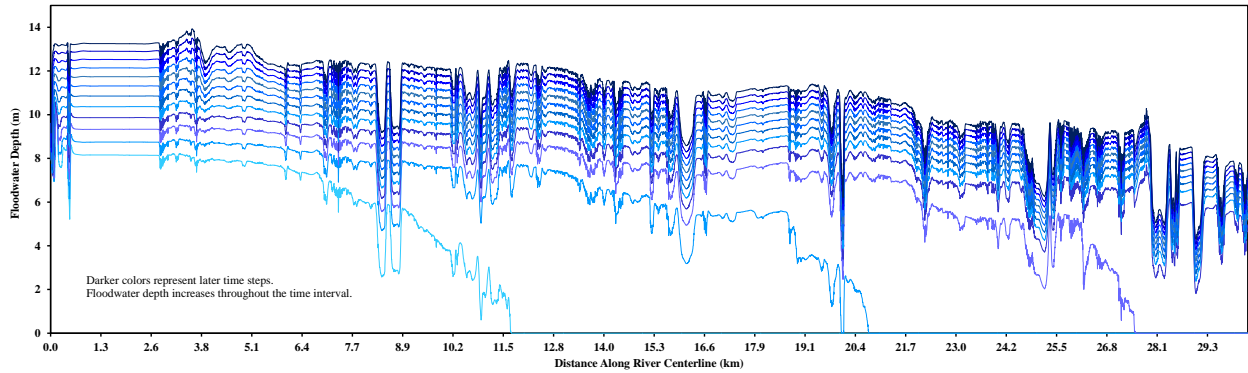


Figure 14. Simulated floodwater depth for time interval 0 – 12 h

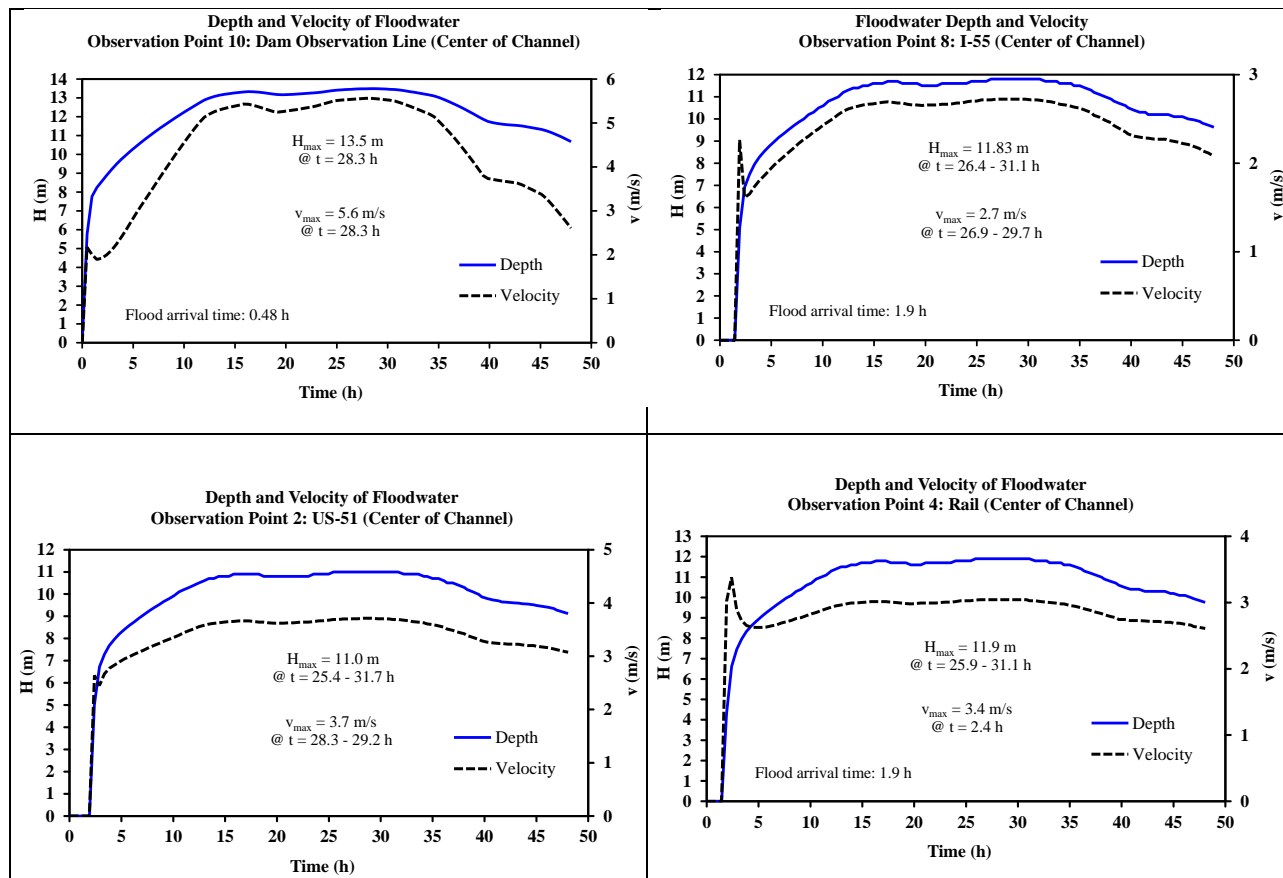


Figure 15. Simulated floodwater depth and velocity at selected observation points

## Flood Simulation Visualization and Impacts on Infrastructure

The Sardis pilot site features I-55, US-51, two minor highways, a rail line, a small airport, churches, and low density residential areas. Visualization of the 10m cell flood simulation results with infrastructure assets impacted by the flood inundation is presented in Figure 16. It shows river downstream CL, cross-sections, transportation features (US 51, Rail line, I-55 and Airport), and calculated flood Depth at Selected infrastructure feature locations along the river CL. The affected infrastructure assets are located within a distance of 10 miles (16 km) from the simulation start point (Figure 16). Several major and local highways and one rail line including 24 bridges are affected by simulated flood inundation, as shown in Figure 4. Geospatial analysis shows that total flood inundation covers an area of 31 sq mi (80 km<sup>2</sup>), where floodwater reaches up to 39 ft (12 m) within the flood inundation area. The nearest building to the simulation start point is Sardis Lake Baptist Church at a linear distance of 4.4 miles (7.03 km). Batesville Public Library is located 10.2 miles (16.51 km) away from the simulation start point.

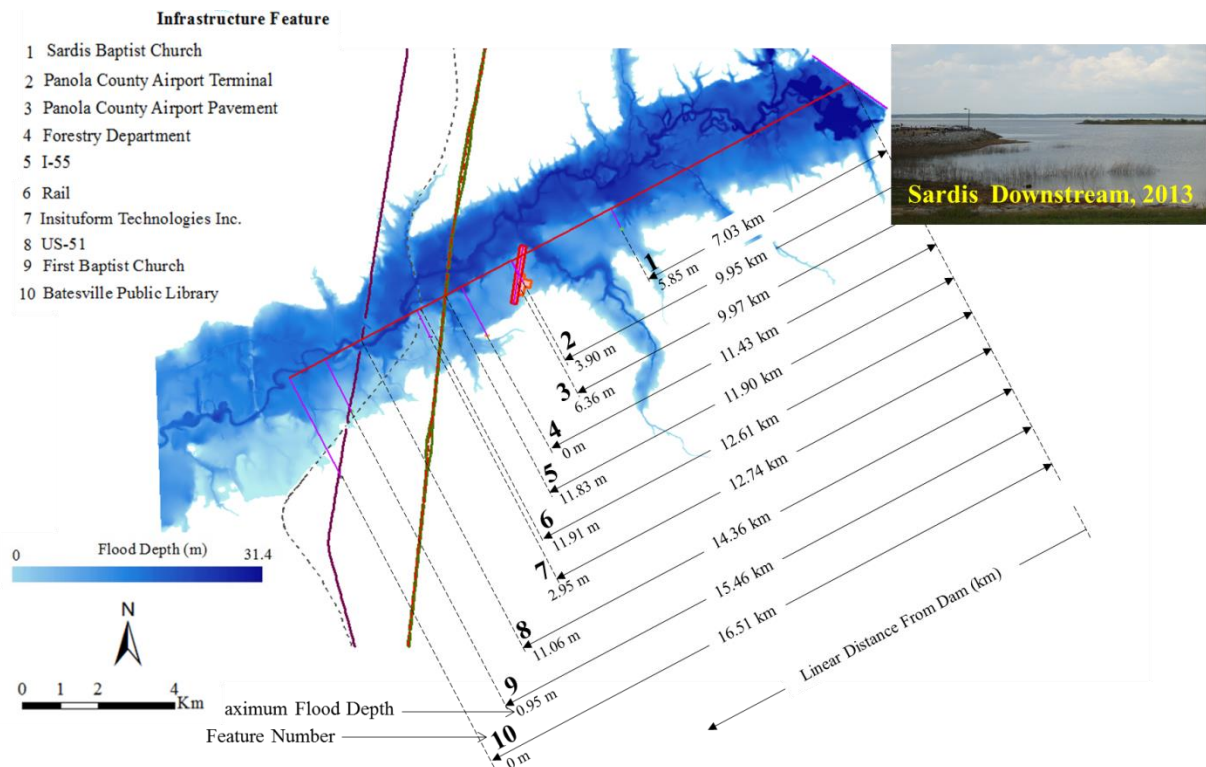


Figure 16. Infrastructure feature description on 10m cell simulation of flood inundation map

Affected transportation infrastructure assets are shown in Figures 4 and 16 and summarized as follows:

- *I-55*: Interstate highway, principal artery for people and freight, located north of Batesville, eight bridges with total length of 1,700 ft (522 m), affected feature length 2.60 mi (4.19 km).

- *US-51*: Non-interstate highway, principal artery for people and freight, parallel to I-55 in the pilot study area, three bridges with total length of 2,500 ft (762 m), affected feature length 2.92 mi (4.70 km).
- *Rail*: Freight rail, located between I-55 and US-51, four bridges with total length of 830 ft (253 m), affected feature length 4.88 mi (7.86 km).
- *Highway 35*: State highway, junctions with I-55 in Batesville, nine bridges with total length of 1,901 ft (333 m), affected feature length 10.60 mi (17.06 km).
- *Highway 315*: State highway, junctions with Highway 35, affected feature length 3.29 mi (5.29 km).

Impacts of flood inundation on transportation infrastructure assets are presented in Table 2 (Durmus et al. 2015, Uddin et al. 2015). Some examples of flood inundation ranges are:

- Affected length of transportation infrastructure is 0.94 mile (1.52 km) at Airport Pavement, 2.60 miles (4.19 km) at I-55, 4.88 miles (7.86 km) at Rail, 2.92 miles (4.70 km) at US-51, 10.60 miles (17.06 km) at Highway 35 and 3.29 miles (5.29 km) at Highway 315.
- Maximum flood depth above ground is 20.9 ft (6.36 m) at Airport Pavement, 38.8 ft (11.83 m) at I-55, 39.1 ft (11.91 m) at Rail, 36.3 ft (11.06 m) at US-51, 33.1 ft (10.09 m) at Highway 35 and 39.3 ft (11.97 m) at Highway 315.
- Maximum floodwater depth above feature is 17.6 ft (5.36 m) at Airport Pavement, 12.6 ft (3.83 m) at I-55, 16.1 ft (4.91 m) at Rail, 13.3 ft (4.06 m) at US-51, 28.2 ft (8.59 m) at Highway 35 and 36.0 ft (10.97 m) at Highway 315.

Table 2. Simulated flood inundation impacts on transportation infrastructure assets

Feature	Feature No.	Distance From Start (km)	Feature Height From Ground (m)	Maximum		Affected Length of Feature (km)
				Floodwater Depth Above Ground (m)	Floodwater Depth Above Feature (m)	
Airport Pavement	3	9.97	1.00	6.36	5.36	1.52
I-55	5	11.90	8.00	11.83	3.83	4.19
Freight Rail Line	6	12.61	7.00	11.91	4.91	7.86
US-51	8	14.36	7.00	11.06	4.06	4.70
Highway 35	*	0.00	1.50	10.09	8.59	17.06
Highway 315	*	0.00	1.00	11.97	10.97	5.29

\*Feature included due to its close proximity to the study area

Table 3 presents the impacts of flood inundation on selected buildings in the flood simulation area. The floodwater is several meters higher than the feature elevation at some locations. The

Forestry Department and Batesville Public Library buildings are not affected by the simulated flood inundation given the fact that they are outside the floodplain.

Table 3. Simulated flood inundation impacts on transportation building infrastructure assets

Feature	Feature No.	Distance From Start (km)	Feature Height From Ground (m)	Maximum		Footprint Area (m <sup>2</sup> )
				Floodwater Depth Above Ground (m)	Floodwater Depth Above Feature (m)	
Sardis Lake Baptist Church	1	7.03	5.00	5.85	0.85	2,059
Airport Terminal	2	9.95	6.00	3.90	0.00	95,106
Forestry Department	4	11.43	4.50	0.00	0.00	3,225
Insituform Technologies Inc.	7	12.74	6.50	2.95	0.00	3,218
First Baptist Church	9	15.46	5.00	0.95	0.00	1,368
Batesville Public Library	10	16.51	3.50	0.00	0.00	1,754

Floodwater depths for building and other structures are as follows (Durmus et al. 2015, Uddin et al. 2015):

- Sardis Lake Baptist Church with a building height of 16.4 ft (5.00 m), maximum floodwater depth above ground 19.2 ft (5.85 m), floodwater depth above feature 2.8 ft (0.85 m), implying that this building will be completely inundated.
- Airport Terminal with a building height of 19.7 ft (6.00 m), maximum floodwater depth above ground 12.8 ft (3.90 m), implying that the terminal building will be under floodwater and unusable.
- Insituform Technologies Inc. with a building height of 21.3 ft (6.50 m), maximum floodwater depth above ground 9.7 ft (2.95 m), implying that this industrial site will be under floodwater and unusable.
- First Baptist Church with a building height of 16.4 ft (5.00 m), maximum floodwater depth above ground 3.1 ft (0.95 m).

The 30 m and 10 m cell size simulations do not consider built infrastructure, whereas the transportation and building infrastructure features are included in 5 m and 3 m cell-size simulations. Detailed results are presented and discussed NCCHE’s final project report in Appendix (Altinakar et al. 2015a). The summary results follow:

- The flow depths computed with 3 m and 5 m cell sizes give almost identical results. Flow depths computed with 10 m and 30 m cell sizes are also almost identical.
- The flood elevation and flow velocities are almost the same for all cell sizes.

### 3. ASSESSING FLOOD IMPACTS ON PAVEMENT AND BRIDGES

#### 3.1 Extreme Flood Inundation Impact Assessment for the Pilot Study Site

The following steps of the research methodology (Figure 3) are discussed in this section:

- Assessing the impacts of floodwater inundation on selected features
- Evaluating structural integrity of highways and bridges

#### Field Evidence of Flood Related Bridge Failures

Evidence of bridge destruction by flood is shown in Figures 5 and 17 where several photos are compiled from recent flood related bridge failures (InfrastructureGlobal 2011, Uddin et al. 2015). The failure analysis of these bridges under extreme floods indicates the most vulnerable conditions:

- When the floodwater reaches the bottom of the deck and top of the girders.
- When floodwater rises more and washes over the bridge deck at high velocity causing large hydrodynamic forces.
- When the floodwater causes severe scouring around bridge piers which may cause it to fail.



Figure 17. Field evidence of catastrophic failure of bridges caused by floods

## Simulated Floodwater Depth Over Selected Infrastructure Features

Figure 18 plots maximum flood water depth vs. height of feature based on Sardis flood simulation for 10m computational cell size. The floodwater will be overflowing on highway and rail bridges by 3.8 to 4.9 m over the bridge decks. All other minor highways, local roads and airport in the study site will be completely inundated if such extreme flood happened. This flood risk vulnerability assessment is possible by using the 2D flood simulation capability.

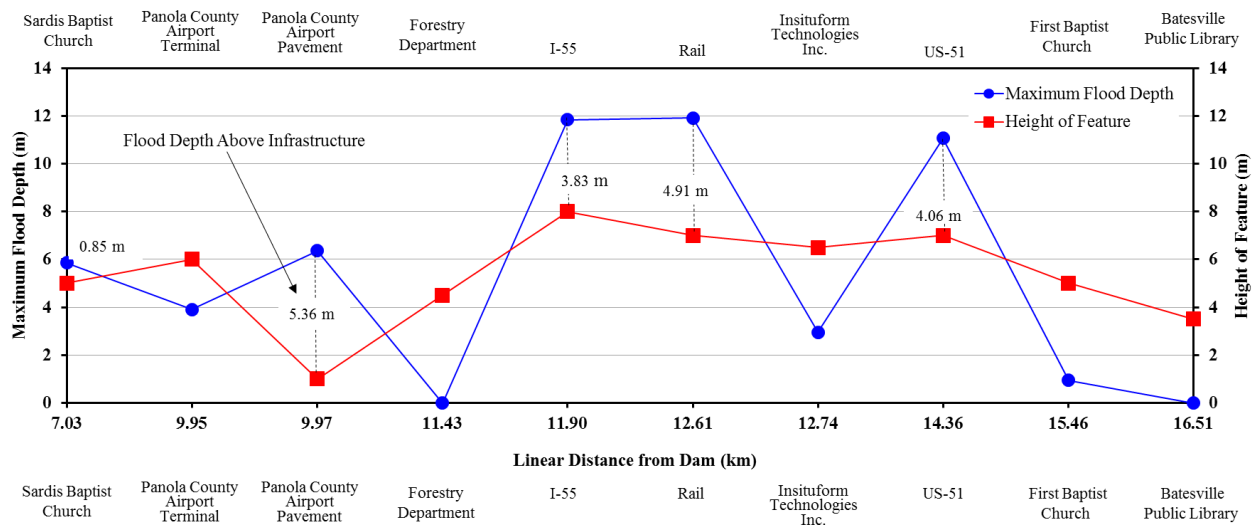


Figure 18. Maximum flood water depth vs. height of feature for Sardis flood simulation



Figure 19. Photos bridge over Tallahatchie River at pilot study site area: (Left) A view of I-55 bridge and (Right) A view of US-51 bridge (credit: Mississippi DOT Bridge Division)

One of the outputs of the simulation is flood depth and velocity at a desired pre-defined observation point on the CL profile or cross section lines. The two major highway bridges in the pilot study site are I-55 and US-51 over Tallahatchie River (Figure 19) and the simulation shows:

- Floodwater depth vs. velocity plot for I-55 is presented in Figure 15 (top right). Figure shows that flood arrives at I-55 bridge in less than two hours. Maximum floodwater depth is 38.8 ft (11.83 m) whereas floodwater velocity reaches 8.9 ft/s (2.7 m/s).
- Floodwater depth vs. velocity plot for US-51, presented in Figure 15 (bottom left), shows that that flood arrives at US-51 bridge in less than two hours. Maximum floodwater depth at US-51 Bridge is 11 m and the maximum floodwater velocity is 3.7 m/s.

Vulnerability assessment of transportation infrastructure assets is an essential component of flood risk modeling. Protection of critical transportation infrastructure assets from extreme weather events such as floods would require the use of flood simulation results and evaluation of structural integrity.

### 3.2 Evaluation of Highway Embankment Stability Subjected to Floodwater

#### Analysis Assumptions and Inputs

A typical embankment was analyzed for slope stability for varying depth of floodwater. For 3m inundation depth, the embankment is assumed moist with a unit weight of 20.6 kN/m<sup>3</sup> and cohesion of 23.9 kPa. For 7 m inundation depth, embankment is assumed to have a unit weight of 20.9 kN/m<sup>3</sup> and cohesion of 18 kPa. Finally, for 11 m inundation depth, embankment is assumed saturated with a unit weight of 21.2 kN/m<sup>3</sup> and cohesion of 12 kPa. Internal friction angle is assumed 25° for all cases. Subsoil is assumed to carry the same properties as the embankment. Unit weight, cohesion and the internal friction angle of the pavement are assumed to be 22.8 kN/m<sup>3</sup>, 0 kPa and 40°, respectively. Analyses were performed using Janbu's Method. Soil properties used in different analysis scenarios are presented in Table 4.

#### Slope Stability Analyses for Highway Embankment

Slope stability analyses for US-51 highway embankment were performed using GeoSlope Software (Student License) to assess the structural integrity of the embankment (GeoSlope 2012). Three different inundation scenarios were considered for the analyses. Slope stability analyses for 3 m floodwater inundation yielded a Factor of Safety (FS) against sliding of 3.12. FS for the opposite side slope was lower (2.88). When the embankment was inundated on both sides, slope stability analysis yielded a FS of 2.68.

Finally, slope stability analyses for 7 m floodwater inundation yielded a FS against sliding of 3.41. FS for the opposite side slope was lower (2.56). It is seen from Janbu and Ordinary Method results that opposite side slope at 7 m inundation are the most critical case (Figure 20).

Table 4. Soil properties used in slope stability analyses

Analysis No.	1		2		3		
Inundation Depth (m)	3		7		11		
	Moist Unit Weight	Cohesion	Unit Weight	Cohesion	Saturated Unit Weight	Cohesion	Internal Friction Angle
	(kN/m <sup>3</sup> )	(kPa)	(kN/m <sup>3</sup> )	(kPa)	(kN/m <sup>3</sup> )	(kPa)	(°)
$\gamma_{\text{pavement}}$	22.78	0	22.78	0	22.78	0	40
$\gamma_{\text{embankment}}$	20.56	23.94	20.90	17.96	21.24	11.97	25
$\gamma_{\text{subsoil}}$	20.56	23.94	20.90	17.96	21.24	11.97	25

Janbu’s and Ordinary Methods yielded lowest FS in undertaken slope stability analyses. However, Janbu’s Method does not consider the equilibrium of internal forces. Therefore, in determination of FS for different slope angles, Spencer’s Method is employed. Results are provided in Figure 21. It is observed that the factor of safety against sliding decreases with increasing slope and also with increasing unit weight/decreasing cohesion of the embankment.

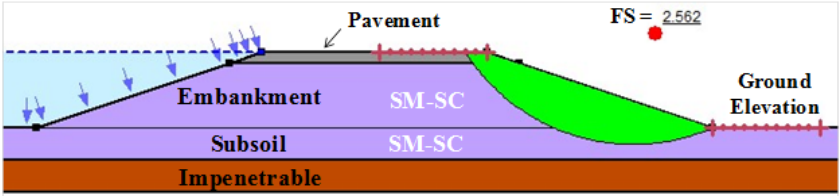


Figure 20. US-51 Embankment at 7 m inundation (most critical Factor of Safety against sliding)

**3.3 Evaluation of Scouring Potential Around Bridge Piers**

For all three bridges (I-55, Rail, and US-51), the depth-averaged local velocity of the floodwater at the central observation point can be as high as 3 m/s, approximately. This is a relatively high flow velocity, which will be able to erode and transport sediment particles up to a diameter of 0.10m. Pier scour under both live-bed and clear-water conditions is computed by the equation developed by Colorado State University and later modified by Richardson et al. (1993). The methodology is discussed in detail in the NCCHE final report in Appendix (Altinakar et al. 2015a).

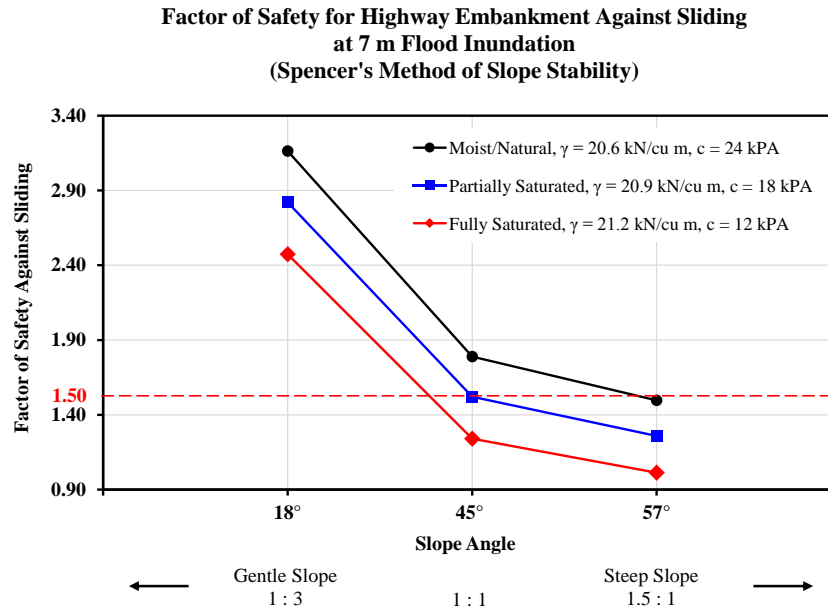


Figure 21. Factor of Safety Against Sliding at 7 m Flood Inundation

*I-55 Bridge:* The local scour around the 10ft-diameter I-55 bridge piers in the main channel (Figure 19 left) is estimated as 5.27m (17.30ft). Unless the pier foundations are sufficiently deep and/or appropriate local scour prevention measures are taken, the bridge may be at risk due to excessive scour.

*Rail Bridge:* The flow overtops the rail bridge with a depth close to 3m. Based on the estimated size of piers, the local scour around the slender piers in the main channel is estimated as 5.36m (17.58ft). This is a quite substantial scour depth. Unless the pier foundations are sufficiently deep and/or appropriate local scour prevention measures are taken, the integrity of the bridge may be in danger due to excessive scour.

*US-51 Bridge:* The local scour around the rectangular pier (0.584 m by 0.26 m) in the main channel of US-51 bridge (Figure 19 right) is estimated as 2.00m (6.57 ft). This is a reasonable scour depth. The piers are founded deep into the ground. Thus, there is no significant danger to the structure.

### 3.4 Extreme Flood Impacts on Bridge Superstructure

According to the Federal Highway Administration, there are 605,411 bridges in the U.S. as of December 31, 2013 (FHWA 2013). Figure 22 shows spatial distribution of deficient bridges by states. Ten states have 20,000 or more bridges. The state of Texas ranks first with 52,561 bridges which make up almost nine percent of the total bridge inventory. “Deficient” defines those bridges which are structurally deficient or functionally obsolete. Unfortunately, more than 24% of

the total bridges in the U.S. are deficient (146,583). Bridge structures, being the backbone of transportation infrastructure, are under a constant threat of being washed away and/or overturned due to exerted forces generated by floodwater.

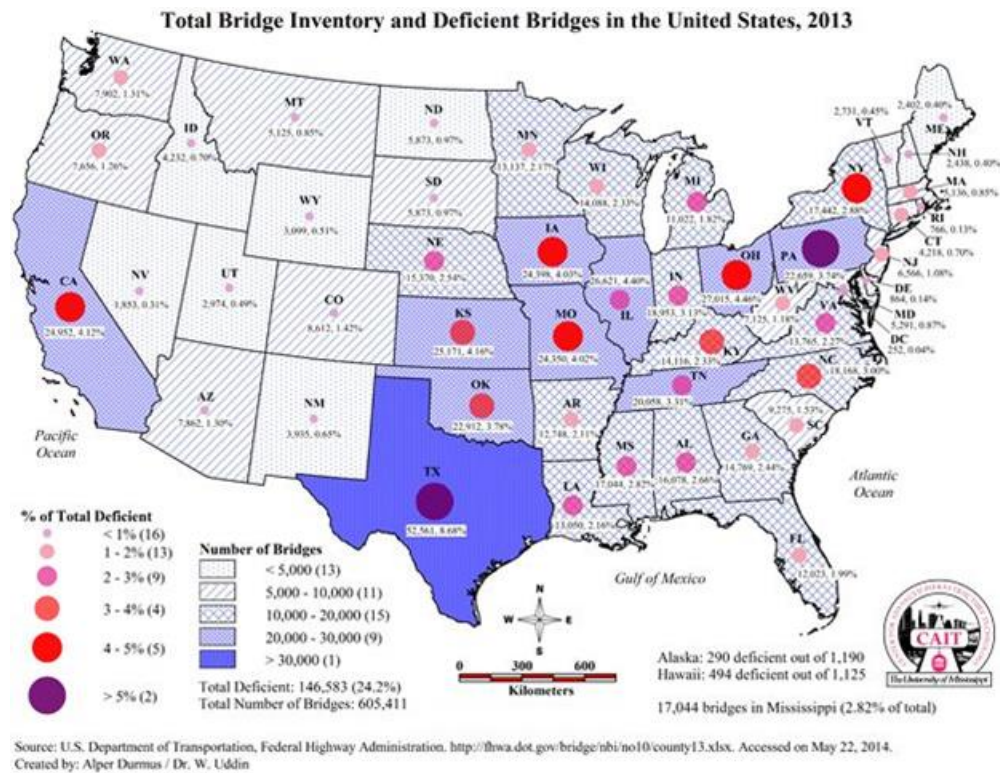


Figure 22. Spatial map of bridge inventory and deficient bridge percentages by state

There is no known reference on computational analysis of the structural integrity of bridge superstructures subjected to extreme floodwater flow. Therefore, in this project a practical approach is presented to assess the structural integrity of the US-51 bridge superstructure. For this purpose, Factor of Safety against overturning was assessed for different inundation scenarios.

### Structural Integrity Assessment of Bridge Superstructure

The structural integrity analysis presented in this section is for floodwater inundation results generated using 10 m cell size. The structural analysis assumes that the floodwater flow exerts pseudo-static force, i.e. not stagnant and is enough to generate the lateral forces on the bridge structure. Besides this, the following assumptions are made after studying the design drawings of the US-51 Bridge (courtesy of The MDOT Bridge Division):

- Girder type: AASHTO I-Beam Type IV (PCI 2013)
- Girder height: 4.5 ft
- Girder cross-section bottom width: 1.83 ft (Xanthakos 1994)
- Girder cross-section area: 4.16 sq ft (Xanthakos 1994)

- Girder spacing: 6 ft
- Bridge deck/slab width: 30 ft (typical 2-lane highway bridge)
- Bridge slab thickness: 1 ft
- Number of girders: 6
- Span width: 30 ft (i.e. girder and slab lengths)
- Unit weight of slab and girders: 150 pcf
- Unit weight of floodwater: 62.4 pcf

A photo of a section of the US-51 Bridge is shown in Figure 23. The bridge superstructure rests on the pile caps. It is assumed that the bridge pile caps, as well as bridge piers and foundations, are capable of withstanding the generated lateral flowing floodwater forces. An examination of photos from several bridge failure cases during the 2005 Hurricane Katrina and the 2011 Hurricane Irene (InfrastructureGlobal 2011) shows that most bridge superstructures washed away when the floodwater reached the height of the girders. For this reason, overturning moments are investigated in this study, and calculated with respect to the interface (edge) of girders and pile caps.

A general schematic of the highway bridge is represented in Figure 24 based on the MDOT drawings of the US-51 Bridge (Uddin 2014).

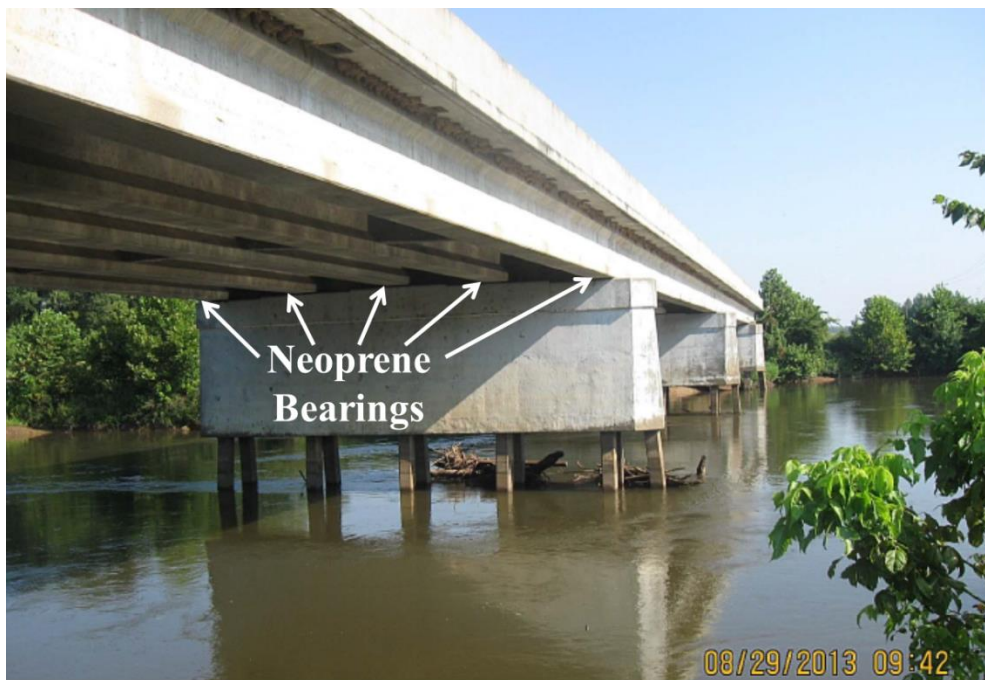


Figure 23. US-51 Bridge (Photo credit: MDOT Bridge Division)

In this study, a 30-ft section of bridge superstructure is analyzed (Figure 25). The section extends 15 ft on each side of a pile cap. This is based on the assumption of a typical superstructure/pile

interface for the entire bridge (Figure 24). Bridge railings etc. are not considered in the calculations.

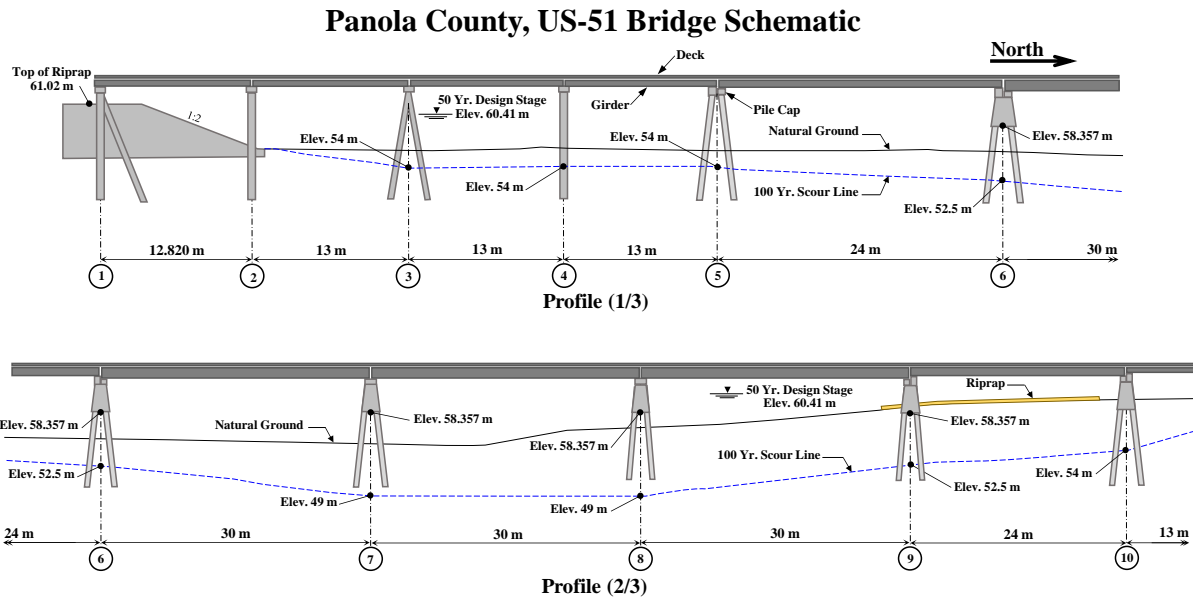


Figure 24. General schematic of the highway bridge (based on MDOT drawings)

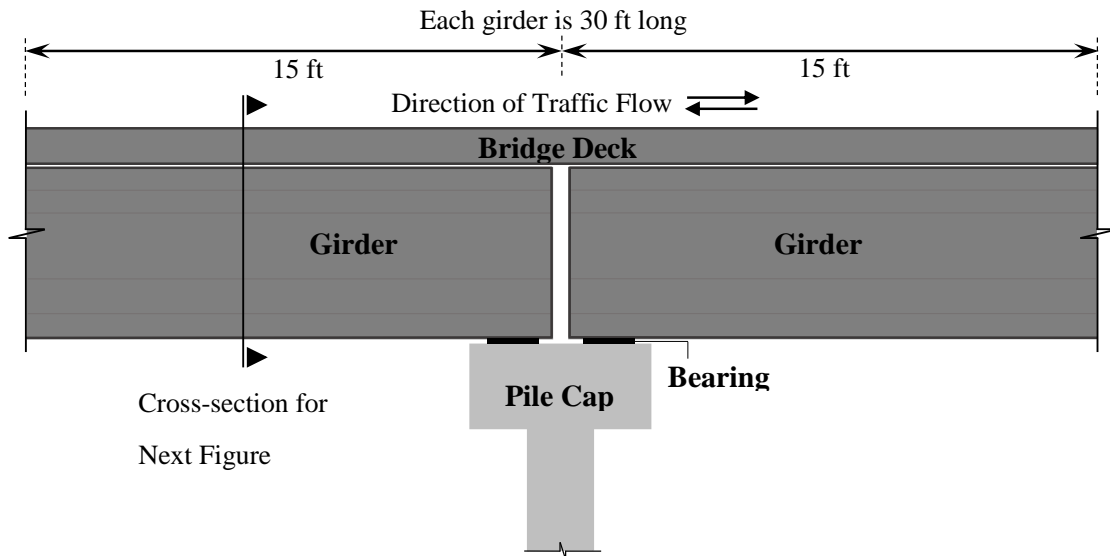


Figure 25. Schematic of a 30 ft section of the bridge superstructure

A schematic of a single girder is shown in Figure 26 (a). A schematic of the entire bridge structure is presented in Figure 26 (b). Three scenarios of floodwater inundation are considered for the analyses:

- The first scenario is where the floodwater is at the bottom of the bridge slab.

- In the second scenario, floodwater is level with the top of the bridge superstructure.
- Finally, the bridge superstructure is under 4 m of floodwater flow.

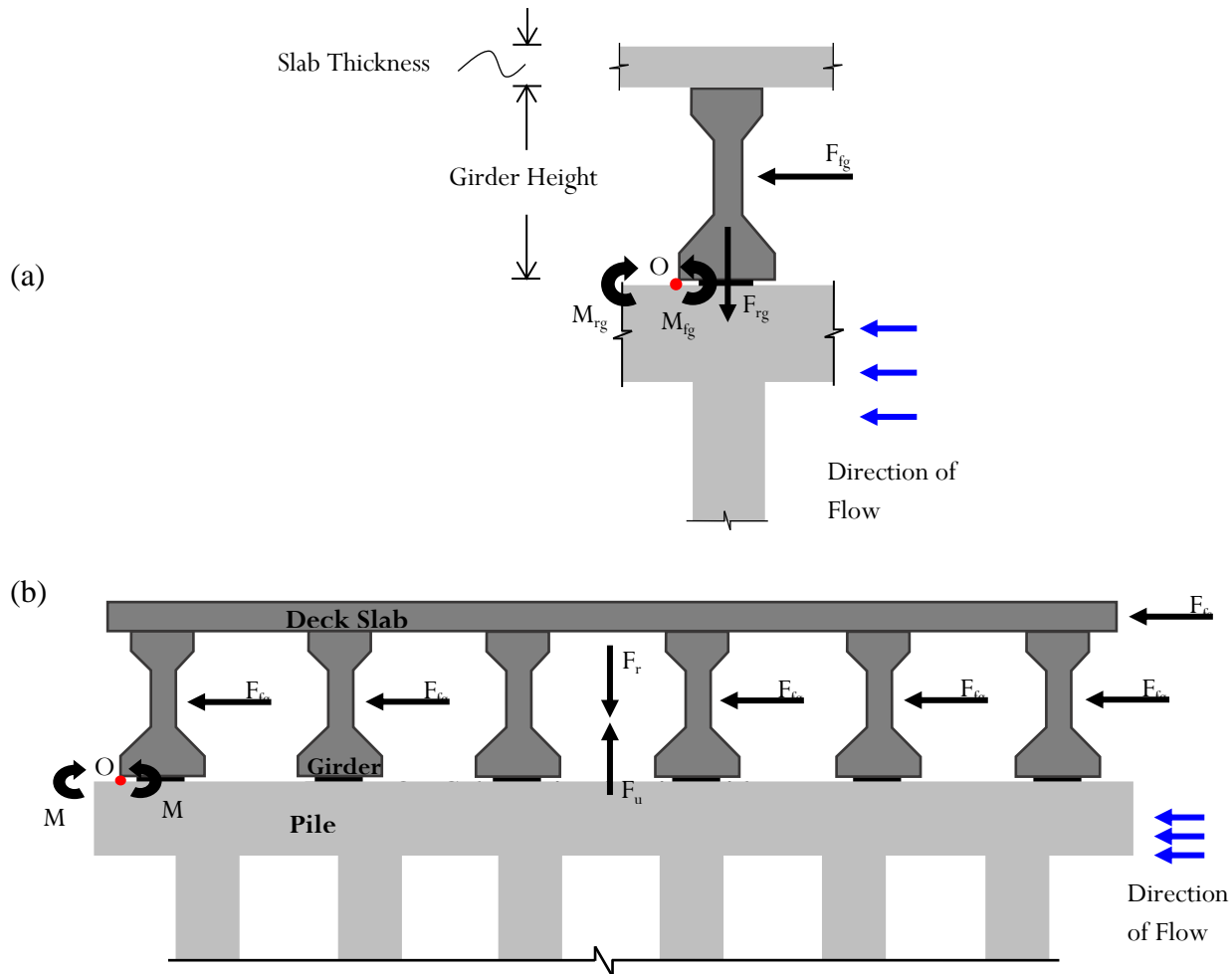


Figure 26. Schematic of (a) Single Girder (b) Entire Superstructure

The bridge superstructure rests on the pile caps. It is assumed that the bridge pile caps, as well as bridge piers and foundations, are capable of withstanding the generated lateral flowing floodwater forces. An examination of photos from several bridge failure cases during 2005 Hurricane Katrina and 2011 Hurricane Irene shows that most bridge superstructures washed away when the floodwater reached the height of the girders. Consequently, overturning moments are calculated in this study with respect to the interface (edge) of girders and pile caps. A general schematic of the highway bridge is represented in Figure 24 based on the MDOT drawings of the US-51 Bridge. For analysis purposes, a 30-ft section of bridge superstructure is considered which extends 15 ft on each side of a pile cap (Figure 25). This is based on the assumption of a typical superstructure/pile interface for the entire bridge. Bridge railings etc. are not considered in the calculations.

## Scenario 1: Floodwater Force at the Bottom of Slab

Before investigating the entire bridge superstructure, overturning analysis is performed for a single girder. The case is a lateral loading generated by the floodwater flow.

### Single Girder Case

Lateral flowing floodwater force ( $F_{fg}$ ) is acting on the mid-height of the girder as a concentrated force. Floodwater force generates the floodwater moment ( $M_{fg}$ ) which acts for overturning of the girder. On the other hand, resisting moment by girders ( $M_{rg}$ ) is generated by the weight of the girders ( $F_{rg}$ ) and acts against  $M_{fg}$ . Moments are calculated with reference to point O as shown in Figure 26 (a).

#### *Calculation of Resisting Moment*

Resisting force,  $F_{rg} = \text{Effective girder length} \times \text{Girder cross-section area} \times \text{Unit weight of girder} = (15+15) \text{ ft} \times 4.16 \text{ ft} \times 150 \text{ pcf} = 18\,720 \text{ lbs}$

Resisting lever arm,  $L_{rg} = (\text{Girder cross-section bottom width}) / 2 = 1.83 \text{ ft} / 2 = 0.92 \text{ ft}$

(See Figure 25 for girder length explanation.)

Resisting moment,  $M_{rg} = F_{rg} \times L_{rg} = 18\,720 \text{ lbs} \times 0.92 \text{ ft} = 17\,129 \text{ lbs}\cdot\text{ft}$

#### *Calculation of Floodwater (Overturning) Moment*

Lateral force of floodwater flow,  $F_{fg} = \text{Girder height} \times \text{Effective girder length} \times \text{Unit weight of floodwater} = 4.5 \text{ ft} \times (15+15) \text{ ft} \times 62.4 \text{ pcf} \times 1 \text{ ft} = 8424 \text{ lbs}$

(Note that the force calculated in this example is for 1 foot of floodwater in the flow direction, and acting on the girder on the side.)

Floodwater force lever arm,  $L_{fg} = (\text{Girder height}) / 2 = 4.5 \text{ ft} / 2 = 2.25 \text{ ft}$

Floodwater moment,  $M_{fg} = F_{fg} \times L_{fg} = 8424 \text{ lbs} \times 2.25 \text{ ft} = 18\,954 \text{ lbs}\cdot\text{ft}$

#### *Factor of Safety*

FS against overturning =  $M_{rg} / M_f = 17\,129 \text{ lbs}\cdot\text{ft} / 18\,954 \text{ lbs}\cdot\text{ft} = 0.90$

(Note that this analysis does not consider the dead load of the deck.)

It can be seen from the results that a single girder is vulnerable to overturning even for 1 ft of floodwater force. The FS will be even less than 0.90 when there is more than 1 ft of floodwater force. Once the girder is displaced, it will possibly hit a neighbor girder and this may cause catastrophic failure of the bridge superstructure. However, this is an extreme case based on flood simulation results.

As shown in the above calculation, full girder height is considered for calculations of lateral floodwater flow forces. However, it should be mentioned that the actual vertical surface perimeter (i.e. side of the girder) is greater than the height of the girder.

The case presented so far analyzed the effect of floodwater flow exerting lateral force to the girder. Uplift force is not included in this single girder analysis, which will further reduce the FS. It will be investigated next.

## Entire Superstructure

The schematic of the entire superstructure is illustrated in Figure 26 (b). Lateral flowing floodwater force on the slab ( $F_{fs}$ ) and the girders ( $F_{fg}$ ), as well as uplift floodwater force ( $F_u$ ), also contribute to overturning moment ( $M_f$ ). Resisting moment ( $M_r$ ) is generated by the weight of the superstructure ( $F_r$ ). Key results are as follows:

- Total resisting moment,  $M_r = M_{rg} + M_{rs} = 1\,684\,800 \text{ lbs}\cdot\text{ft} + 2\,025\,000 \text{ lbs}\cdot\text{ft} = 3\,709\,800 \text{ lbs}\cdot\text{ft}$
- Floodwater moment on girders,  $M_{fg} = F_{fg} \times L_{fg} = 252\,720 \text{ lbs} \times 2.25 \text{ ft} = 568\,620 \text{ lbs}\cdot\text{ft}$
- Total overturning moment,  $M_f = M_{fg} + M_{ug} = 1\,269\,495 \text{ lbs}\cdot\text{ft}$

### *Factor of Safety*

FS against overturning =  $M_r / M_f = 3\,709\,800 \text{ lbs}\cdot\text{ft} / 1\,269\,495 \text{ lbs}\cdot\text{ft} = 2.92$

## Scenario 2: Floodwater Force on Top of Superstructure

For illustration purpose, all calculation steps are shown for Scenario 2 (Figure 26). This scenario is also a lateral loading case as well as uplift forces caused by floodwater flow. The bearings are ignored in the calculations.

### *Calculation of Resisting Moment*

Resisting moment by girders,  $M_{rg} = 1\,684\,800 \text{ lbs}\cdot\text{ft}$  (same as in Scenario 1)

Resisting force by slab,  $F_{rs} = \text{Volume of slab} \times \text{Slab Unit Weight} = 30 \text{ ft} \times 30 \text{ ft} \times 1 \text{ ft} \times 150 \text{ pcf} = 135\,000 \text{ lbs}$

Resisting lever arm of slab,  $L_{rs} = (\text{Slab width}) / 2 = 30 \text{ ft} / 2 = 15 \text{ ft}$

Resisting moment by slab,  $M_{rs} = F_{rs} \times L_{rs} = 135,000 \text{ lbs} \times 15 \text{ ft} = 2\,025\,000 \text{ lbs}\cdot\text{ft}$

Total resisting moment,  $M_r = M_{rg} + M_{rs} = 1\,684\,800 \text{ lbs}\cdot\text{ft} + 2\,025\,000 \text{ lbs}\cdot\text{ft} = 3\,709\,800 \text{ lbs}\cdot\text{ft}$

### *Calculation of Floodwater Moment*

Lateral force of floodwater flow on girders,  $F_{fg} = \text{Girder height} \times \text{Effective girder length} \times$

Number of girders  $\times$  Unit weight of floodwater =  $4.5 \text{ ft} \times (15+15) \text{ ft} \times 6 \times 62.4 \text{ pcf} \times 5 \text{ ft} = 252\,720 \text{ lbs}$

(Note that 5 ft of floodwater in the flow direction is assumed to act on the side of each girder.)

Floodwater lever arm of girders,  $L_{fg} = (\text{Girder height}) / 2 = 4.5 \text{ ft} / 2 = 2.25 \text{ ft}$

Floodwater moment on girders,  $M_{fg} = F_{fg} \times L_{fg} = 252\,720 \text{ lbs} \times 2.25 \text{ ft} = 568\,620 \text{ lbs}\cdot\text{ft}$

Floodwater force on slab,  $F_{fs} = \text{Slab thickness} \times \text{Slab length} \times \text{Unit weight of floodwater} = 1 \text{ ft} \times 30 \text{ ft} \times 62.4 \text{ pcf} \times 5 \text{ ft} = 9360 \text{ lbs}$

(Note that 5 foot of floodwater in the flow direction is assumed to act on the side of the slab.)

Floodwater lever arm of slab,  $L_{fs} = (\text{Slab thickness}) / 2 + \text{Girder height} = \frac{1}{2} \text{ ft} + 4.5 \text{ ft} = 5 \text{ ft}$

Floodwater moment on slab,  $M_{fs} = F_{fs} \times L_{fs} = 9360 \text{ lbs} \times 5 \text{ ft} = 46\,800 \text{ lbs}\cdot\text{ft}$

Total floodwater moment,  $M_f = M_{fg} + M_{fs} = 568\,620 \text{ lbs}\cdot\text{ft} + 46\,800 \text{ lbs}\cdot\text{ft} = 615\,420 \text{ lbs}\cdot\text{ft}$

#### *Calculation of Uplift Moment*

Floodwater uplift force on girders,  $F_{ug} = \text{Total volume of girders} \times \text{Unit weight of floodwater} = 6 \times 30 \text{ ft} \times 4.16 \text{ sq ft} \times 62.4 \text{ pcf} = 46\,725 \text{ lbs}$

Floodwater uplift force on slab,  $F_{us} = \text{Volume of slab} \times \text{Unit weight of floodwater} = 1 \times 30 \text{ ft} \times 30 \text{ ft} \times 62.4 \text{ pcf} = 56\,160 \text{ lbs}$

Total floodwater uplift force,  $F_u = F_{ug} + F_{us} = 46\,725 \text{ lbs} + 56\,160 \text{ lbs} = 102\,885 \text{ lbs}$

Floodwater lever arm of superstructure,  $L_{fss} = (\text{Slab width}) / 2 = 30 \text{ ft} / 2 = 15 \text{ ft}$

Uplift moment on superstructure,  $M_{fss} = F_u \times L_{fss} = 102\,885 \text{ lbs} \times 15 \text{ ft} = 1\,543\,277 \text{ lbs}\cdot\text{ft}$

Total overturning moment,  $M_f = 615\,420 \text{ lbs}\cdot\text{ft} + 1\,543\,277 \text{ lbs}\cdot\text{ft} = 2\,158\,697 \text{ lbs}\cdot\text{ft}$

#### *Factor of Safety*

FS against overturning =  $M_r / M_f = 3\,709\,800 \text{ lbs}\cdot\text{ft} / 2\,158\,697 \text{ lbs}\cdot\text{ft} = 1.72$

The factor of safety of the bridge girders against overturning assumed 5 ft of floodwater acting upon each girder and slab. It should be noted that thousands of feet of floodwater are flowing at an approach velocity of 3.3 m/s or 10.7 feet/sec (7.3 miles/hour) near the US-51 Bridge. This presents an even a higher force on the floodwater-facing girder, as was analyzed by the flood simulation.

### **Scenario 3: Floodwater Overflowing 4 m above Superstructure**

This scenario combines lateral, uplift and dead load of flowing floodwater. It is different from Scenario 2. Full 4 m floodwater overflowing the bridge superstructure introduces the weight of the floodwater acting against the overturning risk of the superstructure, which will result in a higher FS. Therefore, the analysis is not pursued further.

In Scenario 3, the force of floodwater flowing above the superstructure can be considered analogous to dead weight in the structural analysis. The standing floodwater is by no means a threat to the structure as long as the depth of the floodwater remains below the equivalent design truck loading (AASHTO 2012), and no other truck loading should be present during flooding. Nevertheless, these forces must be considered in the structural analysis.

## Vulnerability of Bearings

It is noted that the bearings used in the US-51 Bridge are of neoprene/elastomeric type (Uddin 2014). The thickness of the bearings is generally less than 2 inch which is ignored in the following calculations (Figure 27). A dowel type steel rod is used to maintain the alignment of the girder during temperature-related movements of the girder. The dowel is inserted through a hole in the bearing plate such that the top end of the dowel is inside the bottom part of the girder and the bottom end of the dowel is secured inside the top part of the pile cap. The sole purpose of the bearing/dowel assembly for the girder is to facilitate the girder movement during thermal expansion and contraction.



Figure 27. A typical neoprene bridge bearing (Photo credit: The MDOT Bridge Division)

Table 5 presents calculated factor of safety or FS values for given lateral extents of the floodwater flow.

Table 5. Calculated FS for different floodwater lateral extents

Lateral Extent of Floodwater in Flow Direction (ft)	Scenario 1	Scenario 1 FS	Scenario 2 FS
	FS	(top of girder)	(top of deck slab)
	<i>Single Girder</i>	<i>Entire Superstructure</i>	
1	<u>0.90</u>	4.55	2.23
5	< 0.90	2.92	1.72
10	< 0.90	2.02	1.34
20	< 0.90	1.25	<u>0.93</u>
30	< 0.90	<u>0.90</u>	< 0.93
Critical Lateral Extent	1 ft	20 ft	10 ft

It is shown that 1ft of floodwater is enough to overturn a single girder. When the lateral extent of floodwater is 20ft, the FS of the entire superstructure is 1.25, which is less than the commonly used FS criterion of 1.50.

When the floodwater is on the top of the slab, the superstructure FS is 1.34 at 10 ft of floodwater at which it fails ( $FS < 1.50$ ). The critical lateral extent of floodwater flow for each case is summarized at the bottom of Table 4.

Neoprene bearings between girders and pile caps are provided to accommodate movement of girders due to daily and seasonal temperature changes. As explained earlier, they are held in a desired location by a small steel rod embedded in girders and pile caps. Their purpose is to ensure that the neoprene bearings stay in place. Any movement of the girder (above the pile cap) will destabilize and potentially rupture the bearings. Consequently, they will fail to function properly and allow for the temperature-related movement. Depending on the contact pressure and the type of the neoprene bearing, it would be reasonable to assume a coefficient of friction of 0.1 or less (AASHTO 2012). On the other hand, concrete-to-concrete coefficient of friction is between 0.6 and 1.0 (ACI 2008). When bearings fail, the stress in girders will also increase and the temperature-related girder movement would be restrained due to bearing failure.

Unit weight of floodwater is expected to be more than fresh water due to the suspended soil and debris it carries. Stones, wood, debris etc. will, depending on their masses/dimensions, have additional impact force that will act as a concentrated load on some of the bridge elements. This aspect and hydrodynamic forces acting on the bridge pile caps and superstructure are not considered in the preceding analysis.

### **Summary of Superstructure Structural Integrity Evaluation Results and Discussion**

This study analyzed factors of safety related to bridge superstructure for several different floodwater inundation scenarios based on numerical simulations. Principal findings are as follows:

- Single girder fails when subjected to 1ft of lateral floodwater flow.
- Entire bridge superstructure fails when there is less than 20 ft of lateral floodwater flow. Considering a critical factor of safety of 1.5, the structural integrity of the bridge superstructure is marginal when there is 10 ft of lateral floodwater flow.
- Bridge bearings will fail to perform their function of allowing intended movement of girders for daily and seasonal temperature changes.
- Due to the possible failure of bearings, the girders may misalign, damage the pile cap, overturn the entire superstructure, and eventually crack and fail.

These 2D flood simulations can be used to calculate hydrodynamic forces for assessing future structural integrity of levees and bridges. The current models of hydrodynamic force calculation require expected velocity, which is difficult to obtain (FEMA 2011). As shown in this study that floodwater velocity is possible to get from 2D simulations.

### Three Dimensional Visualization of Infrastructure

It will be a powerful visualization of the impact of floodwater on infrastructure if the flood simulation output of flood inundation and maximum flood depth can be superposed on three dimensional (3D) representation of infrastructure. The 3D visualization of infrastructure assets on a known terrain model can be created using an overlapping set of aerial imagery and/or multispectral satellite imagery. A preliminary 3D feature extraction was conducted by the project collaborator IAVO using overlapping aerial imagery sets and the GeoSphere®/Geogenesis®/FeatureXTract™ software packages (IAVO 2014). The final product was included in a KMZ file that can be loaded into Google Earth to see the models as places on the earth. Unfortunately, no commercially imagery was found for Sardis site. Figure 28 shows the imagery set for a site with two bridges and several buildings. The 3D views of extracted features are shown in Figure 29.

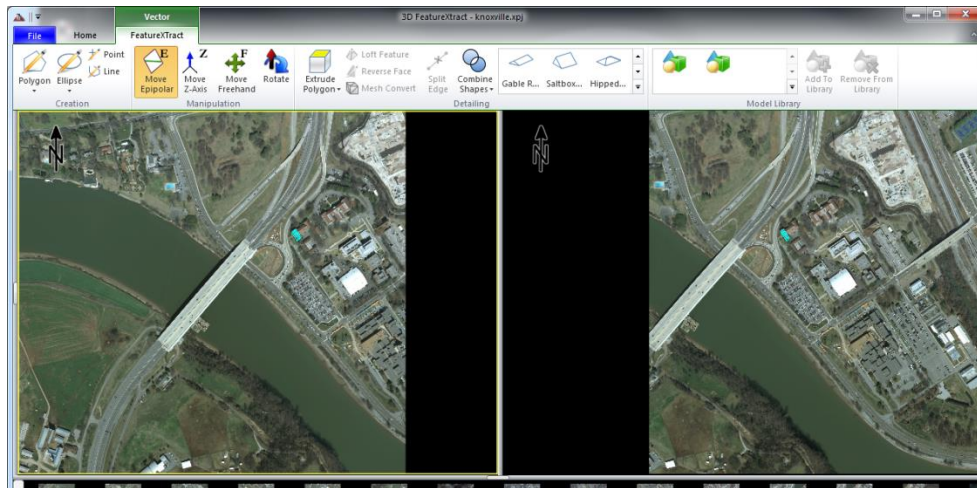


Figure 28. IAVO's Imagery for a site on Tennessee River, Knoxville

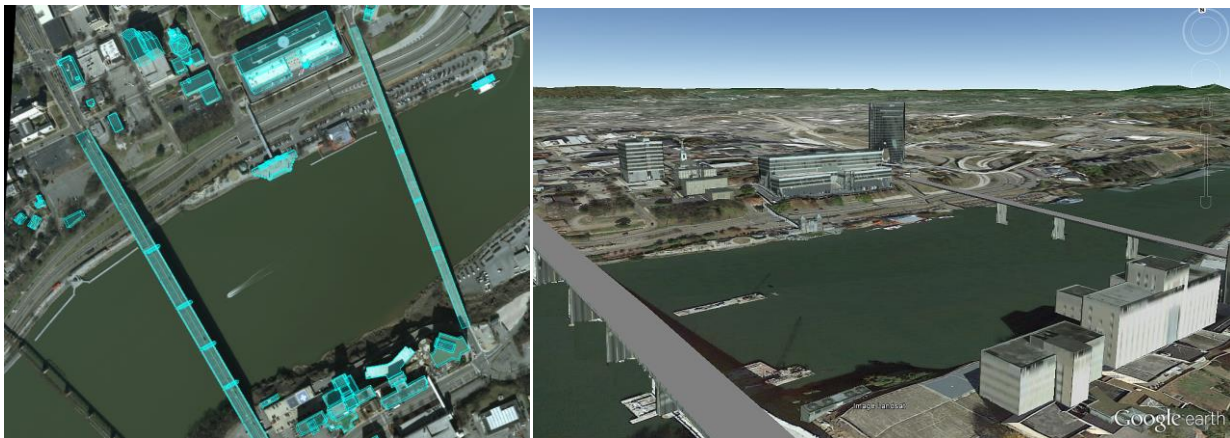


Figure 29. Geosphere/Geogenesis 3D Feature Extraction for (credit: IAVO)

## 4. IMPLEMENTATION OF RESEARCH RESULTS

### 4.1 Summary Results

The overall goal of this study was to identify infrastructure vulnerability to flood hazard risks and catastrophic failures so that preventive steps can be planned to protect transportation infrastructure assets and communities. This report describes flood risk mapping, flood impact simulations on roads and bridge structures, and geospatial methodologies to visualize the potential disaster risk vulnerabilities. This technology can be used to enhance critical transportation infrastructure protection from extreme weather events and natural disasters such as floods.

#### Extreme Flood Simulation Results and Impacts on Infrastructure

A flood inundation simulation was performed for the Sardis pilot study area and results were presented in terms of flood propagation, flood inundation depth, floodwater velocity and flood arrival time. Flood inundation simulation results showed that a total area of 31 mi<sup>2</sup> (80 km<sup>2</sup>) was inundated, where floodwater depth at infrastructure locations reached up to 39 ft (12 m) above the ground level and 13–16 ft (4 – 4.9 m) over the top of the two major highways and rail infrastructure bridges.

There were a total of 24 bridges and four buildings that were affected by the simulated flood inundation. Selected transportation assets were completely inundated with standing floodwater up to 36 ft (10.97 m) above the feature. Further analysis showed that 2.6 miles of I-55, 4.9 miles of Rail, 2.9 miles of US-51, 10.6 miles of Highway 35 and 3.3 miles of Highway 315 were inundated by the simulated flood. The floodwater overflowed as much as 13–16 ft (4–5 m) above major roads and airfields.

The flood simulation with the 3m DEM floodwater flowed 3 m above the I-55 highway. The local scour around the 10 ft-diameter bridge piers in the main channel is estimated as 17.30 ft (5.3 m). Similar results are obtained for the piers of the rail bridge. Unless the pier foundations are sufficiently deep and/or appropriate local scour prevention measures are taken, the bridge may be at risk due to excessive scour.

Furthermore, the flood inundation simulation based on 10 m cell size showed floodwater overflowing 12.6 ft (3.83 m) above the bridge deck on I-55. This floodwater will be flowing beneath the bridge deck with uplift force, pushing laterally in the direction of flow, and overflowing.

Given that the bridge structures are traditionally not designed for lateral floodwater loading, structural integrity assessment of bridges as well as embankments during a flooding event

becomes crucial. This study shows how flood risk mapping and geospatial analysis can be used for vulnerability assessment of critical transportation infrastructure.

## Results of Bridge Structural Integrity Assessment

Currently, there is no comprehensive approach for structural integrity assessment of bridge structures subjected to lateral floodwater forces. Reference points on the bridge cross-sections for overturning moments (at the center of mass) are not correctly positioned (they are positioned at the center of mass), or otherwise it has been assumed that the bridge superstructure is fixed to the substructure, which is often not the case. Furthermore, no results were reported for assessing the structural integrity of bridge structures, and impacts of inland floodwater forces on bridge structures have not been investigated. The project showed a practical approach to analyze the force of lateral floodwater flow for assessing the structural integrity of bridges.

A detailed structural integrity analysis of the US-51 bridge model considered the overturning floodwater moment from lateral floodwater forces and the corresponding moment of resistance by the concrete girders. The most critical condition is when the floodwater level at the top of the concrete girder and the factor of safety approaches 1.0, which is observed for bridge destruction cases during high floodwater levels in both 2005 Katrina and 2011 Irene hurricane disasters.

### 4.2 Sustainable Bridge Management System

Apart from the percentage of structurally deficient bridges (24.2%) in the United States, it is likely that most of the bridges across rivers and streams in the U.S. are vulnerable to being washed away and/or overturning should an extreme flood disaster occur. Once flood risk is incorporated into the existing bridge management system (BMS) practice in the U.S., this will help towards a more sustainable BMS for future implementation. Then, such vulnerable bridges can be prioritized for mitigation and maintenance.

Based on the literature review, “vertical underclearance” data under river-crossing bridges are not a part of the NBIS. Even though the NBIS appears to consider flooding risk, current state-of-practice of bridge management systems do not include vertical underclearance as part of their priority optimization criteria.

The project results show that bridges over rivers and stream have a high risk of failure. The decks on these bridges have the potential to wash away if the expected level of floodwater flow above the channel bed reaches the top of the girders and destabilizes the girder-bearing areas. This important finding of optimum clearance of bridge superstructure above the channel bed is recommended to implement in state bridge management systems for flagging such vulnerable bridges and prioritizing for mitigation.

### **4.3 Overall Benefit to Transportation Infrastructure and Society**

Floods are the most common and damaging among all weather related natural disasters. Billions of dollars in repair and replacement costs of transportation assets were needed after the disasters of 2005 Hurricane Katrina and 2012 Hurricane Sandy. Washing away of bridges and highway segments disrupt public mobility, freight traffic and supply chain, emergency management, and even disaster evacuation routes. Each year millions of dollars are devoted to emergency funds and mitigation of damaged transportation infrastructure. Additionally, disruptions in transportation services lead to huge economic losses. Higher frequency and ferocity of rainfall and coastal hurricanes due to climate change impacts have increased the risk of flood hazards.

As demonstrated in this project, extreme flood simulation and evaluation of structural integrity of bridge structures during a flooding event help to understand the possible catastrophic failures of bridges and road segments. Based on the flood simulation results mitigation alternatives such as strengthening of levees and bridges for protection from flood disasters are important treatments for reducing damage to the infrastructure and economic losses. Additionally, vulnerable areas in the flood plains that can affect surface transportation corridors can be identified and steps taken to enhance infrastructure resilience to flood hazards.

When implemented, a geospatial decision support system approach will help to prioritize critical lifeline transportation infrastructure most vulnerable to extreme flood hazards, take safeguard measures, enhance disaster resilience, and save billions of dollars in cost avoidance of infrastructure destruction and reconstruction. This approach will improve efficiency of emergency management operations and save communities from flood disaster related damage and displacement from their homes.

### **4.4 Recommendations and Future Work**

Spaceborne and airborne remote sensing data and geospatial technologies are available for worldwide coverage at affordable prices for managing built infrastructure assets and implementing decision support systems for disaster resilience management. These geospatial technologies and flood simulations are imperative for impact assessment of extreme floods, mitigation, infrastructure protection and disaster resilience management. In view of increased frequency of worldwide extreme weather related flood occurrences, it is recommended to use these tools, as demonstrated in the project, for flood risk mapping and assessing infrastructure vulnerability to extreme flood events.

A follow up project for developing a geospatial decision support system is also recommended, in cooperation with a state transportation agency, to enhance state bridge management system for identifying vulnerable bridges over streams and rivers and implementing mitigation treatments.

## 5. REFERENCES

AASHTO. (2012). LFRD Bridge Design Specifications, American Association of State Highway and Transportation Officials (AASHTO), Washington DC.

ACI. (2008). Building Code Requirements for Structural Concrete (ACI 318-08) and Commentary. American Concrete Institute (ACI), Michigan, 2008.

Altinakar, M.S., E.E. Matheu, M. McGrath. (2009). New Generation Modeling and Decision Support Tools for Studying Impacts of Dam Failures, Proceedings, ASDSO Dam Safety 2009 Annual Conference, September 27 – October 1, 2009, Hollywood, FL.

Altinakar, M.S., Marcus McGrath, and Vijay Ramalingam, (2015a). 2D Numerical Simulation of a Hypothetical Flood Downstream of Sardis Dam. NCITEC Project: 1202 - 25 Report, Document No. 2014-02, UM-NCICHE, The National Center for Computational Hydroscience and Engineering, The University of Mississippi, January 2015.

Altinakar, M. S., M. McGrath, V. P. Ramalingam, and W. Uddin. (2015b). Two-Dimensional Flood Modeling for the Assessment of Impacts on Critical Infrastructures. University Transportation Center (UTC) Conference for the Southeastern Region, University of Alabama at Birmingham. Birmingham, Alabama, March 26-27, 2015. (presented by Altinakar and Uddin, regional UTC conference)

CAIT. (2014). Center for Advanced Infrastructure Technology, The University of Mississippi, <http://www.olemiss.edu/projects/cait>, Accessed May 10, 2014.

Cook, A.C. (2009). Comparison of One-Dimensional HEC-RAS with Two-Dimensional FESWMS Model in Flood Inundation Mapping, M.S. Thesis, Purdue University, May 2008, [http://web.ics.purdue.edu/~vmervade/reports/2008\\_02.pdf](http://web.ics.purdue.edu/~vmervade/reports/2008_02.pdf), Accessed October 3, 2014.

Durmus, A. Geospatial Assessment of Sustainable Built Infrastructure Assets and Flood Disaster Protection. M.S. Thesis, University of Mississippi, August 2012.

Durmus, A., Q. Nguyen, M. Z. McGrath, M. S. Altinakar, W. Uddin. (2015). Numerical Modeling and Simulation of Extreme Flood Inundation to Assess Vulnerability of Transportation Infrastructure Assets. TRB 94<sup>th</sup> Annual Meeting, The National Academies, Washington DC. Online Proceedings, January 10-14, 2015. (published and presented by Uddin, international conference)

EA. (2009). Desktop Review of 2D Hydraulic Modelling Packages, Science Report: SC080035, Environment Agency, UK. [https://www.gov.uk/government/uploads/system/uploads/attachment\\_data/file/290901/scho0709bqse-e-e.pdf](https://www.gov.uk/government/uploads/system/uploads/attachment_data/file/290901/scho0709bqse-e-e.pdf), Accessed October 3, 2014.

EM-DAT. (2012). The OFDA/CRED International Disaster Database. Université Catholique de Louvain, Brussels, Belgium, 2012. <http://www.emdat.be> Accessed 25 July 2014.

FEMA. (2011). Coastal Construction Manual: Principles and Practices of Planning, Siting, Designing, Constructing, and Maintaining Residential Buildings in Coastal Areas. 4th Ed. FEMA P-55, Volume II. Federal Emergency Management Agency (FEMA). August 2011. [http://www.fema.gov/media-library-data/20130726-1510-20490-1986/fema55\\_volii\\_combined\\_rev.pdf](http://www.fema.gov/media-library-data/20130726-1510-20490-1986/fema55_volii_combined_rev.pdf). Accessed March 2, 2015.

FHWA. (2013). Bridges by State and County, 2013. U.S. Department of Transportation, Federal Highway Administration (FHWA). <http://www.fhwa.dot.gov/bridge/nbi/no10/county13.xlsx>, Accessed May 22, 2014.

GeoSlope. (2012). Download GeoStudio 2012. GeoSlope International, <http://www.geoslope.com/downloads/2012.aspx> Accessed April 4, 2015.

HEC-RAS. (2014). Hydrologic Engineering Center, U.S. Army Corps of Engineers, 2014, <http://www.hec.usace.army.mil/software/hecras/>, Accessed July 25, 2014.

IAVO. (2014). Imagery. IAVO Research and Scientific. <http://www.iavo-rs.com/> Accessed December 15, 2014.

InfrastructureGlobal. (2011). Eastern United States Devastated By Hurricane Irene – No Break from Onslaught of Natural Disasters, 2011, <http://infrastructureglobal.com/?p=485> Thailand's Post-Flood Seminar: Lessons Learned from 2011 Great Flood Disaster and Future Directions for Flood Prevention, 2011, <http://infrastructureglobal.com/?p=1834>, Accessed July 14, 2014.

Munich Re. (2012). Severe Weather in North America, Munich Re, 2012. <http://www.munichre.com/en/media-relations/publications/press-releases/2012/2012-10-17-press-release/index.html> Accessed April 23, 2015.

NCICHE. (2014). The National Center for Computational Hydroscience and Engineering, The University of Mississippi, <http://www.ncche.olemiss.edu>, Accessed July 23, 2014.

NOAA. (2010). Billion Dollar U.S. Weather Disasters. National Oceanic and Atmospheric Administration (NOAA) Satellite and Information Service, 2010. <http://www.ncdc.noaa.gov/>

oa/reports/billionz.html Accessed 10 June 2012.

NOAA. (2015). Billion Dollars Weather Disasters: Table of Events. 2005-2014. National Oceanic and Atmospheric Administration, 2015. <http://www.ncdc.noaa.gov/billions/events> Accessed June 1, 2015.

PCI. (2013). Precast Prestressed Concrete Bridge Design Manual. Precast/Prestressed Concrete Institute (PCI), Second Edition, Chicago, Illinois, 2003.

Richardson, E.V., L.J. Harrison, J.R. Richardson, and S.R. Davis. (1993). Evaluating scour at bridges (2nd ed.). U.S. Department of Transportation Hydraulic Engineering Circular 18, 132 p.

Singh, J. M.S. Altinakar, Y. Ding. (2011). Two-dimensional Numerical Modeling of Dam-break Flows Over Natural Terrain Using a Central Explicit Scheme, *Advances in Water Resources*, Vol. 34, No. 10, 2011, pp. 1366–1375.

Uddin, W., M. S. Altinakar, and A. Durmus. (2015). Extreme flood simulations to assess inundation impacts and structural integrity of transportation infrastructure assets. *International Journal of Critical Infrastructure Protection*, April, 2015. (submitted for publication review and presented by Uddin at The TISP 2015 Critical Infrastructure Symposium, Baltimore, Maryland, 20-22 April 2015, national conference)

USGS. (2014). Accuracy Assessment of the U.S. Geological Survey National Elevation Dataset, and Comparison with Other Large-Area Elevation Datasets – SRTM and ASTER, U.S. Department of Interior, U.S. Geological Survey, Open-File Report 2014-1008, 2014.

Weiss, D. J., and S. Manning. Extreme Weather, Extreme Damage. Center for American Progress, 2013. <http://www.americanprogress.org/issues/green/news/2014/03/27/86532/2013-extreme-weather-extreme-damage> Accessed 10 May 2014.

White House. (2014). Fact Sheet: The President’s Climate Data Initiative: Empowering America’s Communities to Prepare for the Effects of Climate Change, 2014, <http://www.whitehouse.gov/the-press-office/2014/03/19/fact-sheet-president-s-climate-data-initiative-empowering-america-s-comm>, Accessed March 28, 2014.

Xanthakos, P.P. (1994). *Theory and Design of Bridges*. John Wiley & Sons, Inc., New York, 1994.

# **APPENDIX**

**Project 2012-25 Progress Report**

**NCCHE Final Project Report**

# **Program Progress Performance Report for University Transportation Centers**

**Federal Agency and Organization Element to Which Report is Submitted:**

U.S. Department of Transportation  
Research and Innovative Technology Administration

**Federal Grant or Other Identifying Number Assigned by Agency:** DTRT12-G-UTC14

## **Progress Report for the National Center for Intermodal Transportation for Economic Competitiveness**

**Project Title:**

Disaster Protection of Transport Infrastructure and Mobility Using Flood Risk Modeling and Geospatial  
Visualization

Project Number: 2012 – 25

**Principal Investigator (PI) Name, Title and University Contact Information:**

Dr. Waheed Uddin (PI)  
Professor of Civil Engineering and Director, Center for Advanced Infrastructure Technology  
University of Mississippi  
[cvuddin@gmail.com](mailto:cvuddin@gmail.com) [cvuddin@olemiss.edu](mailto:cvuddin@olemiss.edu) (662) 915-5363

**Name of Submitting Official, Title, and Contact Information (e-mail address and phone number), if  
other than PI:** same as PI

**Submission Date:** January 15, 2015

**DUNS and EIN Numbers:** 64-6000819

**Recipient Identifying Number or Account Number, if any:** 363277-061300-021000

**Project Period (Start Date, End Date):** July 1, 2012 - December 31, 2014

**Reporting Period End Date:** December 31, 2014

**Report Term or Frequency:** Semi-annual

---

## 1. Accomplishments

### 1.1. What are the major goals of the project?

#### 1) Goals

Major goals of this project are to develop geospatial visualization models of flood disasters and evaluate their impacts on road infrastructure. Flood disasters cause catastrophic damages to transportation road infrastructure including road pavements and bridges. Washing away of bridges and highway segments disrupt public mobility, freight traffic and supply chain, emergency management, and even disaster evacuation routes. Each year millions of dollars are devoted to emergency funds and mitigation of damaged transport infrastructure. This project addresses the NCITEC theme of *efficient, safe, secure, and sustainable national intermodal transportation network* that can be made *resilient to disasters*.

#### 2) Specific objectives

The specific objective is to identify and implement computational and geospatial visualization technologies to enhance decision support systems for transport infrastructure *protection from extreme weather related natural disasters* such as floods.

The project objective is accomplished by using airborne and spaceborne remote sensing and geospatial technologies for modeling and visualization of terrain and built environment, adapting computational modeling and simulation of flood scenarios, flood risk mapping on regional and local levels, and simulating extreme events for estimating flood disaster impacts on transport infrastructure network assets.

#### 3) Project timeline

The timeline and project activity schedule were updated in view of one year extension to December 31, 2014. Figure 1 shows the planned activities and time line, as well as actual completion dates. There are no significant changes in research approach or methods described in the approved plan.

#### 4) Significant results

- Key outcomes or other achievements.
  1. This project developed a geospatial decision support system for flood risk assessment and protection of infrastructure including roads and bridges. The methodology was implemented for a pilot case study.
  2. Computer simulations for flood risk mapping and vulnerability assessment of highway and bridge assets were evaluated. The pilot case study shows the importance of this approach disaster resilience for saving lives and billions of dollars in flood damages that can be avoided.
  3. The developed approach is able to assess flood related vulnerabilities of traditional urbanization processes and infrastructure systems, which create negative impacts on the environment and the natural cycle of the ecosystem.
  4. Training of UG and graduate students for geospatial workforce development and enhancing infrastructure asset management are additional benefits.

During this reporting period Tasks 1,2, 3, 4, 5, 6, 7, 8, and 9 were continued related to recruiting staff, reviewing literature, collecting spatial data and information about pilot study site and other selected sites, preparing initial computer simulation of flood modeling, installing 3D geospatial visualization software, making external contacts for collaborations, and completing reports.

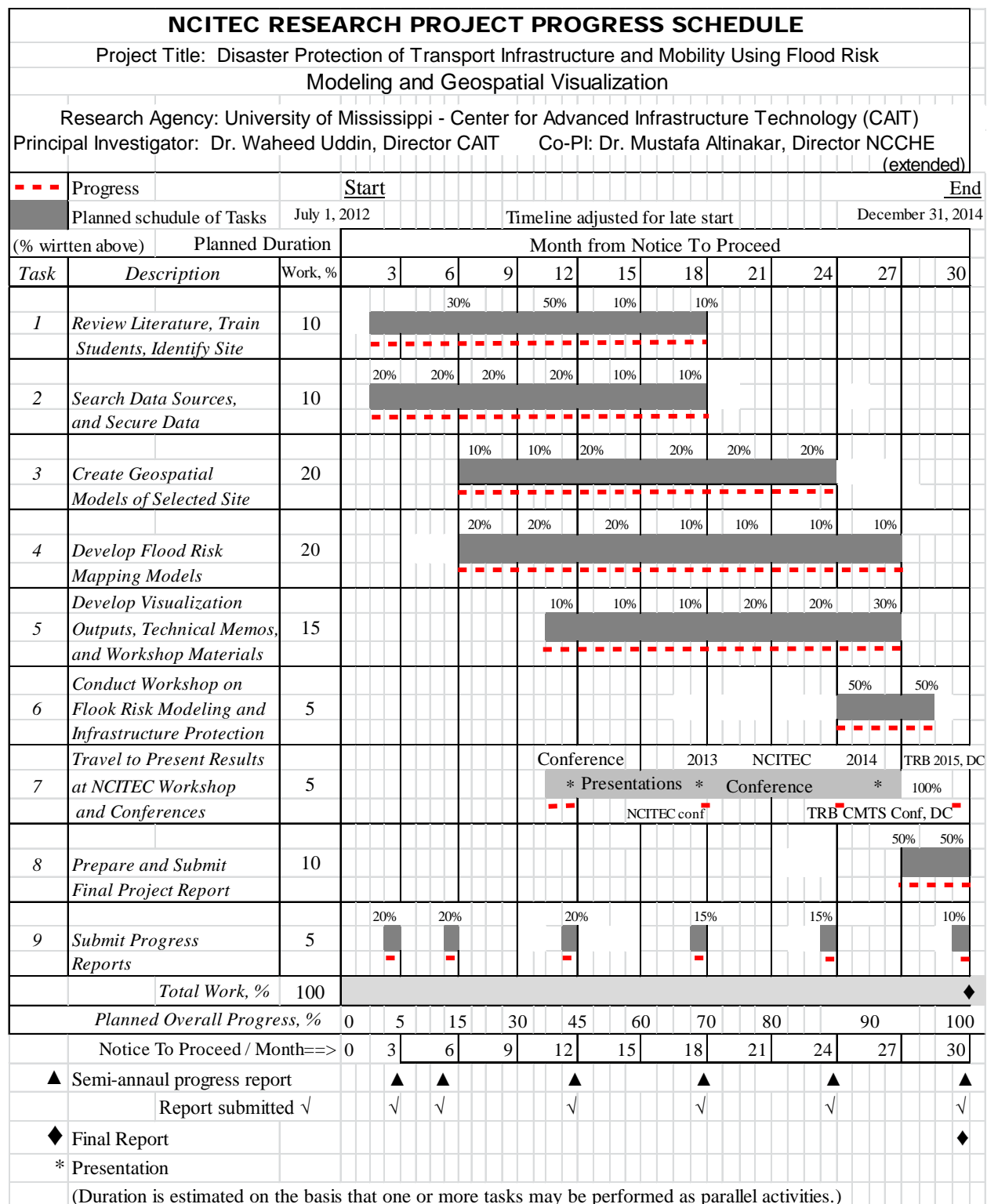


Figure 1. Research project tasks and timeline (planned and percent completion during the report period)

---

## 1.2. What was accomplished under these goals?

- The National Center for Computational Hydroscience and Engineering (NCCHE) completed its computer simulation tasks using one PhD student for flood simulation tasks and other assigned research staff on the project.
- Center for Advanced Infrastructure Technology (CAIT) recruited a new PhD student Alper Durmus in Spring 2014 who worked throughout 2014 taking the lead on the project to analyze flood simulation data and planimetrics of infrastructure features at the pilot flood simulation site. Additionally, a self-funded PhD student Quang Nguyen (with financial support of the country of origin Vietnam) assisted in during 2014 for computer modeling and geospatial visualization of infrastructure assets. The researchers were assisted by UG student workers. All work was conducted in the CAIT Transportation Modeling and Visualization Lab at the off-campus location of the Ole Miss Jackson Avenue Center (JAC).
- The CAIT project team completed literature review on flood simulation and geospatial visualization of built infrastructure including a previous CAIT graduate research project on flood inundation mapping conducted under Dr. Uddin's supervision in 2012. Alper Durmus has been the lead PhD student on this project with assistance in geographical information system (GIS) tasks and related contributions by PhD student Quang Nguyen.
- The PI, co-PI, and NCCHE flood simulation staff (post-doc research scientists and new graduate student) are using Sardis site for primary simulation and analysis. This is one of the identified four candidate sites in northern Mississippi where floods may occur due to levee breaches. The four sites are located in Panola, Lafayette, Greenville, and Tunica counties. The Sardis-Batesville area is the pilot study site in northwestern Mississippi
- The Co-PI and assigned key NCCHE staff members completed following the literature, evaluating NCCHE's two dimensional (2D) flood simulation computer model, and improving the computational models using selected topographic data and computational domains.
- The PI and co-PI directed their project staff to use publicly available high resolution georeferenced imagery and digital elevation model (DEM) data for the pilot site from MARIS, which are required for flood simulation. Figure 2 illustrates the research approach and workflow.
- Traditional one-dimensional (1-D) models are inadequate and do not handle mixed flow regimes. In this study, a 2-D numerical flood modeling software CCHE2D-FLOOD is implemented by the NCCHE in its DSS-WISE software package. The CCHE2D-FLOOD modeling software has following features:
  - Uses finite volume discretization and shock capturing scheme to solve conservative form of full dynamic 2-D shallow water flow equations.
  - Based on multi-core, multi-threaded parallel programming to increase speed.
  - Handles mixed flow regimes, disconnected flow domain, and wetting and drying.
  - Generates spatial maps of flood depth, flood arrival time, and flow velocity vectors.
  - Captures shocks, handles mixed flow regimes and wetting and drying. Also, handles discontinuous flow domains.
- The digital elevation model (DEM) data at 5 ft resolution and aerial imagery for the pilot site were secured from Mississippi Automated Resource Information System (MARIS) by NCCHE researchers for implementation of research methodologies by NCCHE and CAIT researchers and students. Dr. Uddin contacted both Mississippi DOT IT section (Mike Cresap) and MARIS (Steve Walker) to access 2 ft resolution aerial imagery and 5 ft DEM data for the Sardis site. The georeferenced imagery data was used by the CAIT researchers to extract built infrastructure features by creating geospatial planimetrics of all major transportation infrastructure and some

---

building features. Dr. Uddin led the planimetrics effort to extract features of the built infrastructure at the Sardis pilot site using GeoMediaPro geospatial software in CAIT Transportation Modeling and Visualization Lab.

- The site planimetrics included centerline (CL) of the river, cross section lines perpendicular to the CL, major highways and rail, airport, and selected buildings, which were created during Fall 2013 using 2 ft high resolution aerial imagery acquired through cooperation of Mississippi DOT and MARIS.
- The Sardis site features I-55, US51, a rail bridge, a small airport, churches, local roads, and low density residential areas. Figures 3 and 4 show planimetric results of extracted features and river CL feature, as well as cross sections for computational outputs.
- Dr. Altinakar led the flood simulation effort of NCCHE staff for the pilot study site. These simulation studies are needed for evaluating infrastructure structural integrity and flood disaster vulnerability. In order to implement the numerical modeling of flood simulation domain, initially a low resolution DEM data of the selected site was used with 30 m computational cell size of the spatial domain.
- The first flood simulation of the pilot site of Sardis-Batesville area for further flood risk mapping was conducted in January 2014 by NCCHE using high resolution ground contour data of the bare ground, 10 m computational cell size and DSS-WISE software (Figure 5).
- Dr. Uddin and dedicated CAIT PhD student processed the 10 m cell flood simulation outputs. The CCHE2D flood simulation module provided two-dimensional raster maps of flood propagation over 48 hours of simulation and data files of flood arrival times, flood depths, and velocities along the river centerline and at given cross section points. Figure 5 shows the flood map.
- Examples of the flood simulation visualization and affected infrastructure features are shown in Figure 6 and embedded table. Several places floodwater is several meters higher than the feature elevation.
- CAIT staff created further planimetrics data sets of selected infrastructure features in the region of interest (ROI) on GIS map. Height of selected infrastructure planimetrics (buildings, airport, major highways and rail, and major highway/rail bridges) above the ground level.
- This dataset was provided to NCCHE in Spring 2014 semester for a follow up second flood simulation considering built infrastructure and using 5 ft DEM of the site, 10 m spatial cell size, and DSS-WISE flood simulation package. Subsequently, Dr. Altinakar led further flood simulations considering smaller spatial cell sizes of 5 m and 3 m to enhance the accuracy of computational results around the 3-D models of key extracted features. Figure 7 compares the DEM used and flood inundation visualization.
- Dr. Uddin contacted the Information division and bridge divisions of the Mississippi DOT to obtain photos of highway bridges at the pilot Sardis site from bridge inventory databases. Dr. Uddin had detailed meetings with the Bridge Engineer to explain the project goals, understand the traditional approach of bridge design for river crossings, learn the role and types of bearings, and obtain design documents of the two major highway bridges on the Sardis site. Figure 8 shows views of major bridges located in the floodplain.
- A workshop was held on December 5, 2014 in NCCHE conference room to present key milestones and key results of the project, "Extreme Flood Inundation Mapping and Risk Modeling of Transportation Infrastructure Assets".
- Next, structural integrity of highway bridges was analyzed for assessing the impacts of floodwater inundation due to the extreme flood event simulation. Figure 9 shows a spatial map of U.S. highway bridge inventory and condition by state. Total 17,038 Bridges are located in Mississippi.

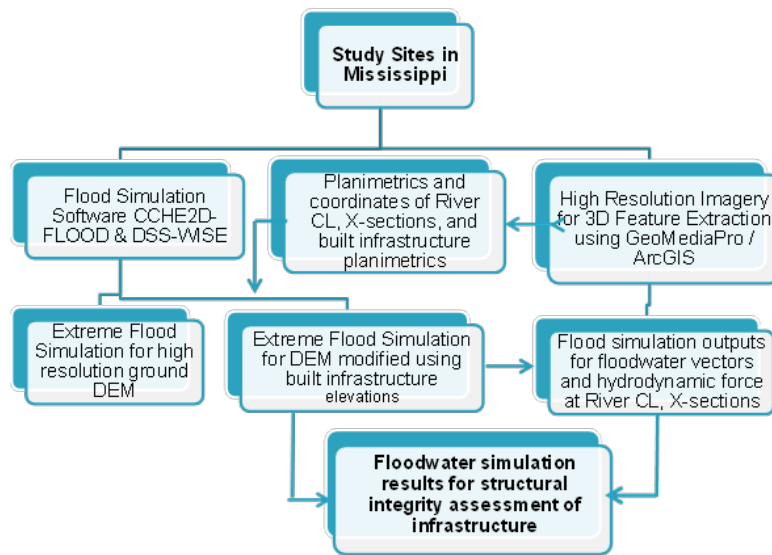


Figure 2. Research workflow chart

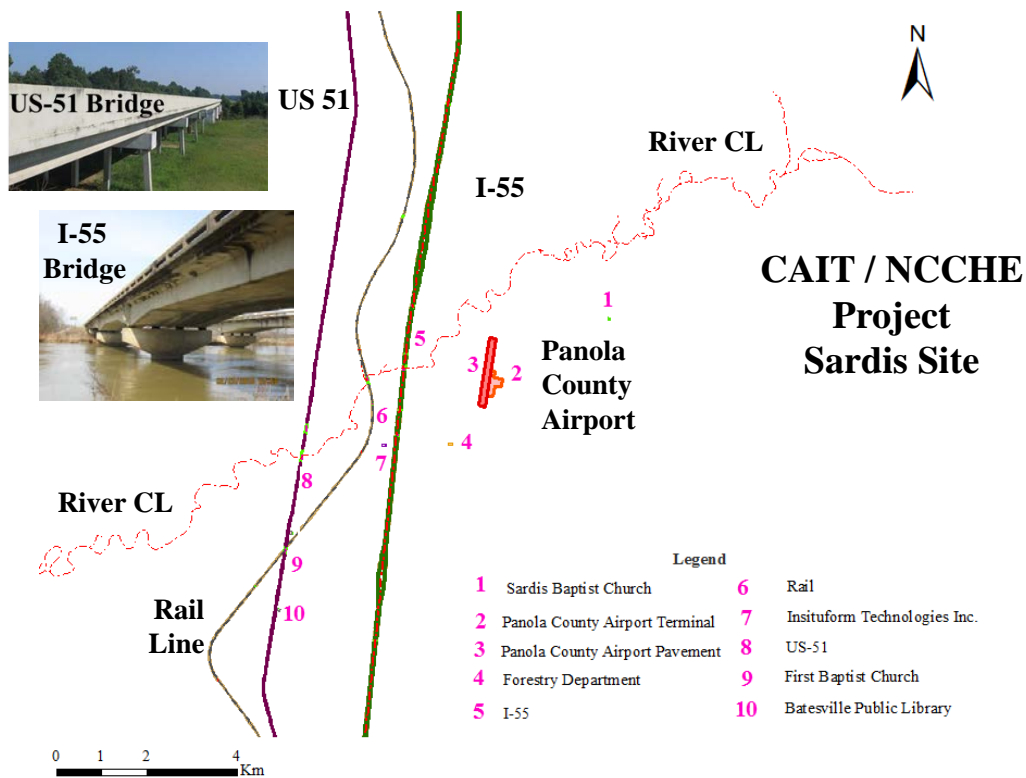


Figure 3. Tallahatchie River CL downstream at Sardis Dam pilot study site and planimetrics visualization of transportation assets (Bridge Photo credit: Mike Cresap of Mississippi DOT)

Sardis River Cross Sections and 2-Ft (60.96 cm) Aerial Imagery (C)

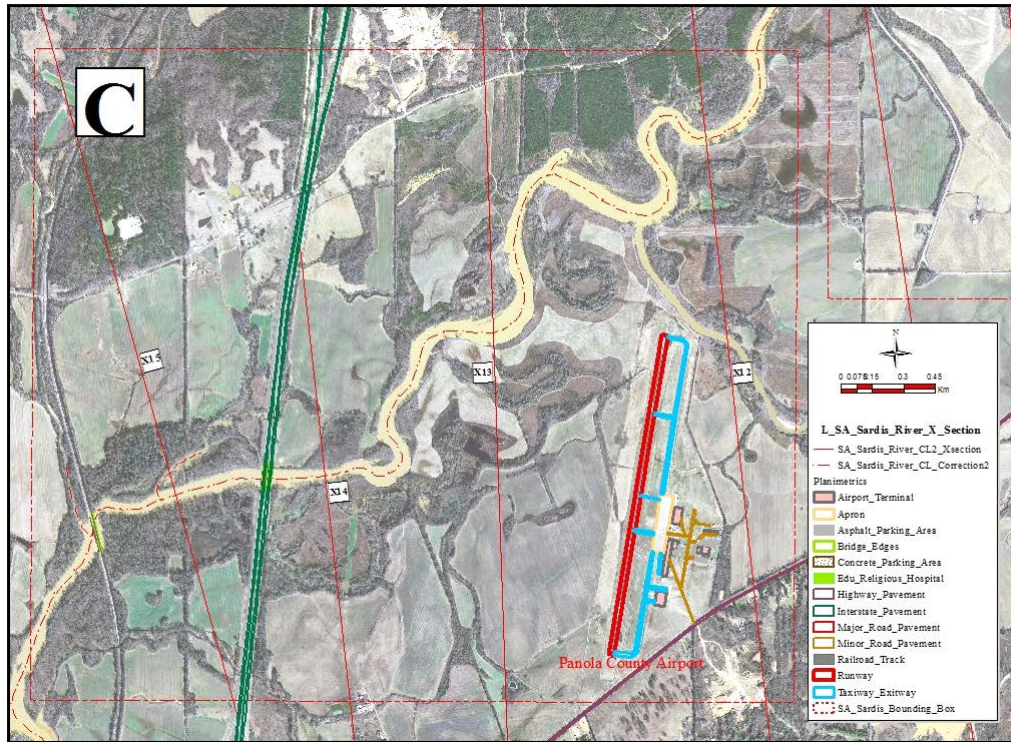


Figure 4. River downstream centerline and cross sections, as well as I-55 and airport features

Flood Simulation 1 (January 2014) and Infrastructure Assets

CAIT / NCCHE  
Project  
Sardis Site  
Flood Inundation Area = 80 sq km

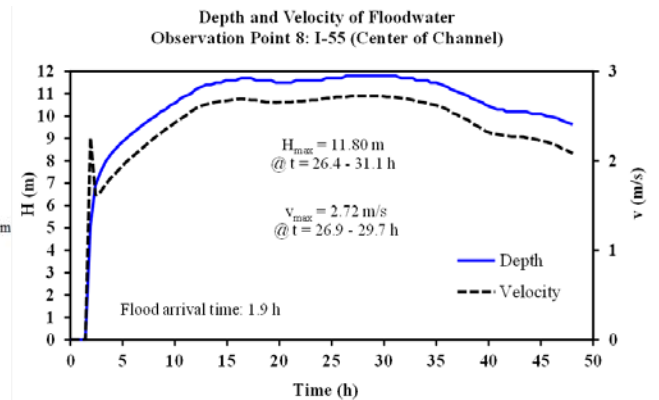
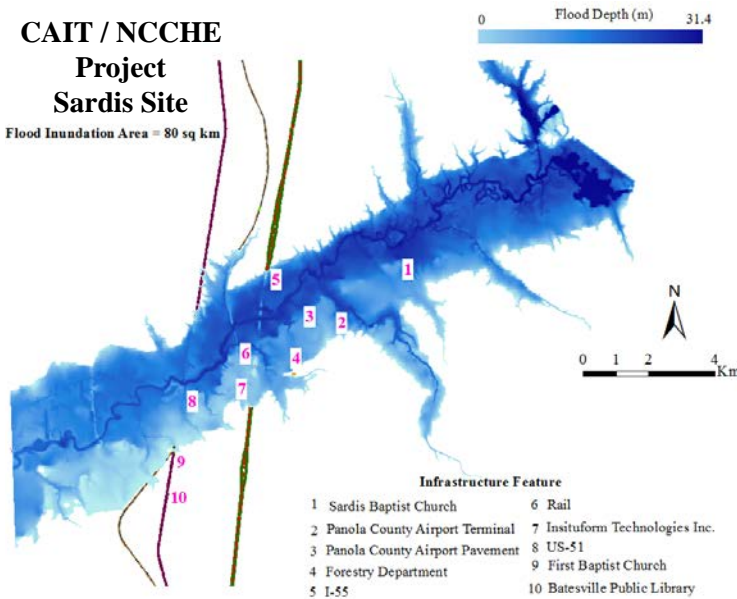
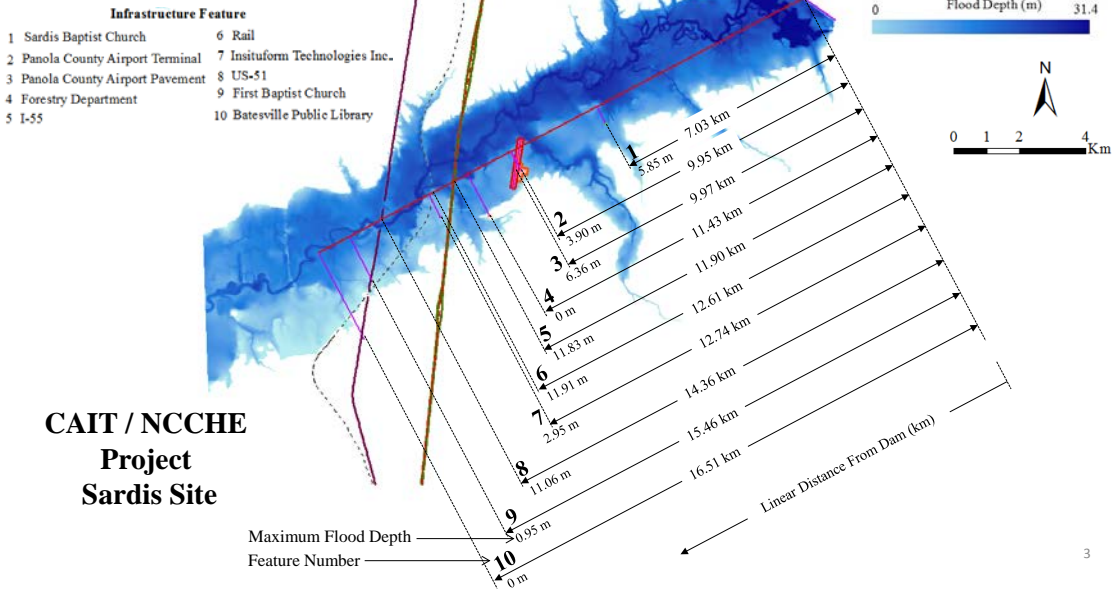


Figure 5. (Left) Flood simulation (20 km long westward and 80 sq km area inundated by simulated flood), (Right) Depth and velocity of flood water at river CL and I-55 bridge

### Infrastructure Feature Descriptions and Locations on Flood Simulation 1 - Inundation Map



Feature	Linear Distance From Start	Maximum Flood Depth	Height of Feature	Flood Depth Above Infrastructure
	(km)	(m)	(m)	(m)
	A	B	C	D = B - C
1. Sardis Lake Baptist Church	7.03	5.85	5.00	0.85
2. Panola County Airport Terminal	9.95	3.90	6.00	(-2.10) Below Infra.
3. Panola County Airport Pavement	9.97	6.36	1.00	5.36
4. Forestry Department	11.43	0	4.50	(-4.50) Below Infra.
5. I-55	11.90	11.83	8.00	3.83
6. Rail	12.61	11.91	7.00	4.91
7. Insituform Technologies Inc.	12.74	2.95	6.50	(-3.55) Below Infra.
8. US-51	14.36	11.06	7.00	4.06
9. First Baptist Church	15.46	0.95	5.00	(-4.05) Below Infra.
10. Batesville Public Library	16.51	0	3.50	(-3.50) Below Infra.

Figure 6. River downstream centerline and cross sections, transportation features (US 51, Rail, I-55 and airport), visualization of the flood simulation inundation, and flood depth at selected feature locations

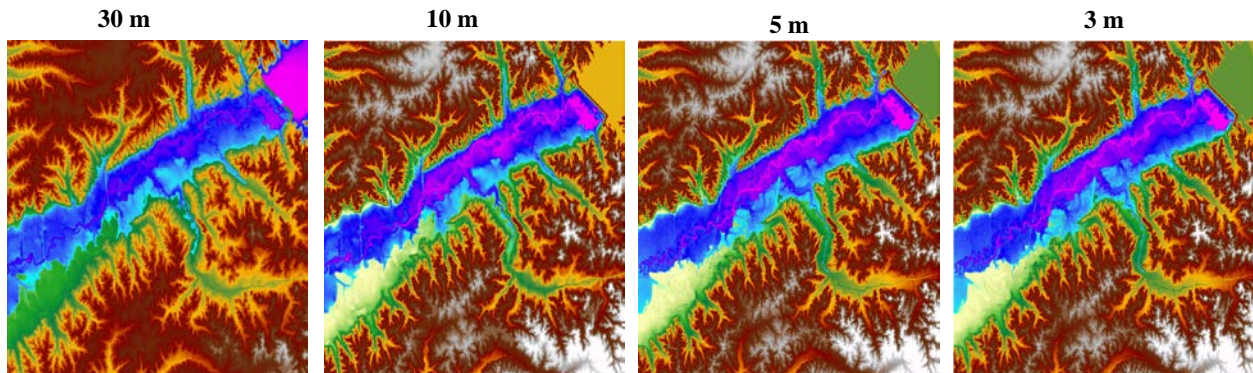


Figure 7. Different Cell Sizes for Computational Modeling, DEM, and Resulting Flood Inundation Results



Figure 8. Photos bridge over Tallahatchie River at pilot study site area: (Left) A view of I-55 bridge and (Right) A view of US-51 bridge (credit: Mississippi DOT Bridge Division)

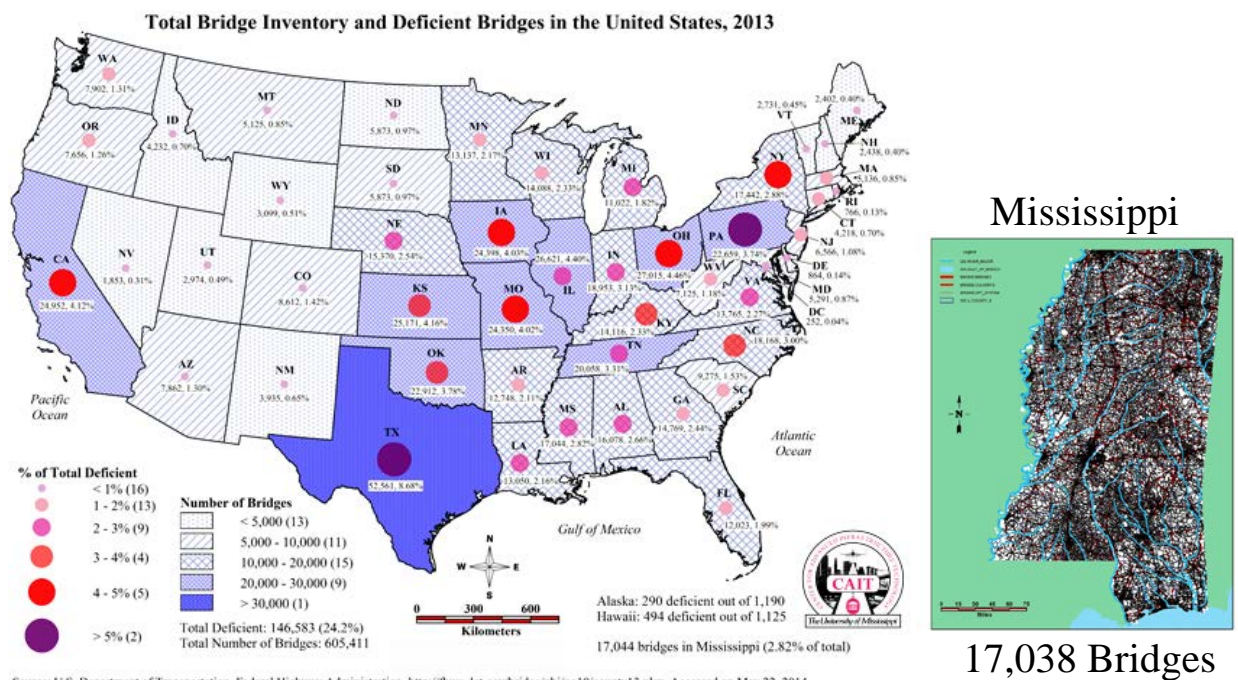


Figure 9. A spatial map of highway bridge inventory and condition by state

- An important component of the research methodology was the extraction of 3-D models of infrastructure features for the study site. This requires special 3-D modeling software and an overlapping set of imagery scenes. An enhanced version of the 3D geospatial feature extraction software GeoGenesis, included in Geospheric and provided by IAVO at no-cost to the project, was installed on seven computers in CAIT Transportation Modeling and Visualization Lab (part of in-kind cost share). Later, IAVO's in-house aerial imagery of the Tennessee River scenes in Knoxville were used to develop 3-D models of two bridges and a few buildings. The final results are shown in GoogleEarth animation (Figure 10).
- Dr. Uddin's efforts showed that no stereo satellite imagery is available in the archived imagery database of commercial satellite imagery providers and the collection of new imagery is cost

---

prohibitive and outside the scope of this small study. The overlapping imagery scenes and DEM are needed for the extraction of 3D features using 3D geospatial software on high performance graphics computers in the CAIT Transportation Modeling and Visualization Lab.

- Dr. Uddin made personal contacts with the Mississippi DOT and Mississippi Automated Resource Information System but could not find any stereo or overlapping aerial imagery set for the Sardis site.
- An alternate approach for creating 3D solid CAD models due to unavailability of stereo imagery for the pilot site is possible by: (1) exporting the planimetrics of selected transportation and building infrastructure assets on the test site to CAD programs, (2) adding elevations in CAD, and (3) exporting and importing back in the geospatial workspace. In the interest of time the heights of all selected features including I-55 highway, US-51 highway, and the rail line were estimated from available highway drawings and field visits. These heights were provided to the NCCHE researchers who made simple 3D solid models for flood simulations using different computational cell sizes (Figure 7).



Figure 10. A 3-D model of bridges and buildings extracted from overlapping imagery (credit: IAVO)

- The structural analysis, based on flood simulation results, included: estimation of floodwater depth and inundation of infrastructure features, embankment slope stability, scouring damage to bridge piers, and structural vulnerability of bridge substructure and superstructure. Key results follow:
  - Total area of 31 sq miles (80 km<sup>2</sup>) was inundated that included: 2.6 miles of I-55, 4.9 miles of freight rail line, 2.9 miles of US-51, 10.6 miles Highway 35 and 3.3 miles of Highway 315, 24 bridges, airfield, and many buildings. The floodwater overflowed as much as 10–16 ft (3–5 m) above major highways, rail, and airfield.
  - The flood simulation with the 3 m DEM shows floodwater flow 3 m above the I-55 highway. The local scour of 17.30 ft is estimated around the 10 ft-diameter I-55 bridge piers in the main river channel. Unless the pier foundations are sufficiently deep and/or

- 
- appropriate local scour prevention measures are taken, the bridge may be at risk due to excessive scour.
- A detailed structural integrity analysis of US-51 highway concrete bridge model considered the overturning floodwater moment from horizontal floodwater forces and the corresponding moment of resistance by the concrete girders. The results show the most critical condition when the Factor of Safety (FS) approaches about 1.0 for the floodwater level at the top of the concrete girders. This indicates the vulnerability of all those bridges on rivers/stream, which do not have adequate height above the channel and maximum floodwater level. This is a useful criterion to identify vulnerable bridges in the inventory of any transportation agency.
- The project has been an important milestone towards flood risk mapping and improving disaster resilience of critical infrastructure assets considering the following summary of the damage and economic loss due to extreme flood events:
    - About 60% of all disasters costing one billion dollars or more in the United States were related to weather.
    - Extreme weather events are occurring at an increasing frequency as experienced by devastating floods in recent years on the East Coast and Gulf Coast.
    - Extreme weather events caused \$208 billion of economic cost in the United States with more than 1,200 lives lost between 2011 and 2013.
    - 2005 Hurricane Katrina disaster on Louisiana and Mississippi Gulf Coast resulted in more than \$100 billion in infrastructure and economic costs.
    - Critical transportation infrastructure assets are under a continuous risk of flood hazards and are subject to significant damage, such as washing away of pavements and bridges.
    - The extreme flood simulations and structural integrity studies carried out in this NCITEC project provide useful criteria to identify vulnerable bridges by using bridge inventory and inspection databases. This is an important step to develop a geospatial decision support system framework for enhancing disaster resilience of lifeline transportation infrastructure assets.
  - This study addressed the National Center for Intermodal Transportation for Economic Competitiveness (NCITEC) theme of efficient, safe, secure, and sustainable national intermodal transportation network being resilient to disasters.
  - The products of this pioneering research project include: (1) flood risk mapping using computational and geospatial tools for flood risk mapping, (2) structural integrity assessment methodologies for pavements and bridges, (3) the framework of a geospatial decision support system to identify vulnerable bridges over rivers and streams based on simple criteria that can be implemented in bridge inspection programs, and (4) guidelines for mitigation of flood damage risks and adaptation of strategies to improve flood disaster resilience of these lifeline infrastructure assets and avoid huge economic losses from catastrophic failures of these assets.

### **1.3. How have the results been disseminated? If so, in what way/s?**

Both Dr. Uddin and Dr. Altinakar were involved in outreach activities associated with the project objectives and results.

- A summary SlideShare presentation, based on key projects results used in the December 2014 workshop presentations and 2015 TRB paper, was posted. <http://slidesha.re/1CiiDnK>

- 
- The NCCHE's extreme flood simulation results for the Sardis site in northwestern Mississippi were used by Dr. Uddin to develop and post the following YouTube video on *infrastructureglobal* channel and embedded on CAIT web page. [http://youtu.be/h\\_FRfj-i8IA](http://youtu.be/h_FRfj-i8IA)
  - Dr. Altinakar's PhD student Marcus McGrath was announced as 2013 Student of the Year (SOY) awardee. This news was posted on the CAIT/NCITEC web page.
  - On December 22, 2014, the Maine RRAP Team was awarded the Trailblazer Award by the Department of Homeland Security (DHS).

"...in recognition of their exceptional leadership and innovative thinking in performing the first RRAP to focus on the potential impacts of climate change. Their work has significantly furthered national climate change policy objectives as directed by the President and will serve as the model for other communities to better understand the risks and impacts of climate change and how to promote planning and resilience. Their leadership, teamwork, and initiative are a great credit to themselves and the Office of Infrastructure Protection."

NCCHE is part of the Maine RRAP Team and carried out all the storm surge and flood simulations with different climate change and sea-level rise scenarios.

- December 5, 2014 Workshop: "Extreme Flood Inundation Mapping and Risk Modeling of Transportation Infrastructure Assets"  
The workshop was opened to all by email invitations and CAIT web page posting. It was held in NCCHE Conference Room, Brevard 3rd Floor, University of Mississippi Oxford campus. Presentations were made by Dr. Uddin, Dr. Altinakar (jointly with NCCHE researchers Marcus McGrath and Vijay Ramalingam), Alper Durmus, Quang Nguyen, with closing remarks by Dr. Altinakar.
- The UM team's outreach activities and presentations related to the project objectives and expected results are summarized in the following list:
- Dr. Altinakar made several presentations to his flood research funding agencies, visiting delegations, and abroad
  - December 10, 2014: Representatives of MEMA Led by Mr. Billy Patrick visited NCCHE. Results of the levee breach flood simulations in Mississippi Delta were presented and discussed.
  - Drs. Altinakar and Ding participated in the Portland Maine Capstone meeting and presented the results of a study regarding the protection against floods and storm surges under climate change scenarios.
  - September 9, 2014: Dr. Altinakar visited USDA NRCS in Jackson Mississippi to present flood models developed by NCCHE and to discuss their potential applications for the flood impact analyses to be performed by the USDA.
  - DSS-WISE Software used for the NCITEC project is now being employed by several federal agencies and Mississippi state agencies. The agencies that use DSS-WISE include: (a) DHS Dams Sector Branch; (b) USACE HQ; (c) USACE MMC; (d) USACE-ERDC; (e) USACE Vicksburg District; (f) Mississippi Department of Environmental Quality.
  - Dr. Altinakar continued offering presentations and courses in the U.S. and abroad about the current use of DSS-WISE by federal and state agencies.

- 
- Dr. Uddin presented project overview and examples of on-going work to the following international visiting university delegations during their scheduled visits to CAIT Transportation Modeling & Visualization Lab in UM Jackson Ave Center (JAC):
    - October 30, 2014: Visiting attendees of the winter workshop of the Gulf Region Intelligent Transportation Society (GRITS) toured the Lab. The workshop was held at the University of Mississippi Campus in Oxford, Oct 29-30, 2015. Dr. Uddin provided brief overview of the Lab facilities, the NCITEC projects, and history of the Lab evolution in cooperation with the Mississippi DOT Traffic Engineering Division.
    - October 29 - 30, 2014: Acey Roberts, Mississippi DOT ITS Engineer and GRITS President, lectured both days on the video panel wall, which was installed in the CAIT Transportation lab as a part of the establishment of a model ITS Lab. The lab has been given access to real-time video streams from all video surveillance facilities across the state, as well as the four bridges on the Mississippi River bridges. This is a tremendous opportunity for CAIT's graduate students to monitor both highway traffic and barge traffic passing under these bridges and use the data for modeling barge traffic performance.
    - October 3, 2014: Dr. Lucy P. Priddy visited the Lab. She is Research Civil Engineer with the ERDC Airfields and Pavements Branch in Vicksburg, Mississippi. After welcome remarks by Dr. Uddin, Dr. Lucy Priddy talked with the current CAIT students/researchers about job opportunities at ERDC, her PhD research summary, and reflected on her experience during her University of Mississippi years as one of the first UG RAs who worked on CAIT research projects during 1999-2002.
  - October 24-25, 2014: Dr. Uddin teaching and research profile was compiled and presented at the annual banquet on 24th October in Austin, Texas to honor 2014 inductees of the University of Texas CAEE Academy of Distinguished Alumni where he received the award. On 25<sup>th</sup> Oct at the Academy annual meeting on the Austin campus Dr. Uddin briefed the CAEE faculty, fellow attendees, and former professors about his journey of education, teaching, research, service, and current research projects.
  - October 21, 2014: Dr. Uddin attended the annual board meeting as 2014 appointed member and the conference of the Mississippi Transportation Institute (MTI), in Convention Center, Jackson, Mississippi. Briefly met State Senator and Representative speakers, the Mississippi DOT Executive Director, as well as, Chief Engineer, Bridge Engineer, Aviation Engineer, and Research Division engineers.
  - September 14-17, 2014: Dr. Uddin attended the ITS3C regional conference and presented overview of NCITEC projects and Gulf Coast rail study results. The conference was organized by the Gulf Region Intelligent Transportation Society (GRITS), the Intelligent Transportation Society of Florida (ITSFL) and the Intelligent Transportation Society of Georgia (ITSGA). The joint conference was held September 14-17, 2014 at the Arthur R. Outlaw Convention Center in Mobile, Alabama.
  - Dr. Uddin included an overview of NCITEC transportation system and flood disaster risk assessment projects as a part of a new proposal in cooperation with the Quaid-E-Awam University of Engineering, Science and Technology (QUEST), Nawab Shah, Sindh, Pakistan. The proposal was prepared jointly by the two universities to the National Academy of Sciences/USAID and Higher Education Commission (HEC) as a part of the Pakistan-United States
-

---

joint Science and Technology Program. The final proposal was submitted on January 5, 2015. This was possible on the invitation of QUEST who made a memo of understanding with UM.

- Dr. Uddin promoted his 2013 book “Public Infrastructure Asset Management” through blog pages and tweets. The book was published by McGraw-Hill in July 2013. The book includes several new sections on supply chain management, flood disaster impact examples, use of remote sensing imagery and geospatial technologies, asset management practice for transportation and other lifeline public infrastructure, and value engineering applications for investment decision making. The highlights of the book are discussed in the following blog post. <http://infrastructureglobal.com/dr-robert-khayat-ole-miss-chancellor-emeritus-infrastructure-improvement-cannot-be-delayed-if-we-are-to-continue-as-a-vital-nation/>  
See a YouTube video on *InfrastructureGlobal* channel introducing the book (authors: Uddin, Hudson, Haas) and Amazon video. <http://youtu.be/LiHqJlnrFy0>  
<http://amzn.to/1BokzrY>
- Dr. Uddin presented the flood disaster simulation poster and co-chaired aviation workshop 143 at the January 2015 Annual Meeting of the Transportation Research Board (TRB), Washington DC, January 11-14, 2015. The flood paper and two other presentations are included in online TRB 2015 annual meeting proceedings.
- Dr. Uddin prepared and posted slideshare presentations that include project updates on supply chain, flood simulation, Gulf passenger rail restoration, and highway-waterway freight intermodal integration.
- Dr. Uddin has been following marine/waterborne transportation news, supply chain stakeholders, logistics associations, and rail industry on Twitter social media. He used web sharing about the NCITEC projects through YouTube video, SlideShare, and Twitter.
- DropBox folders were created for all 2014 project backups and sharing project related data, geospatial files, electronic data files, and other project documents.
- The NCITEC project tab on the University of Mississippi CAIT web site was updated with UM projects, the 2013 Student of the Year award, supply chain survey form, Gulf Coast Rail white paper, and linked to the MSU web site. <http://www.olemiss.edu/projects/cait/ncitec/>
- Dr. Altinakar and Dr. Uddin submitted abstracts for conference presentations at:
  - 2015 University Transportation Center (UTC) Conference for the Southeastern Region: University of Alabama at Birmingham, March 26-27, Birmingham, Birmingham, Alabama.
  - 2015 Critical Infrastructure Symposium: The Infrastructure Security Partnership (TISP) and the Society of American Military Engineers (SAME), April 20-21, Baltimore, Maryland.
- Dr. Uddin submitted the following abstracts for papers and presentation on NCITEC project related research and spatial mapping outputs:
  - 6th ICONF BMP: 6th International Conference Bituminous Mixtures and Pavements: Aristotle University of Thessaloniki (AUTH), June 10-12, 2015, Thessaloniki, Greece.
  - 2015 International Symposium on Systematic Approaches to Environmental Sustainability in Transportation (ISSAEST): University of Alaska Fairbanks, August 2-5, Fairbanks, Alaska.
  - 2015 IJPC - International Journal of Pavements Conference: September 10-12, Weimar, Germany.

**1.4. What do you plan to do during the next reporting period to accomplish the goals and objectives? <List any summits, webinars, seminars, you will host. Any work you will be doing with local agencies. Education related activities, etc. >**

Table 1 shows effort for each task activity (with assigned research team) that the research team has completed to accomplish the goals and objectives by the termination date of December 31, 2014.

Table 1. Research project tasks completion during the report period and effort planned for the next period

Project Tasks	Completed To Date	Planned for Next Report
<i>Task 1: Review Literature, Train Students for 3D Modeling and Flood Risk Mapping Methodologies, and Identify Sites. (CAIT/NCCHC)</i>	100%	-
<i>Task 2: Search Imagery and LIDAR Data Sources, Contact Potential Agencies, and Secure Data for Selected Sites. (CAIT/NCCHC)</i>	100%	-
<i>Task 3: Create Geospatial Models for Selected Site Using Remote Sensing Data. (CAIT/NCCHC)</i>	100%	-
<i>Task 4: Develop Flood Risk Mapping Models Using Normal and Extreme Flood Scenarios for Selected Site. (NCCHC)</i>	100%	-
<i>Task 5: Develop Visualization Outputs, Technical Memos, and Workshop Presentation Materials. (CAIT/NCCHC)</i>	100%	-
<i>Task 6: Conduct Workshop on "Flood Disaster Risk Modeling and Simulations for Protection of Lifeline Transport Infrastructure." (CAIT/NCCHC)</i>	100%	-
<i>Task 7: Travel to Present Research Results at NCITEC/MSU Workshop and Selected Conferences. (CAIT/NCCHC)</i>	100%	-
<i>Task 8: Prepare and Submit Final Project Report. (CAIT/NCCHC)</i>	100%	-
<i>Task 9: Submit Progress Reports. (CAIT/NCCHC)</i>	100%	-

The project ended on December 31, 2014. The comprehensive final report is completed.

**Outreach activities and papers/presentations planned during the next reporting period:**

The PI and Co-PI are planning to prepare papers and make presentations in coming months.

**2. Products**

**2.1. Publications, conference papers, and presentations:**

The following papers/conference presentations are related to the goals of this project:

Uddin, W. (2014). Chapter 23 "Mobile and Area Sources of Greenhouse Gases and Abatement Strategies," *Handbook of Climate Change Mitigation and Adaptation*, edited by Wei-Yin Chen, John M. Seiner, Toshio Suzuki and Maximilian Lackner, Springer. (Updated Chapter 23 of the 2012 Handbook in December 2014. The reference book will be available in early 2016).  
<http://www.springer.com/energy/renewable+and+green+energy/book/978-3-319-14408-5>

A. K. M. Azad Hossain, Yafei Jia, Xiaobo Chao, Mustafa Altinakar. (2014). Advances in Application of Remote Sensing Techniques to Enhance the Capability of Hydrodynamic Modeling in Estuary. Chapter in *Remote Sensing and Modeling: Advances in Coastal and Marine Resources*, Coastal

- 
- Research Library (CRL) series, vol. 9, First edited by Charles W. Finkl, Christopher Makowski, 06/2014: chapter 12: pages 295-313; Springer International Publishing., ISBN: 9780123847034
- Singh, J., Altinakar, M.S., and Ding, Y. (2014). Numerical Modeling of Rainfall-Generated Overland Flow Using Nonlinear Shallow-Water Equations. *J. Hydrol. Eng.*, 10.1061/(ASCE) HE.1943-5584.0001124 , 04014089.
- Yan Ding, Yaoxin Zhang, Yafei Jia, Afshin Gazerzadeh, Mustafa S. Altinakar. (2014). Simulation and Prediction of Storm Surges and Waves Driven by Hurricanes and Assessment of Coastal Flooding and Inundation. DOI: 10.13140/2.1.5094.8164 Conference: 11th Int. Conf. on Hydro science and Engineering (ICHE-2014), Hamburg, Germany.
- Durmus, A., Nguyen, Q., McGrath, M.Z., Altinakar, M.S., and Uddin, W. (2014). Numerical Modeling and Simulation of Extreme Flood Inundation to Assess Vulnerability of Transportation Infrastructure Assets. Paper No. 15-1606, On-line Proceedings, Paper Presented at the 94th Annual Meeting of The Transportation Research Board, Washington, DC, January 10-15, 2015.
- Uddin, W. (2015). Aircraft Safety on Airfield Pavements with Standing Water and Slush. Workshop 143- Influence of Airfield Surface Irregularity on Aircraft Life, Presented at the 94th Annual Meeting of The Transportation Research Board, Washington, DC, January 10-15, 2015.
- Uddin, W., Cobb, S., Sherry, P. and Eksioğlu, B. (2015). Economically Viable Intermodal Integration of Surface and Waterway Freight Transport for Sustainable Supply Chain. *University Transportation Center (UTC) Conference for the Southeastern Region*, University of Alabama at Birmingham, March 26-27, 2015, Birmingham, Birmingham, Alabama.
- Durmus, A., Nguyen, Q., McGrath, M.Z., Altinakar, M.S., and Uddin, W. (2015). Numerical Modeling And Simulation of Extreme Flood Inundation To Assess Vulnerability of Transportation Infrastructure Assets. *University Transportation Center (UTC) Conference for the Southeastern Region*, University of Alabama at Birmingham, March 26-27, 2015, Birmingham, Birmingham, Alabama.
- Altinakar, M.S., McGrath, M.Z., Ramalingam, V.P., and Uddin, W. (2015). Two-Dimensional Flood Modeling for the Assessment of Impacts on Critical Infrastructures. *University Transportation Center (UTC) Conference for the Southeastern Region*, University of Alabama at Birmingham, March 26-27, 2015, Birmingham, Birmingham, Alabama.
- Uddin, W, Altinakar, M.S. and Durmus, A. (2015). Extreme Flood Simulations to Assess Inundation Impacts and Structural Integrity of Transportation Infrastructure Assets. *The 2015 Critical Infrastructure Symposium*, The Infrastructure Security Partnership (TISP) and the Society of American Military Engineers (SAME), April 20-21, 2015, Baltimore, Maryland.
- Uddin, W. (2015). Appraisal of Mechanistic-Empirical Pavement Design Guide for Highways Being Implemented in United States and Complimentary Needs for Pavement Asset Management. *6th ICONF BMP, 6th International Conference Bituminous Mixtures and Pavements*, Aristotle University of Thessaloniki (AUTH), June 10-12, 2015, Thessaloniki, Greece.
- Uddin, W., McCarty, T., and Sharma, J. (2015). Environmental Sustainability and Energy Considerations for Life-Cycle Analysis of Transportation Infrastructure Systems. *International Symposium on Systematic Approaches to Environmental Sustainability in Transportation (ISSAEST)*, University of Alaska Fairbanks, August 2-5, 2015, Fairbanks, Alaska.
- Uddin, W. and Merighi, João. (2015). Assessing Aircraft Safety on Airfield Pavements in Presence of Longitudinal Roughness, Standing Water, and Slush. *2015 IJPC - International Journal of Pavements Conference*, September 10-12, 2015, Weimar, Germany.

- Dr. Uddin and Dr. Altinakar will jointly submit new papers involving project results to international journals.
- Dr. Uddin will submit the following manuscripts:

- 
- Chapter 77 “Climate Change Adaptation for the Built Environment,” *Handbook of Climate Change Mitigation and Adaptation*, edited by Wei-Yin Chen, John M. Seiner, Toshio Suzuki and Maximilian Lackner, Springer. (The reference book will be available in early 2016).  
<http://www.springer.com/energy/renewable+and+green+energy/book/978-3-319-14408-5>
  - *ISPRS International Journal of Geo-Information* (ISSN 2220-9964 "Efficient Capturing of 3D Objects at a National Level: With a Focus on Buildings and Infrastructure" New Special Issue IJGI).
  - Dr. Uddin is preparing a new book proposal on natural disaster vulnerability assessment and protection of infrastructure from natural disasters. The motivation of this book is largely based on global supply chain disruptions and related adverse economic impacts of 2011 - 2014 worldwide extreme tsunami, hurricane, and flood disasters. The proposal was initially discussed in a meeting with the editor of Taylor and Francis in Washington DC on January 13, 2014. This was further discussed in Washington DC during the TRB Conference on January 12, 2015.

## 2.2. Website(s) or other Internet site(s): <Any new ones?>

UM CAIT web page: <http://www.olemiss.edu/projects/cait/ncitec/>

The NCITEC project tab on CAIT web site, linked to the University of Mississippi web site, provides useful background of NCITEC goals and university partners.

Blog: <http://infrastructureglobal.com/>

*InfrastructureGlobal* is a blog about infrastructure and natural disasters around the globe. Dr. Uddin created this blog site after the devastating floods of Mississippi River basin in May 2011. Several posts are related to efficient mass transit and benefits of intermodal integration, and freight supply chain, as well as community and supply chain disruptions from floods. Twitter is very effective for outreach and for accessing the latest data and info on project related topics. Over 2,300 followers in 46 countries see tweets by @drwaheeduddin and many more see through retweets (RTs) and mentions from over 91 countries.

SlideShare: Over 3,600 SlideShare views of 9 presentations. A recent SlideShare presentation, based on 2014 workshop presentations and 2015 TRB paper, was posted. <http://slidesha.re/1CiiDnK>  
Another slide presentation was posted on “NCITEC Intermodal Transportation and Disaster Safeguard Research Projects at CAIT.” <https://www.slideshare.net/waheeduddin/uddin-caitncitecprojects11-oct2013slsh>

The top viewed slide presentation (1,251 views in less than two months) is “Mississippi Gulf Coast Rail Revival: NCITEC White Paper Background – CAIT”  
<http://www.slideshare.net/waheeduddin/mississippi-gulf-coast-rail-revival-ncitec-white-paper-background-cait> and “Dr. Uddin/CAIT Infrastructure and Environment Research Areas” with 526 views.

Twitter: <https://twitter.com/drwaheeduddin> Started in January 2012; several lists and “Global Infrastructure” timeline created; over 22,500 tweets to date.

Twitter: <https://twitter.com/disasterglobal> Started in 2012 on topics of protection from natural disasters and managing infrastructure assets; over 3,300 tweets to date.

Twitter: <https://twitter.com/InfrastructureG> Started in January 2014 to focus on built infrastructure and transportation assets; several lists on specific categories such as sustainable transportation; over 930 tweets to date.

YouTube Videos: Over 1,680 views of project related seven YouTube videos were reported to date.  
<http://youtu.be/8JjM2QEexFE>

---

### **2.3. Technologies or techniques: <Have any ongoing projects resulted in any technologies or methods?>**

- Geospatial planimetrics and mapping of built infrastructure assets using aerial imagery.
- Geospatial mapping of floodplains created using NCCHE's two dimensional flood simulation models.
- A simple to use approach to assess structural integrity of concrete girder bridges subject to extreme flood inundation

### **2.4. Inventions, patent applications, and/or licenses:**

Nothing to report

### **2.5. Other products**

Nothing to report

## **3. Participants & Other Collaborating Organizations**

### **Key Investigators**

Dr. Waheed Uddin (PI), University of Mississippi [cvuddin@olemiss.edu](mailto:cvuddin@olemiss.edu) (662) 915-5363

Professor of Civil Engineering and Director, Center for Advanced Infrastructure Technology (CAIT)

Dr. Mustafa Altinakar (co-PI), University of Mississippi [altinakar@ncche.olemiss.edu](mailto:altinakar@ncche.olemiss.edu) (662) 915-7788

Director, National Center for Computational Hydroscience and Engineering (NCCHE)

### **Other UM Research Staff**

Dr. Vijay Ramalingam, NCCHE Research Software Developer

Marcus McGrath (PhD student, NCCHE Graduate Student)

Dr. Azad Hossain, NCCHE Research Scientist

Ms. Leili Gordji (PhD student, NCCHE Graduate Student)

Alper Durmus (CAIT/Civil Engineering Graduate PhD Student) since Spring 2014

Quang Nguyen (CAIT/Civil Engineering Graduate PhD Student) since Fall 2013

Saeed Arab (CAIT/Civil Engineering Graduate PhD Student), Fall 2013 (left in January 2014)

Mohammad Torkjazi (CAIT/Civil Engineering Graduate PhD Student), 2013 (left in January 2014)

William "Tucker" Stafford (UG junior civil engineering student, CAIT) since Summer 2014

Gergo Arany (UG junior civil engineering student, CAIT) since Summer 2014

Haley Lynn Sims (UG junior civil engineering student, CAIT) since Summer 2013

Gi Yong Park (Exchange student from South Korea, UG civil engineer, CAIT) Summer – Fall 2013 (left)

### **Other Collaborating Organizations**

The PI has been contacting and will contact again the following organization as collaborators in this project:

IAVO Research & Scientific, Durham, North Carolina: IAVO has provided licenses of the GeoSPHERIC package that embeds a new version of the GeoGenesis® geospatial software. The software has been installed on seven computer stations in CAIT Transportation Modeling and Geospatial Labs. The value of the software for each computer seat is being used as in-kind cost share for this project. Their help is also acknowledged for identifying imagery specifications and providing training data to CAIT students.

As required by the NCCHE mission, Dr. Altinakar is closely in contact with the following agencies:

- 
- Department of Homeland Security (DHS) Science and Technology Directorate; FEMA
  - USDA Agricultural Research Service (ARS)
  - US Army Research Office (ARO)
  - US Army Corps of Engineers (CoE)
  - Mississippi Department of Marine Resources
  - Mississippi Emergency Management Agency
  - Association of State Dam Safety Officials (ASDSO)

### **3.1. What other organizations have been involved as partners?**

- Intergraph for continuing academic license of GeoMedia Pro at no cost to the University of Mississippi for use on CAIT projects (worth \$118,000 per year).
- As Intergraph Registered Research Lab, CAIT Remote Sensing and Geospatial Analysis Laboratory and CAIT Transportation Modeling and Visualization Laboratory is receiving geospatial industry support for education and training of students in geographical information system (GIS) applications through the project research tasks. This Intergraph software grant is a cooperative feature of this project. Since January 2014 the statewide license has been provided by MARIS. This software and ArcGIS software, provided by Mississippi Mineral Resource Institute, were used to create planimetrics of roads, bridges, and buildings from high resolution aerial imagery.

### **3.2. Have other collaborators or contacts been involved?**

The PI has been contacting the following organization as cooperative features of this project:

- 1) Mississippi Department of Transportation (MDOT): MDOT Roadway Design Division has been contacted for access to aerial imagery for candidate sites(s) in Mississippi. Follow up of initial contacts was made through an EIT who is Dr. Uddin's former student and CAIT staff.
- 2) MDOT Planning Division through contact with Dr. Uddin's former student and EIT for accessing overlapping aerial imagery scenes of the study sites.
- 3) MDOT Transportation Information Director (Mike Cresap) and MDOT Director of Structures - State Bridge Engineer (Justin Walker) have been especially helpful to provide drawings and photos for the I-55/US-51 highway bridges on the Sardis site and updated geospatial database of all state maintained highways and bridges of Mississippi. These were very important and useful contributions to this project.
- 4) Mississippi Automated Resource Information System: MARIS is a statewide resource agency in Mississippi for no-cost Landsat imagery and DEM data sources of selected counties in Mississippi. <http://www.maris.state.ms.us/> Project researchers downloaded bare ground 5 ft DEM/contour data and 2 ft aerial imagery scenes of Sardis site. Additionally, Dr. Uddin contacted MARIS and requested 2 ft aerial imagery and DEM of other candidate sites. We received this data for Tunica site on a USB hard disk.
- 5) US Army ERDC Hydraulics Lab, Vicksburg, Mississippi (Dr. Kenneth Ned Mitchell)

## **4. Impact**

### **4.1. What is the impact on the development of the principal discipline(s) of the program?**

- The UM's CAIT Transportation Modeling & Visualization Lab was provided a video panel wall by the Mississippi DOT ITS section in October 2014 as a part of a model ITS lab to monitor real-time traffic flow on roads and barge under bridges over the Mississippi River. The CAIT lab expanded

---

recently with new high performance computer equipment, new computer furniture, large video monitor for presentations, and seminar/meeting tables, chairs, and accessories. Geospatial course has taught in this facility since 2013 to: 3 UG and 3 graduate students in Fall 2013, 6 UG students in 2014 May Intersession, and 2 UG and 2 new graduate students in Spring 2015. Most of the NCITEC project research work is conducted in this lab.

- Dr. Uddin's NCITEC projects at CAIT supported 5 PhD students, 3 M.S. students, 11 UG Civil Engineering students, and 3 UG non-engineering students during 2013-2014.
- New graduate and CAIT undergraduate student workers were trained or are being trained for data analysis, geospatial analysis, and transportation demand modeling research. The contents of Transportation and Geospatial course are enhanced using the NCITEC project products.
- It is expected that the research accomplishments will lead to specialized transportation course and disaster mitigation and safeguard courses, as well as trained geospatial workforce.
- The contents of geospatial courses CE495 and ENGR597 Section 25, taught by Dr. Uddin, were updated using NCITEC project work. CE495 was offered in the 2014 May intersession. These courses will be offered again in Spring 2015 and future intersemester and/or regular sessions.
- Research results will be incorporated in the existing CE 481 – Transportation Engineering I course (3 credit hours) and CE 570 – Infrastructure Management course (3 credit hours), CE 590 – Airport Planning and Design, and ENGR 692 Section 2 – Numerical Methods and Optimization and Nonlinear Time Series Modeling in the department of Civil engineering. CE 570 course was offered by Dr. Uddin in Fall 2013 and CE 585 – Highway pavement in Fall 2014 to UG seniors and graduate students. The new textbook for this course was 2013 McGraw-Hill book *Public Infrastructure Asset Management* (Uddin, Hudson, Haas). Dr. Uddin will offer ENGR 692 Section 2 in Spring 2015 and CE 590 in Fall 2015.
- It is hoped that the research accomplishments will lead to specialized infrastructure courses involving flood risk assessment, disaster mitigation and safeguard, and transportation courses, as well as trained geospatial workforce.

#### **4.2. What is the impact on other disciplines?**

It is expected that research accomplishments from this project will be introduced in the computational hydroscience graduate program courses offered by Dr. Altinakar.

Dr. Uddin has interacted with Dr. Mustafa Altinakar of the UM's National Center of Computational Hydroscience who collaborated on the flood modeling project and is partnering in related research efforts.

Students in the Journalism department at the University of Mississippi often contact Dr. Uddin for their video projects on sustainability related topics for George Washington University's Planet Forward web site every year. This is a part of the on-going collaboration of Dr. Uddin with another NCITEC project PI, Dr. Kristen Swain. Dr. Uddin discusses with potential Journalism students the findings and significance of their project so that sustainable intermodal transportation integration topics can become one of their projects. The following example of Planet Forward video on the use of waste glass for sustainable road applications was produced by UM journalism student in May 2013. Earlier another student's YouTube video on life cycle analysis for sustainability projects was posted on *Planet Forward* web site.

<http://infrastructureglobal.com/sustainable-infrastructure-by-recycling-waste-glass-to-enhance-road-safety-and-reduce-emissions-guest-post-22/>

<http://planetforward.org/idea/life-cycle-analysis-of-sustainable-technologies/>

A YouTube video by Mason Herman (Public Policy/Journalism UG student), "Dr. Uddin Interview on Transportation and Air Quality Mitigation," April 30, 2014. <http://youtu.be/ulcvqaOHVc4>

---

Lakyn Birks, a journalism student, interviewed Dr. Uddin on November 18, 2014 on the topic of “Why trees on the University Campus are important to promote sustainability”. Ms. Birks posted her (planet forward) sustainability video assignment “Tree Recovery Sustainability video” on YouTube.

<http://youtu.be/tdZgnMr0WXo>    <http://youtu.be/Qu48hmwUq20>

#### **4.3. What is the impact on the development of transportation workforce development?**

The project has significant impacts on transportation workforce development. For example, the project:

- Provided opportunities to UG students, Master’s and Doctoral graduate students, other participating specialists for research in transportation management of commodities, supply chain logistics, intermodal network optimization, geospatial visualization, and related disciplines.
- Enhanced intermodal transportation education by supporting graduate and UG students. Led four PhD graduate students, two M.S. students, and five UG students to work on project related assignments at UM. Some of them completed their course projects on project related topics.
- One M.S. student completed his graduating research report by using his geospatial and CO<sub>2</sub> prediction results accomplished in passenger train and freight mobility projects. He implemented the research framework to his own country Indonesia by analyzing traffic related emissions and impacts of the loss of tropical forest cover on CO<sub>2</sub> production.
- Improved the performance and modern computer modeling and visualization skills of main stream professionals and members of underrepresented groups (minority students) that will improve their access to or retention in transportation research, teaching, supply chain management, or other related professions.
- Developed and disseminated new educational/training materials and provide exposure to transportation, science and technology for practitioners, public works professionals, teachers, young people, media, supply chain stakeholders, and general public. This has been accomplished through geospatial workforce training in the teaching lab, classroom, tweets, YouTube videos, and SlideShare presentations, as listed in section 2.2.

#### **4.4. What is the impact on physical, institutional, and information resources at the university or other partner institutions?**

The project made significant impact on enhancing current capabilities and research infrastructure at both CAIT and NCCHE units of the University of Mississippi:

- *Physical infrastructure resources:* Computing facilities, geospatial laboratory, geospatial software, and transportation corridor/traffic flow simulation capabilities. (Additionally, 8 new computer workstations and visualization equipment were procured using project funds and installed in CAIT Transportation Modeling & Visualization Laboratory in UM Jackson Center after approval by the DOT RITA sponsors.) These new computers and 6 old computers from CE Graphics Lab have been functioning fully since Fall 2013 after installation of geospatial software and other programs. Most project staff and graduate students used this lab in 2014.

The Mississippi DOT’s Intelligent Transportation System (ITS) section is collaborating with the University of Mississippi to provide traffic video display wall and extend the fiberoptic backbone to JAC building and CAIT Transportation Modeling & Visualization Laboratory facility in order to establish a model ITS lab. In October 2014 the CAIT Transportation laboratory was provided a video panel wall by the Mississippi DOT ITS section as a part of a model ITS lab to monitor real-time traffic flow on roads and barge under bridges over the Mississippi River. The lab will be

---

used for real-time traffic data collection and flow attributes for use in this project and teaching UG and graduate students.

- *Institutional resources*: Involving the Student Chapter of Institute of transportation Engineers (ITE) and both graduate and undergraduate transportation students in project activities. A major goal to support undergraduate students is to motivate them to pursue graduate studies in transportation systems and professional careers in transportation engineering discipline.
- *Information resources and electronic means*: CAIT web pages, news interviews by journalism students, You Tube video and SlideShare production, blog posts, tweets, and scientific papers. (Over 3,600 SlideShare views of 8 presentations on transportation and infrastructure and over 1,680 views of project related YouTube videos to date.)

#### **4.5. What is the impact on technology transfer?**

The project is making positive impacts on technology transfer to students and transportation workforce, as well as public use, including:

- Transfer of flood risk maps and decision support system framework for disaster vulnerability reduction to local and state government agencies for enhancing flood related emergency management.
- Collaboration with geospatial industry and other stakeholders for enhancing modeling of built infrastructure and offer added value of flood disaster visualization.
- Presentation of research results at conferences and workshop and participation in other conferences will be used for government and industry outreach, implementation in practice, and future training courses for interested agencies and consulting service providers.
- We will continue preparation of refereed papers, making conference presentations, and participating in regional and international conferences, NCITEC conferences and workshops, and annual Transportation Research Board meeting.
- Using these research dissemination and outreach efforts for establishing contacts with government and industry stakeholders, academia, implementing in practice, and offering future presentations to interested agencies and emergency management authorities.

#### **4.6. What is the impact on society beyond science and technology?**

The project is likely to make an impact beyond the bounds of science, engineering, and the academic world on areas such as:

- Enhancing public understanding of flood disaster, prevention, and mitigation through visualization products which are easy to understand and communicate with government stakeholders, businesses, media, and general public.
- Adapting the developed approach for flood disaster mitigation practices, decision support systems for disaster evacuation routing and emergency management, and landuse and flood control policies.
- Implementing disaster protection methodologies and web-based social networking tools to build disaster resilience infrastructure and communities, improve community preparedness and infrastructure defense against flood disasters, and protect social fabric, economic viability, civic facilities, and environmental conditions against flood disasters.

### **5. Changes/Problems**

#### **5.1. Changes in approach and reasons for change:**

None

---

**5.2. Actual or anticipated problems or delays and actions or plans to resolve them:**

The no-cost extension has allowed the research team to complete the research tasks, submit journal/conference papers to adequately document the research results, and complete the final report.

**5.3. Changes that have a significant impact on expenditures:**

None

**5.4. Significant changes in use or care of animals, human subjects, and/or biohazards:**

Not applicable

**6. Special Reporting Requirements**

**6.1. Information on matching funds:**

Table 2 shows the source of matching funds. IAVO’s grant of necessary number of licenses for the GeoGenesis® geospatial software is essential for CAIT Transportation and Remote Sensing Labs. It provides in-kind cost share. Additionally, IAVO’s help is sought to provide training data set for CAIT students.

Table 2. Cost sharing sources, expected amount, and amount realized to date

Source of Matching Fund	Cost Sharing Realized To Date
IAVO Research and Scientific for GeoGenesis® software licenses	100.0% (software installed on seven computer stations)

US DOT/RITA NCITEC funds approved:

Expended To Date: 100.0%

**6.2. RITA Performance Indicators for NCITEC:**

**Part I – Program-Wide Indicators**

1. Number of transportation-related courses offered during the reporting period that were taught by faculty and/or teaching assistants who are associated with the UTC at UM
  - Undergraduate courses: 1 (CE 481 Transportation Engineering I; 3 credit hours)
  - Graduate/UG course: 1 (CE585 Highway Pavements; 3 credit hours)
  - Graduate courses: 1 (ENGR 699 Special Topics in Engineering Science Section 25, M.S. Graduate Report; 3 credit hours)
2. Number of students participating in transportation research projects funded by this grant at UM
  - Undergraduate students: 3 (CAIT)
  - Graduate students: 3 (CAIT/NCICHE)
3. Number of transportation-related advanced degree programs that utilize grant funds to support graduate students at UM
  - Master’s Level: 1 (CE)
  - Doctoral Level: 2 (CE/NCICHE)
4. Number of graduate students supported by this grant at UM
  - Master’s Level: 0
  - Doctoral Level: 3 (CAIT/NCICHE)
5. Number of students supported by this grant who received degrees at UM

- 
- Master's Level: none
  - Doctoral Level: none

## **Part II – UTC-Specific Indicators**

(Related to projects where Dr. Uddin and Dr. Altinakar are involved.)

1. Research Capability Performance Metrics
  - Transportation research projects with an impact on intermodal transportation: 4
  - Peer-reviewed intermodal transportation research reports published: 9  
(2 Journal and Peer Reviewed TRB Papers/ 1 M.S. Thesis/2 Book Chapters)
  - Intermodal transportation research papers accepted for presentation at academic/professional meetings: 11
2. Leadership Performance Metrics
  - Leadership positions held by NCITEC researchers in regional, national and international organizations: 6  
(including 2 Intl conferences, Mississippi Transportation Institute, ASCE, ITE, Journal)
  - Number and diversity of NCITEC partners and collaborators: 0 (other than PIs)
  - Keynote speeches and invited presentations given by NCITEC faculty and staff: 1
  - Number of awards received by NCITEC faculty and staff: 4  
(Uddin's 2014 ASCE Life member and 2014 University of Texas CAEE Academy of Distinguished Alumni, student's ITE Southern District First prize paper, DHS Trailblazer Award to NCCHE/ Maine RRAP Team)
3. Education and Workforce Development Performance Metrics
  - Students completing transportation related courses: 135
  - Students involved in transportation research projects: 20
  - Educational tools specific to intermodal transportation, e.g., case studies, historical materials, computer simulations, and other models: 5
  - Students enrolled in advanced degree programs affiliated with NCITEC: N/A
  - Graduate students and their theses supported by NCITEC projects: 9
  - Students receiving degrees from education programs affiliated with NCITEC: 1 (M.S. degrees)
  - Faculty participating in NCITEC research projects and educational programs and activities: 2
4. Technology Transfer Performance Metrics
  - Intermodal transportation seminars, symposia, and educational programs conducted for and attended by practicing transportation professionals: 1 workshop (UM NCCHE/CAIT)
  - People attending the above-mentioned events: 10
5. Collaboration Performance Metrics
  - Number of projects (research, educational, and technology transfer) that have investigators from two or more institutions: 3 (Uddin's projects)
  - Collaborative efforts with state and local transportation and public works agencies: 5

# University of Mississippi School of Engineering

**National Center for Computational Hydroscience & Engineering**  
**Center for Advanced Infrastructure Technology**

## NCITEC WORKSHOP

**“Extreme Flood Inundation Mapping and Risk Modeling of  
Transportation Infrastructure Assets”**

**December 5, 2014**

**Friday 9:00 - 11:30 am NCCHE Conference Room, Brevard 3<sup>rd</sup> Floor**

The workshop provides an overview and key accomplishments made by NCCHE and CAIT for the NCITEC funded project. More info: <http://www.olemiss.edu/projects/cait/ncitec/>

### **Workshop Agenda**

9:00 - 9:10 Welcome: Dr. Altinakar

9:10 - 9:30 Project Overview, Research Methodology, and Key Products: Dr. Uddin

9:30 - 10:15 Flood Simulation Results: Dr. Altinakar, Marcus McGrath, Vijay Ramalingam

10:15 - 10:30 Break

10:30 - 11:00 Flood Impact Evaluation of Infrastructure: Alper Durmus

11:00 - 11:20 Geospatial Mapping of Flood Impacts Based on Imagery Spectral  
Multicriteria: Quang Nguyen

11:20 - 11:30 Concluding Remarks: Uddin and Altinakar

Adjourn



## NCITEC Project: 1202 - 25

### Disaster Protection of Transport Infrastructure and Mobility Using Flood Risk Modeling and Geospatial Visualization



### 2D Numerical Simulation of a Hypothetical Flood Downstream of Sardis Dam, MS



Prepared by  
Mustafa S. Altinakar, Ph.D.  
Marcus McGrath, M.Sc.  
Vijay Ramalingam, M.Sc.

January 2015

# Acronyms

---

ANL	Argonne National Laboratory
ArcGIS	A geographical information system software developed and marketed by ESRI®
CFL	Courant-Friedrichs-Lewy condition for convergence
DEM	Digital Elevation Model
DHS	U.S. Department of Homeland Security
DSAT	Dams Sector Analysis Tool
DSS-WISE™	Decision Support System for Water Infrastructural Security is a two-dimensional flood modeling and consequence analysis platform developed by the National Center for Computational Hydroscience and Engineering
ERDC	USACE Engineer Research and Development Center located in Vicksburg, MS
FEMA	Federal Emergency Management Agency
GRP	Generalized Riemann Problem
HAZUS-MH	Hazard U.S.-Multi Hazard (a geographic information system-based natural hazard loss estimation software package developed and freely distributed by the Federal Emergency Management Agency (FEMA))
HLLC	Harten-Lax-van Leer with Contact wave (an approximate numerical solver for Generalized Riemann Problem)
MMC	USACE Modeling Mapping and Consequence center
NED	National Elevation Dataset
RMSE	Root Mean Square Error
SWE	Shallow Water Equations
USACE	United States Army Corps of Engineers
USGS	United States Geological Survey Agency

## Table of Contents

<b>CHAPTER 1 INTRODUCTION.....</b>	<b>1</b>
1.1 Project Goal .....	1
1.2 Testbed Areas and Selection of the Simulation Area .....	1
<b>CHAPTER 2 DESCRIPTION OF DSS-WISE™ MODEL.....</b>	<b>5</b>
2.1 Governing Equations.....	6
2.1.1 Discretization of Governing Equations and Numerical Model .....	7
2.2 Boundary Conditions .....	9
2.3 Verification and Validation of DSS-WISE™ Model .....	9
<b>CHAPTER 3 COMPUTATIONAL MESH, INPUT DATA AND SIMULATION SET UP .....</b>	<b>10</b>
3.1 Computational Domain for Testbed No. 2.....	10
3.2 Transportation Infrastructures and Buildings of Interest.....	10
3.3 List of Simulations Performed.....	13
3.4 Digital Elevation Models (DEMs) and Representation of Structures .....	16
<b>CHAPTER 4 RESULTS FILES PRODUCED BY THE SIMULATIONS WITH DSS-WISE .....</b>	<b>26</b>
4.1 Observation Lines.....	29
4.2 Observation Points .....	36
4.3 Observation Profile .....	37
<b>CHAPTER 5 SIMULATION RESULTS.....</b>	<b>39</b>
5.1 Maximum Flow Depth .....	39
5.2 Flood Arrival Time.....	44
5.3 Maximum Specific Discharge .....	48
5.4 Discharge Hydrographs for Observation Lines .....	51
5.5 Observation Points at Bridge Locations .....	56

<b>5.6</b>	<b>Depth and Tangential Velocity along the Observation Profile .....</b>	<b>60</b>
<b>CHAPTER 6 CONCLUSIONS .....</b>		<b>65</b>
<b>6.1</b>	<b>Comparison of Flow Parameters Computed with Different Cell Sizes.....</b>	<b>65</b>
<b>6.2</b>	<b>Bridge Scour .....</b>	<b>68</b>
6.2.1	Bridge Pier Scour Estimation for I-55 Bridge.....	70
6.2.2	Bridge Pier Scour Estimation for Railroad Bridge.....	72
6.2.3	Bridge Pier Scour Estimation for US-51 Bridge .....	74
<b>CHAPTER 7 REFERENCES.....</b>		<b>76</b>

# Chapter 1 INTRODUCTION

## 1.1 Project Goal

Floods are one of the most widely occurring disasters. Floods may be caused by natural hydro-meteorological phenomena, such as rainfall and/or snowmelt, storm surges, etc., or by the operation and/or failure of manmade control structures, such as dams and levees. Floods may impact transportation systems by damaging roads, railroads and bridges. Road closures due to floods may not only hinder disaster response and emergency relief operations but also cause indirect damages in other critical sectors.

This report documents the research tasks carried out as a part of the NCITEC project 1202-25 “Disaster Protection of Transport Infrastructure and Mobility Using Flood Risk Modeling and Geospatial Visualization”. The methodology for achieving the objective is to 1) simulate extreme flood inundation using two dimensional numerical modeling of flood propagation and visualize on a geospatial map of the study area, 2) extract infrastructure features for I-55 highway, rail structure, US-51 highway, local airport and some buildings including their height elevation above ground levels, 3) simulate extreme flood inundation and its impacts on selected infrastructure features, and 4) evaluate structural integrity of highways and bridges. Traditionally, flood simulation and risk mapping of transportation critical infrastructures relied mostly on one-dimensional flood modeling. In this study, two dimensional modeling of the propagation of floods over large areas are simulated. Specifically, the project aims to identify and implement computational and geospatial visualization technologies to enhance decision support systems for transport infrastructure protection from extreme weather related natural disasters such as floods.

The NCCHE research tasks are primarily focused on flood modeling and simulation for the pilot testbed. The approach used to achieve this objective is to combine the results of two dimensional numerical modeling of flood propagation with geospatial data layers to visualize, and quantitatively evaluate the damages to road infrastructure for the purposes of risk mapping at local and regional levels.

## 1.2 Testbed Areas and Selection of the Simulation Area

Initially, four locations were selected as candidate testbed areas (Figure 1):

- Testbed No 1 is located near Tunica, Mississippi (Figure 2). Likely breach scenario is breaching of the Mississippi levee. There are a number of small bridges, and culverts around the town of Tunica.
- Testbed No 2 is located downstream of Sardis Dam, Mississippi (Figure 3). There are two highway bridges and one railroad bridge crossing the Little Tallahatchie River, which evacuates the flows released from the dam.
- Testbed No 3 is located near Greenville, Mississippi (Figure 4). Likely breach scenario is breaching of the Mississippi levee.
- Testbed No 4 is located in Oxford, Mississippi, and covers an area to the east of the intersection between Highway 6 and the Jackson Avenue (Figure 5). The likely flood scenario is a flash flood in a small creek flowing in the area.

All these four locations involve roads, bridges, residential and urban development areas. Based on the availability and the quality of the data, it was decided to focus the current study on the Testbed No 2. In order to consider the worst case flood scenario that may impact the road infrastructure downstream, a sunny-day, partial and gradual breaching of Sardis Dam is considered. The water surface elevation at the time of failure is assumed to be flush with the crest elevation.

The flood simulations are performed using a state-of-the-art two-dimensional (2D) numerical model called DSS-WISE™ developed at the National Center for Computational Hydroscience and Engineering. The 2D model directly provides the depth grid, arrival time, specific discharge, and two dimensional velocity components in the horizontal plane directly. Detailed information about the DSS-WISE model is provided in the next chapter.

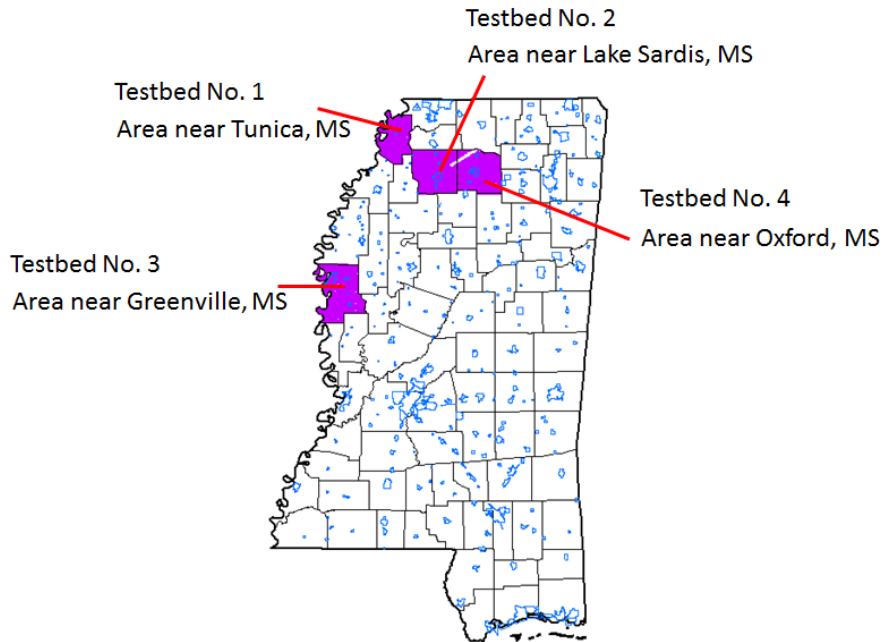


Figure 1 Map showing the locations of the four candidate testbed areas selected initially.

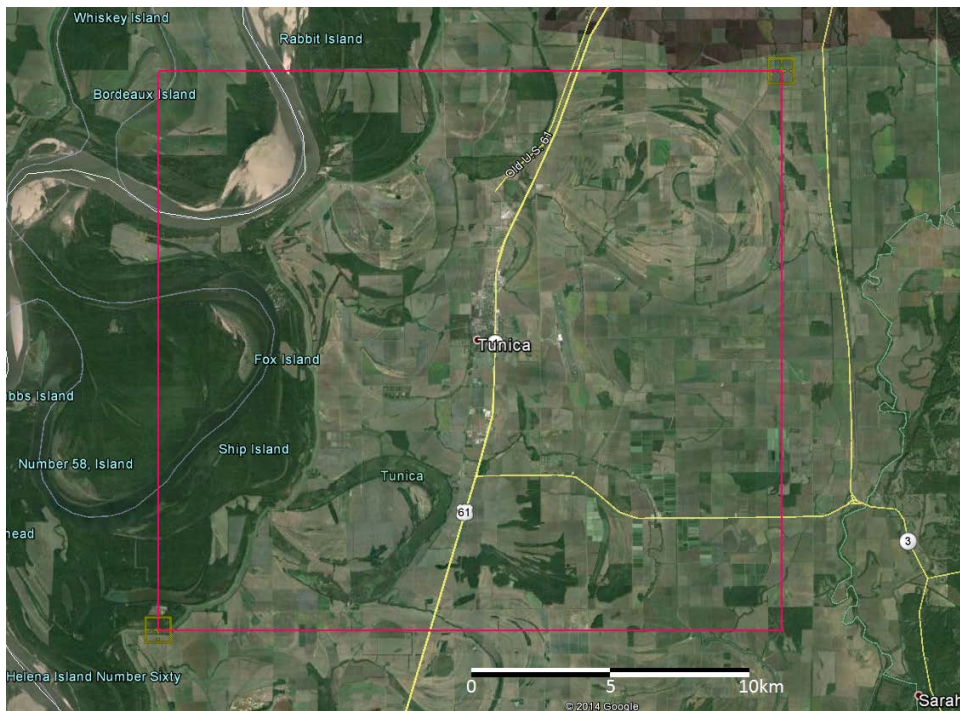


Figure 2 The Testbed No 1 as seen on Google Earth.



Figure 3 The Testbed No 2 as seen on Google Earth.

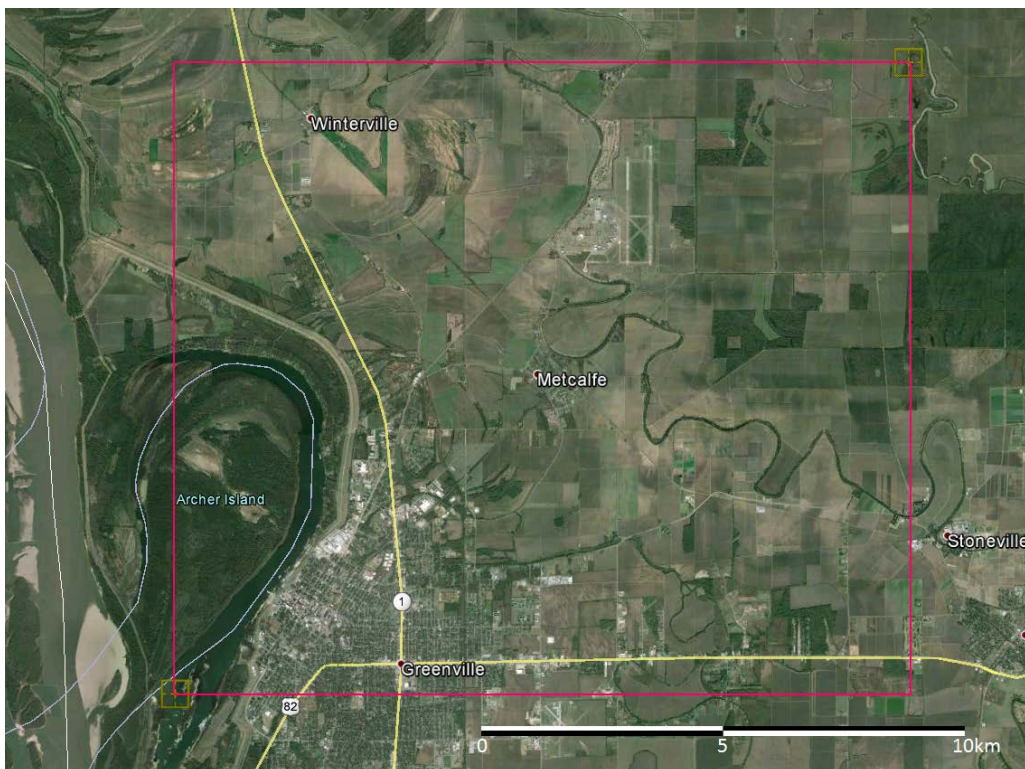


Figure 4 The Testbed No 3 as seen on Google Earth.



Figure 5 The Testbed No 4 as seen on Google Earth.

## Chapter 2 DESCRIPTION OF DSS-WISE™ MODEL

Two-dimensional numerical simulation of flood propagation in the Testbed No 2 was carried out using the DSS-WISE™ software, which was developed at the National Center for Computational Hydroscience and Engineering at the University of Mississippi.

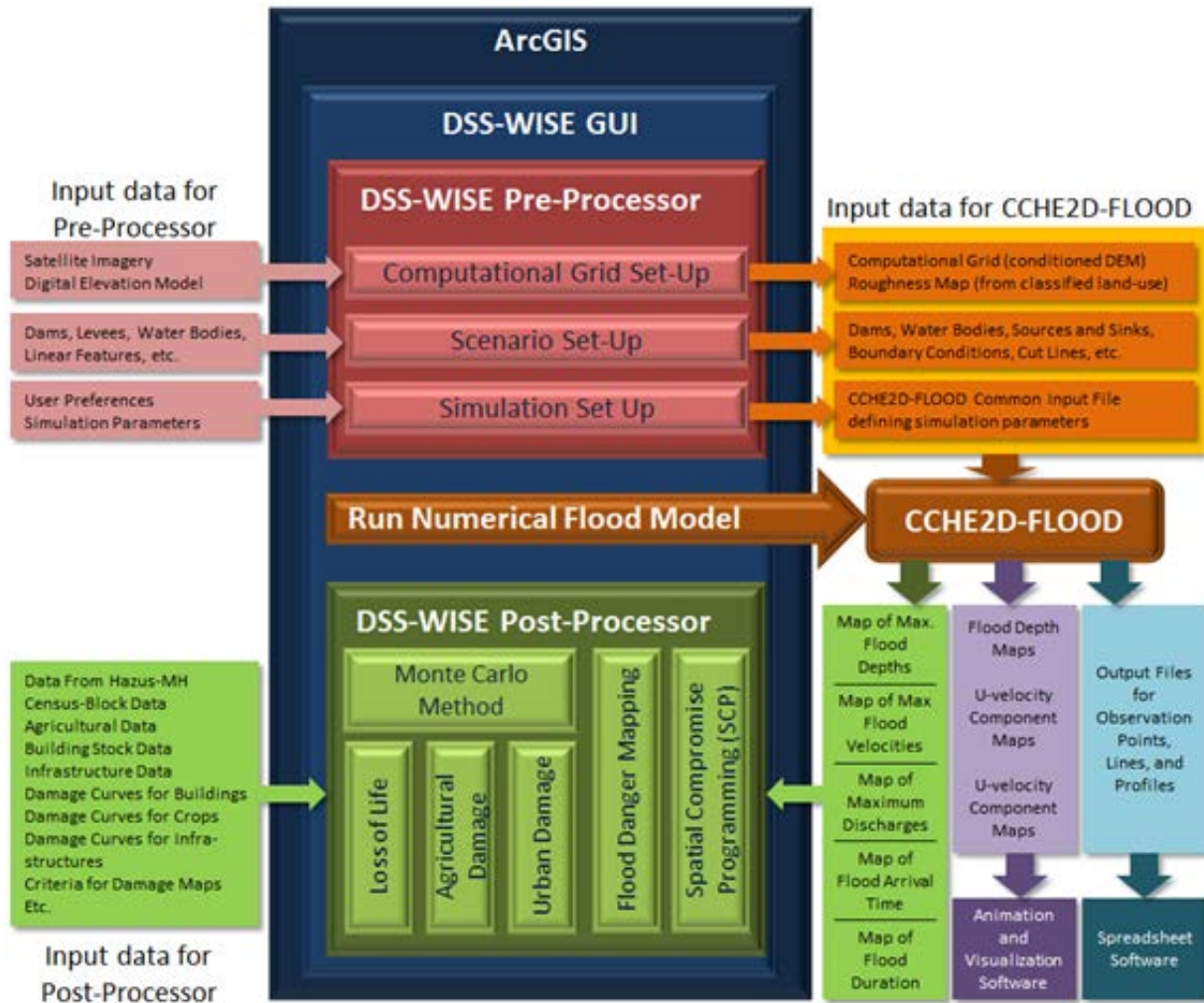


Figure 6 Conceptual diagram showing the overall structure of DSS-WISE™ and the data flow.

DSS-WISE™ is an integrated flow modeling and consequence analysis platform that combines a state-of-the-art two dimensional numerical model with GIS-based pre-processor and post-processor. Figure 6 shows the overall structure of DSS-WISE™ and the data flow. A graphical user interface (GUI), which is designed as an extension of ArcGIS® software developed and commercialized by ESRI®, allows the user to interact with the pre-and post-processors and the numerical model.

The preprocessor provides the functionalities to import various types of geospatial data files to be used as input data and scenario set-up. The DSS-WISE is designed to work with different levels of information availability. Using the pre-processor, the user can (1) import a DEM and condition it to be used as computational domain; (2) define initial water bodies and fill with water; (3) define hydraulic structures such as dams and levees; (4) assign boundary conditions to edges; and (5) define simulation parameters.

Controlled releases from various types of structures, such as gated or non-gated spillways, bottom outlets, pumping stations, etc. can be modeled as sources and sinks, and source and sink pairs. Source and sink pairs can also be used to model bridges and culverts. The user can define observation points, observation lines and observation profiles. Altinakar et al. (2010a) provides information on the preprocessor and various options that are implemented in an early version of the preprocessor module.

The raster results files generated by DSS-WISE™ can be imported into the ArcGIS platform for mapping and further analysis using the post-processor module (Altinakar et al., 2008). The post-processor includes a number of modules. The loss-of-life module uses a modified version of the USBR method (Graham, 1999, Dise, 2002) to compute potential loss of life. The agricultural damage module (Qi et al., 2006) uses the method developed by the United States Department of Agriculture, National Resources Conservation Service (NETSC Technical Note – Watersheds-16 Rev. 2, 1978). The postprocessor provides tools for performing an uncertainty analysis using Monte Carlo method (Qi et al., 2005a and b; Qi and Altinakar, 2011a and b). Urban damage can be calculated by using the maximum flood depth and velocity raster maps with the HAZUS-MH software (<http://www.hazus.org/>), which was developed by the United States Federal Emergency Management and is freely available. Post-processor also includes a module for flood hazard risk mapping for humans, vehicles and buildings based on FEMA/FIA (undated) and FEMA (2000), USACE (1985) and RESCDAM (2000) criteria (Altinakar et al, 2010b). The spatial compromise programming (SCP) module (Qi et al., 2005a) can be used to analyze and rank flood mitigation projects based on a GIS-based multi-criteria decision making technique, which takes into account spatial variability of their advantages and disadvantages (Tkach and Simonovic, 1997).

## 2.1 Governing Equations

DSS-WISE™ model solves the conservative form of shallow water equations that govern the flood propagation over complex topography. Referring to the definition sketch in Figure 7, the conservative form of shallow water equations in vector format can be written as

$$\mathbf{U}_t + [\mathbf{F}(\mathbf{U})]_x + [\mathbf{G}(\mathbf{U})]_y = \mathbf{S}(\mathbf{U}) \quad (1)$$

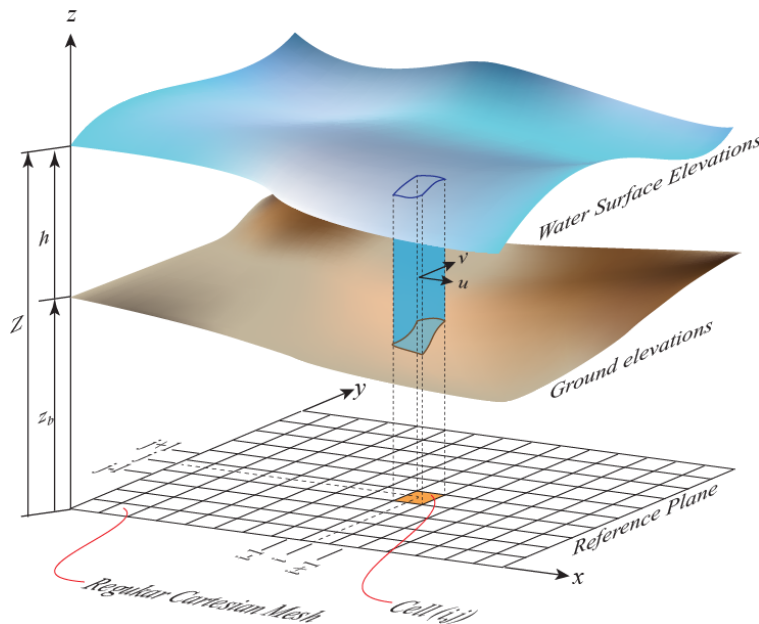


Figure 7 Definition sketch for modeling of shallow water flow over complex topography.

Bolded symbols in Eq. (1) represent vectors with  $\mathbf{U}$  being the vector of conserved variables,  $\mathbf{F}(\mathbf{U})$  and  $\mathbf{G}(\mathbf{U})$  the fluxes in  $x$  and  $y$  directions, respectively.

$$\mathbf{U} = \begin{bmatrix} h \\ hu \\ hv \end{bmatrix}, \mathbf{F}(\mathbf{U}) = \begin{bmatrix} hu \\ hu^2 + gh^2/2 \\ huv \end{bmatrix}, \mathbf{G}(\mathbf{U}) = \begin{bmatrix} hv \\ hvu \\ hv^2 + gh^2/2 \end{bmatrix} \quad (2)$$

The term on the right side of the equation,  $\mathbf{S}(\mathbf{U})$ , is the vector of source terms due to topography and friction.

$$\mathbf{S}(\mathbf{U}) = \begin{bmatrix} q_v \\ -ghS_{fx} - gh(\partial z_b/\partial x) \\ -ghS_{fy} - gh(\partial z_b/\partial y) \end{bmatrix} \text{ with } S_{fx} = \frac{u n^2 \sqrt{u^2+v^2}}{h^{4/3}} \text{ and } S_{fy} = \frac{v n^2 \sqrt{u^2+v^2}}{h^{4/3}} \quad (3)$$

In these equations,  $u$  and  $v$  are the local velocity components in  $x$  and  $y$  directions,  $h$  the flow depth,  $z_b$  the bed elevation,  $g$  the gravitational acceleration, and  $q_v$  the net source/sink discharge (or mass per cell area per unit time) added without momentum input. The system of equations is closed by assuming that the source terms due to friction,  $S_{fx}$  and  $S_{fy}$ , can be expressed using the Manning's equation for steady uniform flow. The symbol  $n$  stands for Manning's friction coefficient, which depends on the characteristics of the terrain and the land use/cover.

### 2.1.1 Discretization of Governing Equations and Numerical Model

DSS-WISE™ assumes that the solution domain can be represented as a regular Cartesian mesh defined in  $x$ - $y$  horizontal plane (see Figure 8 and Figure 7), such as a DEM (Digital Elevation Model). The step sizes in  $x$  and  $y$  directions are in  $\Delta x$  and  $\Delta y$ , respectively. The  $z$  axis represents elevation with respect to an arbitrary datum. Gravitational acceleration is normal to the plane and points in the negative  $z$  direction. Referring to Figure 8, the finite volume method is used to obtain an explicit discrete time marching equation for solving the three unknowns, i.e.  $h$ ,  $hu$ , and  $hv$ , by integrating the shallow water equations given in Eq. (1) over the cell  $(i,j)$ :

$$U_{i,j}^{m+1} = U_{i,j}^m - \left(\frac{\Delta t}{\Delta x}\right) \left(F_{i+\frac{1}{2},j} - F_{i-\frac{1}{2},j}\right) - \left(\frac{\Delta t}{\Delta y}\right) \left(G_{i,j+\frac{1}{2}} - G_{i,j-\frac{1}{2}}\right) + \Delta t S_{i,j} \quad (4)$$

In the above equation,  $F_{i+1/2,j}$  and  $F_{i-1/2,j}$  express the fluxes through the east and west intercell boundaries, and  $G_{i+1/2,j}$  and  $G_{i-1/2,j}$  through north and south intercell boundaries, respectively (see Figure 8 and the computational stencil in Figure 9). Developing a robust and stable shock-capturing upwind numerical model requires the selection of appropriate expressions to compute the intercell fluxes. DSS-WISE™ adopts a Godunov (Godunov 1959 and Godunov et al. 1976) type upwind scheme based on the approximate solution of Generalized Riemann Problem (GRP) at each cell interface using the first-order HLLC Riemann solver (Toro et al., 1992, 1994). The HLLC method is a modified version of the HLL (Harten, Lax and van Leer) Riemann solver originally proposed by Harten, Lax, and van Leer (1983). The C in HLLC method stands for the contact wave (when solving equations in one direction; the variation of variables in the other direction behave as contact waves). The HLLC method offers several advantages. It is relatively simple and straightforward to implement. It does not require entropy fixes to avoid physically impossible solutions. It can handle wet-dry fronts without having to define a minimum water depth everywhere. The details of the implementation can be found in Altinakar and McGrath (2012b).

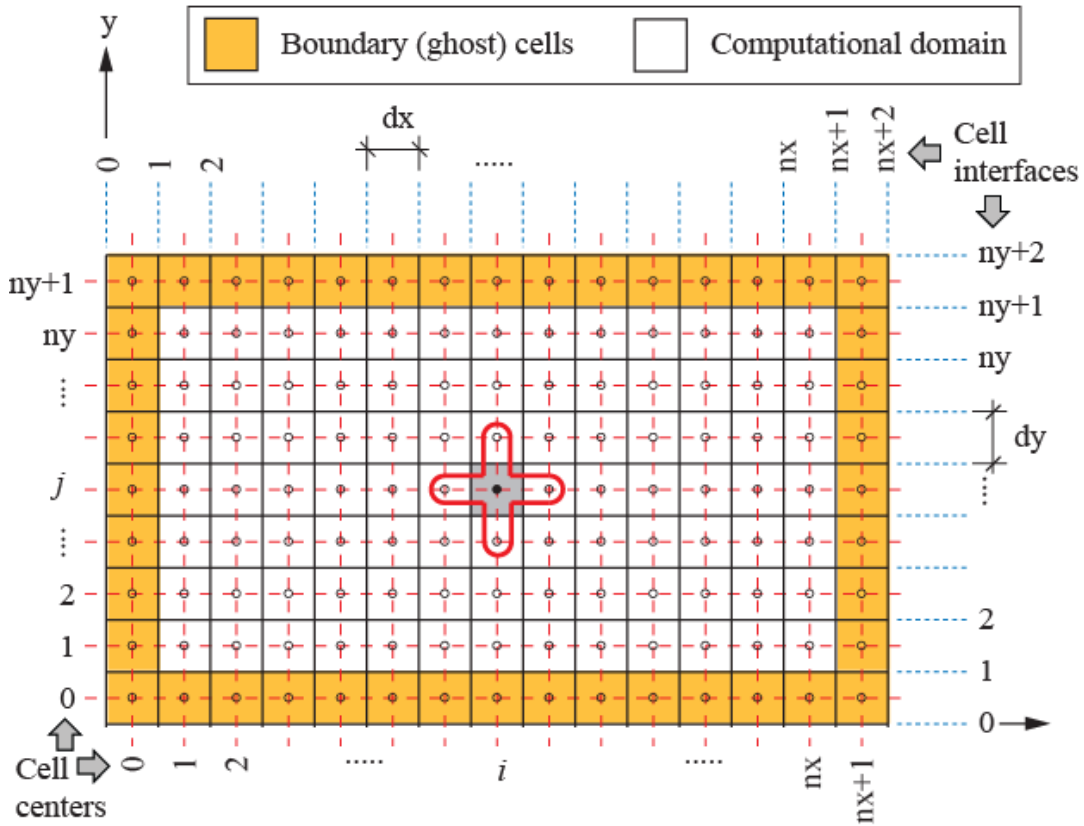


Figure 8 Regular Cartesian computational mesh used by DSS-WISE™.

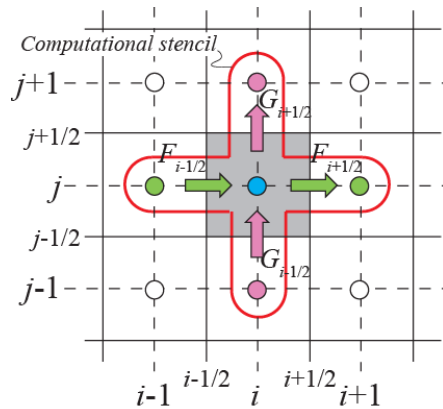


Figure 9 Computational stencil.

The explicit scheme used by DSS-WISE™ is subjected to Courant-Friedrichs-Lewy (CFL) condition for convergence, which states that the fastest wave in the domain should only travel a fraction of the cell size ( $\Delta x = \Delta y$ ) during the time step  $\Delta t$ . Based on the CFL condition, the time step is automatically chosen using the following criteria:

$$N_{CFL} = \text{Max} \left[ \frac{\Delta t}{\Delta x} (|\mathbf{u}| + \sqrt{gh}), \frac{\Delta t}{\Delta y} (|\mathbf{v}| + \sqrt{gh}) \right] \leq 0.5 \quad (5)$$

The automatic selection of the time step based on the CFL condition ensures that the perturbations do not travel over an entire cell during a single time step. The resulting code is robust and reliable. It captures shock waves, such as standing or traveling hydraulic jumps and translatory waves. It also handles wetting and drying and disconnected domains.

The DSS-WISE™ is programmed using multi-core multi-threaded parallelization to increase the computational speed. It also uses special techniques to track and compute only wet cells to further increase the computational speed (Altinakar et al. 2012b).

## 2.2 Boundary Conditions

DSS-WISE™ offers a number of boundary conditions along the edges of the computational domain. The available options are:

- Closed (wall) boundary condition: This type of boundary acts like a fully reflective boundary and does not allow water to exit the domain.
- Open boundary condition: The flow can exit the domain without generating any perturbations.
- Inflow boundary: The discharge flowing into the domain is described as a function of time.
- Outflow boundary: The user imposes the time series of water elevation.

In the present study, open boundary condition was specified along all for edges in all simulations.

## 2.3 Verification and Validation of DSS-WISE™ Model

Originally developed with funding from the U.S. Department of Homeland Security (DHS) Science and Technology Directorate, the DSS-WISE™ has been extensively verified and validated using various analytical solutions and mathematical constructs. It has also been validated using field data from past dam failures (Altinakar et al. 2010). A blind validation study was also performed in collaboration with USACE MMC (Altinakar et al. 2012a). Validation of DSS-WISE using the data from Big Bay Dam failure in Mississippi can be found in Altinakar et al. (2010c).

The DSS-WISE™ software is currently used by various federal and state agencies, which include U.S. Department of Homeland Security Dams Sector; U.S. Army Corps of Engineers (USACE) Headquarters, Washington D.C.; USACE-ERDC (Engineer Research and Development Center), Vicksburg, MS, Military Hydrology Group; USACE-MMC (Modeling Mapping and Consequence); USACE Vicksburg District; Mississippi Department of Environmental Quality. These agencies are using DSS-WISE for dam-break and other flood simulations in civil and military real-life applications.

In collaboration with the Office of Infrastructure Protection, DHS National Protection and Programs Directorate, and the Office of Homeland Security, USACE Headquarters, a simplified version of DSS-WISE™, called DSS-WISE™ Lite, is currently available for web-based automated dam-break flood modeling and mapping tool through, which is accessible via DSAT (Dams Sector Analysis Tool) portal hosted by the Argonne National Laboratory (ANL). This service became available in February 2012 with one pilot state and a year later was opened to all states. As of the end of 2014, the system has handled 3020 simulation requests submitted by 105 users from 41 states have. A new version of this software will be released in 2015.

## Chapter 3 Computational Mesh, Input Data and Simulation Set up

### 3.1 Computational Domain for Testbed No. 2

Figure 10 shows the extent of the computational domain for testbed No. 2 on the Google Earth. The rectangular-shaped area of interest extends 20.58 km in East-West direction and 17.26 km in North-South Direction.



Figure 10 Computational Domain for Testbed No. 2.

### 3.2 Transportation Infrastructures and Buildings of Interest

Numerical simulations were designed to provide information on the impact of the imposed flood scenario on various transportation infrastructures and several buildings of interest, whose locations are shown in Figure 11. There are two road bridges and a railroad bridge crossing the Little Tallahatchie River downstream of the Sardis Dam. In the order from upstream to downstream, and referring to Figure 11, these are:

- I-55 Bridge (double bridge)
- Railroad Bridge, and
- US-51 Bridge

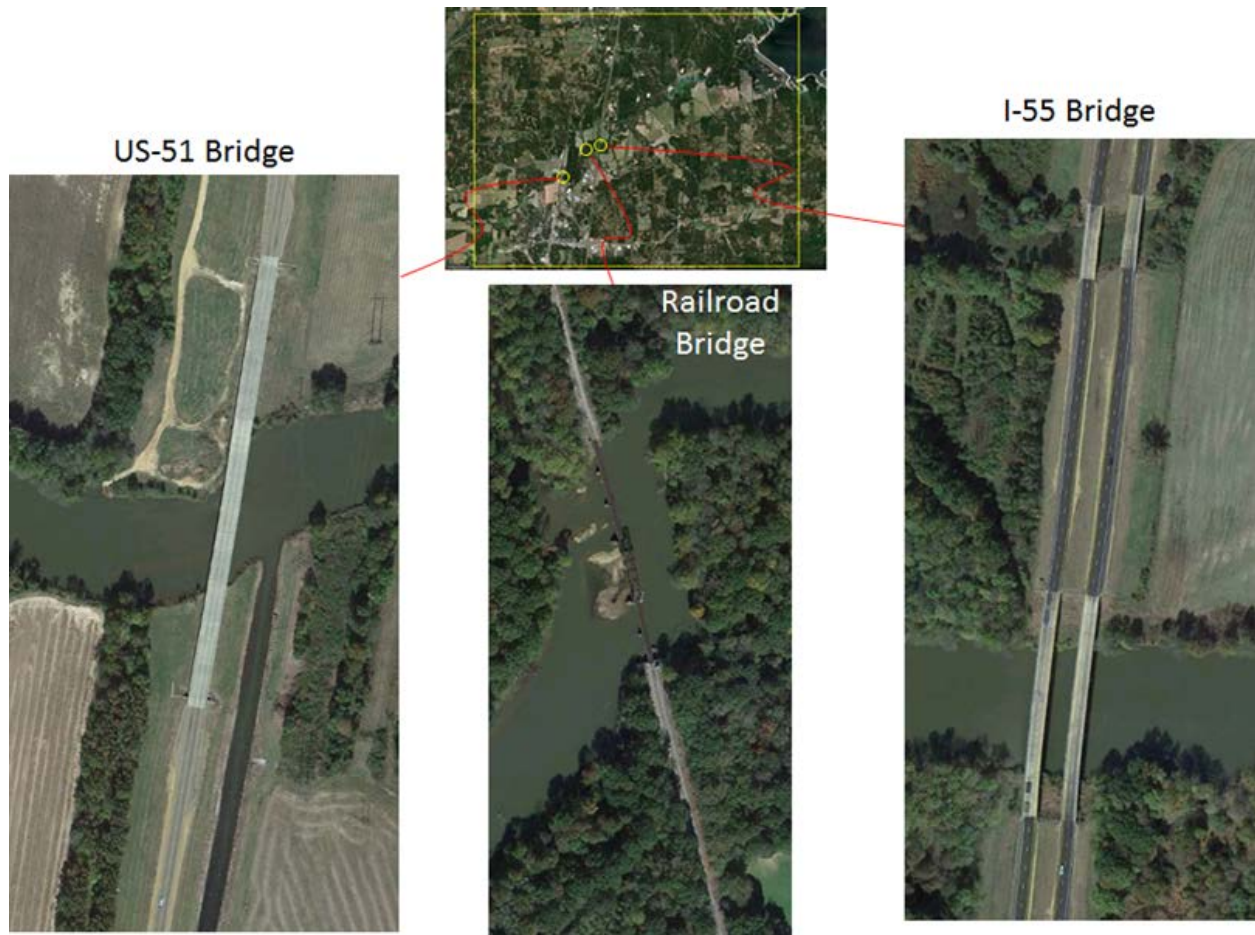


Figure 11 Road and railroad bridges in the area of interest for Testbed No. 2.

Referring to Figure 12, there are also several structures of interest for which the potential flood impact for the selected scenario is to be investigated:

- Sardis Lake Baptist Church
- First Baptist Church
- Batesville Public Library
- U.S. Forestry Department
- Insituform Technologies Inc.
- Panola County Airport (pavement and terminal buildings)

Figure 13 shows the aerial view of these structures as seen in Google Earth. These six structures were represented as elevations in simulations with high-resolution DEMs (3m and 5m cell sizes). In coarser simulations, due to the large cell size (10m and 30m) the structures could not be modeled adequately as elevations; therefore, they were neglected.

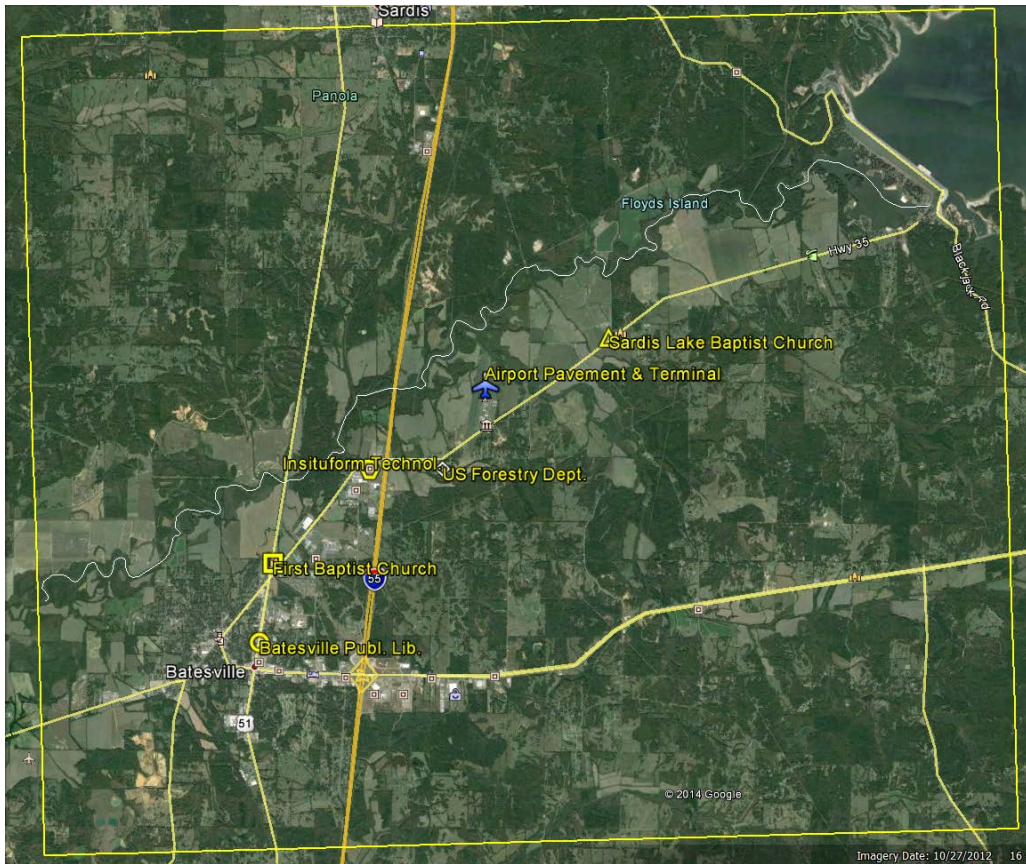


Figure 12 Structures of interest in the computational domain of Testbed No. 2.

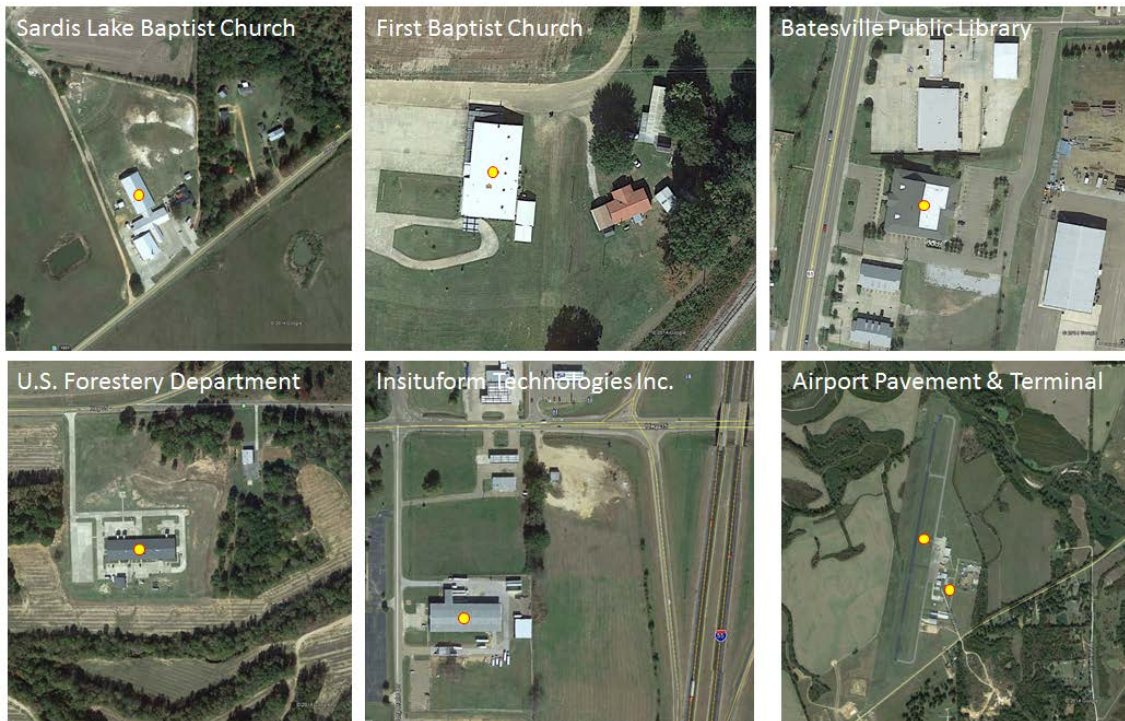


Figure 13 Structures of interest (to be modeled in high resolution simulations) as seen in Google Earth.

### 3.3 List of Simulations Performed

The extreme flood event considered in the present study is the hypothetical partial and gradual breaching of Sardis Dam when the water-surface level in the reservoir is flush with the crest elevation. Since a sunny day failure scenario is considered, the discharge entering the lake at the upstream end and the flows in the downstream channel are both neglected.

The same flood scenario were simulated using four DEMs with different resolutions:

1. Simulation using a DEM with 30m (1 arc-second) cell size sourced from USGS NED  
The computational domain for the simulation with the 30m DEM from USGS NED is much larger than that of the Testbed No. 2 and includes the entire Sardis Lake. Figure 14 shows the extent of the computational mesh. In the same figure, the boundary of the computational domain for the Testbed No. 2 is also shown for comparison purposes.

The DEM is obtained from USGS NED (<http://ned.usgs.gov/>). Transportation infrastructure or buildings of interest are not burned into the DEM. The deck elevation of the bridges are not represented in the DEM. Therefore, the water flow can pass through the bridge openings. The road infrastructure is not burned into the DEM. The road elevations are left as they are represented in the DEM. At 30m resolution, the crown of the road (about 10 m for I-55) and the embankment (about 80 m for I-55) can only be captured very coarsely.

In this simulation, the Sardis Dam is represent as an idealized dam. The DEM includes the entire Sardis Lake. The initial conditions are set by filling the reservoir up to the elevation of the crest. The idealized dam is breached as soon as the simulation starts. The breach scenario considers a trapezoidal final breach profile with a top width of 218 m and a bottom width of 200m. The side slope of the breach are assumed to be 1:1. The time of formation for the breach to reach its final form is assumed to be 0.44 hours.

The simulation is performed for a duration of 48 hours. The discharge passing through the breach cross section was automatically recorded by placing an observation line immediately downstream of the breach. The extracted breach discharge is shown in Figure 15. The peak breach discharge is 16,450 m<sup>3</sup>/s and it occurs 1.97 hours after the beginning of the simulation (i.e. after the initiation of the breach). At the end of the simulation, i.e. 48 hours after the initiation of the breach, the breach discharge has reduced to 192 m<sup>3</sup>/s. This flood hydrograph was directly imposed as a source for simulations with all other DEM resolutions (10 m, 5 m, and 3 m) as a source. This allowed the use of a much smaller computational area (Testbed No.2) with higher resolutions (smaller cell sizes) and eliminated the need to represent the entire reservoir.

2. Simulation using a DEM with 10m (1/3 arc-second) cell size sourced from USGS NED  
The computational domain is the Testbed No.2 as shown in Figure 10. The DEM is obtained from USGS NED (<http://ned.usgs.gov/>). Transportation infrastructure or buildings of interest are not burned into the DEM. The deck elevation of the bridges are not represented in the DEM. Therefore, the water flow can pass through the bridge openings. The road infrastructure is not burned into the DEM. The road elevations are left as they are represented in the DEM.

Lake Sardis is not included in the domain and thus the reservoir is not modeled. The hydrograph discharge obtained from the simulation with 30m DEM (Figure 15) is directly imposed as a source immediately downstream of the dam. The simulation is performed for a duration of 48 hours.

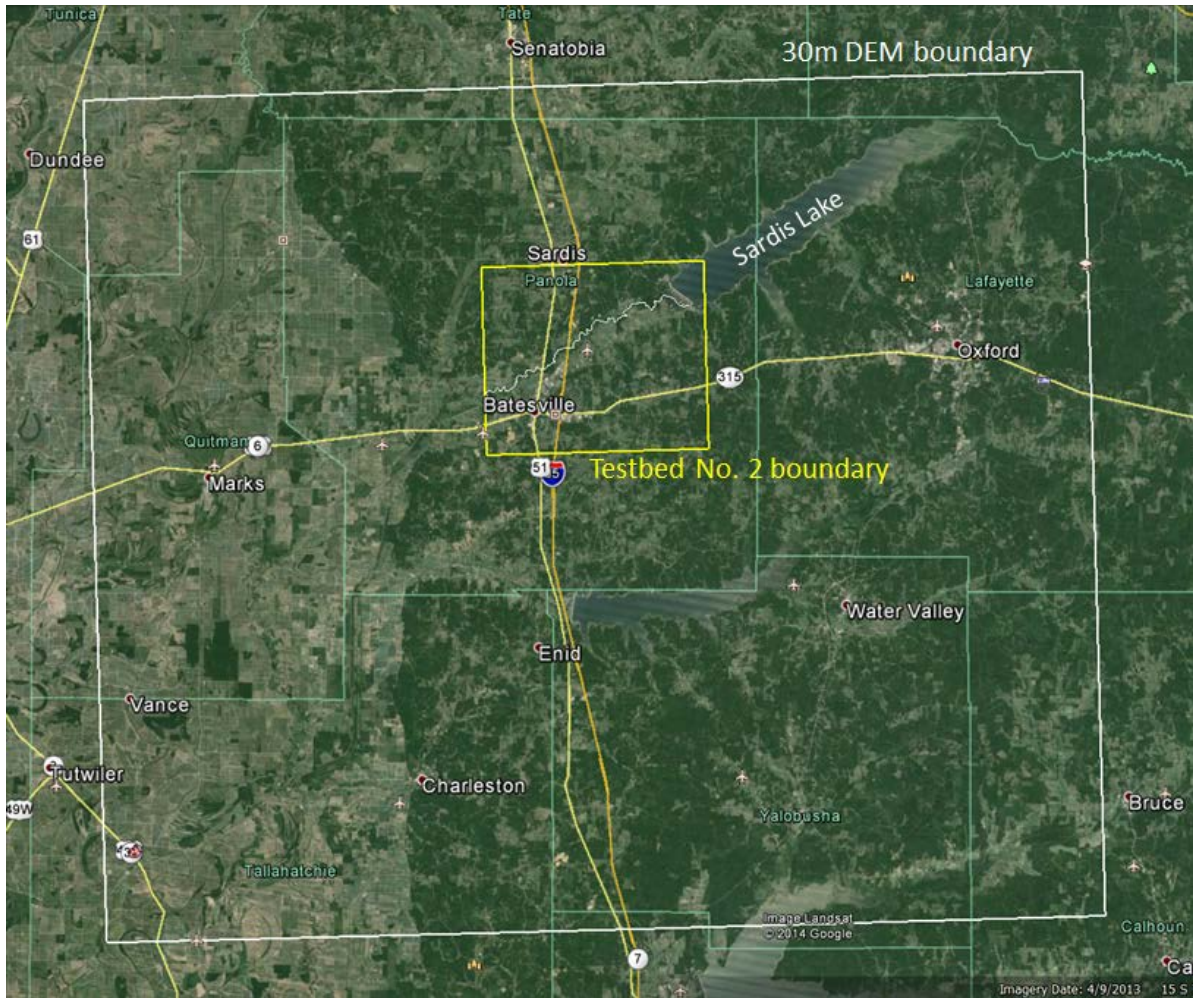


Figure 14 Extent of the simulation with 30m DEM.

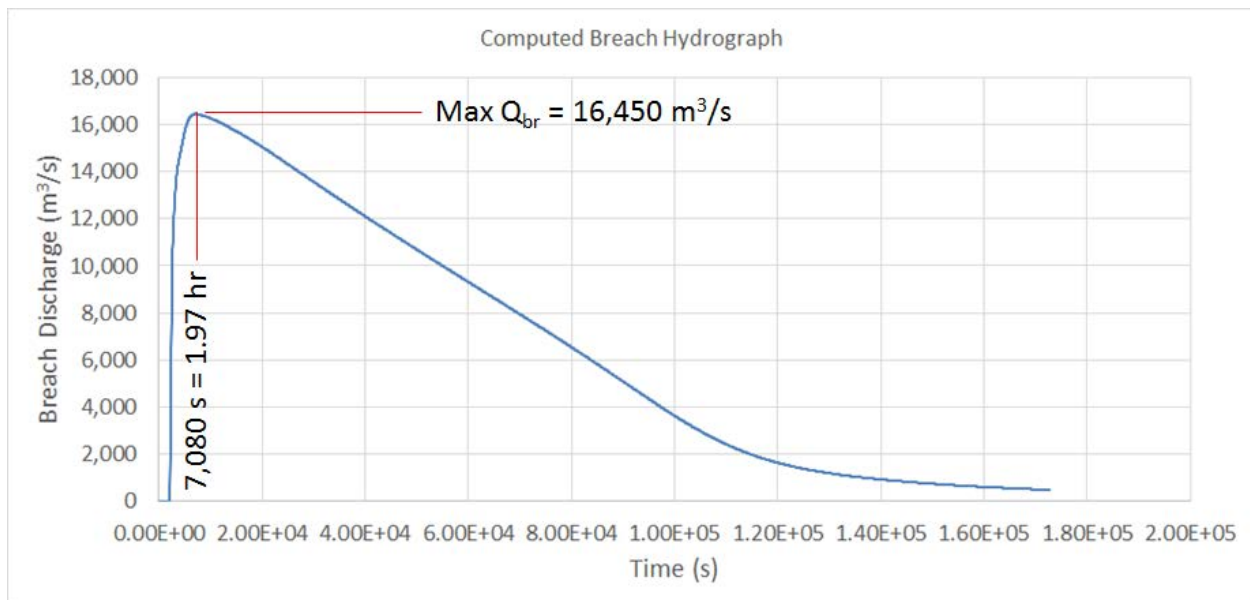


Figure 15 Breach discharge hydrograph obtained with the simulation using the 30m DEM.

3. Simulation using a DEM with 5m cell size sourced from USGS NED  
 The computational domain is the Testbed No.2 as shown in Figure 10. The DEM is obtained by resampling the 3m resolution DEM. The buildings of interest listed in Section 3.2 are burned into the DEM. The deck elevation of the bridges are not represented in the DEM. Therefore, the water flow can pass through the bridge openings. The resolution of the DEM is sufficiently high to have a good representation of the road infrastructure as elevation (road and railroad embankments).

Lake Sardis is not included in the domain and thus the reservoir is not modeled. The hydrograph discharge obtained from the simulation with 30m DEM (Figure 15) is directly imposed as a source immediately downstream of the dam. The simulation is performed for a duration of 48 hours.

4. Simulation using a DEM with 3m (1/9 arc-second) cell size sourced from USGS NED  
 The computational domain is the Testbed No.2 as shown in Figure 10. The DEM has a spatial resolution of 3m. The buildings of interest listed in Section 3.2 are burned into the DEM. The deck elevation of the bridges are not represented in the DEM. Therefore, the water flow can pass through the bridge openings. The resolution of the DEM is sufficiently high to have an excellent representation of the road infrastructure as elevation (road and railroad embankments).

Lake Sardis is not included in the domain and thus the reservoir is not modeled. The hydrograph discharge obtained from the simulation with 30m DEM (Figure 15) is directly imposed as a source immediately downstream of the dam. The simulation is performed for a duration of 48 hours.

All simulations presented in this report were performed assuming an overall Manning's roughness coefficient of  $0.035 \text{ m}^{-1/3}$ s over the entire computational domain.

Table 1 List of Simulations and their properties

	Simulation with 30m DEM	Simulation with 10m DEM	Simulation with 5m DEM	Simulation with 3m DEM
Cell size	30	10	5	3
Number of Columns	3085	2058	4116	6860
Number of Rows	2589	1726	3452	5753
Number of Cells	7,987,065	3,552,108	14,208,432	39,465,580
East-West Extent (km)	92.550	20.580	20.580	20.580
North-South Extent (km)	77.670	17.260	17.260	17.259
Spatial Reference	NAD_1983_UTM_Zone_16N			
Datum	D_North American_1983			
Min Elevation (m)	37.964	53.410	53.147	53.147
Max Elevation (m)	189.784	136.070	139.868	139.900
Structures Burned into the DEM	No	No	Yes	Yes
Bridge Openings	Cleared	Cleared	Cleared	Cleared
Flood Scenario				
Discharge Hydrograph	Computed during the simulation by imposing a trapezoidal breach forming in 0.44 hours	Discharge hydrograph obtained during the simulation with 30m DEM is directly imposed as a source at the downstream of the dam.		
Manning's Roughness	Overall Manning's roughness of $0.035 \text{ m}^{-1/3}$ s			

### 3.4 Digital Elevation Models (DEMs) and Representation of Structures

The digital elevation data for the two-dimensional flood simulations were obtained from USGS National Elevation Dataset (NED)<sup>1</sup>. Figure 16 shows a screen shot from the national Map Viewer website<sup>2</sup>. The digital elevation data with 1/9 arc-second spatial resolution is available for the highlighted area, which covers the region of interest for the present. For the area of interest the digital elevation data is available at resolutions of 1/9 arc-second (~3 m), 1/3 arc-second (~10 m), 1 arc-second (~30 m), and 2 arc-second (~60 m).

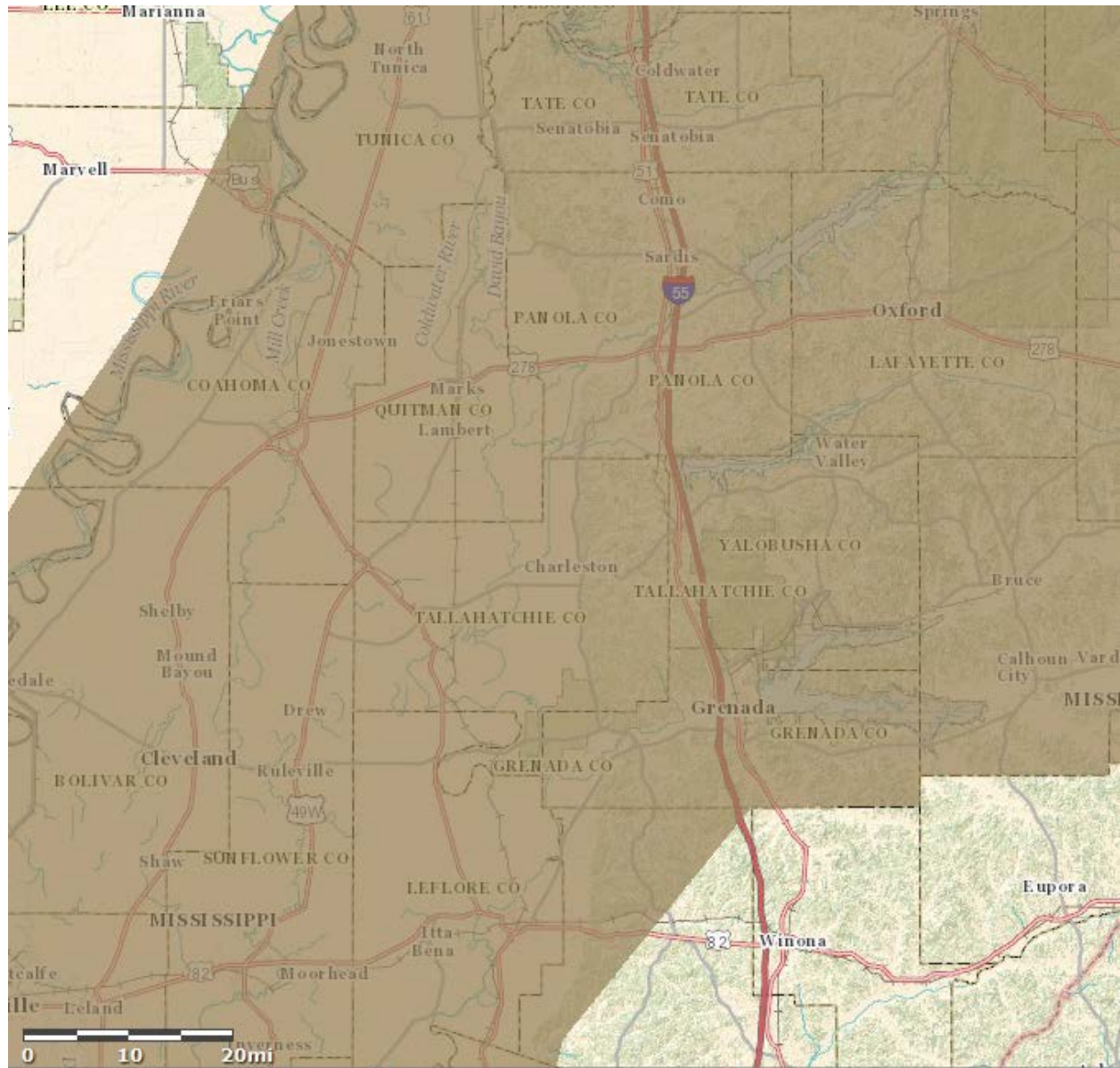


Figure 16 Availability of elevation data from USGS NED website: 1/9 arc-second elevation data is available for the highlighted area.

<sup>1</sup> <http://ned.usgs.gov/>

<sup>2</sup> <http://viewer.nationalmap.gov/viewer/>

Figure 17 shows the 30 m DEM used for flood simulation, mapping and risk analysis. This DEM covers a much larger area than the area for Testbed No. 2, whose extent is shown in the figure as a white rectangle. The 30 m DEM was obtained by resampling the 1/3 arc-second (~10 m) USGS NED data downloaded from the USGS NED website (<http://ned.usgs.gov/>). Only bridge openings were cleared to create a free passage for the flow. No other modifications were made in the DEM. The DEM served as the regular Cartesian grid for numerical simulations.

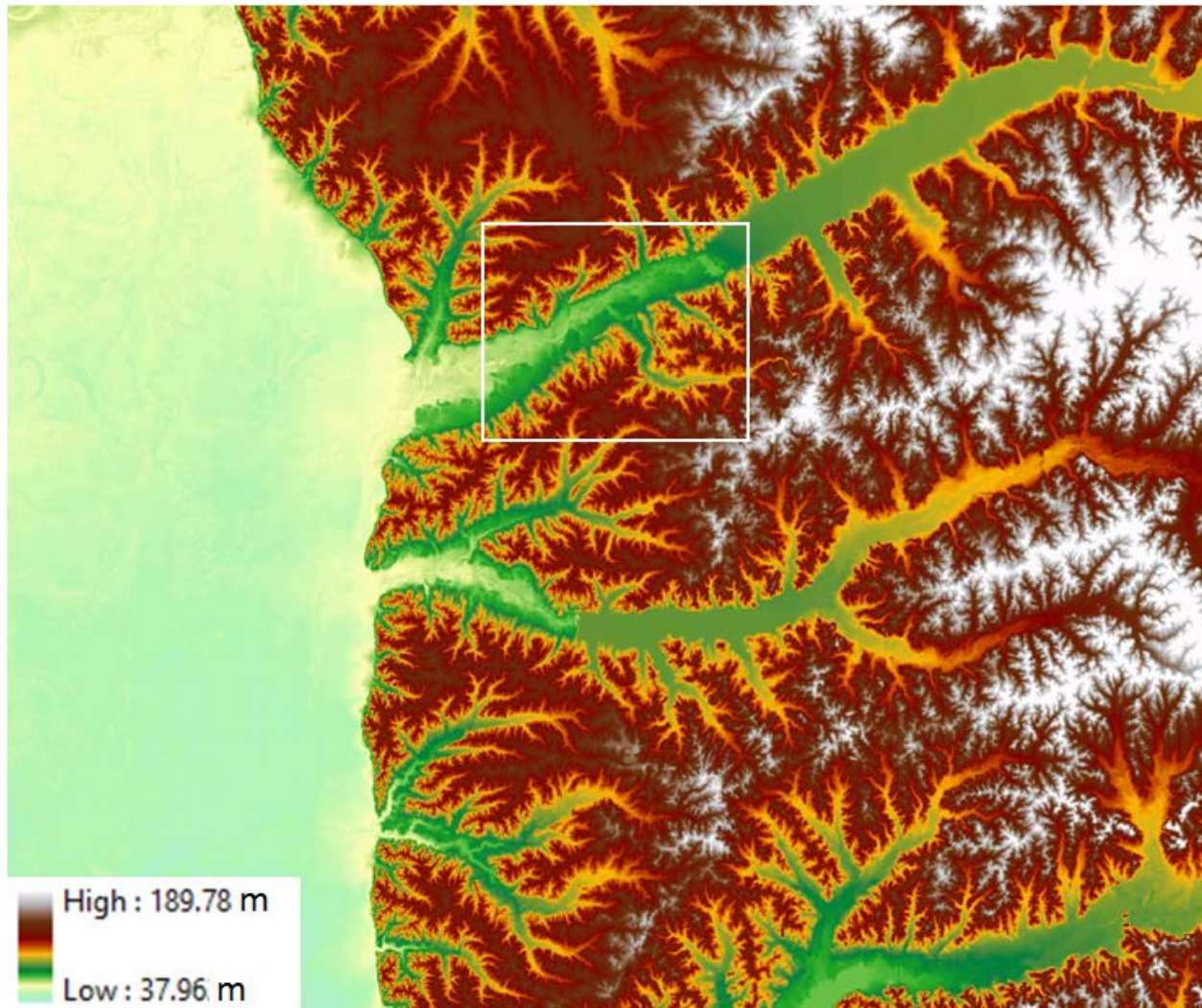


Figure 17 DEM with a resolution of 30 m (structures of interest are not burned into the DEM).

Figure 18 shows the 10 m DEM used for flood simulation, mapping and risk analysis in Testbed No. 2. This DEM was obtained by downloading 1/3 arc-second (~10 m) USGS NED data from the USGS NED website (<http://ned.usgs.gov/>). Only bridge openings were cleared to create a free passage for the flow. No other modifications were made in the DEM. The DEM served as the regular Cartesian grid for numerical simulations.

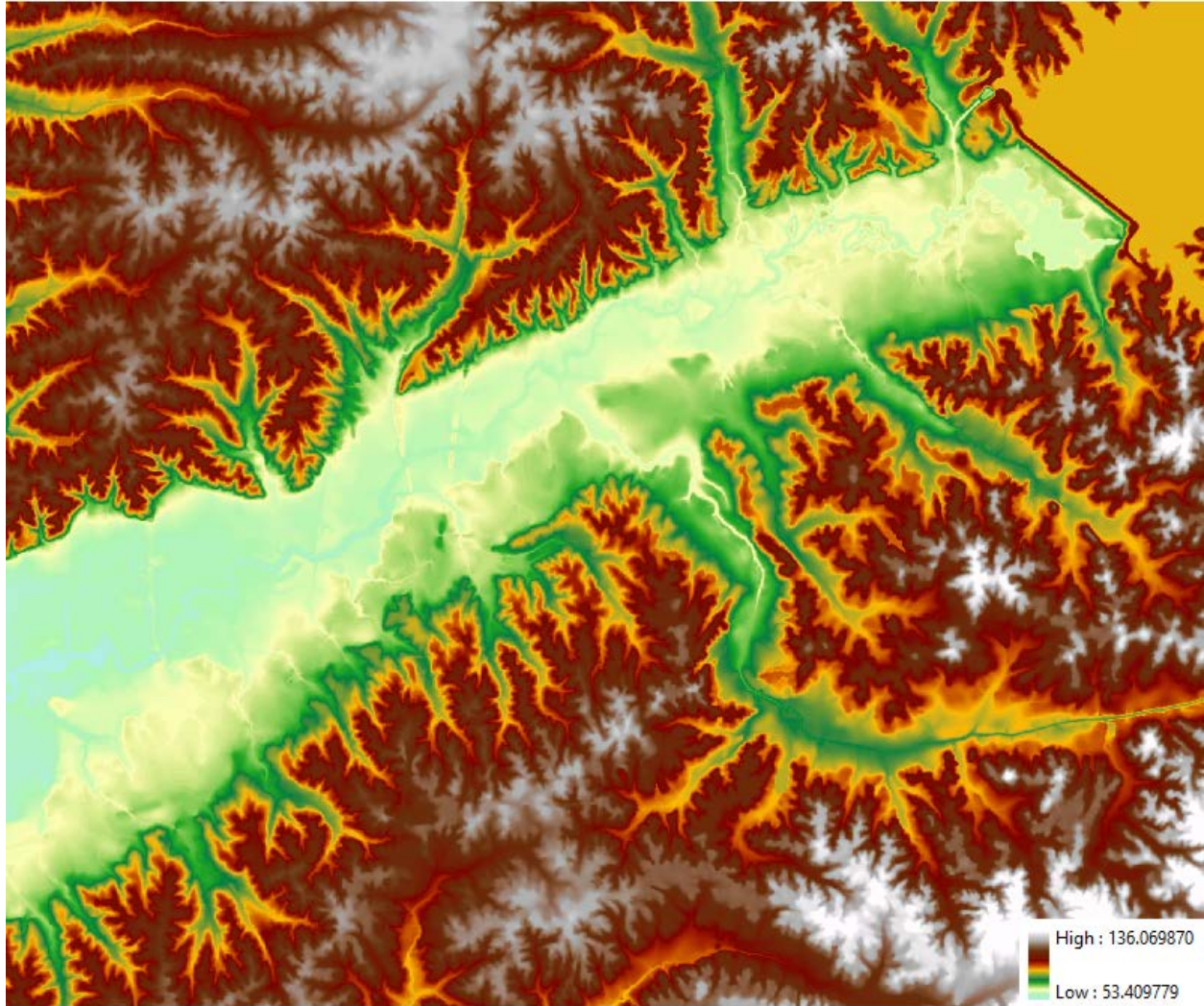


Figure 18 DEM with a resolution of 10 m (structures of interest are not burned into the DEM).

Figure 19 shows the 5 m DEM used for two-dimensional flood simulation, mapping and risk analysis in Testbed No. 2. The 5 m DEM was obtained by resampling the 1/9 arc-second (~3 m) USGS NED data downloaded from the USGS NED website (<http://ned.usgs.gov/>). Bridge openings were cleared to create a free passage for the flow. The structures listed in Section 3.2 were burned into the DEM as elevation. The modified DEM served as the regular Cartesian grid for numerical simulations.

Figure 20 shows the 3 m DEM used for two-dimensional flood simulation, mapping and risk analysis in Testbed No. 2. The 3 m DEM was obtained by resampling the 1/9 arc-second (~3 m) USGS NED data downloaded from the USGS NED website (<http://ned.usgs.gov/>). Bridge openings were cleared to create a free passage for the flow. The structures listed in Section 3.2 were burned into the DEM as elevation. The modified DEM served as the regular Cartesian grid for numerical simulations.

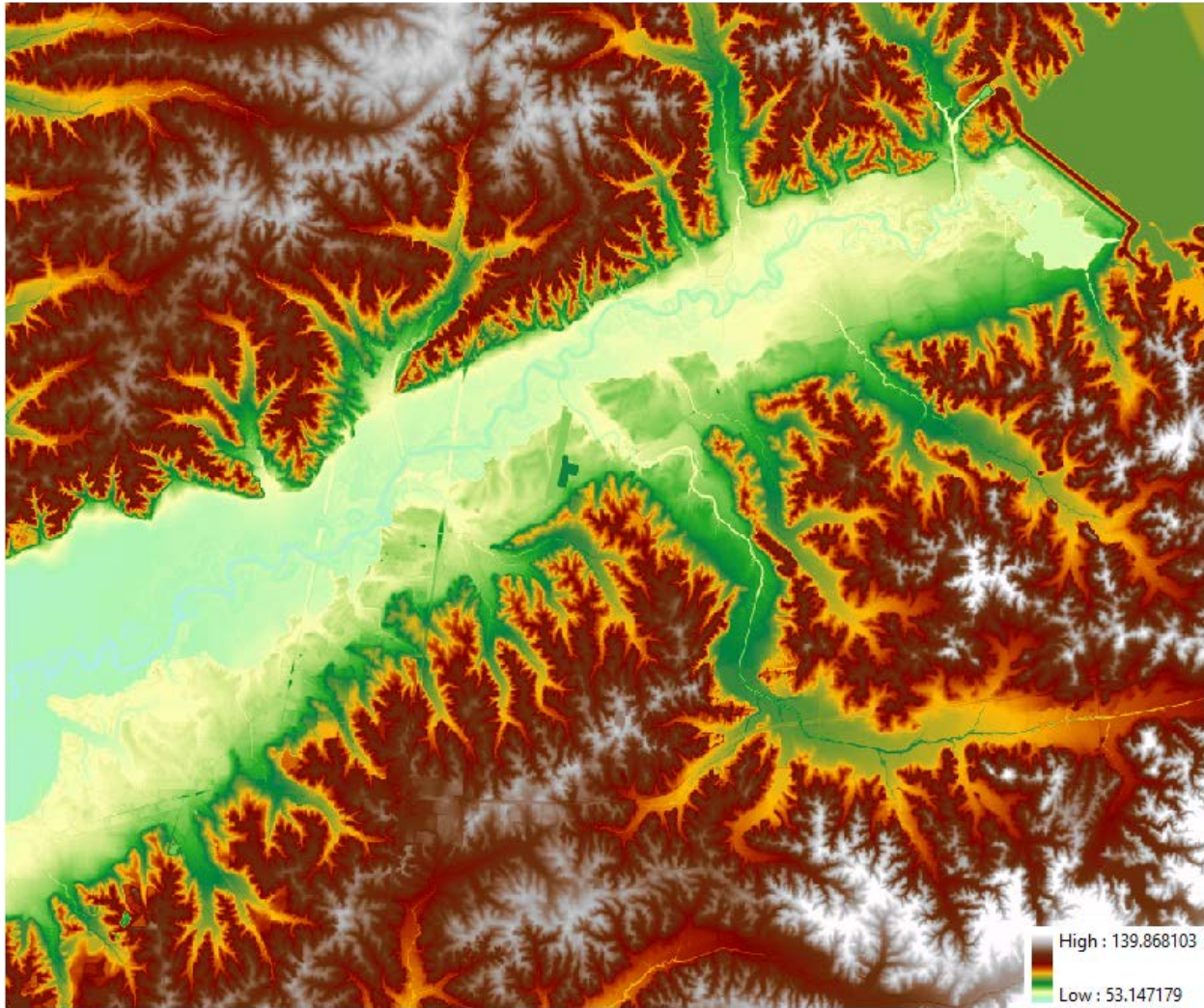


Figure 19 DEM with a resolution of 5 m (structures of interest are burned into the DEM).

Gesch et al (2014) provides information about the vertical accuracy of USGS NED and its comparison with other datasets such as SRTM (Shuttle Radar Topography Mission) and ASTER (Advanced Spaceborne Thermal Emission and Reflection Radiometer). The accuracy of the NED dataset was investigated by comparing it with the highly accurate geodetic control points used by the National Geodetic Survey (NGS) for creating the latest hybrid geoid model called GEOID12A. More than 25,000 geodetic control points spread over the entire North America (Figure 21) were used for assessing the elevation accuracy of USGS NED elevation data.

The investigation using 25,310 geodetic control points (see Figure 22) showed that the absolute vertical accuracy of the data for the conterminous United States has a mean value of -0.29 m with a standard deviation of 1.52 m and a root mean square error (RMSE) value of 1.55 m.

For two-dimensional flood simulation over relatively small areas, the relative vertical accuracy, which is the point-to-point vertical accuracy, is generally more important than the absolute vertical accuracy. Gesch et al. (2014) investigated the relative vertical accuracy of NED elevation using 15,509 points for which the NED elevation and the distance between the points were recorded. When averaged from the 1,068 point pair with point-to-point distances less than 500 m, a relative vertical accuracy has a mean

value of 0.81 m with a standard deviation of 1.19 meters and a 95<sup>th</sup> percentile value of 2.93 m. The mean value of slope accuracy is 0.77° with a 95<sup>th</sup> percentile value of 2.79°.

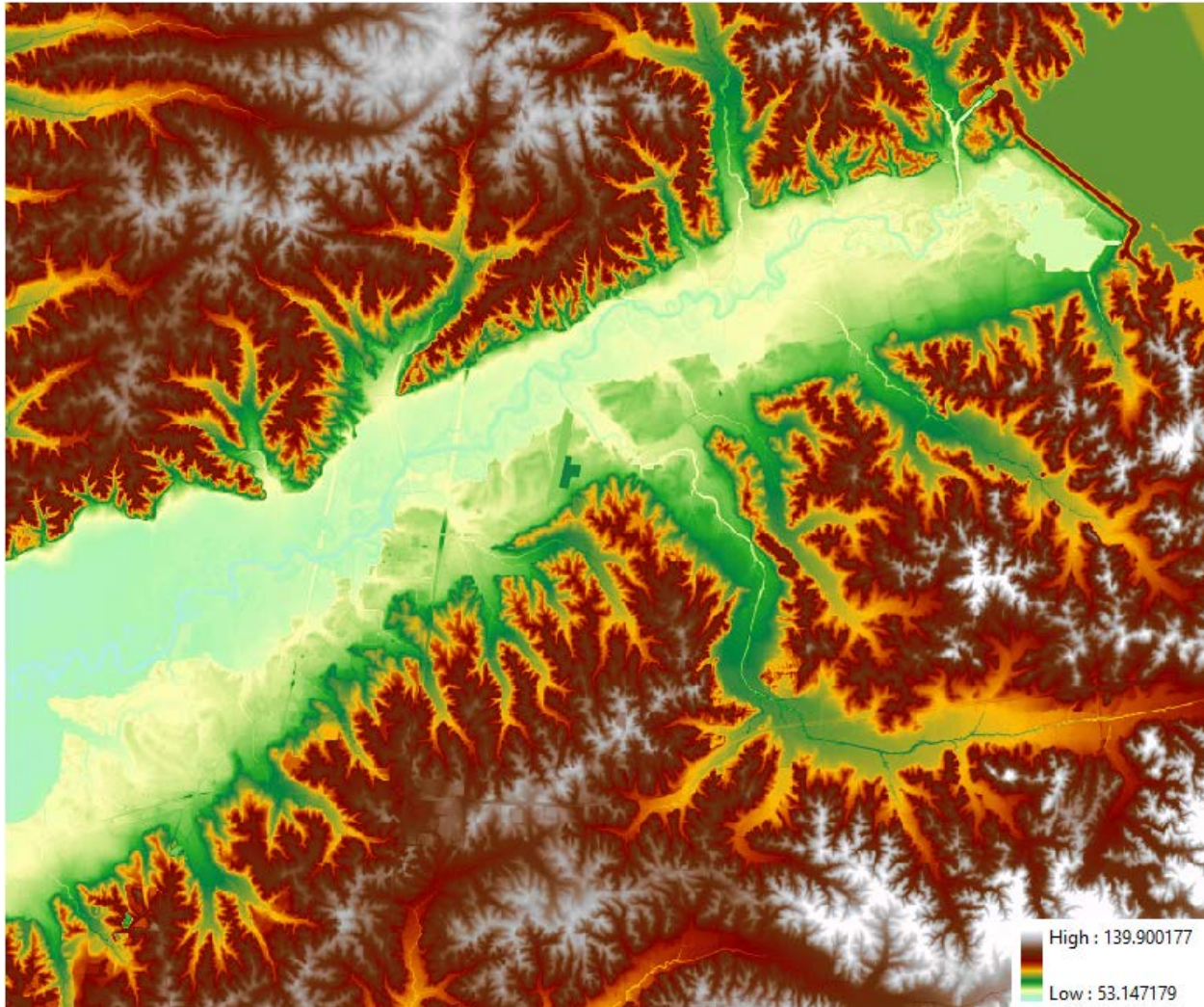


Figure 20 DEM with a resolution of 3 m (structures of interest are burned into the DEM).

Due to the use of a regular Cartesian grid as computational mesh, the structures cannot be burned into the DEM with their exact shape. The smaller the cell size, the better approximated shape of the structure. Figure 23, Figure 24, Figure 25, Figure 26, Figure 27, and Figure 28 show how the six structures listed in Section 3.2 are captured as elevation in DEMs with 5m and 3m resolution. In general, the shape of the structure is better captured with 3 m DEM. Nevertheless, unless the structure is rectangle aligned with north-south or east-west direction, the structured burned into the DEM presents jagged edges. This is an unavoidable but acceptable compromise in the present context. The use of body fitted non-orthogonal coordinate system would lead to unreasonable computational times.

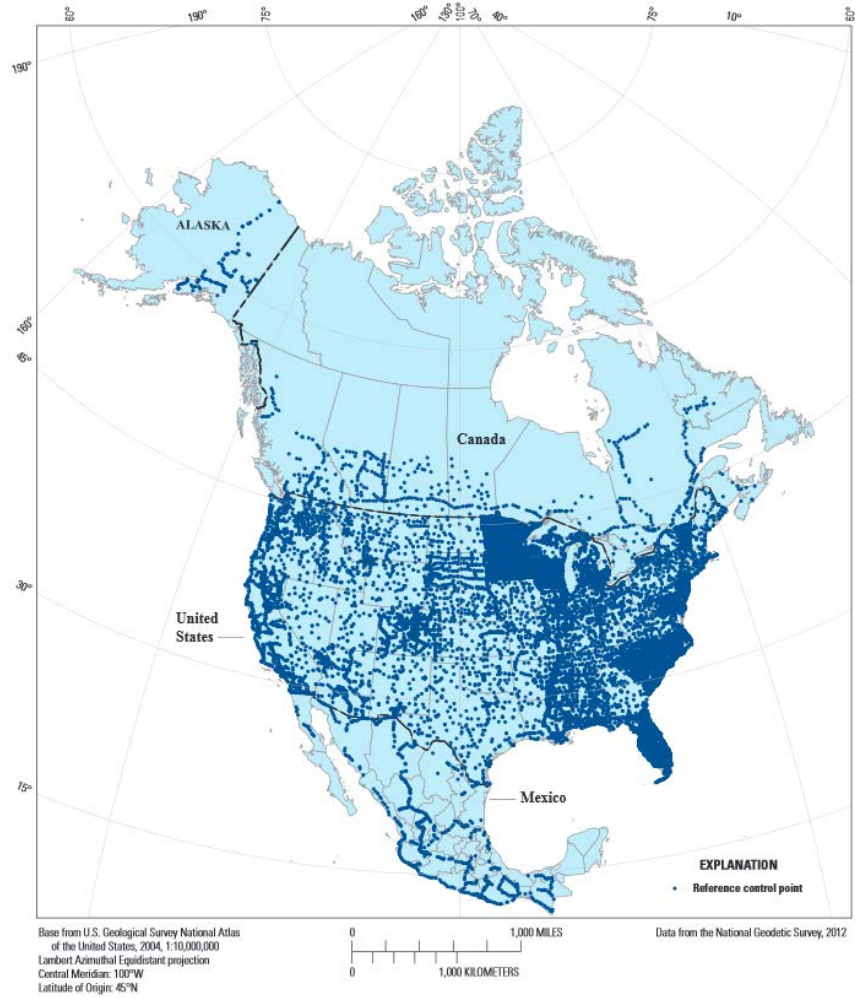


Figure 21 Map showing the locations of NGS geodetic control points used for assessing the vertical accuracy of USGS NED elevation data (taken from Gesch et al. 2014).

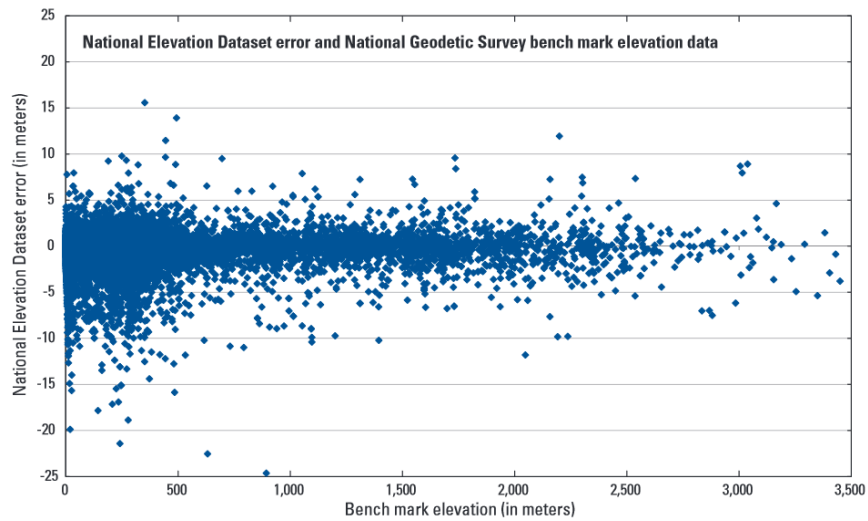


Figure 22 National Elevation Dataset (NED) errors (in meters) plotted against National Geodetic Survey (NGS) bench mark elevation data (taken from Gesch et al. 2014).

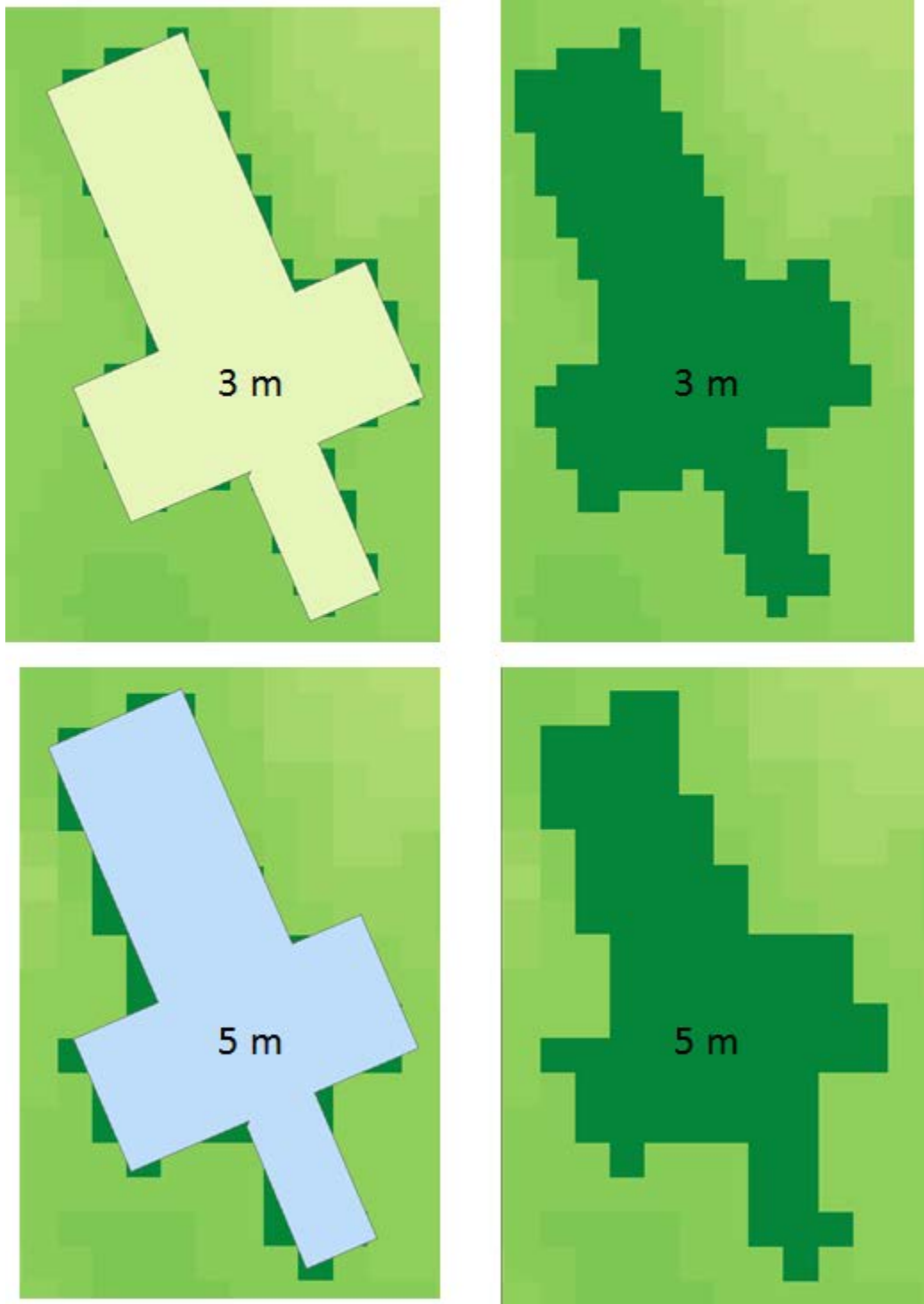


Figure 23 Sardis Lake Baptist Church building represented as elevation in 3m DEM (1<sup>st</sup> row) and 5m DEM (2<sup>nd</sup> row). The polygon in the left images represent the footprint of the building. The images on the right show how the shape of the building is captured as elevation with the cell size of the DEM.

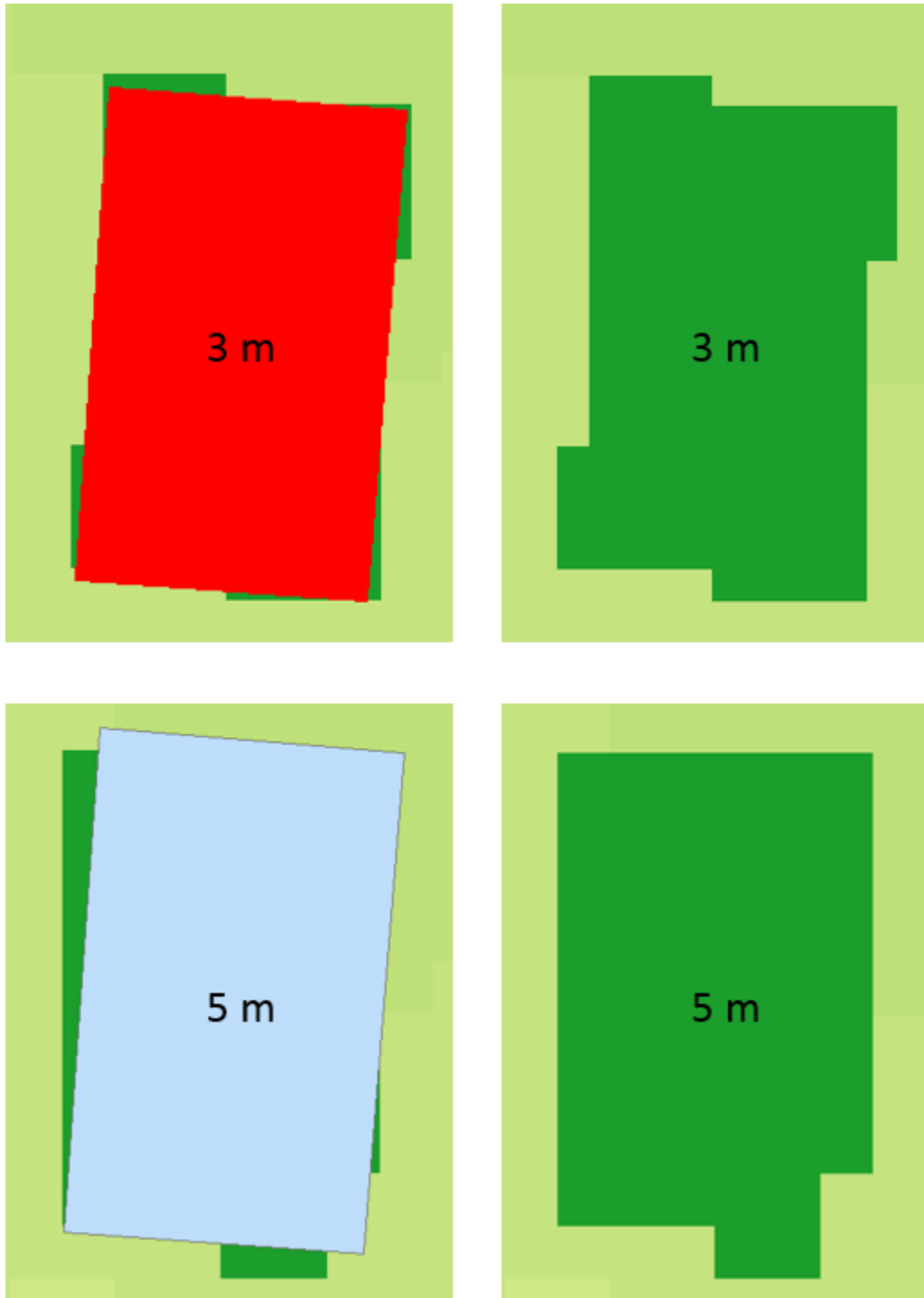


Figure 24 First Baptist Church building represented as elevation in 3m DEM (1<sup>st</sup> row) and 5m DEM (2<sup>nd</sup> row). The polygon in the left images represent the footprint of the building. The images on the right show how the shape of the building is captured as elevation with the cell size of the DEM.

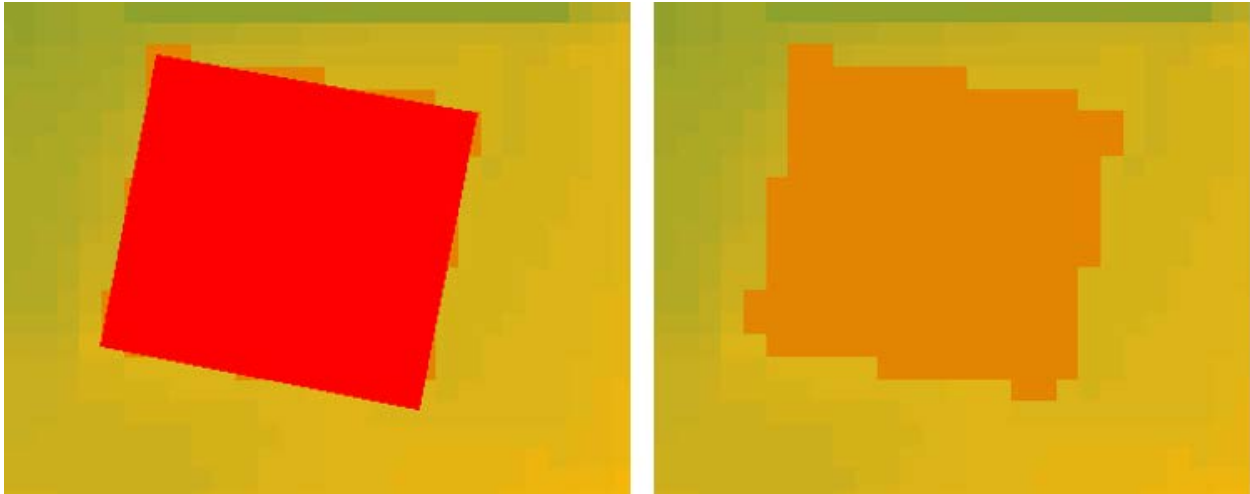


Figure 25 Batesville, MS, Public Library building represented as elevation in 3m DEM (1<sup>st</sup> row) and 5m DEM (2<sup>nd</sup> row). The polygon in the left images represent the footprint of the building. The images on the right show how the shape of the building is captured as elevation with the cell size of the DEM.

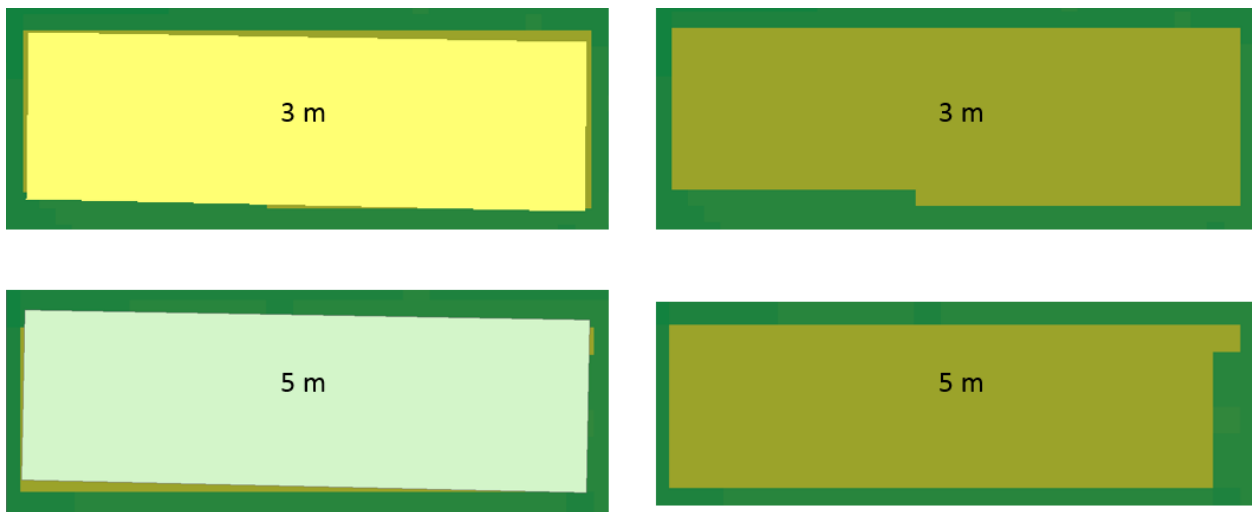


Figure 26 U.S. Forestry Department building represented as elevation in 3m DEM (1st row) and 5m DEM (2nd row). The polygon in the left images represent the footprint of the building. The images on the right show how the shape of the building is captured as elevation with the cell size of the DEM.

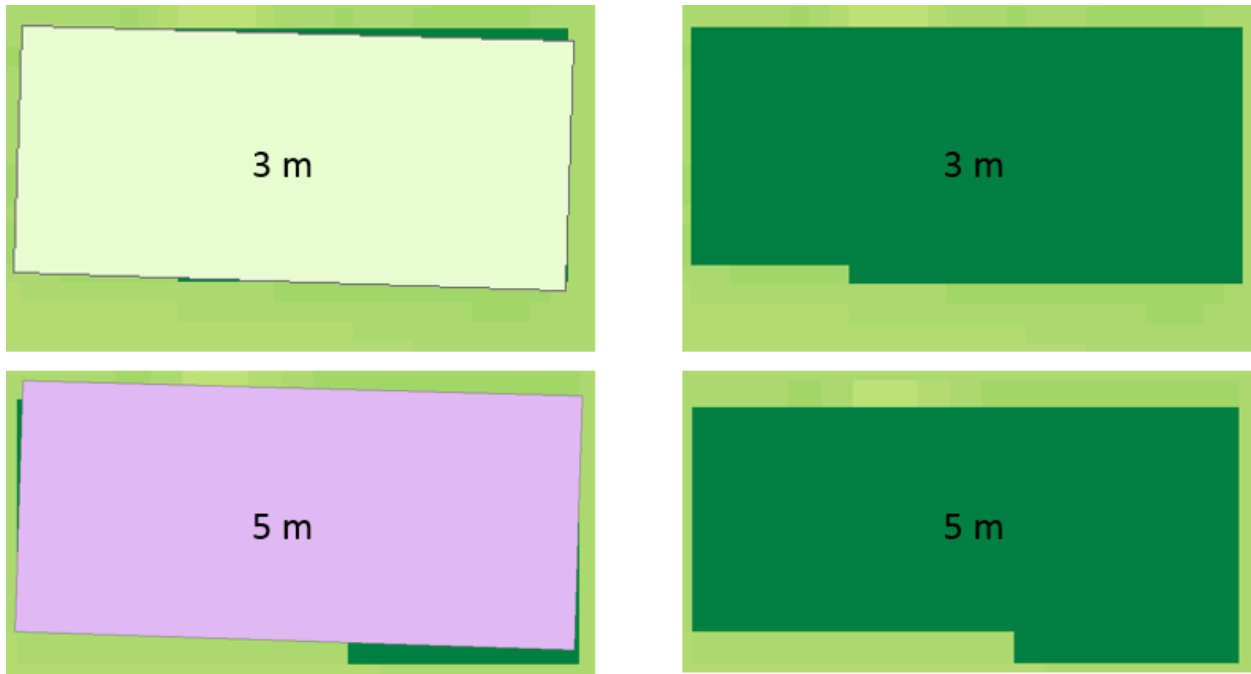


Figure 27 Insituform Technologies Inc. represented as elevation in 3m DEM (1<sup>st</sup> row) and 5m DEM (2<sup>nd</sup> row). The polygon in the left images represent the footprint of the building. The images on the right show how the shape of the building is captured as elevation with the cell size of the DEM.

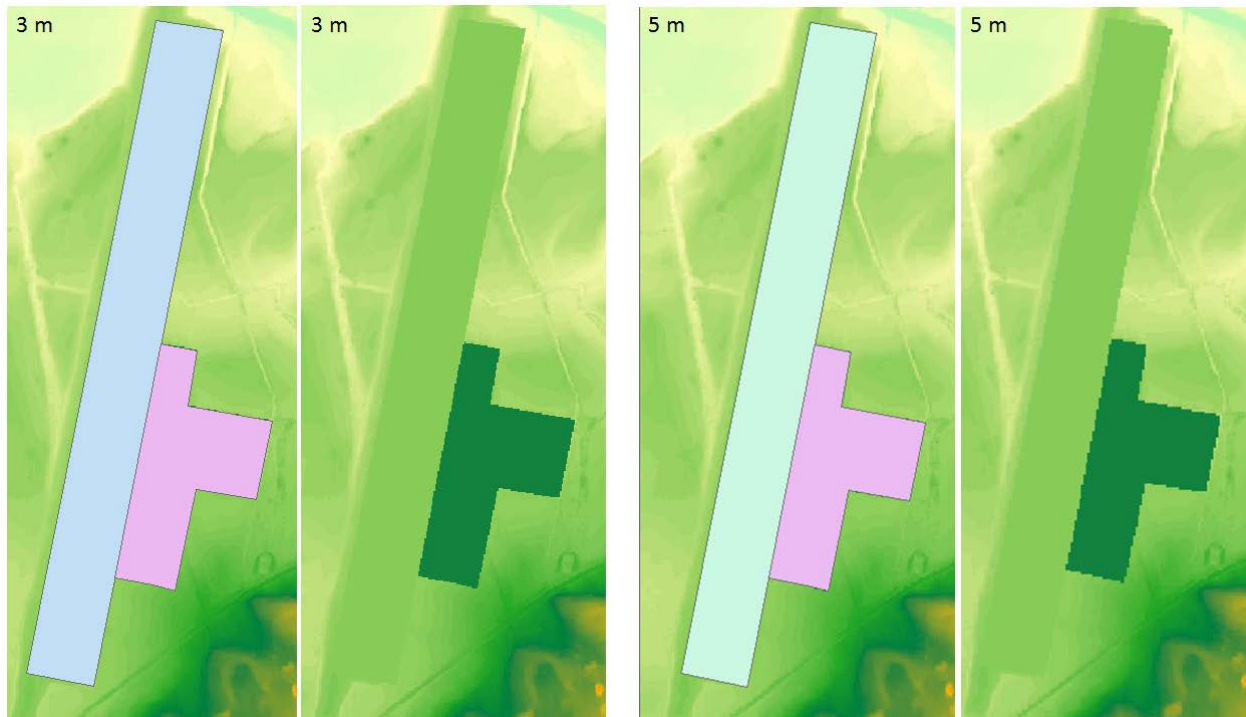


Figure 28 Airport pavement and terminal buildings represented as elevation in 3m DEM (left two images) and 5m DEM (right two images). The polygons represent the footprint of the building. The images without the polygon show how the shape of the building is captured as elevation with the cell size of the DEM.

## Chapter 4 Results Files Produced by the Simulations with DSS-WISE

The simulations with DSS-WISE™ produce a variety of results files. For the present study the results files produced by the simulations can be listed in three general categories:

1. Geo-referenced raster files and shapefiles (general risk mapping)
  - a. Extent of the flood
  - b. Map of maximum flood depths (maximum depth achieved during the simulation)
  - c. Map of flood arrival time (dry area becoming wet regardless of the depth of flow)
  - d. Map of maximum specific discharge (velocity times depth), which also gives an idea about the momentum
  
2. Time series data (csv files) at selected locations (especially for evaluation of potential impacts to structures, transportation network, and buildings)
  - a. Discharge hydrographs at selected cross sections  
To extract discharge hydrograph at a cross section DSS-WISE™ provides the user with the capability of defining “Observation Lines”. An observation line can be a straight line or a polyline. The program records the discharge crossing the line (flow perpendicular to the observation line) in both directions as a function of time. Results for each observation line are made available as a comma separated file (csv file) at the end of the simulation. Detailed information on observation lines, the contents of a typical csv output file and the list of the observation lines defined for the present study are provided in Section 4.1.
  - b. Time history of flow depth, flood water surface elevation, velocity components and magnitude and flow direction at selected observation locations  
DSS-WISE™ allows the user to specify an unlimited number of “Observation Points” in the computational domain to extract information as a function of time. Results for each observation point are made available as a comma separated file (csv file) at the end of the simulation. Detailed information on observation points, the contents of a typical csv output file and the list of the observation points defined for the present study are provided in Section 4.2.
  - c. Time history of flow depth, velocity vector (x and y components) along specified longitudinal profile  
DSS-WISE™ provides the capability of defining a polyline in the computational domain for along which the flow data is extracted as a function of time at a user specified number of regularly spaced points. The observation lines are generally used to gain a longitudinal profile view of the evolution of flow along a specified path. The extracted flow data includes depth and tangential velocity. The results for each observation profile is made available as a comma separated file (csv file) at the end of the simulation. Detailed information on observation lines, the contents of a typical csv output file and the list of the observation lines defined for the present study are provided in Section 4.3.
  
3. Products for easy dissemination of results and information
  - a. KMZ file of the results for visualization on Google Earth (does not necessitate any special software)  
DSS-WISE™ produces KMZ files of the simulation results to be viewed on Google Earth. Since Google Earth is a freely available software and only requires a computer with an internet connection, KMZ files provide an excellent way to disseminate information to local authorities and to the general public. Moreover, the KZ files can be published on the internet for web-access or can be viewed on tablets and smart phones.

Figure 29 shows the KMZ file of the results of the simulation with the 3 m DEM as viewed on Google Earth. The KMZ file of results contain multiple layers that can be turned on or off individually. These layers are listed in the left panel. When the KMZ file is first uploaded, by default the maximum depth map is displayed along with observation lines, observation points and observation profiles.

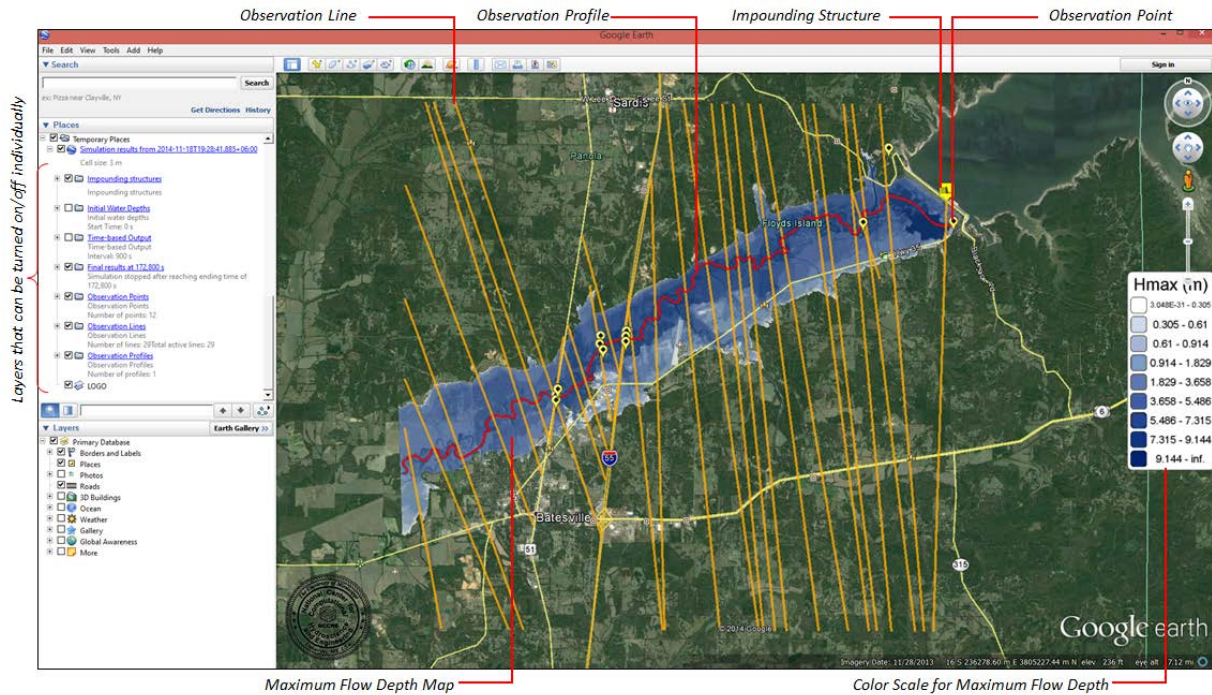


Figure 29 KMZ file for the simulation results with the 3 m DEM as viewed on Google Earth.

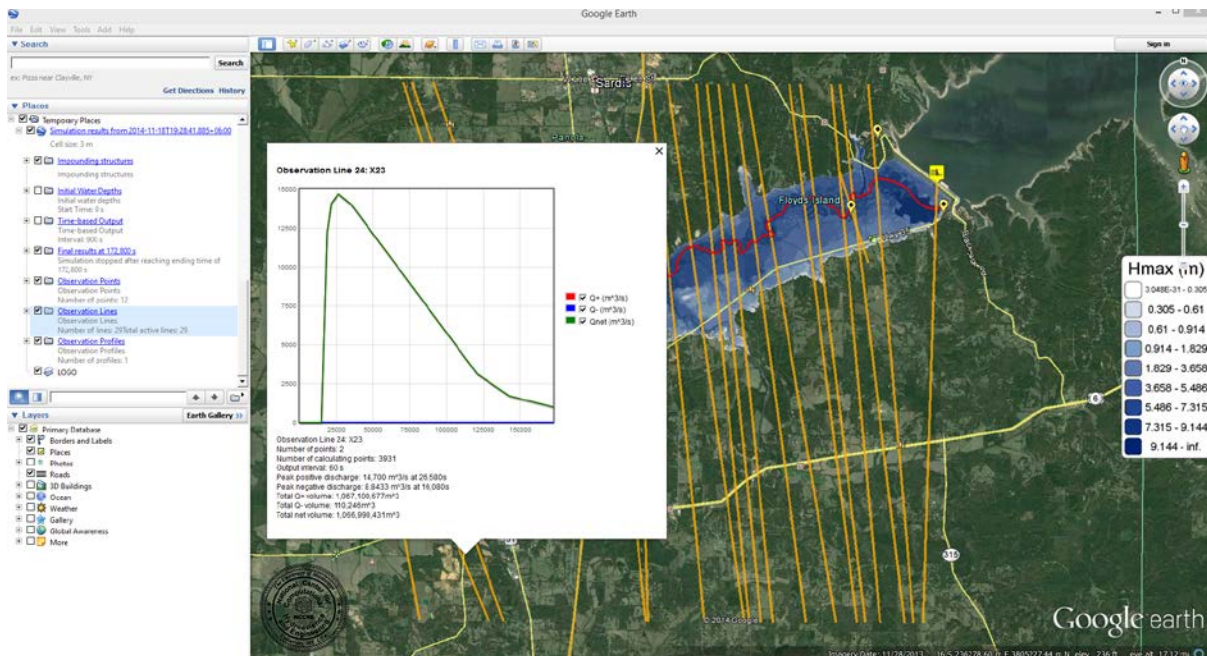


Figure 30 Flow discharge crossing any observation line can be displayed by clicking on it.

The discharge hydrograph crossing any observation line can be displayed by simply clicking on it (Figure 30). Similarly, the variation of the flow depth at any observation point can be visualized by clicking on it (Figure 31).

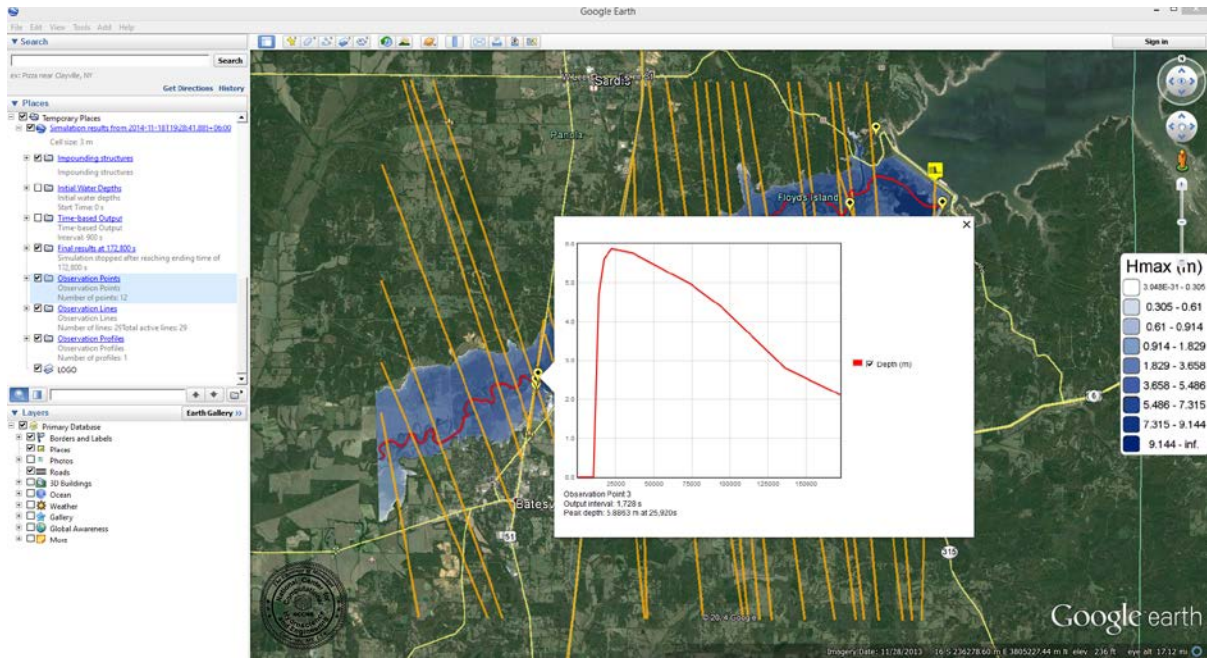


Figure 31 Variation of the flow depth at any observation point can be displayed simply by clicking on it.

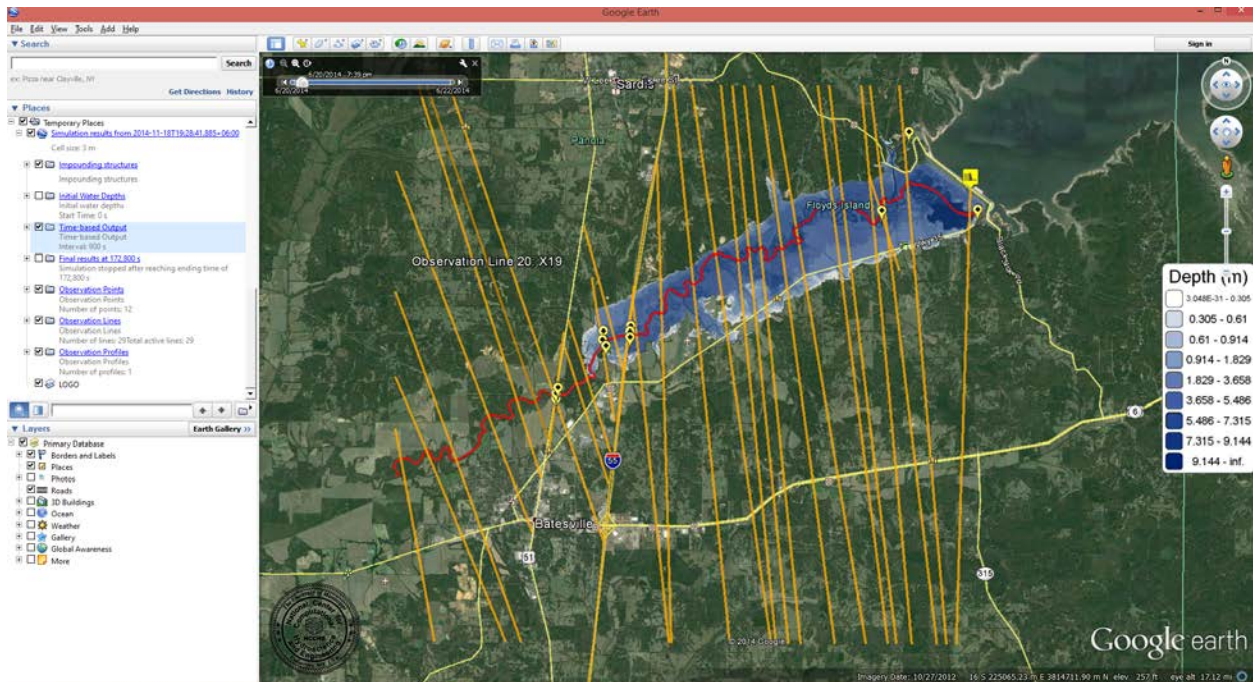


Figure 32 Animation of the propagation of the flood in Google Earth.

The KMZ file also provides the possibility of animating the propagation of the flood. In Figure 32, the final results layer is turned off and the “Time-based Output” layer is turned on. The slider on the top left corner of the display controls the animation.

#### 4.1 Observation Lines

A total of 29 observation lines were defined to record the cross sectional discharge. Figure 33 shows the locations of the observation lines on the computational mesh. Labels of the observation lines are also indicated in this figure. The list of all the observation lines is provided in Table 3. Figure 34 shows all 29 observation lines on Google Earth image.

Since, the simulation is two dimensional, return flows are possible in a cross section. The flow may be crossing the cross section line in both direction. Therefore, the DSS-WISE software records the discharges crossing an observation line in each direction separately as a function of the line.

According to the convention used in DSS-WISE, the positive direction is defined as the right side while going from the first vertex to the last vertex (in the present case the observation lines were straight lines and there are only two vertices). The Little Tallahatchie River immediately downstream of Sardis Dam is flowing in the east to south direction. The observation lines were defined with the first vertex on the north side (on the side of the right bank) and the second vertex on the south side (left bank side). The positive flow direction for the observation lines, therefore, points to the downstream of the river (westward).

A typical output file for an observation line is shown in Table 2. The first column contains the time in seconds since the beginning of the simulation. The results are output at approximately every 60 seconds. The second and third columns contain the total discharges crossing the observation line in positive and negative directions. The fourth and fifth columns contain the total lengths of the observation line with positive and negative discharges.

Table 2 Output file for cross section X0.

X0				
Time (s)	Q+ (m <sup>3</sup> /s)	Q- (m <sup>3</sup> /s)	L+ (m)	L- (m)
0.50	0.00E+00	0.00E+00	0.00E+00	0.00E+00
60.18	6.05E+03	0.00E+00	2.90E+02	0.00E+00
120.14	7.26E+03	1.76E+02	5.85E+02	1.15E+02
180.10	8.48E+03	2.37E+02	7.80E+02	1.60E+02
....	....	....	....	....
172500.11	9.74E+03	2.60E+02	1.18E+03	8.40E+02
172560.01	9.74E+03	2.60E+02	1.18E+03	8.40E+02
172620.13	9.74E+03	2.60E+02	1.18E+03	8.40E+02
172680.08	9.74E+03	2.60E+02	1.18E+03	8.40E+02
172740.05	9.74E+03	2.60E+02	1.18E+03	8.45E+02
172800.05	9.74E+03	2.59E+02	1.18E+03	8.45E+02

Special attention was given to place observation lines near bridges crossing the Little Tallahatchie River in order to be able to evaluate the flow conditions. There are three bridges considered in the present study. Figure 35 shows the locations of these three bridges. The positions of the observation lines with respect to I-55 Bridge, Railroad Bridge, and US-51 Bridge crossing the Little Tallahatchie River are shown in Figure 36, Figure 37, and Figure 38, respectively.

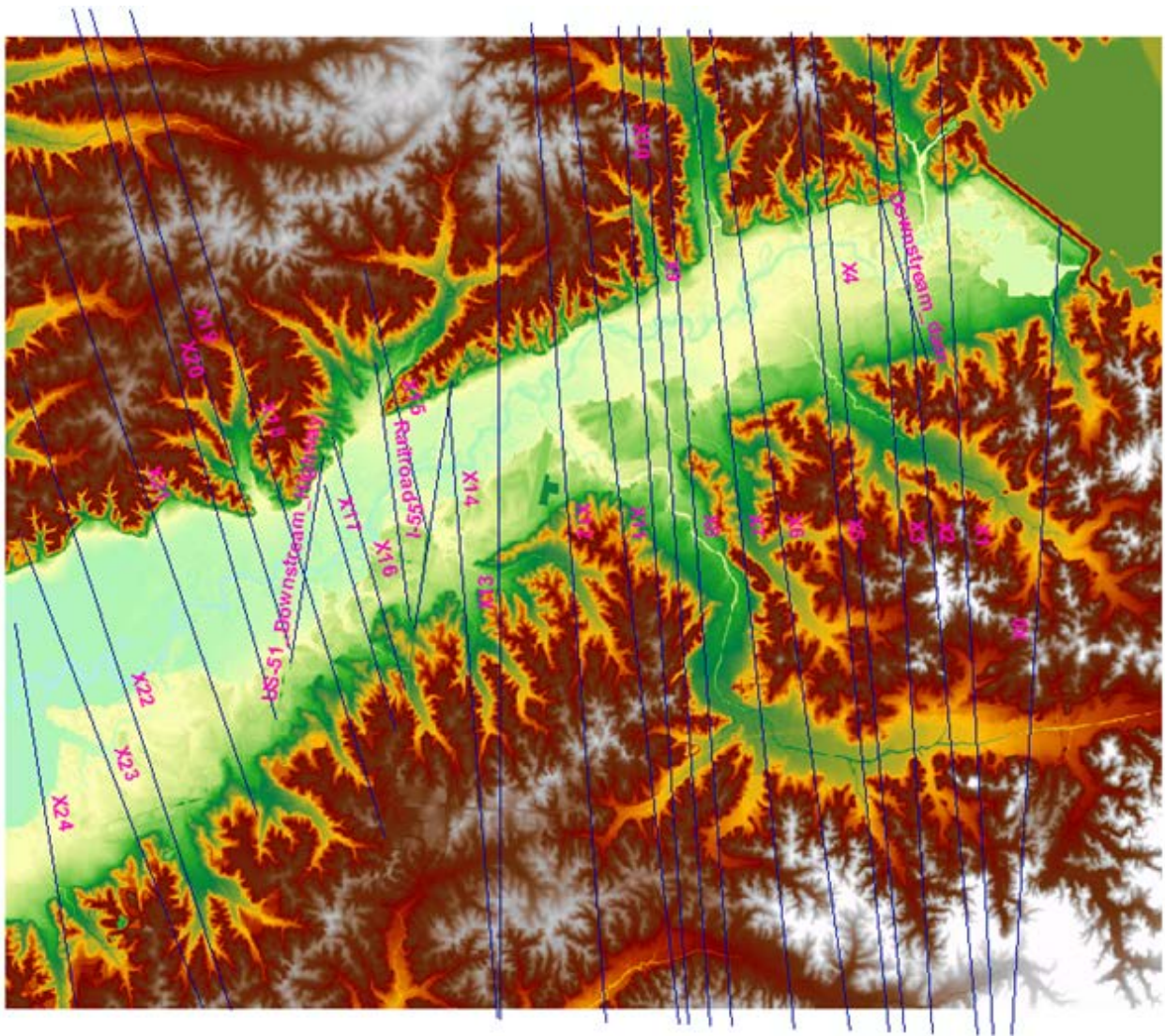


Figure 33 Locations of observation lines on the computational mesh.

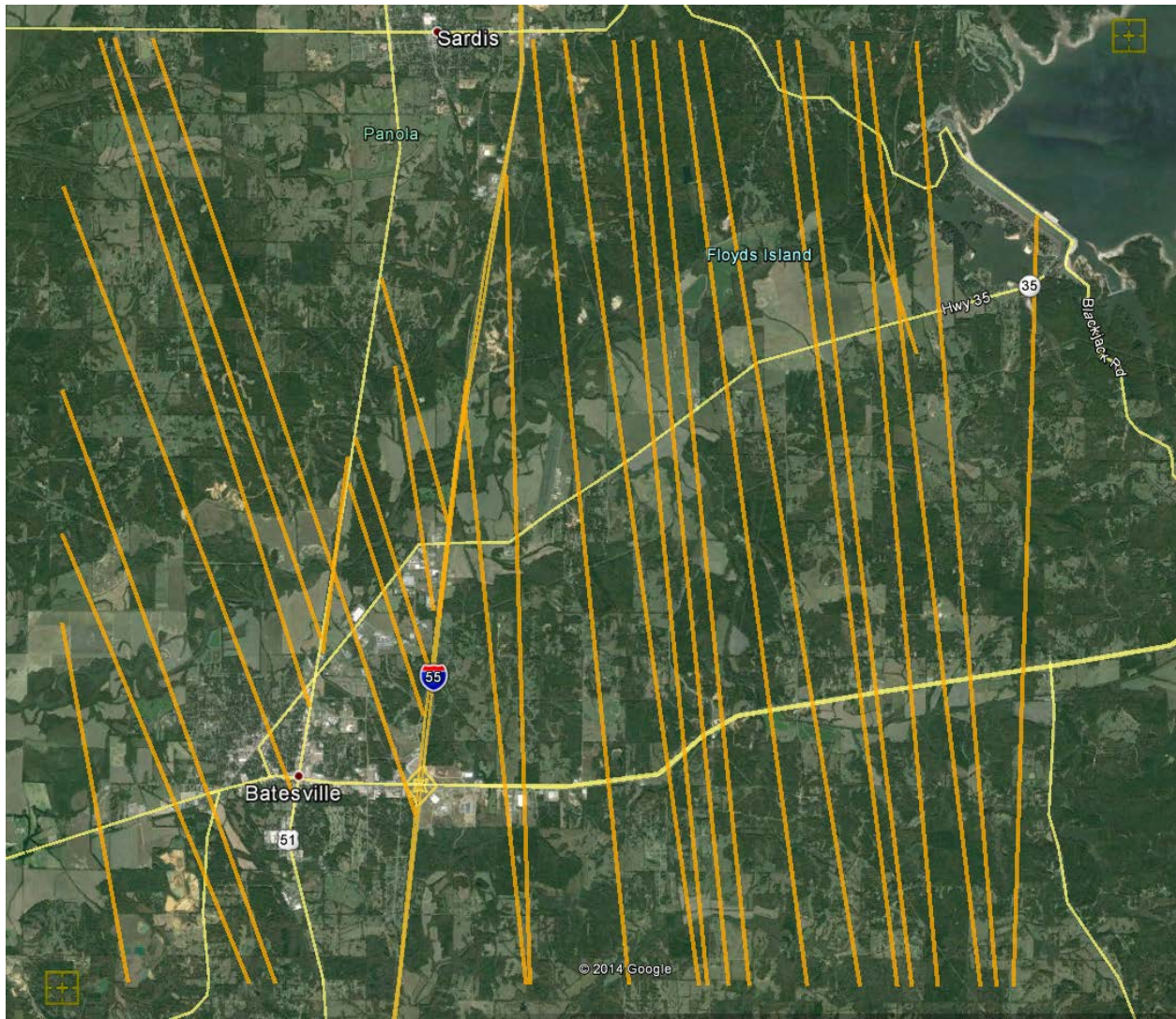


Figure 34 Google Earth image showing the locations of the observation lines (see also Figure 33).

Table 3 List of observation lines at which the computed discharge hydrograph is recorded.

No	River CL Point	CL Coordinates		X section number	X-section North Coordinates		X-section South Coordinates		Remarks
		Longitude	Latitude		Longitude	Latitude	Longitude	Latitude	
1	4	-89.793588	34.398684	X0	-89.793298	34.406103	-89.798379	34.275938	North Side of X-section terminates at the west edge of sardis dam
2	17	-89.815124	34.407665	X1	-89.817945	34.435498	-89.801799	34.275953	
3	50	-89.823469	34.403379	X2	-89.828118	34.435540	-89.805083	34.275968	
4	82	-89.826864	34.396081	X3	-89.831176	34.435553	-89.813773	34.276005	
5	118	-89.837412	34.402003	X4	-89.842313	34.435598	-89.819068	34.276027	
6	135	-89.841020	34.401078	X5	-89.846268	34.435614	-89.822055	34.276040	
7	186	-89.853685	34.395090	X6	-89.861908	34.435675	-89.829646	34.276071	
8	232	-89.858687	34.388865	X7	-89.866284	34.435692	-89.840431	34.276115	
9	285	-89.866077	34.389267	X8	-89.871765	34.435713	-89.852253	34.276162	
10	304	-89.870193	34.389256	X9	-89.875847	34.435728	-89.856460	34.276178	
11	334	-89.873841	34.385732	X10	-89.879824	34.435743	-89.860762	34.276195	
12	377	-89.881575	34.387248	X11	-89.889935	34.435780	-89.862480	34.276202	
13	420	-89.889377	34.378792	X12	-89.896413	34.435804	-89.876746	34.276256	
14	494	-89.900384	34.370484	X13	-89.901923	34.413030	-89.896983	34.276329	North Side of this X-section terminates at the east edge of I-55
15	533	-89.909119	34.364347	X14	-89.910391	34.374213	-89.897790	34.276332	North Side of this X-section terminates at the east edge of I-55
16	543	-89.916826	34.363563	X15	-89.927328	34.395521	-89.913694	34.354028	North Side of this X-section terminates at the east edge of US-51 and South Side of it terminates at the west edge of I-55
17	613	-89.926381	34.352202	X16	-89.932735	34.368661	-89.917281	34.328615	North Side of this X-section terminates at the east edge of US-51 and South Side of it terminates at the west edge of I-55
18	629	-89.929919	34.350436	X17	-89.934011	34.360894	-89.918692	34.321734	North Side of this X-section terminates at the east edge of US-51 and South Side of it terminates at the west edge of I-55
19	653	-89.937384	34.346497	X18	-89.974194	34.436057	-89.920289	34.304835	South Side of this X-section terminates at the west edge of I-55
20	678	-89.944112	34.345224	X19	-89.982043	34.436079	-89.939639	34.334497	South Side of this X-section terminates at the west edge of US-51
21	698	-89.950648	34.345749	X20	-89.985091	34.436088	-89.942035	34.323125	South Side of this X-section terminates at the west edge of US-51
22	749	-89.960425	34.341166	X21	-89.992473	34.411033	-89.945095	34.307701	South Side of this X-section terminates at the west edge of US-51
23	797	-89.971580	34.328449	X22	-89.992612	34.376618	-89.948928	34.276503	
24	841	-89.981974	34.331225	X23	-89.992711	34.352382	-89.954237	34.276520	
25	862	-89.990841	34.328832	X24	-89.992771	34.337386	-89.979065	34.276594	
26		-89.937165	34.346574	US-51 Downstream Highway	-89.934226	34.365392	-89.939408	34.332209	
27		-89.921109	34.362346	Railroad	-89.924605	34.380675	-89.916796	34.339377	
28		-89.911907	34.364275	I-55	-89.909935	34.378371	-89.915548	34.338190	
29		-89.824071	34.398761	Downstream_dam	-89.828301	34.409725	-89.817946	34.382664	

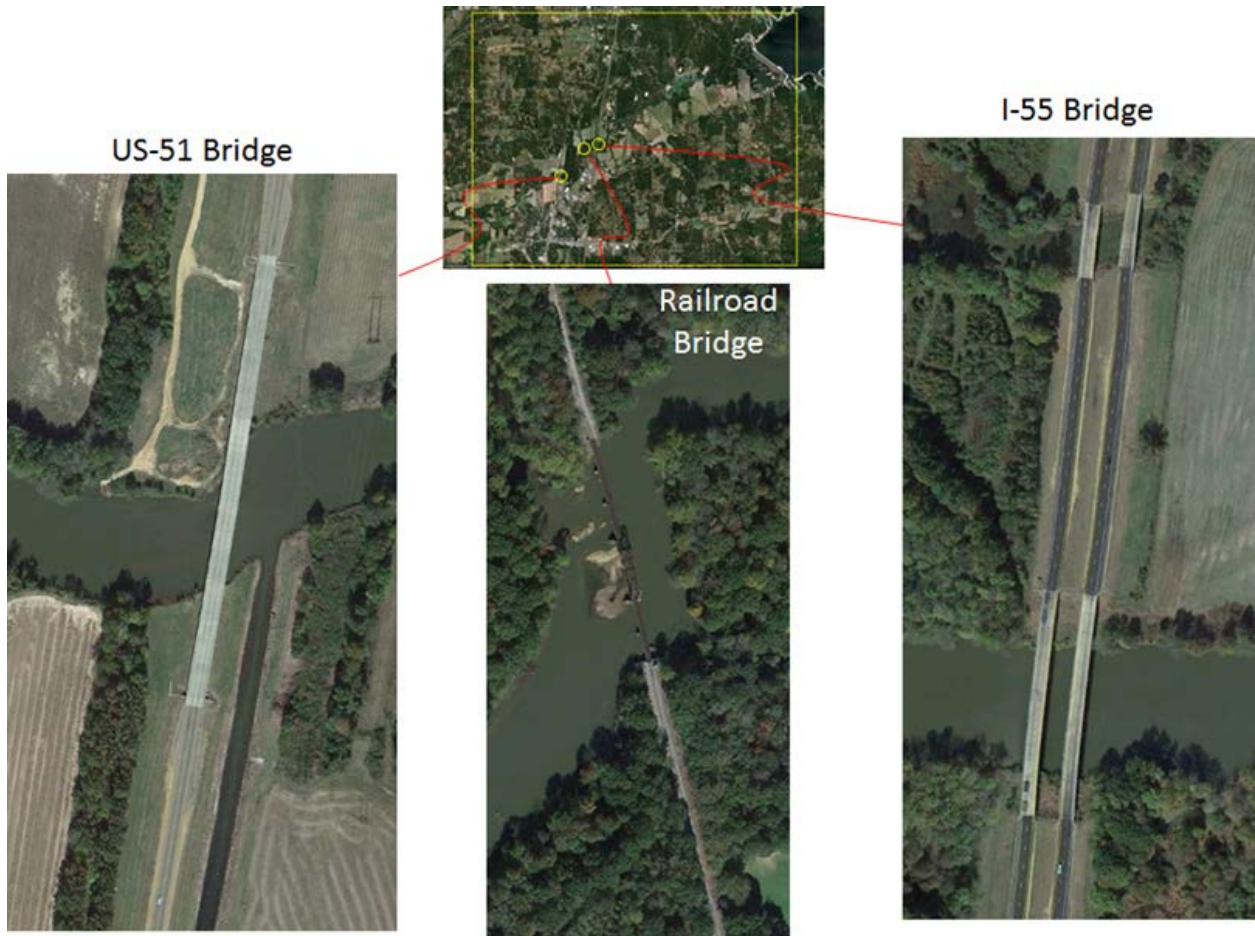


Figure 35 Google Earth images of the three bridges located in the computational domain.



Figure 36 I-55 bridge crossing the Little Tallahatchie River and the observation lines X14, I-55, and X15.



Figure 37 Railroad Bridge crossing the Little Tallahatchie River and the observation lines X15, Railroad, and X16.



Figure 38 US-51 bridge crossing the Little Tallahatchie River and the observation lines X117, US-51\_Down-stream\_Highway, X18, and X19.

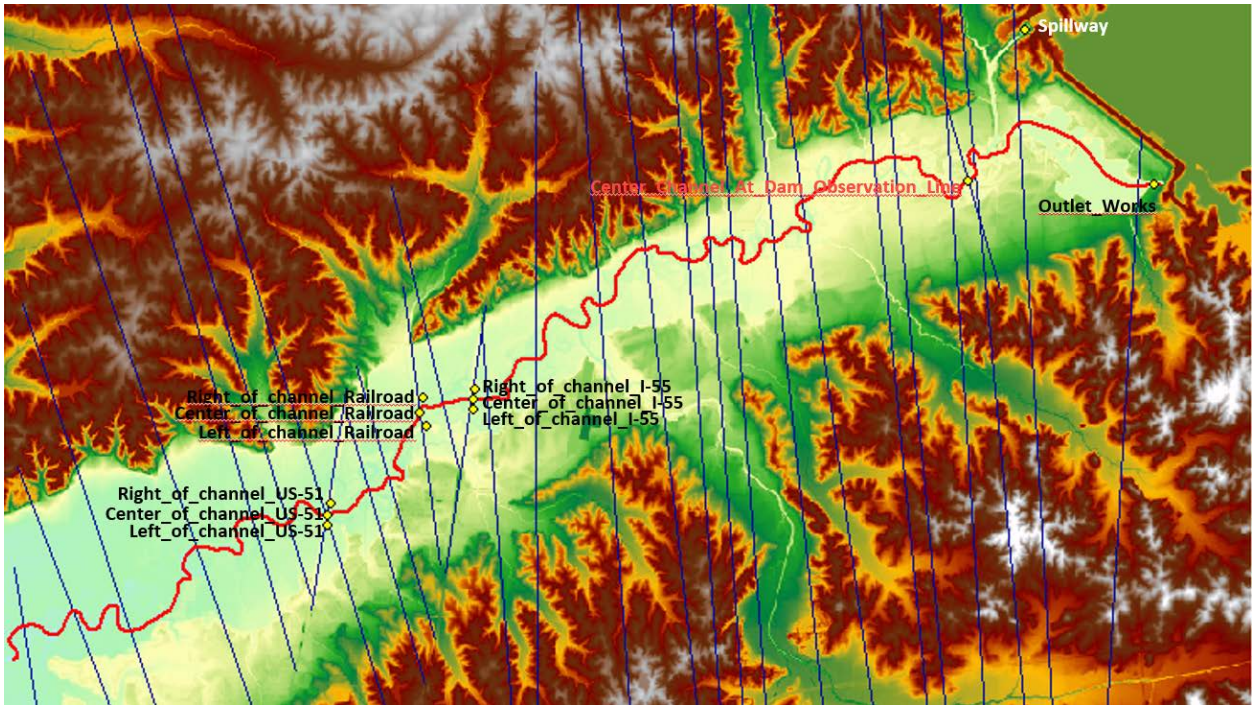


Figure 39 Locations of observation points on the computational mesh.

## 4.2 Observation Points

A total of 12 observation points were defined to record the flow depth, the two velocity components in the horizontal plane (x and y components) and the bed elevation. The list of all observation points are given in Table 4. Figure 39 shows the locations of the observation points on the computational domain. Figure 40 shows the locations of the observation points on the Google Earth image. Referring also to Table 4, the observation points 1 to 3 are located on the I-55 Bridge, observation points 4 to 6 are on the Railroad Bridge, and observation points 7 to 9 are on the US-51 Bridge. The flow depth and flow velocity direction information recorded at these observation points will be used in assessing the potential damage level to the bridges.

Table 4 List of observation points.

No	Longitude	Latitude	Description
1	232278.0566	3806563.894	Right_of_channel_I-55
2	232249.2575	3806391.099	Center_channel_I-55
3	232244.8269	3806211.658	Left_of_channel_I-55
4	231400.7903	3806428.76	Right_of_channel_Railroad
5	231360.9145	3806158.491	Center_channel_Railroad
6	231469.4652	3805959.112	Left_of_channel_Railroad
7	229899.7891	3804677.411	Right_of_channel_US-51
8	229834.991	3804491.324	Center_channel_US-51
9	229825.022	3804310.222	Left_of_channel_US-51
10	240393.3865	3809991.408	Center_Channel_At_Dam_Obs_Line
11	243453.4807	3809935.286	Outlet_Works
12	241329.7281	3812457.796	Spillway

Table 5 Contents of the output file for the first observation point.

Left_of_channel_US-51				
Time (s)	H (m)	U (m/s)	V (m/s)	Zb (m)
0.50	0.00E+00	0.00E+00	0.00E+00	5.96E+01
1728.07	0.00E+00	0.00E+00	0.00E+00	5.96E+01
3456.15	0.00E+00	0.00E+00	0.00E+00	5.96E+01
5184.10	0.00E+00	0.00E+00	0.00E+00	5.96E+01
6912.01	0.00E+00	0.00E+00	0.00E+00	5.96E+01
8640.11	2.16E+00	-4.98E-01	-9.70E-01	5.96E+01
10368.08	3.69E+00	-1.48E+00	-1.61E+00	5.96E+01
....	....	....	....	....
167616.11	6.34E+00	-2.43E+00	-1.93E+00	5.96E+01
169344.13	6.27E+00	-2.40E+00	-1.92E+00	5.96E+01
171072.13	6.19E+00	-2.38E+00	-1.91E+00	5.96E+01
172800.05	6.10E+00	-2.35E+00	-1.89E+00	5.96E+01

The structure and the contents of the output file for an observation point are shown in Table 5. The first column contains the time in seconds since the beginning of the simulation. As it can be seen, the results are output at approximately every 29 minutes. The second column contains the flow depth. The velocity components in x (west-east) and y (south-north) directions are in third and fourth columns, respectively. Finally, the fifth column is the bed elevation, which remains constant throughout the simulation in the present case.

### 4.3 Observation Profile

One observation profile is defined along the thalweg line of the Little Tallahatchie River downstream of the Sardis Dam. Thalweg is a widely used hydraulic term that comes from German. It is a combination of the words "thal" (meaning valley) and "weg" (meaning road). Literal translation of Thalweg from German means the "valley road" or road that follows the lowest points of the valley, or the bottom of the valley. In hydraulics it is used to name the imaginary line that joins the lowest points of the cross sections along the entire length of a stream. In the present case the thalweg line is represented by the centerline of the stream.

The observation profile is a polyline defined by 877 vertices (Figure 40). The DSS-WISE software was programmed to provide the depth and tangential velocity at 6070 points spaced at 5m intervals along the observation line at every hour. The output file for the observation profile is shown in Table 6 together with explanations on the left.

Table 6 Structure of the output file for the observation profile along the thalweg line (centerline).

	Channel_CL					
	Time (s)	X (m)	Y (m)	Distance (m)	H (m)	V-tangential (m/s)
Initial values T = 0 hr 6070 lines	0.50	2.44E+05	3.81E+06	2.50E+00	0.00E+00	0.00E+00
	0.50	2.44E+05	3.81E+06	7.50E+00	0.00E+00	0.00E+00
	0.50	2.44E+05	3.81E+06	1.25E+01	0.00E+00	0.00E+00
	0.50	2.44E+05	3.81E+06	1.75E+01	0.00E+00	0.00E+00
	...	...	...	...	...	...
	0.50	2.25E+05	3.80E+06	30342.50	0.00E+00	0.00E+00
Results for T = 1 hr 6070 lines	0.50	2.25E+05	3.80E+06	30347.50	0.00E+00	0.00E+00
	3600.05	2.44E+05	3.81E+06	2.50	9.60E+00	1.10E+01
	3600.05	2.44E+05	3.81E+06	7.50	8.38E+00	1.19E+01
	...	...	...	...	...	...
	3600.05	2.25E+05	3.80E+06	30342.50	0.00E+00	0.00E+00
	3600.05	2.25E+05	3.80E+06	30347.50	0.00E+00	0.00E+00
Results for 2 hr ≤ T ≤ 46 hr 45×6070 lines	7200.01	2.44E+05	3.81E+06	2.50	9.60E+00	1.10E+01
	7200.01	2.44E+05	3.81E+06	7.50	8.38E+00	1.19E+01
	...	...	...	...	...	...
	...	...	...	...	...	...
	...	...	...	...	...	...
	165600.05	2.25E+05	3.80E+06	30342.50	6.57E+00	2.87E+00
165600.05	2.25E+05	3.80E+06	30347.50	6.63E+00	2.88E+00	
Results for T = 47 hr 6070 lines	169200.00	2.44E+05	3.81E+06	2.50	9.60E+00	1.10E+01
	169200.00	2.44E+05	3.81E+06	7.50	8.38E+00	1.19E+01
	...	...	...	...	...	...
	169200.00	2.25E+05	3.80E+06	30342.50	6.48E+00	2.83E+00
	169200.00	2.25E+05	3.80E+06	30347.50	6.54E+00	2.85E+00
	172800.05	2.44E+05	3.81E+06	2.50	9.60E+00	1.10E+01
Results for T = 48 hr 6070 lines simulation ends	172800.05	2.44E+05	3.81E+06	7.50	8.38E+00	1.19E+01
	...	...	...	...	...	...
	172800.05	2.25E+05	3.80E+06	30342.50	6.35E+00	2.78E+00
	172800.05	2.25E+05	3.80E+06	30347.50	6.41E+00	2.79E+00

The first column is the time in seconds since the beginning of the simulation. At every hour the program writes 6070 lines of data one for every point along the observation profile. The second and third columns contain the coordinates of the point for which the data is written. The value in the third column is the linear distance from the first vertex of the observation line to the specific point. The last two columns are the flow depth and the tangential flow velocity magnitude.

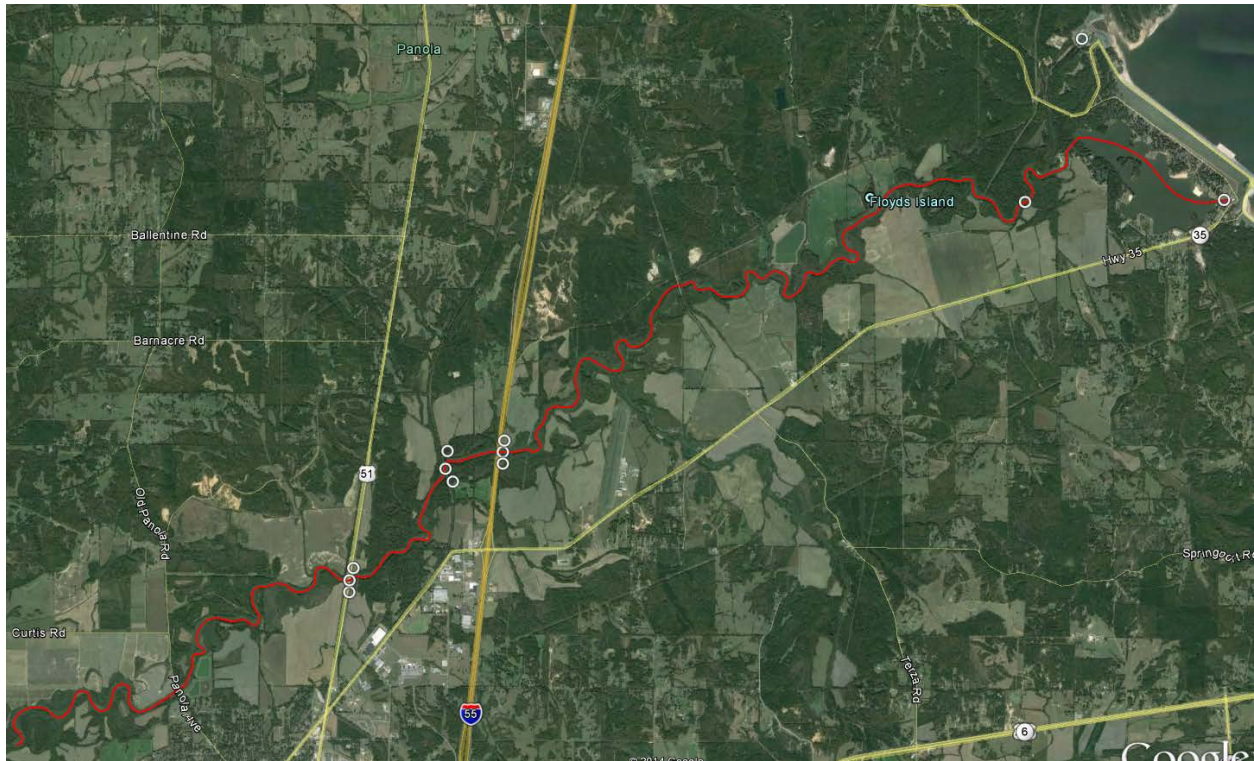


Figure 40 Google Earth Image showing the observation line (red line).

## Chapter 5 Simulation Results

### 5.1 Maximum Flow Depth

Raster maps of flow depth for simulations using DEMs with 30 m, 10 m, 5m and 3m resolution are presented in Figure 41, Figure 42, Figure 43, and Figure 44, respectively. Highest maximum flow depth downstream of the dam is predicted by the simulation with 5 m DEM as 11.5 m.

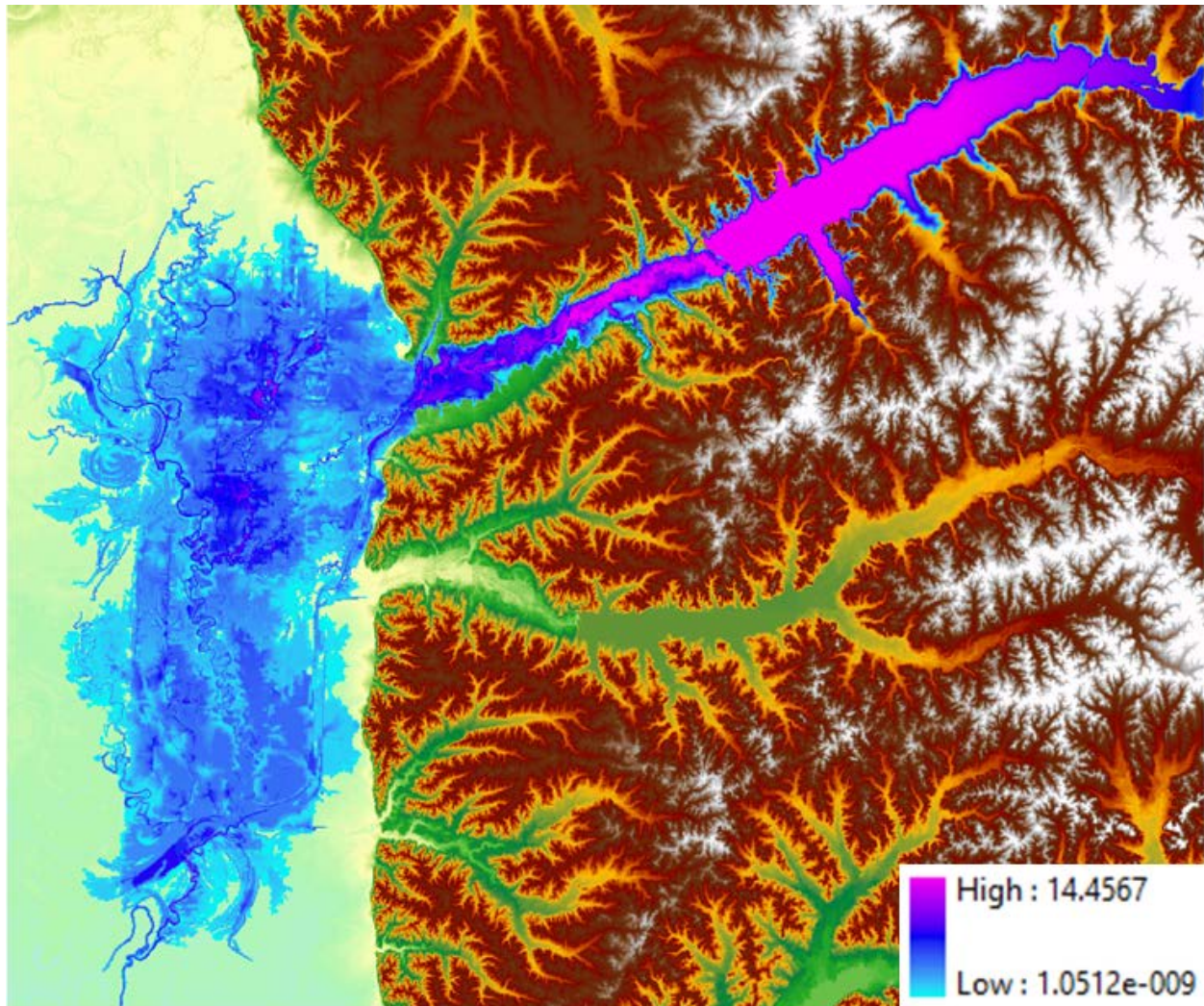


Figure 41 Raster map of maximum flood depth (in m) for the simulation with 30 m DEM.

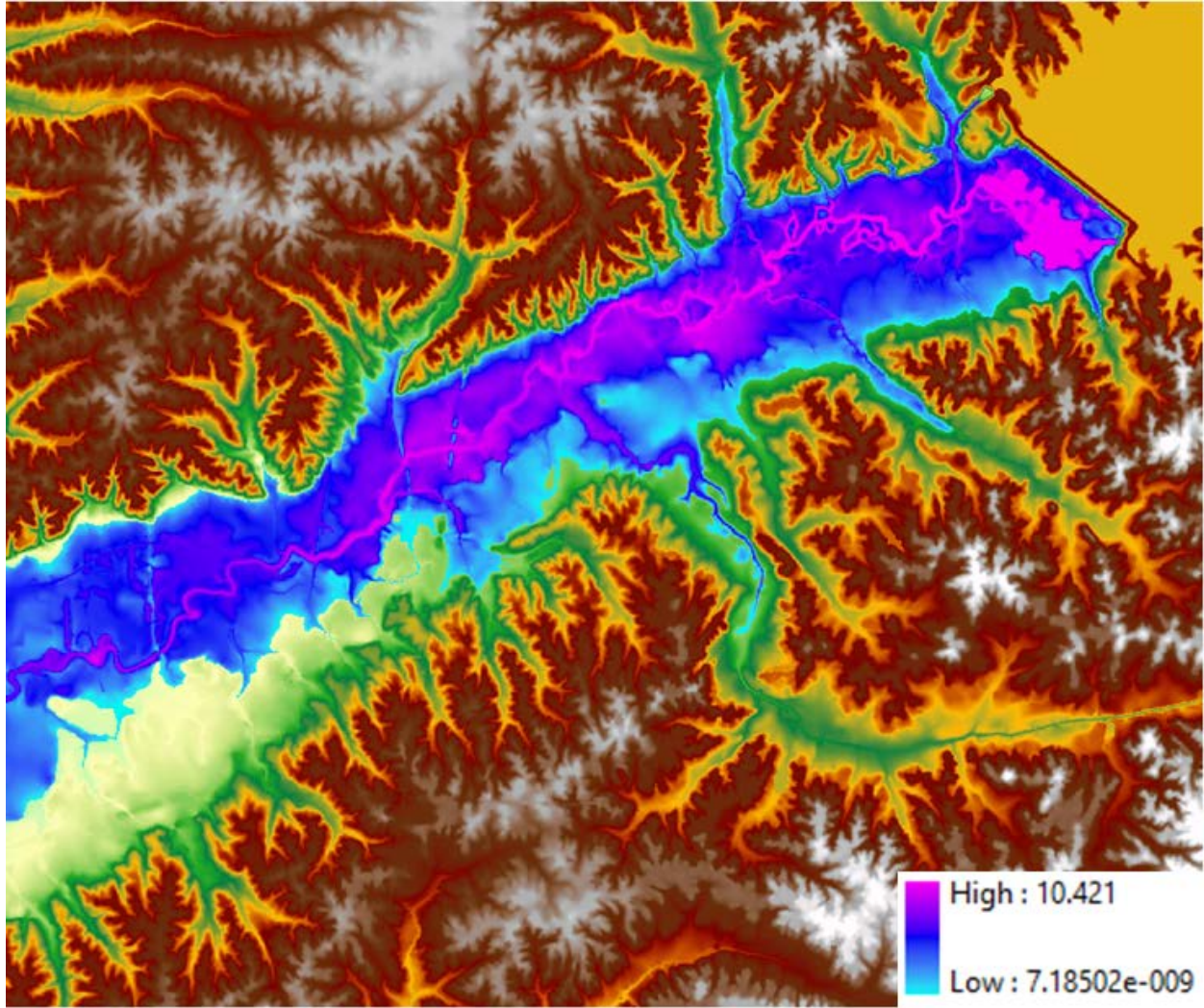


Figure 42 Raster map of maximum flood depth (in m) for the simulation with 10 m DEM.

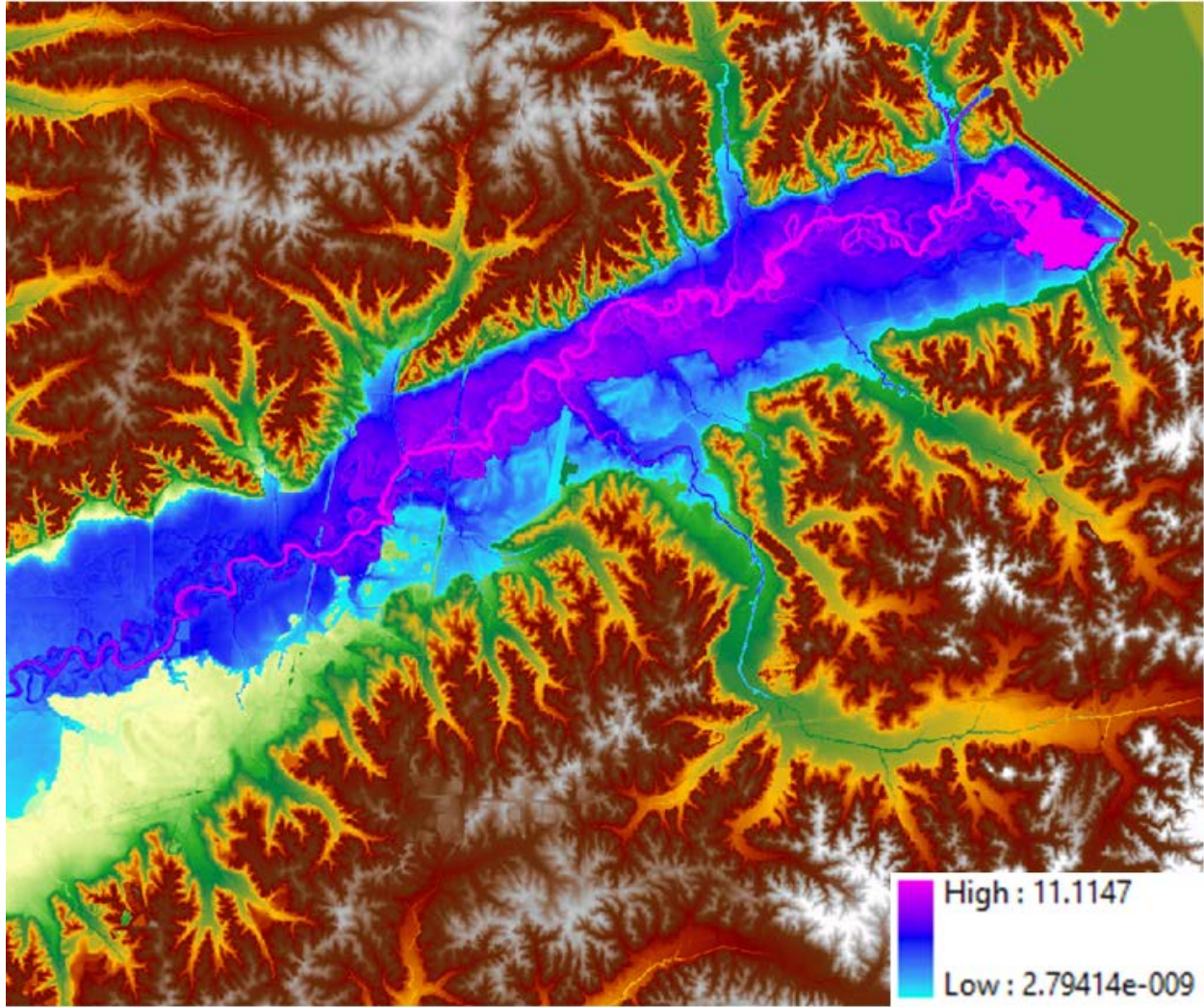


Figure 43 Raster map of maximum flood depth (in m) for the simulation with 5 m DEM.

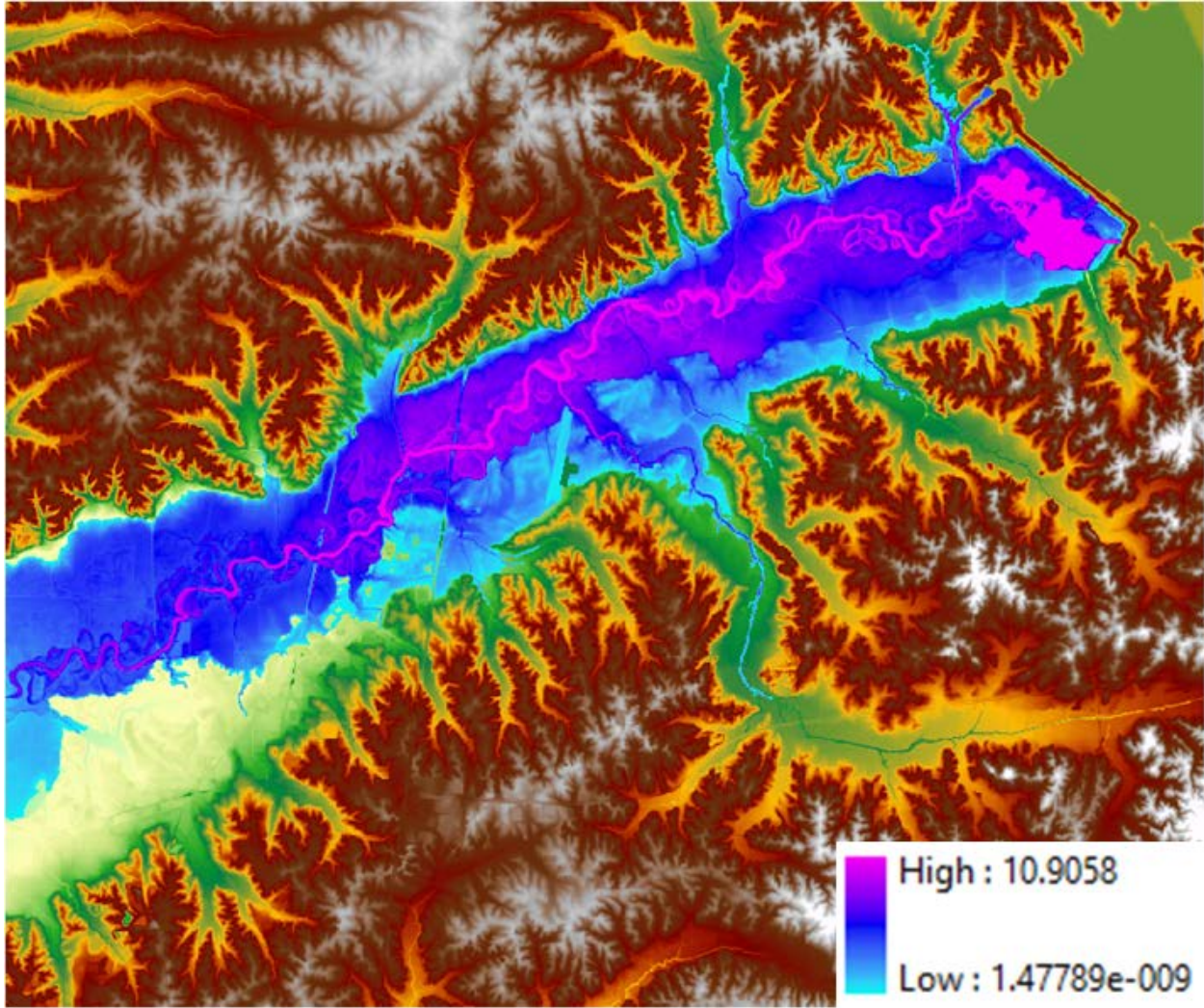


Figure 44 Raster map of maximum flood depth (in m) for the simulation with 3 m DEM.

The following observations can be made:

- Sardis Lake Baptist Church is in the inundated area predicted by the simulations. Maximum water depth around the structure reaches 1.8m. Considerable damage should be expected.
- First Baptist Church is outside of the inundation area predicted by the simulations. It will not be affected by the flood.
- Batesville Public Library is outside of the inundation area predicted by the simulations. It will not be affected by the flood.
- U.S. Forestry Department building is outside of the inundation area predicted by the simulations. It will not be affected by the flood.
- The building of the Insituform Technologies Inc. is in the inundation area predicted by the simulations. Maximum water depth around the structure is about 0.2 m. A modest level of damage should be expected.
- The pavement and the terminal building of the Panola County Airport are in the inundation area predicted by the simulations. The water depth at the northern end of the pavement close to the Little Tallahatchie River is more than 0.50 m. Water depth around the terminal buildings is more than 1 m on the north side.

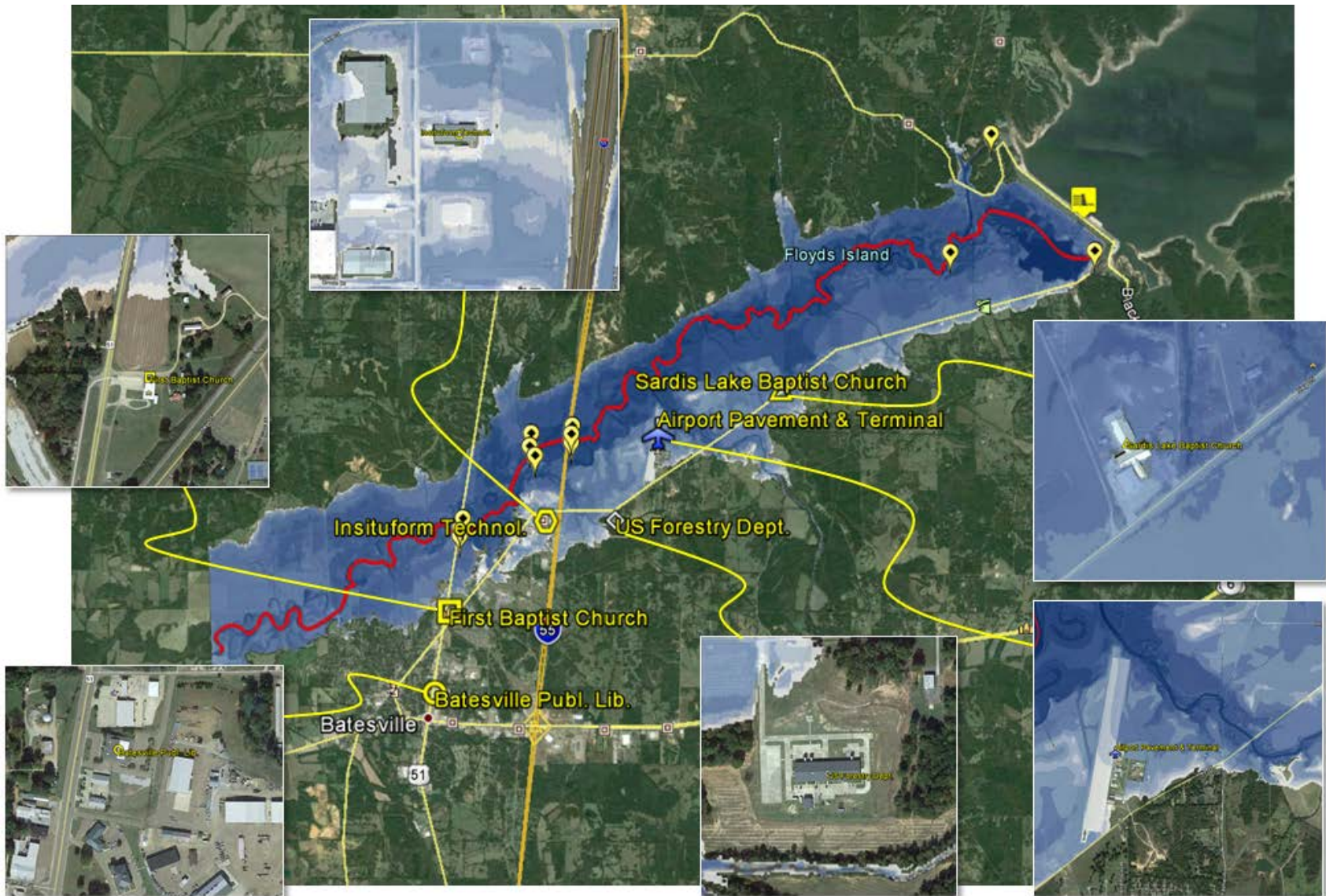


Figure 45 Flood impact on the structures of interest.

## 5.2 Flood Arrival Time

Raster maps of flood arrival time for simulations using DEMs with 30 m, 10 m, 5m and 3m resolution are presented in Figure 46, Figure 47, Figure 48, and Figure 49, respectively. Highest maximum flow depth downstream of the dam is predicted by the simulation with 5 m DEM as 11.5 m.

Based on the simulation with 3 m DEM, the flood reaches the west edge of the computational domain in about 16,223 s (4.51 hrs) in the channel. The floodplain becomes inundated later. The southern part of the floodplain becomes inundated in about 20,370 s (5.65 hrs) after the beginning of the simulation.

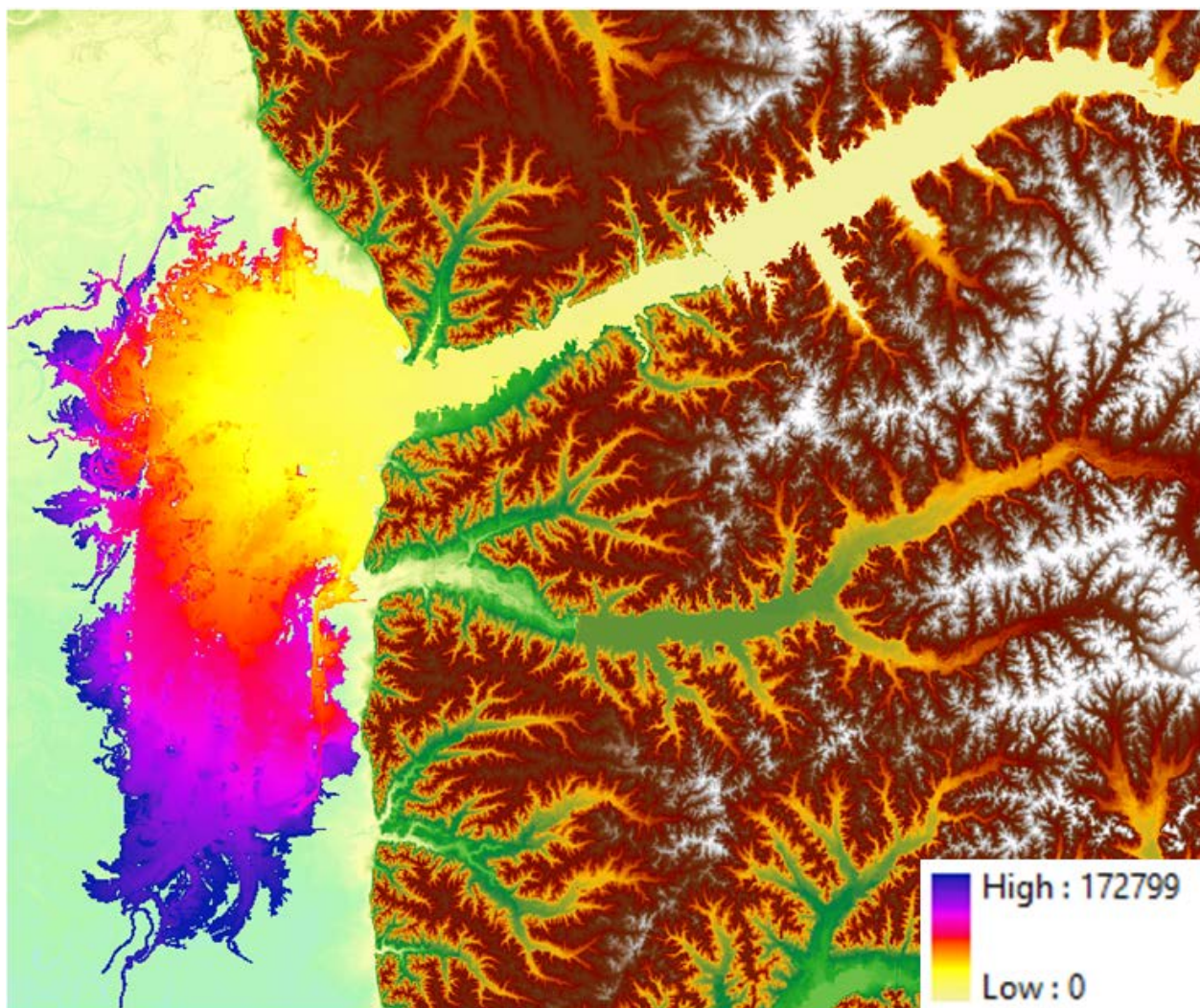


Figure 46 Raster map of flood arrival time (in seconds after the beginning of the simulation, which coincides with the time of initiation of the breach) for the simulation with 30 m DEM.

Referring to Figure 46, the flood reaches the Mississippi Delta about 18,418 s (5.12 hrs) after the initiation of the breach. Once it reaches the flat landscape of Mississippi Delta, the flood spreads in a two-

dimensional manner. It is important to note that in this region a 1D model would not have been applicable due to the fact that the 1D flow assumption is no longer valid. At the end of the simulation, i.e. 48 hours after the initiation of the breach, flood waters extend from Sledge, MS, in the north to Sharkey and Tippto, MS, in the south. The widest part of the inundation area in the Mississippi Delta is more than 27 km and extends to the west of Marks, Lambert, Quitman, Darling, and Falcon, MS.

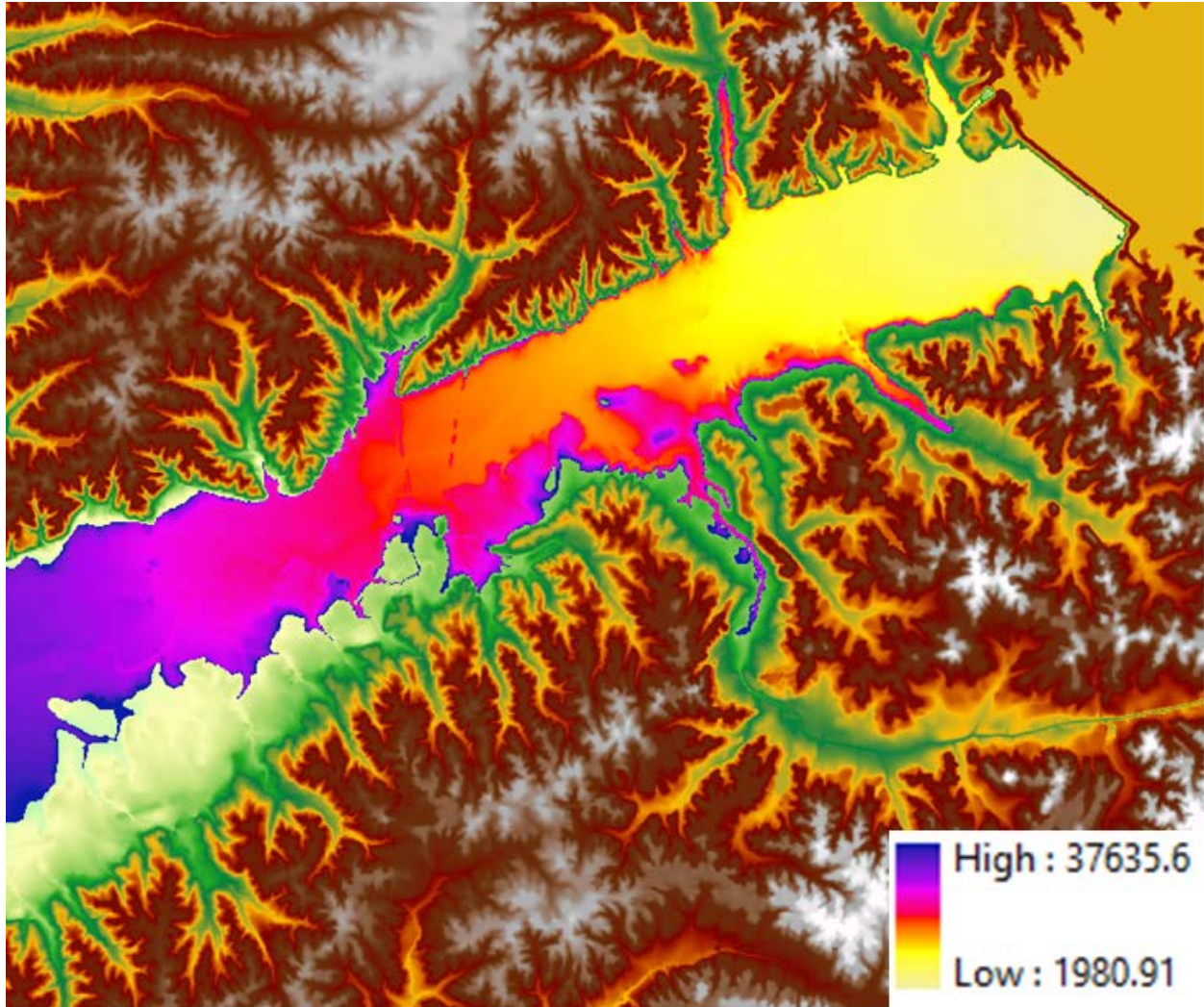


Figure 47 Raster map of flood arrival time (in seconds after the beginning of the simulation, which coincides with the time of initiation of the breach) for the simulation with 10 m DEM.

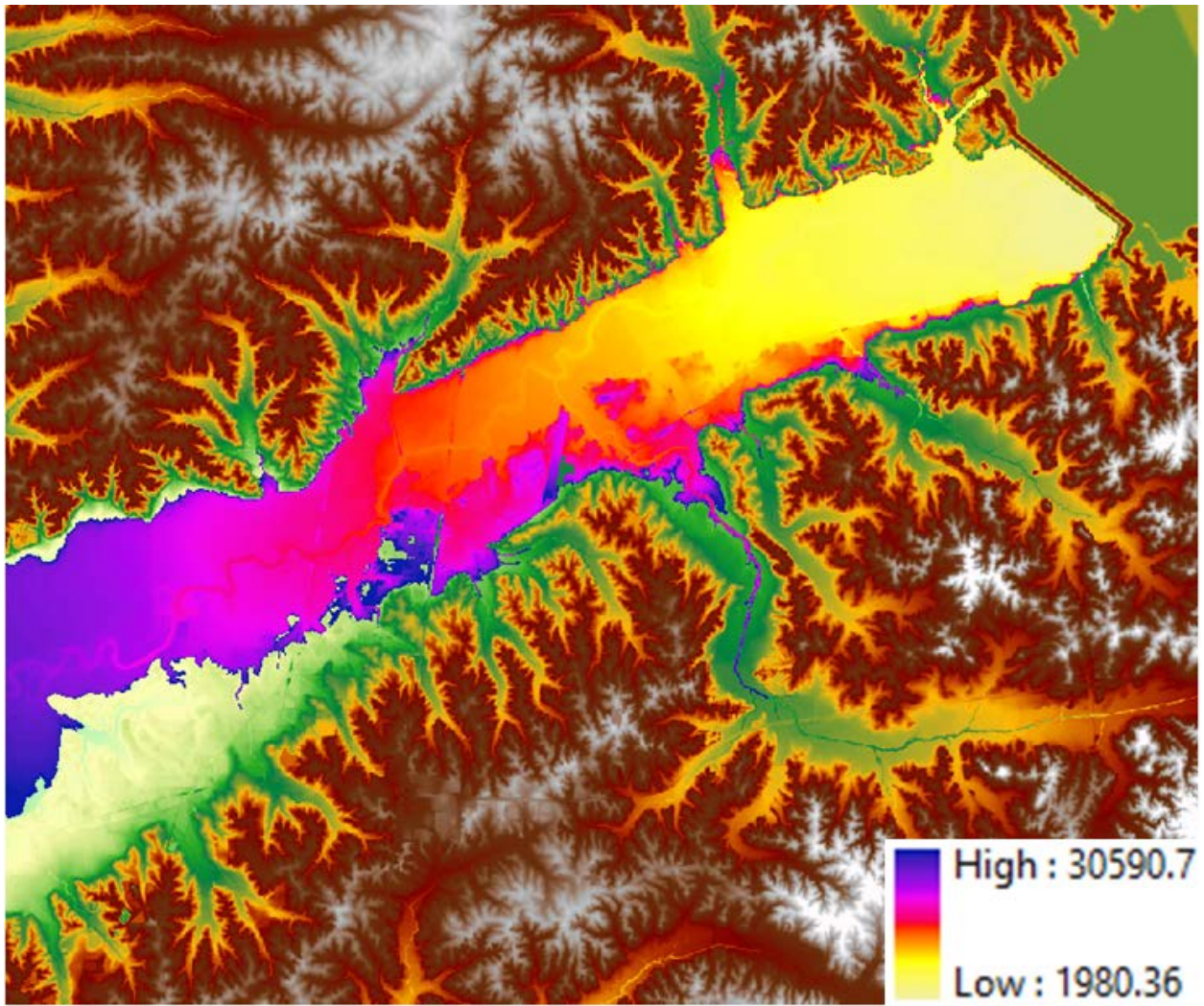


Figure 48 Raster map of flood arrival time (in seconds after the beginning of the simulation, which coincides with the time of initiation of the breach) for the simulation with 5 m DEM.

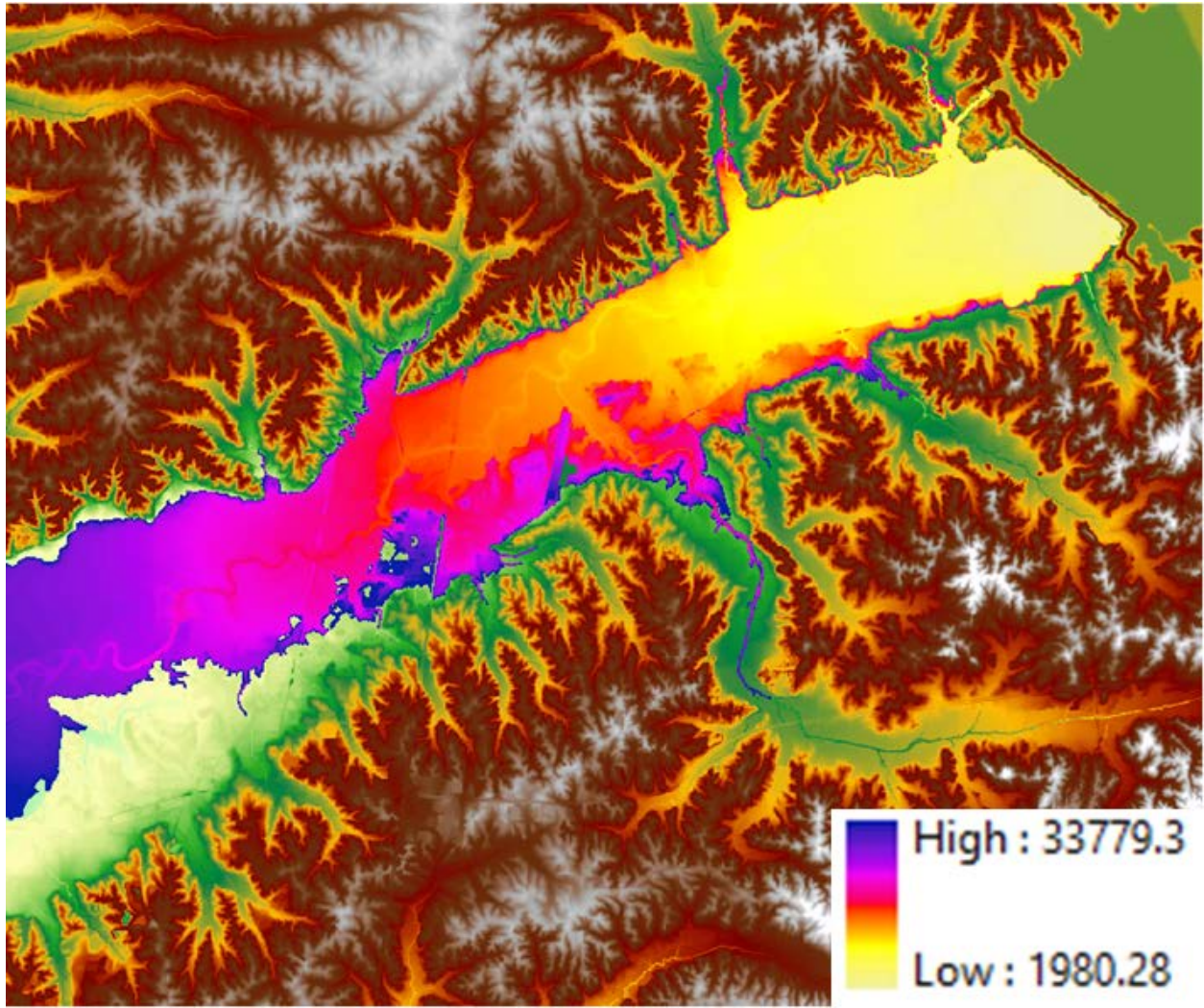


Figure 49 Raster map of flood arrival time (in seconds after the beginning of the simulation, which coincides with the time of initiation of the breach) for the simulation with 3 m DEM.

### 5.3 Maximum Specific Discharge

Maximum specific discharge, i.e. the discharge per unit width (dimensions are  $\text{m}^3/\text{s}/\text{m}$ ) is an important parameter. In addition to providing the discharge information, it is also used in determining the potential damage to humans, buildings and vehicles.

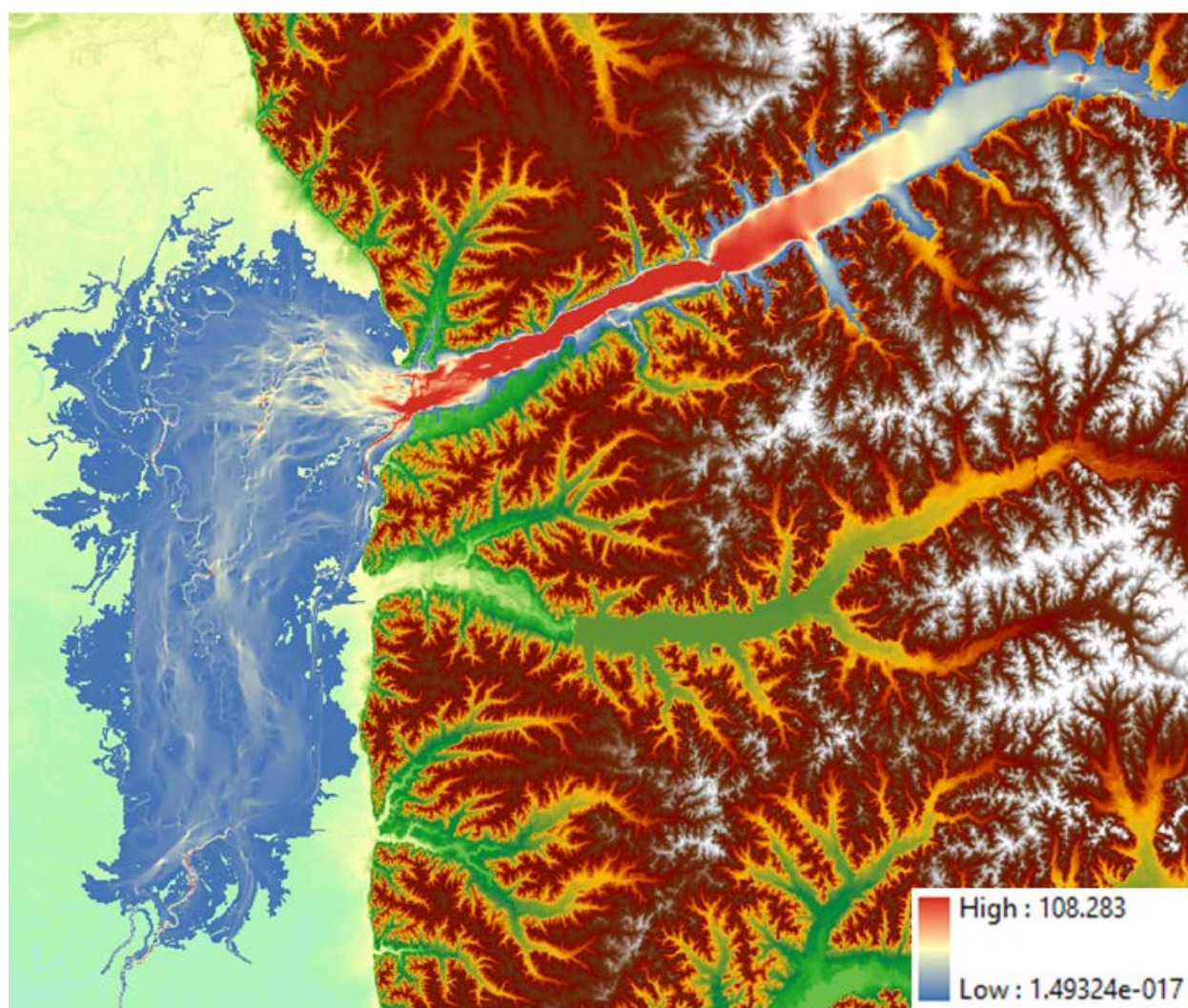


Figure 50 Raster map of maximum specific discharge (in  $\text{m}^3/\text{s}/\text{m}$ ) for the simulation with 30 m DEM.

Raster maps of maximum specific discharge for simulations using DEMs with 30 m, 10 m, 5m and 3m resolution are presented in Figure 50, Figure 51, Figure 52, and Figure 53, respectively. The simulation with 3 m DEM predicts the highest maximum specific discharge near the breach location as  $126 \text{ m}^3/\text{s}/\text{m}$ . It is interesting to note that the maximum specific discharge predicted by the simulation with 5m DEM is  $124 \text{ m}^3/\text{s}/\text{m}$ , which is almost the same, where the maximum specific discharge for the simulation with 10 m DEM is  $80 \text{ m}^3/\text{s}/\text{m}$ , which is much lower. This shows that the values near the imposed source may depend on the cell size. The maximum specific discharge predicted by the simulation with 30 m DEM, which simulates the lake and the breaching process, gives an intermediate value of  $108 \text{ m}^3/\text{s}/\text{m}$ .

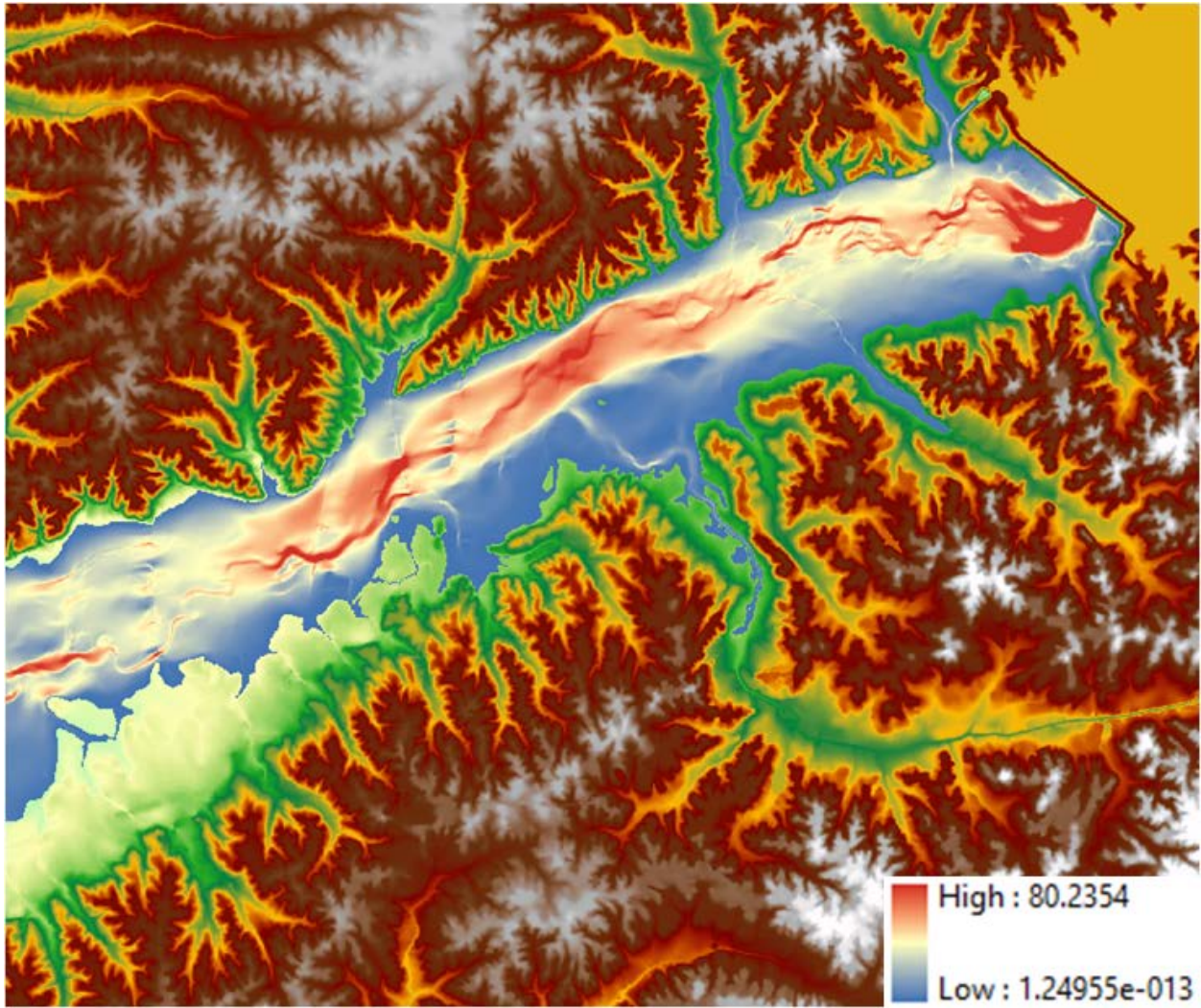


Figure 51 Raster map of maximum specific discharge (in  $\text{m}^3/\text{s}/\text{m}$ ) for the simulation with 10 m DEM.

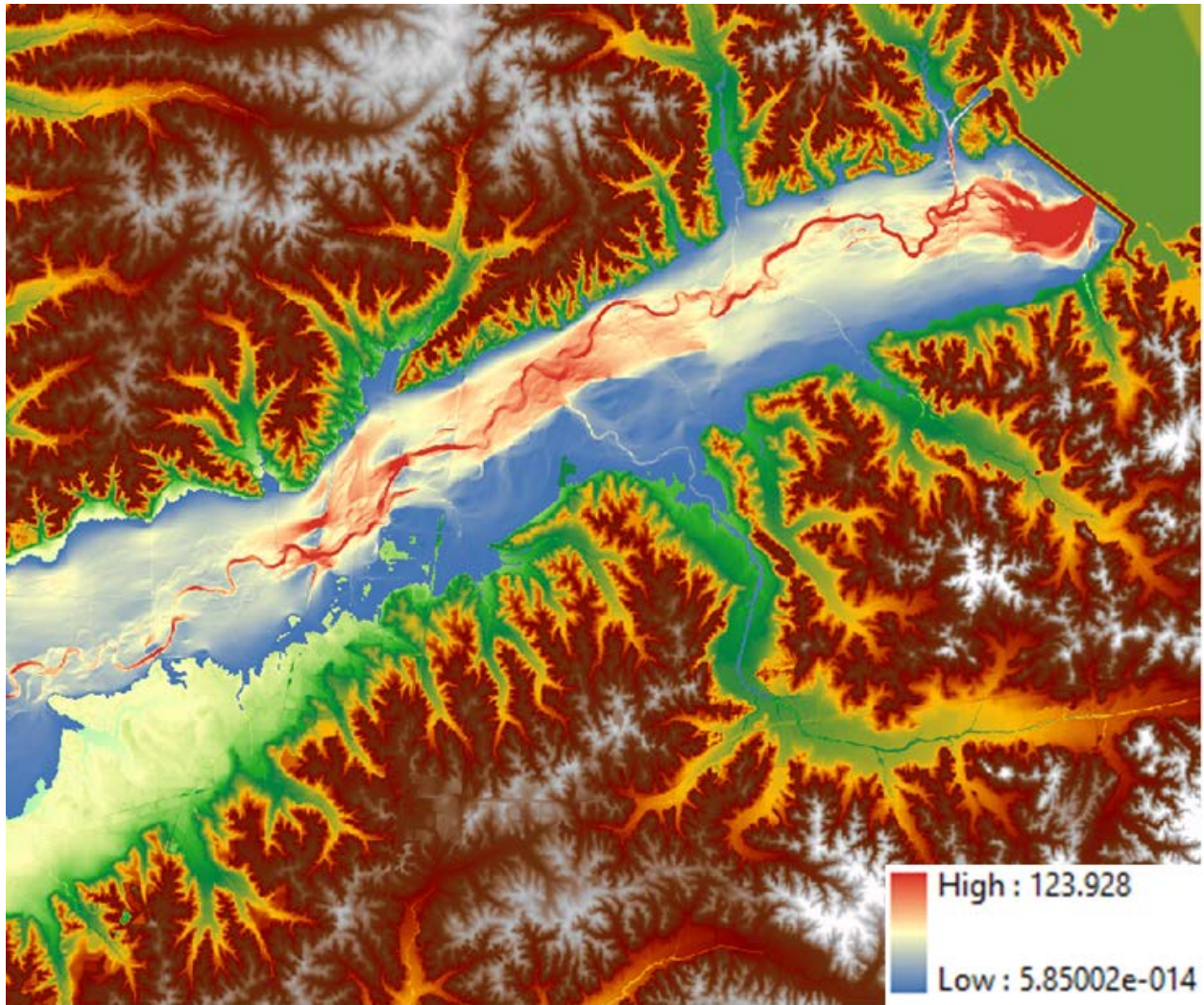


Figure 52 Raster map of maximum specific discharge (in  $\text{m}^3/\text{s}/\text{m}$ ) for the simulation with 5 m DEM.

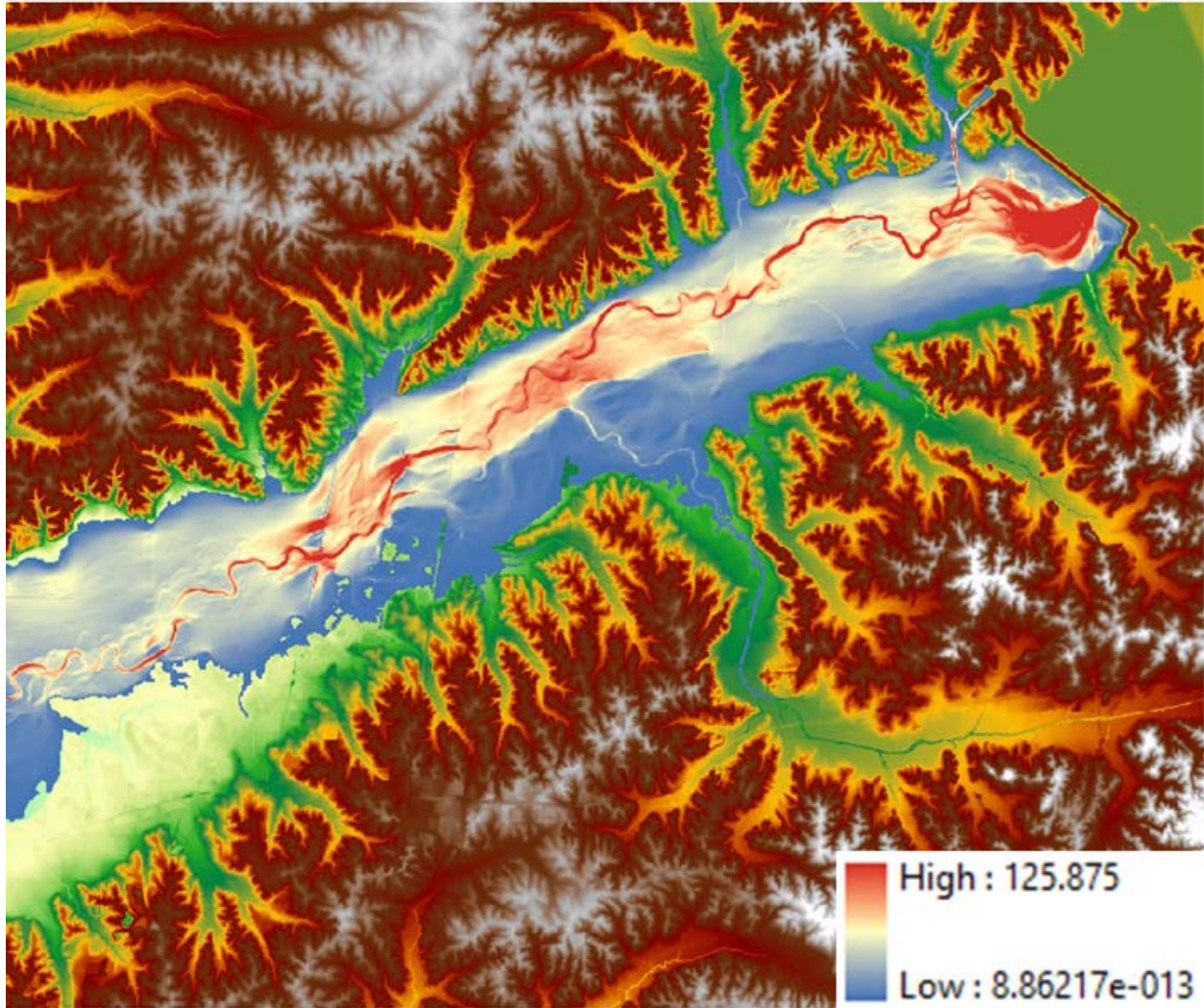


Figure 53 Raster map of maximum specific discharge (in  $\text{m}^3/\text{s}/\text{m}$ ) for the simulation with 3 m DEM.

#### 5.4 Discharge Hydrographs for Observation Lines

For each simulation, DSS-WISE provided the hydrographs computed at 29 observation lines, i.e. cross sections, defined at the simulation setup phase (Figure 33). These hydrographs are output in separate comma separated value (csv) files for further analysis and treatment and can be readily imported into a spreadsheet program (see Table 2). The hydrographs computed at the observation lines can also be visualized in the kmz file generated by the DSS-WISE software by simply clicking on an observation line (Figure 30).

In Figure 54, hydrographs computed at 17 cross sections have been plotted together for all four simulations with different resolutions. Locations of the 17 cross sections are shown in Figure 55. The transformation of the flood hydrograph and the attenuation of its peak discharge as it propagates downstream can be clearly seen in Figure 54. Due to the short distance the attenuation of the peak discharge is not significant.

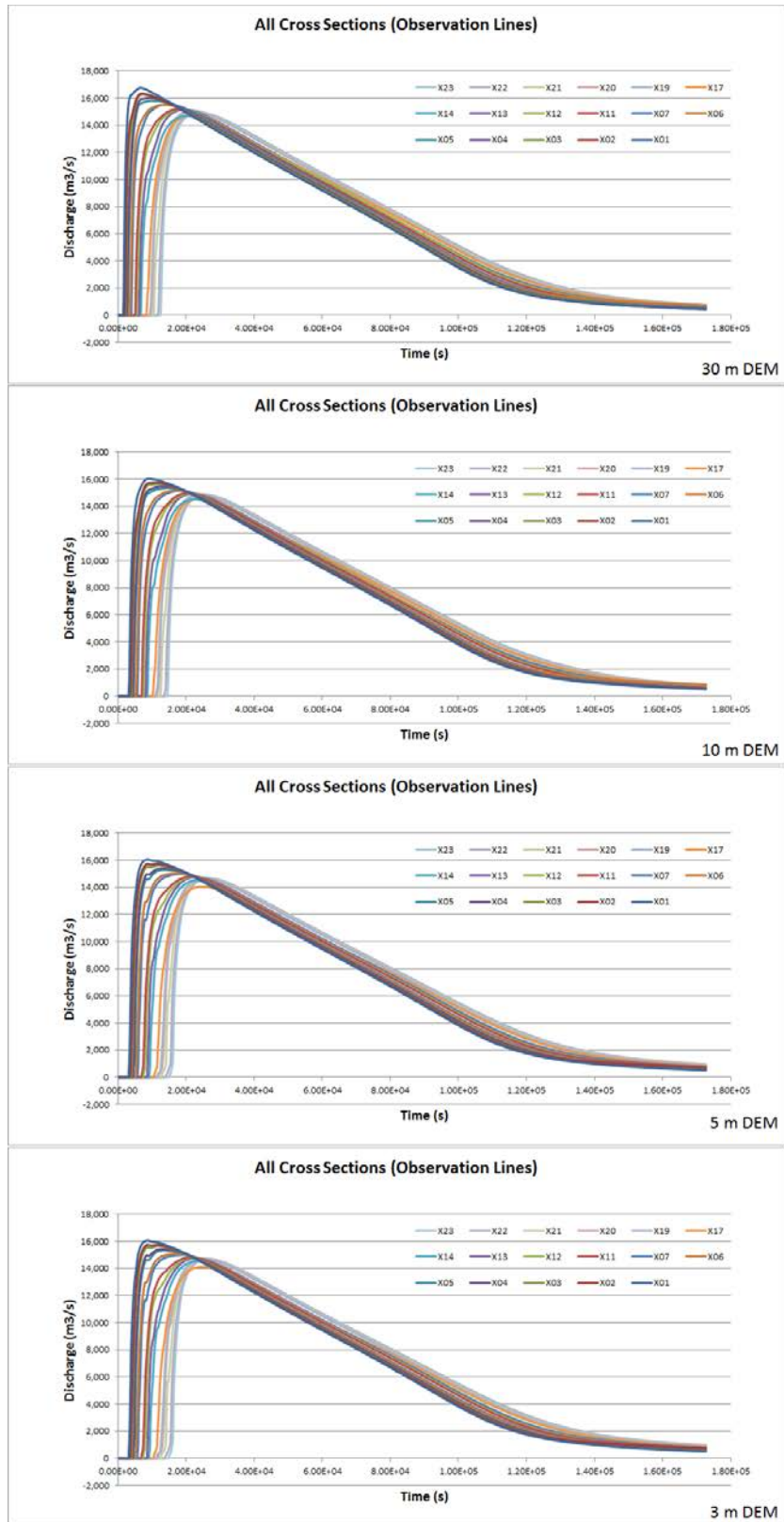


Figure 54 Transformation of the discharge hydrograph as the flood propagates downstream (see Figure 33 for cross section locations).

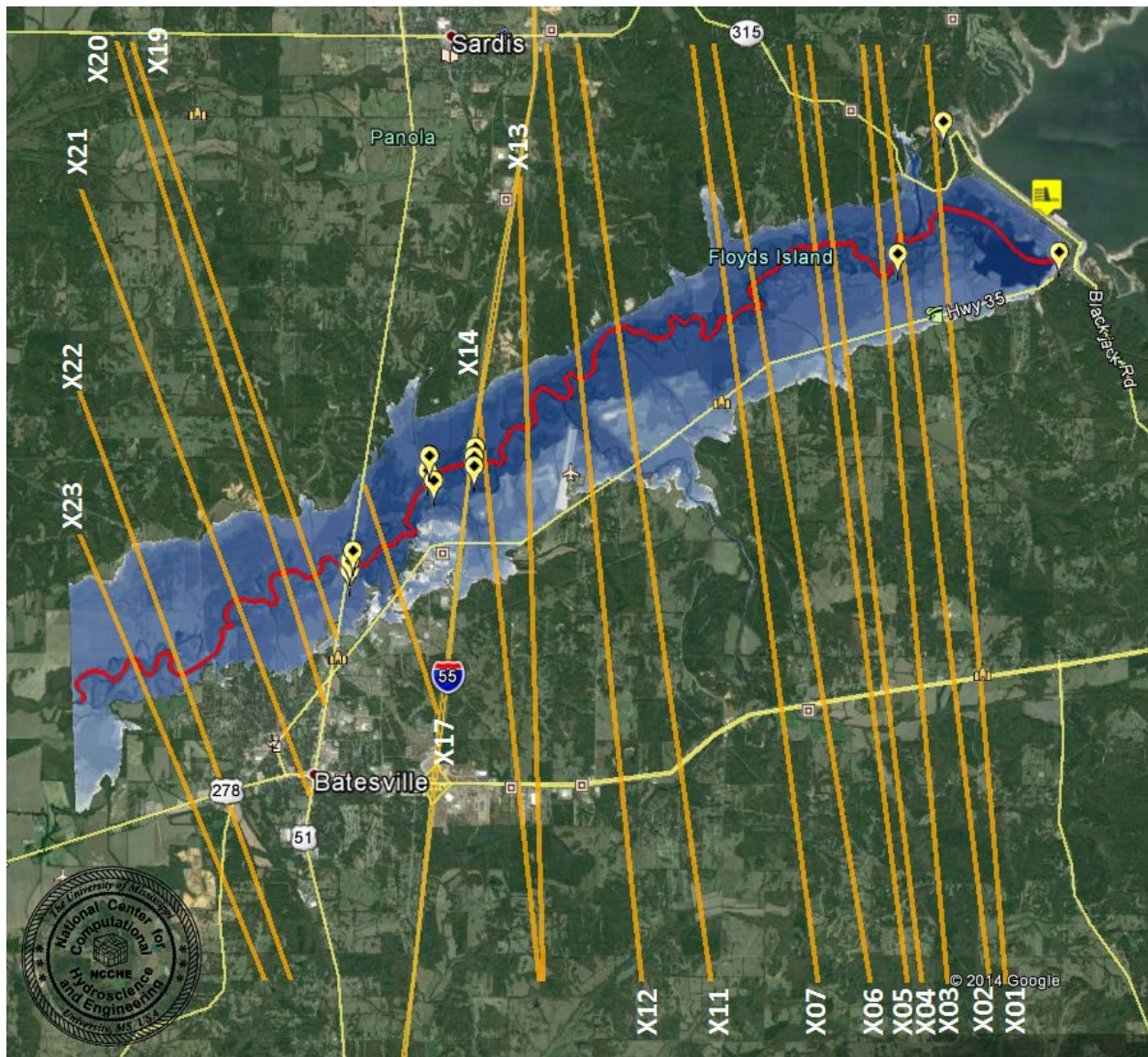


Figure 55 Locations of the 17 selected cross sections whose hydrographs are plotted in Figure 54.

The peak discharge decreases from  $16,057 \text{ m}^3/\text{s}$  at the cross section X01, located downstream of Sardis Dam, to  $14,700 \text{ m}^3/\text{s}$  at the cross section X23, located at the downstream end of the area of interest. The time lag for the peak discharge increases with increasing distance from the dam as expected. The time at which the discharge suddenly starts increasing marks the arrival of the flood at the cross section.

Figure 56 shows how the bridge cross sections for US-51, Railroad, and I-55 are captured as elevation in the DEM. Figure 58 shows the hydrographs at the bridge cross section together with the hydrograph at the cross section X01. The locations of the three bridge cross sections (observation lines) are shown in Figure 57. These cross sections are respectively 11.0 river-miles (I-55), 11.6 river-miles (Railroad) and 13.4 river-miles (US-51) downstream of the dam. Due to the short distance, the peak discharge attenuates only slightly and the peak discharges are around  $14,750 \text{ m}^3/\text{s}$ . This is a significant discharge and considerable amount of sediment transport, and debris transport, should be expected. These large discharges may also lead to bank erosion and local scour that may endanger the structural integrity of the bridges.

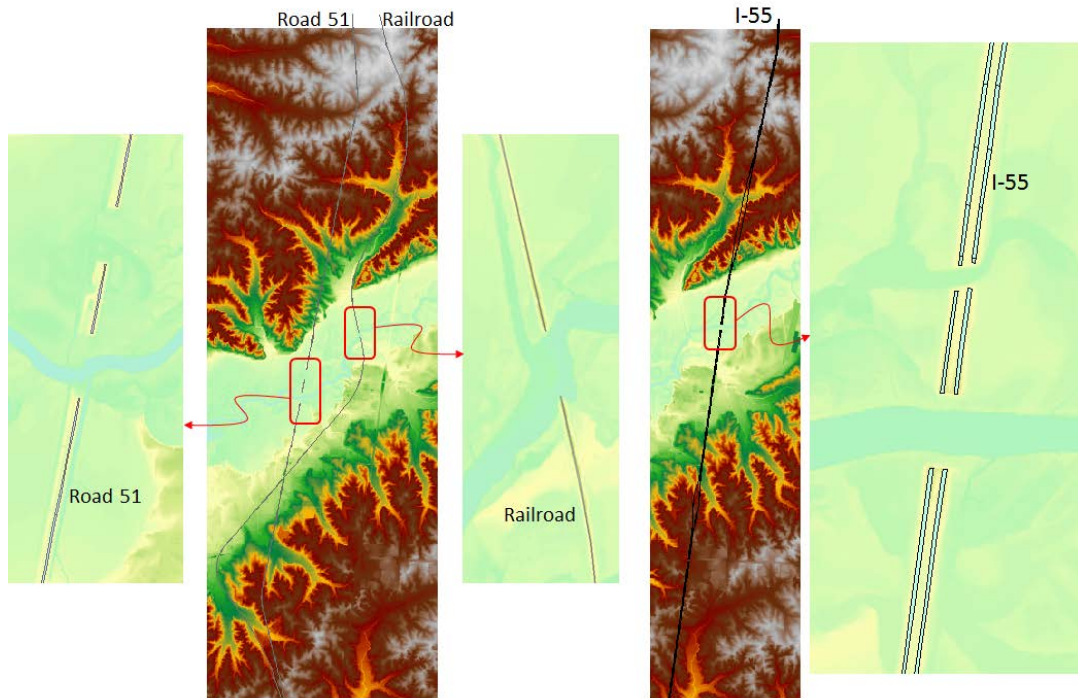


Figure 56 Images showing how the US-51, Railroad, and I-55 are captured in the 3m DEM.

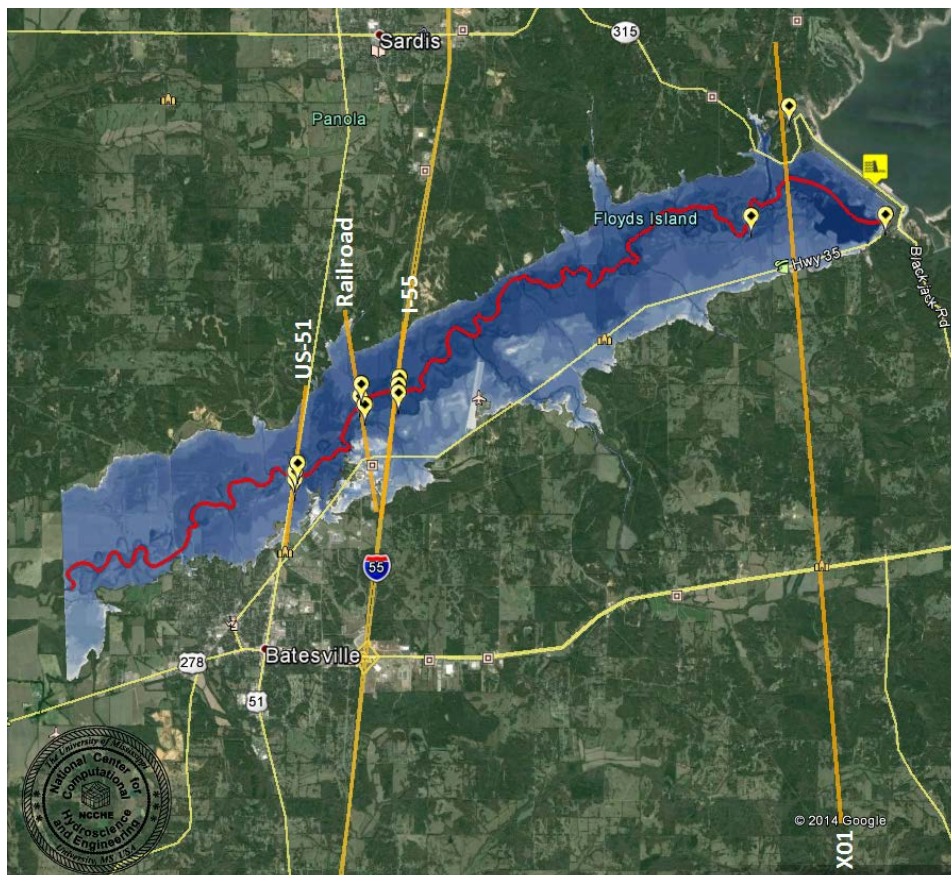


Figure 57 Locations of the bridge cross sections for which hydrographs are plotted in Figure 58.

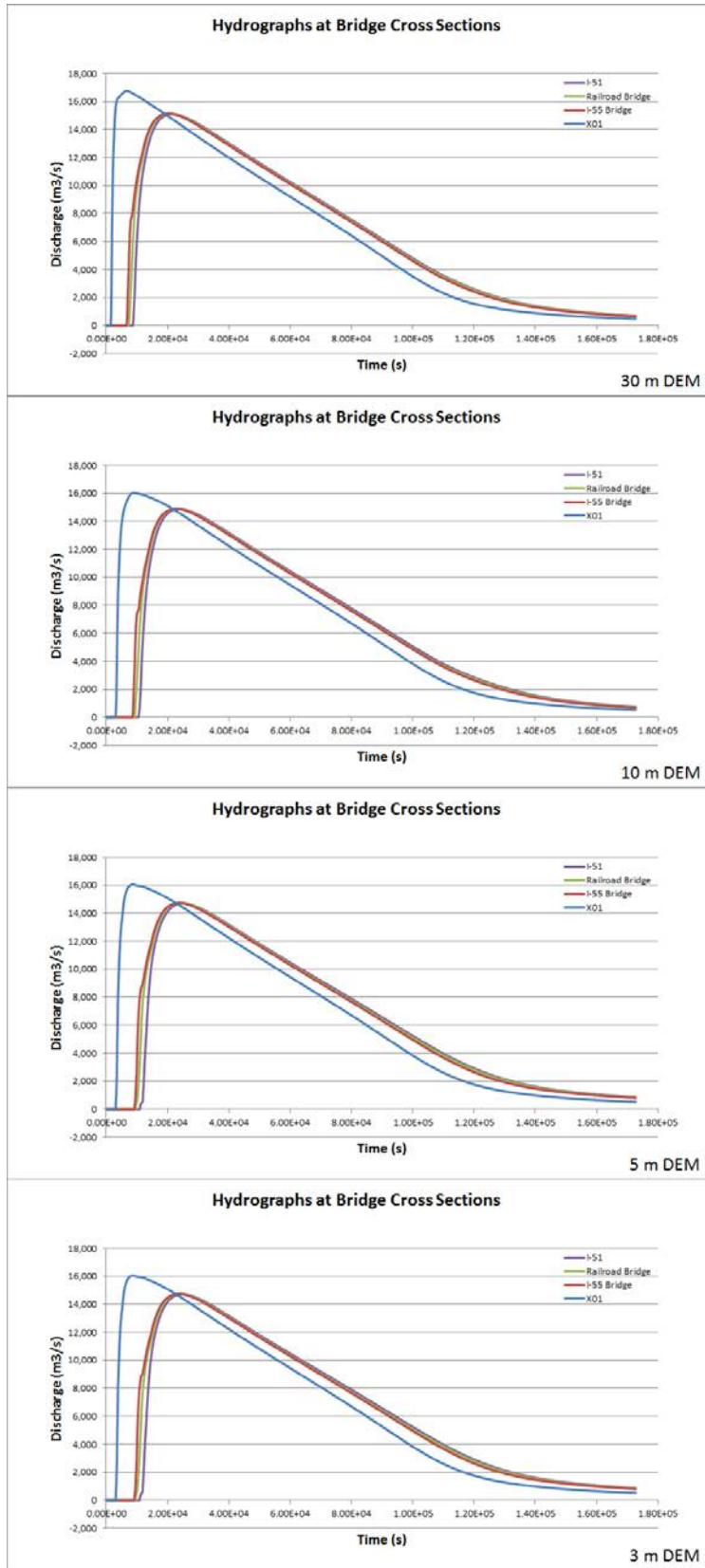


Figure 58 Hydrographs computed at the bridge cross sections (see Figure 57 for cross section locations).

## 5.5 Observation Points at Bridge Locations

Interstate Highway I-55, a railroad and US-51 cross Little Tallahatchie floodplain on embankments with bridges. As shown in Figure 59, the simulation with 3 m DEM predicts that long stretches of all three transportation infrastructures will be overtopped and inundated:

- I-55 is overtopped along a 2,370 m-long stretch and the water depth over the crown of the road is predicted to be as high as 4 m.
- The railroad is overtopped at several locations. Total length of inundated stretch is about 4,000 m. The water depth over the embankment can be as high as 1.6 m.
- US-51 is overtopped by the flood over a stretch of about 3,210 m. The highest water depth over the road crown is close to 2 m.

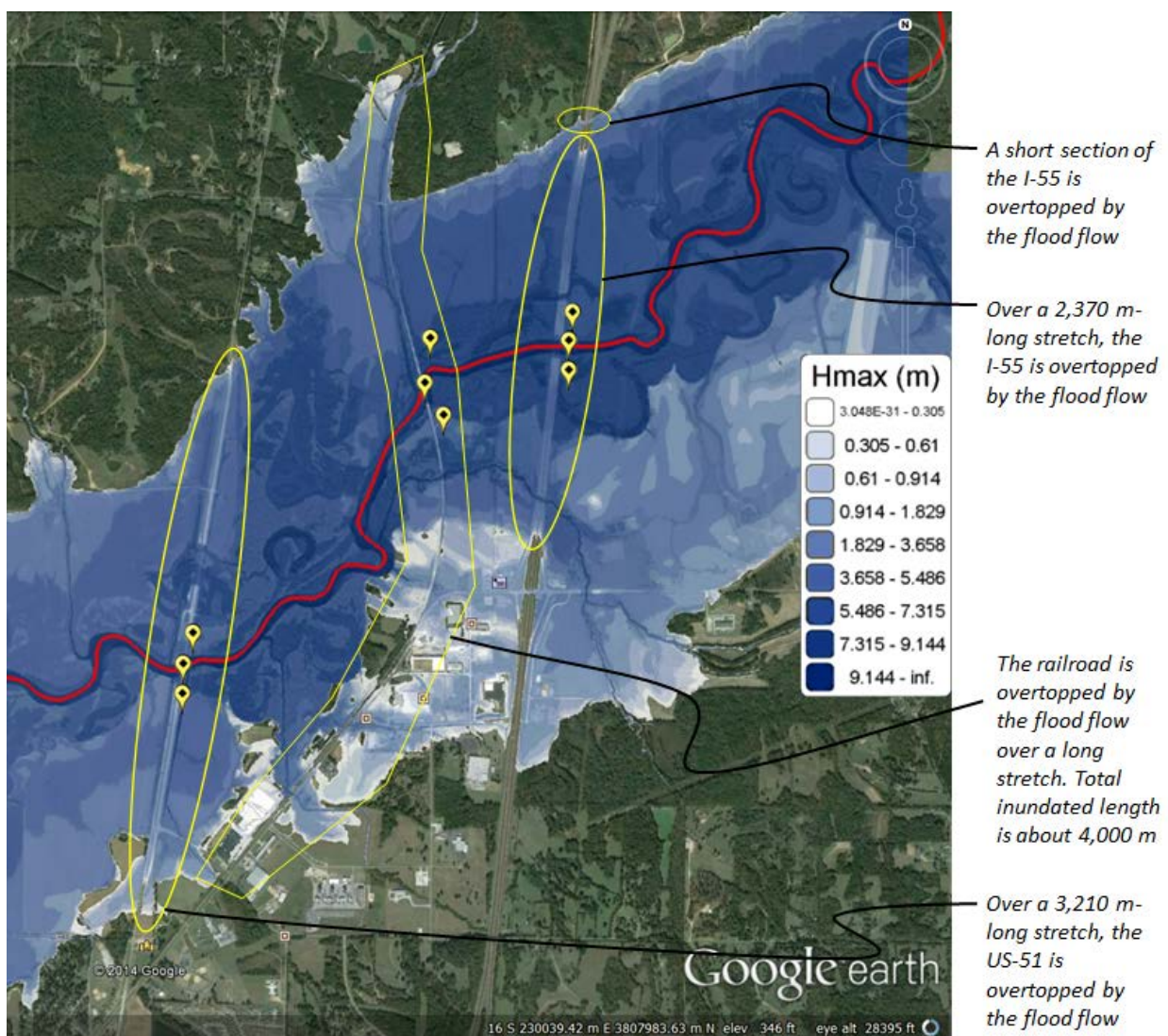


Figure 59 Inundation of I-55, Railroad and US-51.

The discharge hydrographs crossing the observation lines along I-55, Railroad and US-51 were presented in Section 5.4. These discharges is the sum of the flow passing through the bridge openings and the flow overtopping the embankment.

Observation points are defined on left center and right side of the bridges for the I-55, the Railroad and US-51. The extracted data includes the flow depth and the components of the flow depth-integrated velocity in the horizontal plane. The data for each observation is available in a csv file. Using the velocity component data, it is possible to compute the magnitude and the direction of the velocity vector. Flow depth, flow velocity and flow direction computed at the observation points near the I-55 Bridge, Railroad Bridge, and US-51 Bridge are plotted in Figure 61, Figure 62, and Figure 63, respectively.

For all three bridges, the depth-averaged local velocity at the central observation point can be as high as 3 m/s, approximately. This is a relatively high flow velocity. Hjulstrom diagram in Figure 60 (see Graf and Altinakar 2002) shows that the flow will be able to erode and transport sediment particles up to a diameter of 0.10 m. A more correct approach, of course, would be the use of the bed shear stress and the Shields diagram (see Graf and Altinakar 2002). Nevertheless, the Hjulstrom diagram clearly shows that the flow at the observation points near the bridges has considerable potential for eroding and transporting the bed material. The issue of the local erosion is considered in a separate section.

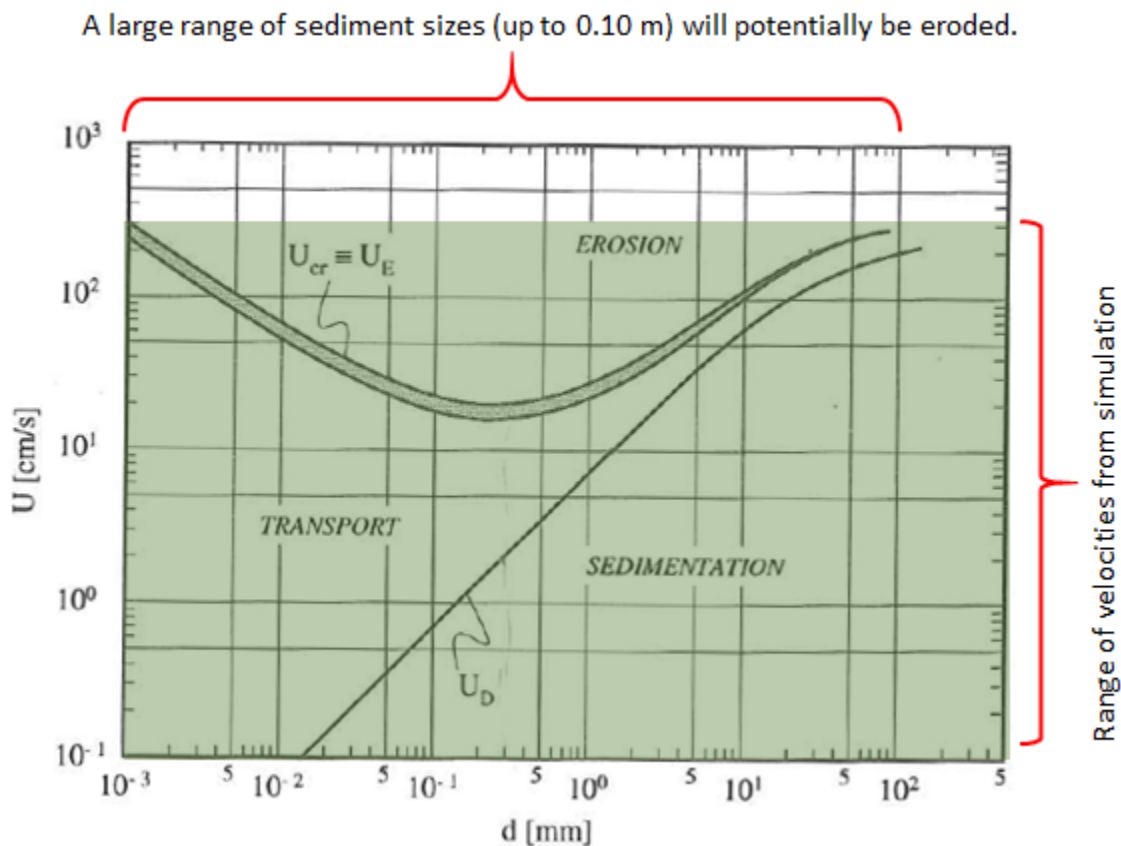


Figure 60 Critical velocities for transport and erosion according to Hjulstrom (taken from Graf and Altinakar, 2000).

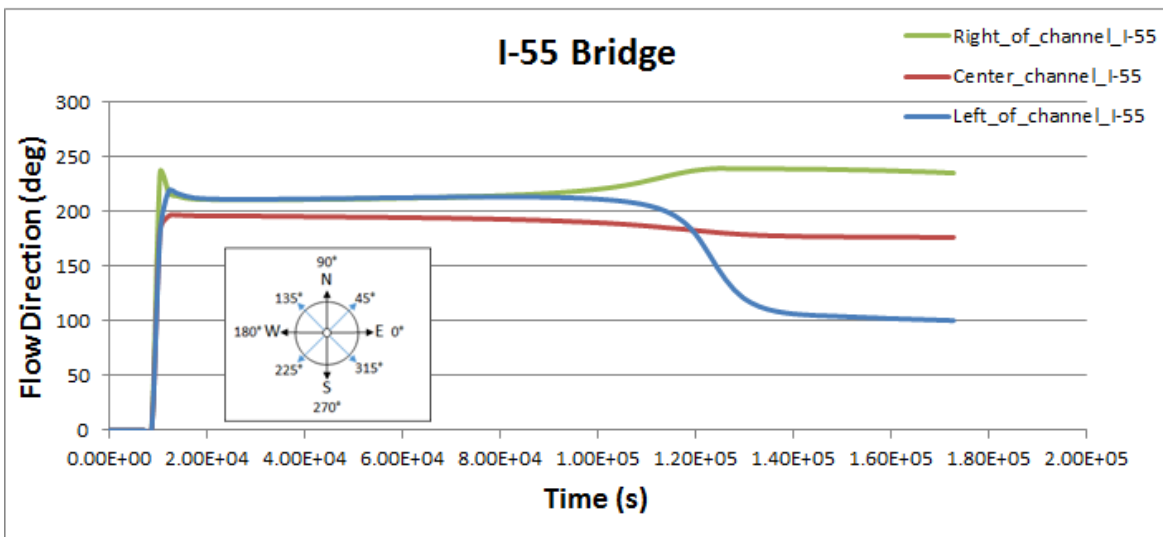
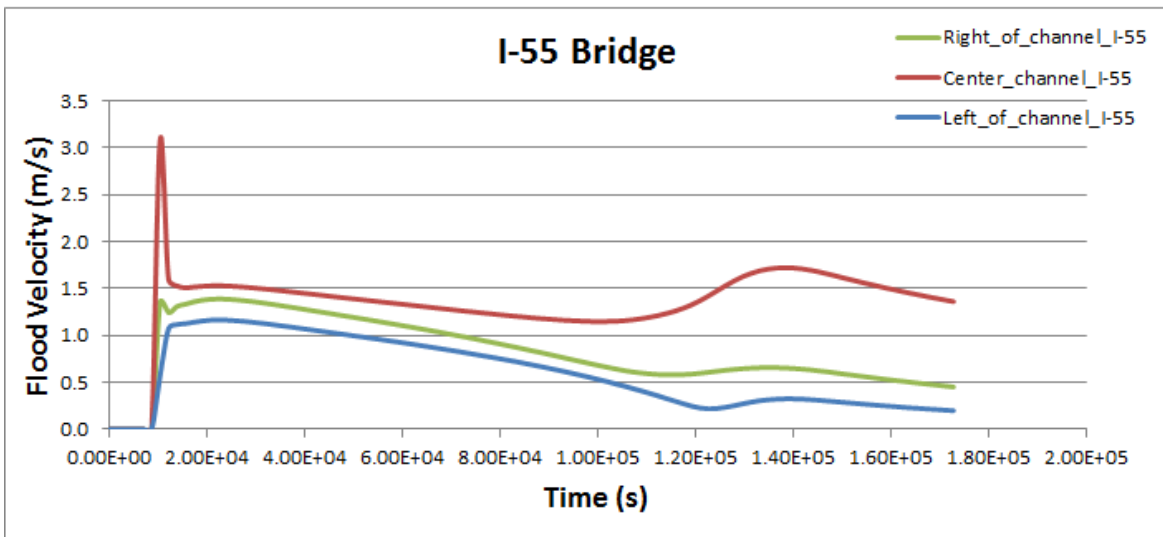
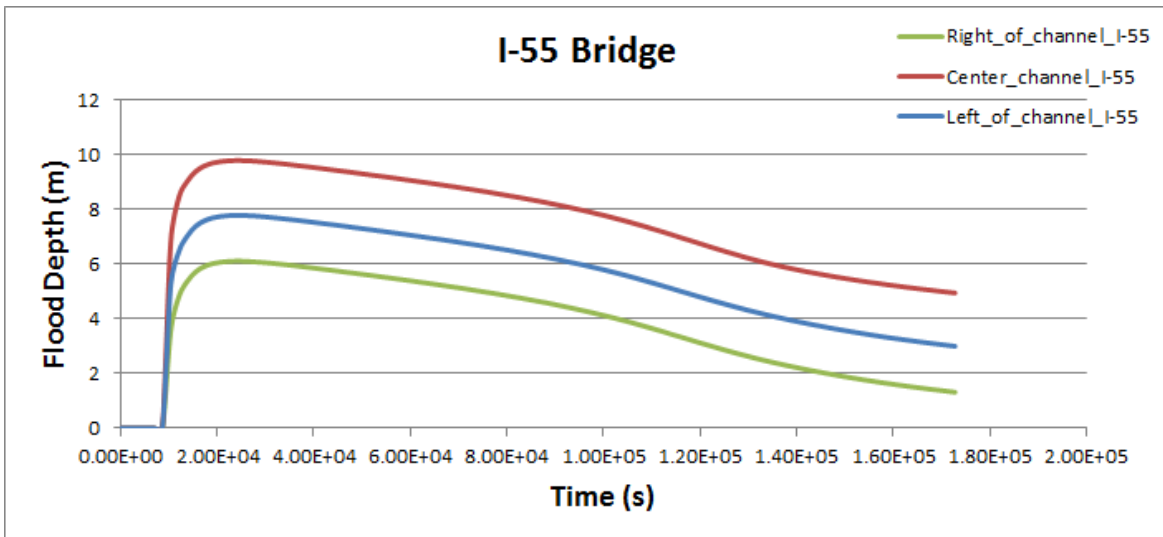


Figure 61 Flow depth, velocity and direction at the three observation points upstream of I-55 Bridge.

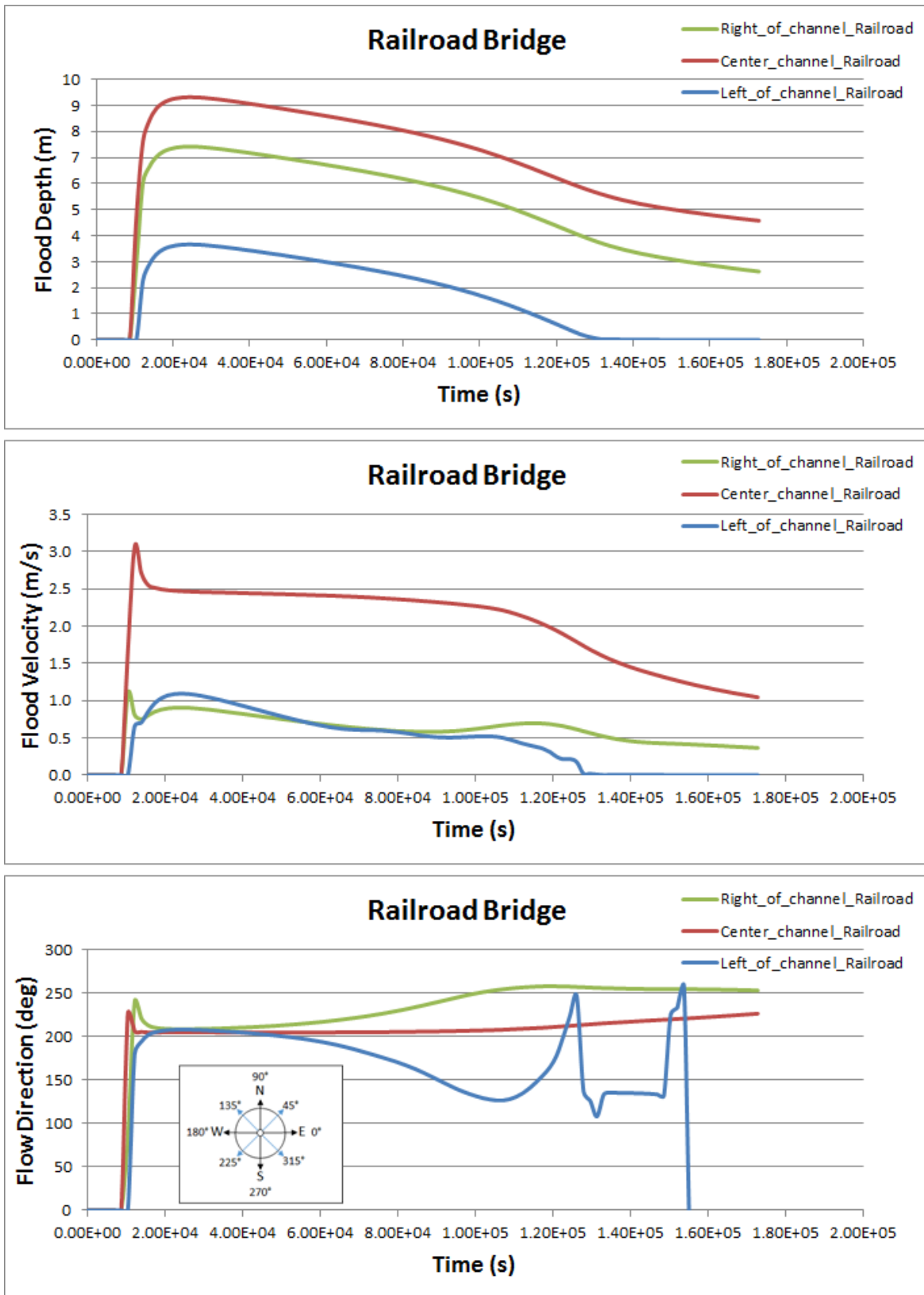


Figure 62 Flow depth, velocity and direction at the three observation points upstream of Railroad Bridge.

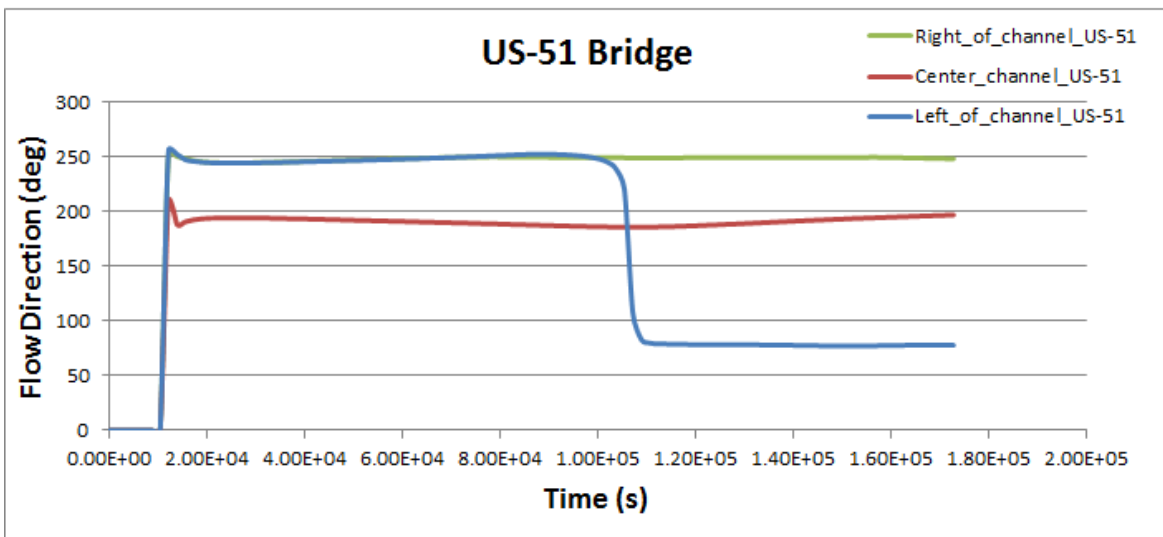
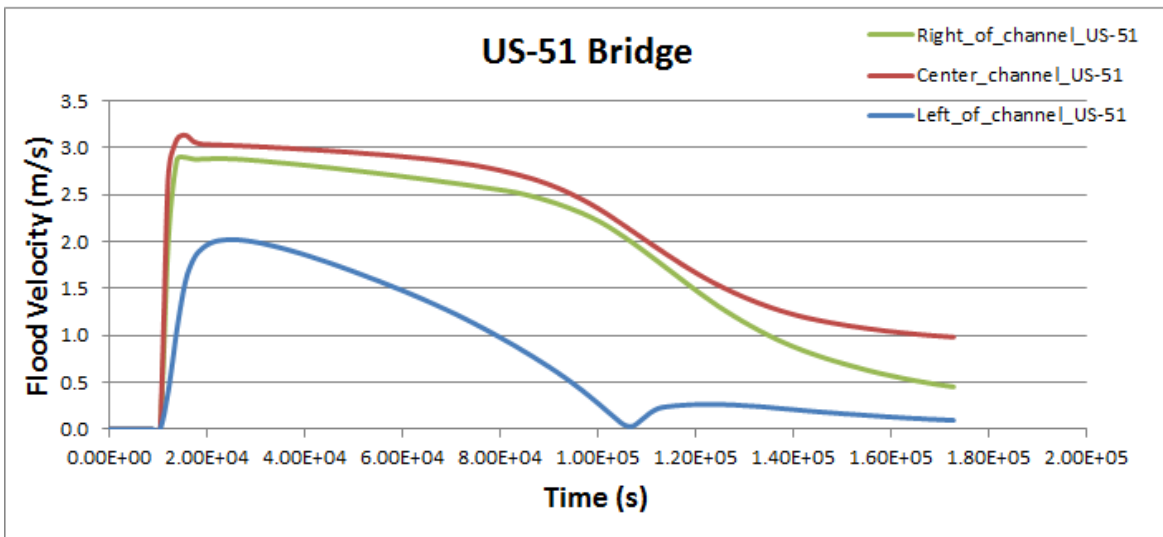
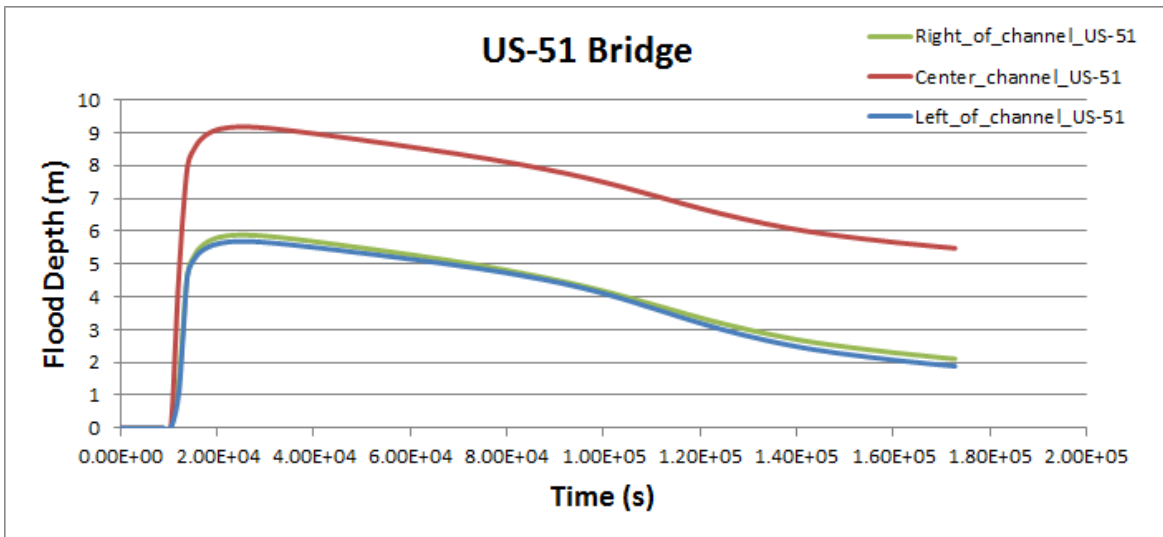


Figure 63 Flow depth, velocity and direction at the three observation points upstream of US-51 Bridge.

## 5.6 Depth and Tangential Velocity along the Observation Profile

The observation profile follows roughly the centerline of the Little Tallahatchie River downstream of the Sardis Dam. Although the straight line distance between the beginning and end points is about 20.481 km, the observation profile following the sinuous river plan-view has a length of 30.350 km. The snapshots of depth and velocity profiles along the observation profile at different times are shown in Figure 64 and Figure 65.

The highest velocities are observed near the advancing front and immediately downstream of the dam. One hour after the breach, the front is at about 4.2 km. The maximum velocity of 5.84 m/s is observed at a downstream distance of 3.33 km, i.e. at about 1.06 km behind the front. Four hours after breaching the front reaches a point 27.70 km downstream. The average propagation velocity of the front is therefore 6.93km/hr (1.92 m/s). Five hour after the breach the front is already beyond the endpoint of the observation profile. The depths along the profile continue to increase until about 6 hours after the breach. Seven hours after the initiation of the breaching the flood depths starts decreasing. At the end of the simulation, i.e. 48 hours after the breach the flood depths along the observation line are in the range of 4 to 6 m. The flood velocities in the first 25 km are less than 1m/s but at certain places peaks reaching more than 2m/s are observed.

In Figure 66, flood discharge versus flood depth curves are plotted at six locations along the observation line: 5 km, 10 km, 15 km, 20 km, 25 km, and 30 km. These plots clearly show that the maximum velocity and depth do not occur at the same. Maximum depth arrived later than the maximum velocity. It is important to note that these curves represent the velocity and depth computed at a point in the center of the stream.

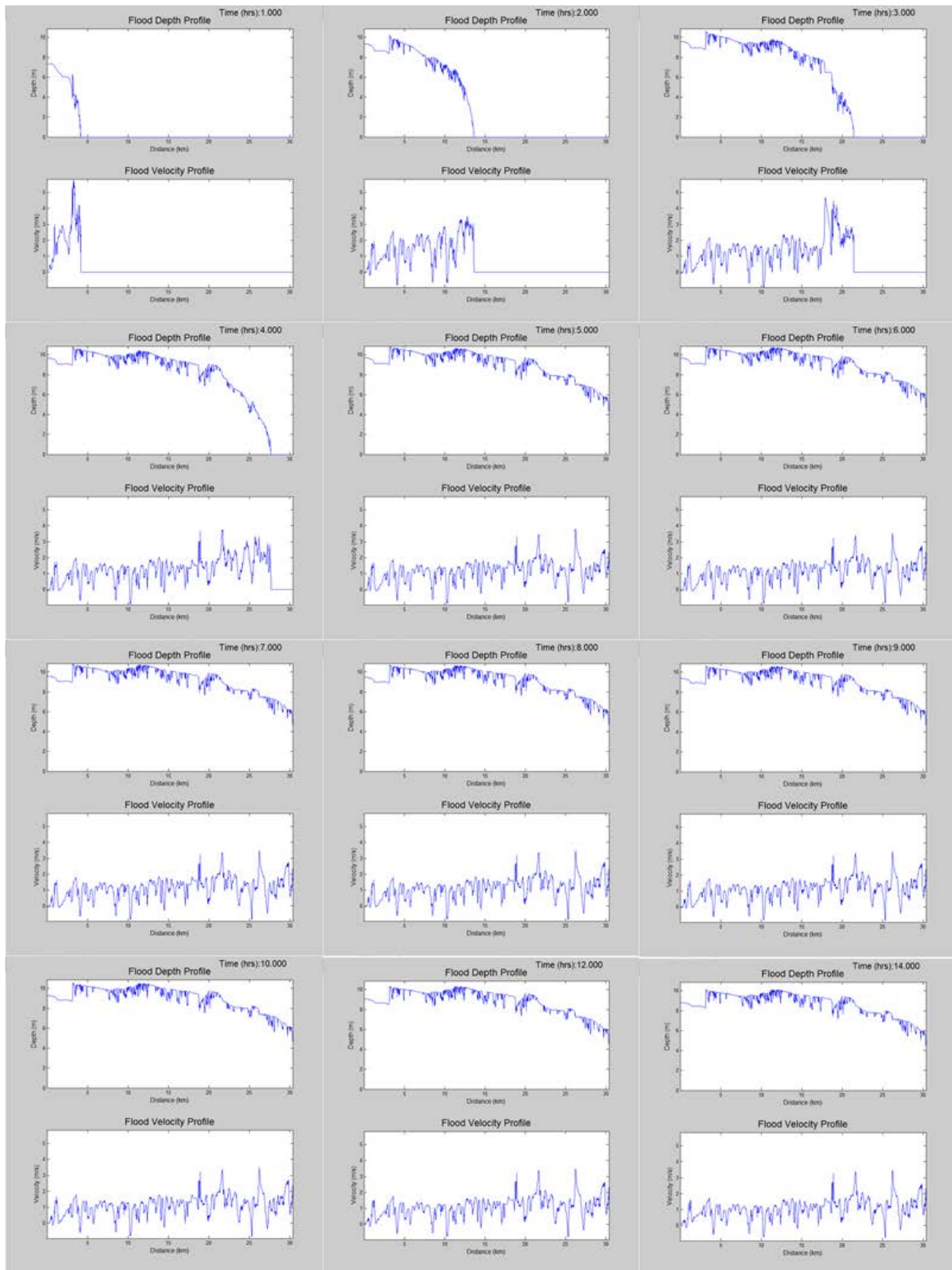


Figure 64 Snapshots of depth and velocity profiles predicted with 3 m DEM: Part 1 (1hr – 14hrs).

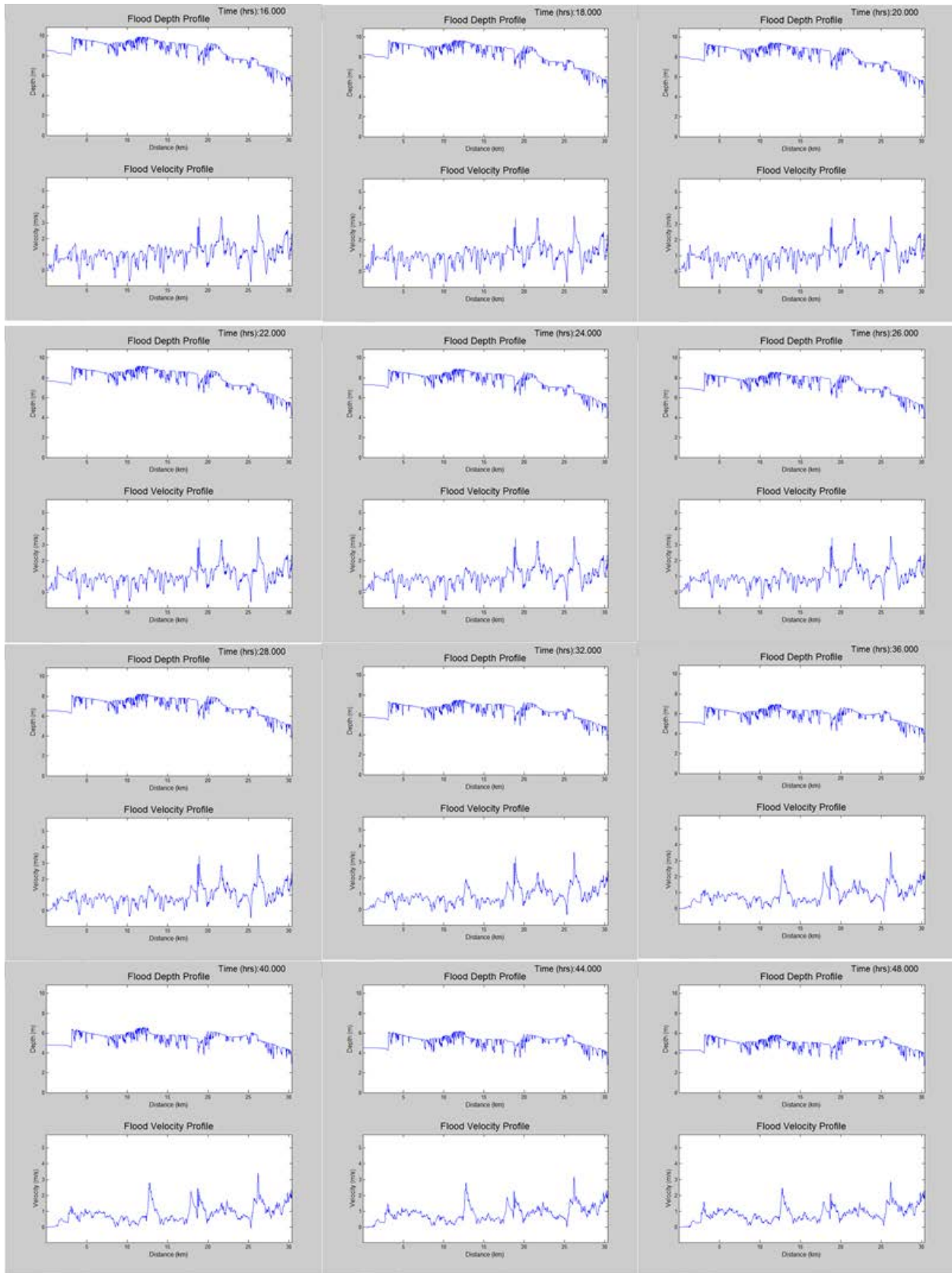


Figure 65 Snapshots of depth and velocity profiles predicted with 3 m DEM: Part 2 (16hr – 48hrs).

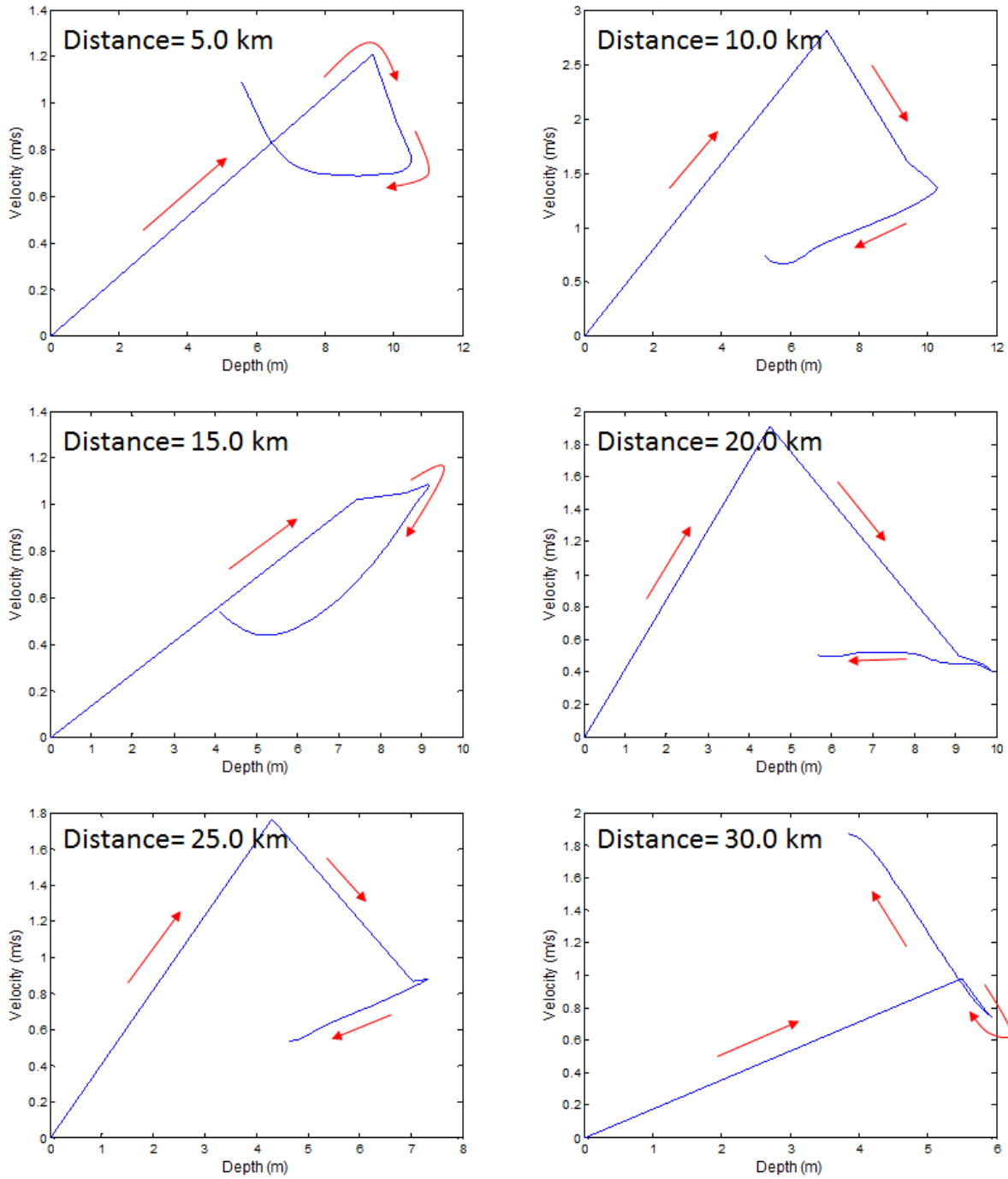


Figure 66 Flood discharge versus flood depth curves at several stations along the observation profile.

## Chapter 6 CONCLUSIONS

### 6.1 Comparison of Flow Parameters Computed with Different Cell Sizes

Flood simulations were carried out using DEMs with four different cell sizes: 3m (1/9 arc-second), 5m, 10m (1/3 arc-second), and 30m (1 arc-second). An understanding of the influence of the resolution of the DEM on the simulation results can be gained by comparing the flow parameters computed at the observation points with different cell sizes. Figure 67, shows the time history of flow depth, flood elevation, flow velocity and flow direction computed at the three observation stations (left bank, center, and right bank) located upstream of the I-55 Bridge. In each sub-plot the results computed with four different cell sizes are superposed. Similar plots are also prepared for the observation stations at the Railroad Bridge (Figure 68) and US-51 Bridge (Figure 69).

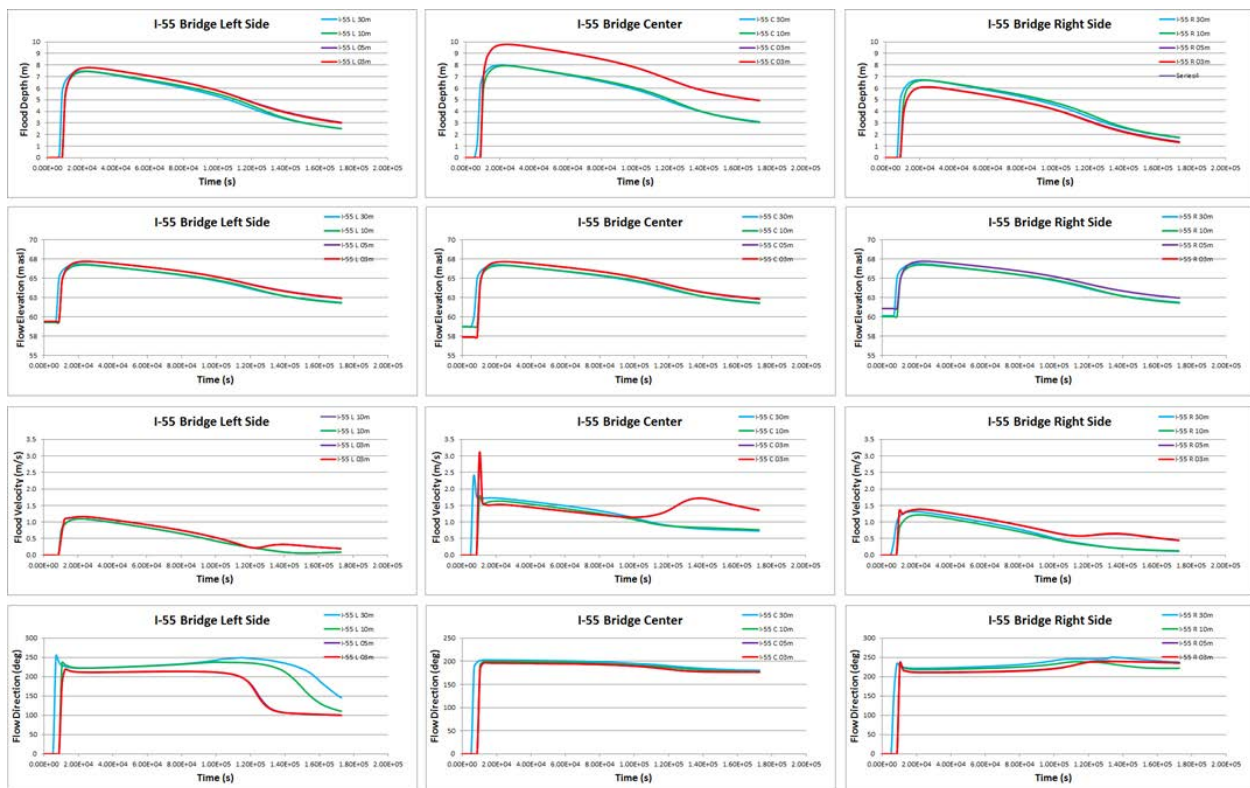


Figure 67 Comparison of flow depth, flood elevation, flow velocity, and flow direction computed at the I-55 Bridge using DEMs with 3m, 5m, 10m, and 30m cell-size.

Based on Figure 67, the following observations can be made:

- The flow depths computed with 3m and 5m cell sizes give almost identical results at all three observation stations. Flow depths computed with 10m and 30m cell sizes are also almost identical. For the left and right observation stations the flow depths computed with 3m and 5m are higher than those computed with 10m and 30m. The reason for this discrepancy is the difference in bed elevations, which are listed in Table 7.
- The flood elevations plotted in the second row are almost the same for all cell sizes. This clearly shows that the water surface elevation is less sensitive to the differences in local depth.
- The flow velocities plotted in the third row are almost the same for all cell sizes.

- The flow directions computed with different cell sizes are reasonable close to each other.

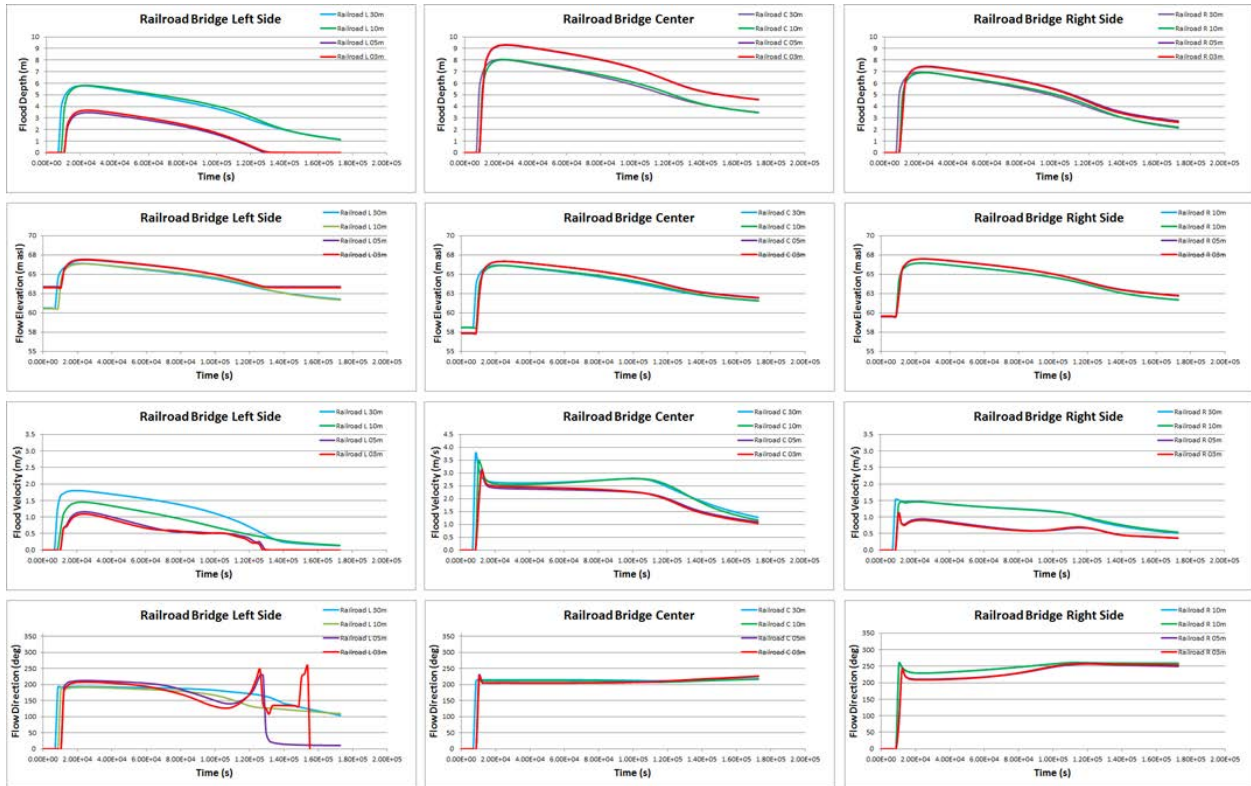


Figure 68 Comparison of flow depth, flood elevation, flow velocity, and flow direction computed at the Railroad Bridge using DEMs with 3m, 5m, 10m, and 30m cell-size.

The plots in Figure 68 and Figure 69 confirm that even if the flow depths computed with different cell sizes show differences, the flood elevations generally remain the same. Unless very detailed information is needed for special purposes, the results computed with 10m cell size, and even with 30m cell size, give reasonable good results for general engineering purposes; at least for the special case of Sardis Dam breach simulation.

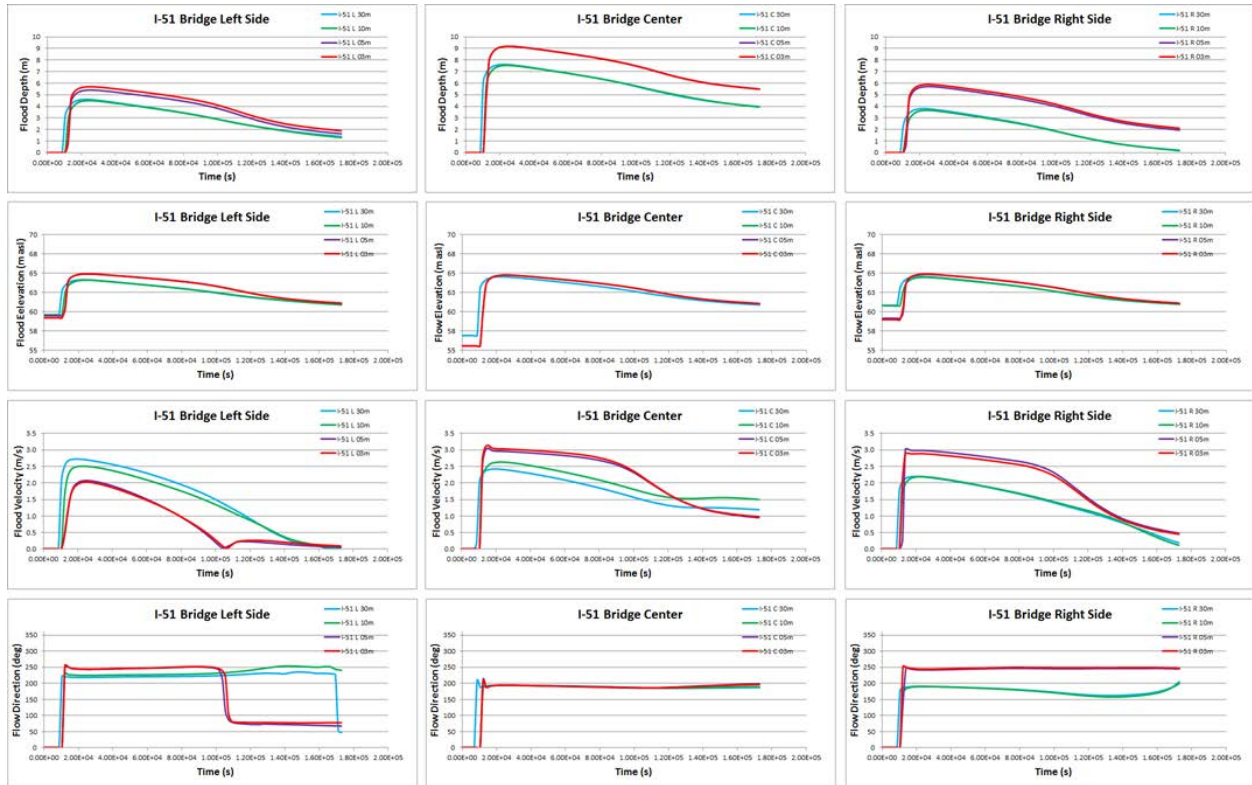


Figure 69 Comparison of flow depth, flood elevation, flow velocity, and flow direction computed at the US-51 Bridge using DEMs with 3m, 5m, 10m, and 30m cell-size.

Table 7 Bed elevations at the observation stations when using DEM's with different cell sizes.

Structure	DEM Cell Size	Bed Elevation (m) at the Observation Point		
		Left	Center	Right
I-55 Bridge	3m (1/9 arc-second)	59.4	57.4	61.1
	5m	59.4	57.4	61.1
	10m (1/3 arc-second)	59.3	58.7	60.1
	30m (1 arc-second)	59.4	58.8	60.2
Railroad Bridge	3m (1/9 arc-second)	63.3	57.3	59.6
	5m	63.4	57.4	59.5
	10m (1/3 arc-second)	60.5	59.3	59.5
	30m (1 arc-second)	60.5	58.1	59.6
US-51 Bridge	3m (1/9 arc-second)	59.2	55.6	59.0
	5m	59.5	55.6	59.2
	10m (1/3 arc-second)	59.6	56.9	60.8
	30m (1 arc-second)	59.6	56.9	60.8

## 6.2 Bridge Scour

Referring to USACE<sup>3</sup>, the equation suggested by Neill (1968) for determining the critical velocity for the initiation of motion can be used to determine whether clear-water or live-bed conditions will occur.

$$V_c = 1.58 [(s_s - 1) g D_{50}]^{1/2} (y_1/D_{50})^{1/6} \quad (6)$$

where  $V_c$  is the critical velocity for movement of bed material (in ft/s),  $y_1$  is the average flow depth in the main channel upstream of the bridge (ft), and  $D_{50}$  is the median diameter of bed material (ft). If the flow velocity is greater than the critical velocity given in Eq. (6), the live-bed scour formulas will be used to calculate the scour; otherwise the clear-water formulas are to be used.

The total scour at a bridge should be considered as a sum of contraction scour, which occurs due to the narrowing of the cross section, and the pier scour and/or abutment scour due to interaction between the flow and the structure. Both the contraction scour and the pier/abutment scour involve sediment flow interaction.

Scour at bridges is a complex phenomenon (see Graf and Altinakar 2002). There are numerous formulae proposed by different authors. The scour depths computed with different formulae for the same conditions may yield results with significant differences. In the present study, we adopt the following formulations adopted and recommended by the federal agencies (Holnbeck and Parrett 1997).

**Contraction scour under live-bed conditions** is computed using the formula developed by Laursen (1960) and modified by Richardson et al. (1993)

$$y_{sc} = y_1 \left[ \left( \frac{Q_2}{Q_1} \right)^{\frac{6}{7}} \left( \frac{W_1}{W_2} \right)^{k_1} \right] - y_1 \quad (7)$$

where  $y_{sc}$  is the contraction scour depth (in ft),  $y_1$  is the average depth in the main channel in the approach section,  $Q_1$  is the discharge in the approach reach of the main channel upstream of the bridge (in cfs),  $Q_2$  is the discharge in the contracted reach of the main channel (in cfs),  $W_1$  is the width of the main channel portion of the approach reach transporting sediment (in ft),  $W_2$  is the width of the main channel portion of the contracted reach transporting sediment (in ft), and  $k_1$  is a coefficient depending on the transport mode of the bed material:  $k_1 = 0.59$  if the sediment is mostly transported as bed load,  $k_1 = 0.64$  if the sediment is mostly transported as bed load but contains some suspended material, and  $k_1 = 0.69$  if the sediment is mostly transported as suspended load.

**Contraction scour under clear-water conditions** is computed using the formula developed by Laursen (1963) and modified by Richardson et al. (1993)

$$y_{sc} = y \left[ \frac{Q}{D_m^{1/3} y^{7/6} W} \right]^{\frac{6}{7}} - y \quad (8)$$

where  $y$  is the average flow depth in the main channel at the contracted section before clear-water scour (in ft),  $Q$  is the discharge through the bridge,  $D_m$  is the effective mean diameter of the bed material (in ft)

<sup>3</sup> <http://www.fhwa.dot.gov/engineering/hydraulics/pubs/hec/hec18ed2.pdf>

in the bridge section and can be assumed to be  $D_m = 1.25 D_{50}$ , and  $W$  is the width of the bridge opening adjusted for skewness to the flow and for effective pier width.

**Pier scour under both live-bed and clear-water conditions** is computed by the equation developed by Colorado State University and later modified by Richardson et al. (1993).

$$y_{sp} = 2.0 K_1 K_2 K_3 \left( \frac{a}{y_p} \right)^{0.65} (Fr_p)^{0.43} y_p \quad (9)$$

where  $y_{sp}$  is the scour depth for the pier (in ft),  $K_1$  is a correction factor for pier-nose shape as listed in Table 8,  $K_2$  is a correction factor that depends on the flow angle of attack on the pier and the ratio of pier length to pier width,  $K_3$  is a correction factor that depends on bedforms,  $a$  is the pier width,  $y_p$  is the flow depth just upstream of the pier (in ft), and  $Fr_p$  is the Froude number upstream of the pier.

The coefficient  $K_2$  can be calculated using the following equation (Brunner 2010):

$$K_2 = \left( \cos(\theta) + \frac{L}{a} \sin(\theta) \right)^{0.65} \quad (10)$$

where  $\theta$  is the flow angle of attack on the pier, and  $L$  is the pier length.

Froude number is given as

$$Fr_p = \frac{V_p}{\sqrt{g y_p}} \quad (11)$$

where  $V_p$  is the velocity in the main channel in the approach reach (in ft), and  $g$  is the gravitational acceleration (32.185 ft/s<sup>2</sup>).

Table 8 Correction factor,  $K_1$ , for pier-nose shape (taken from Brunner 2010)

Shape of Pier Nose	$K_1$
(a) Square nose	1.1
(b) Round nose	1.0
(c) Circular cylinder	1.0
(d) Group of cylinders	1.0
(e) Sharp nose (triangular)	0.9

Table 9 Correction factor,  $K_3$  , for bendforms (taken from Brunner 2010)

Bed Condition	Dune Height H feet	$K_3$
Clear-Water Scour	N/A	1.1
Plane Bed and Antidune Flow	N/A	1.1
Small Dunes	$10 > H \geq 2$	1.1
Medium Dunes	$30 > H \geq 10$	1.1 to 1.2
Large Dunes	$H \geq 30$	1.3

**Abutment scour under both live-bed and clear-water conditions** is computed using the equation developed by Froehlich (Richardson et al. 1993).

$$y_{sa} = \left[ 2.27 K_1 K_2 \left( \frac{L_a}{y_a} \right)^{0.43} (Fr_a)^{0.61} + 1 \right] y_a \quad (12)$$

where  $y_{sa}$  is the abutment scour (in ft),  $K_1$  is a coefficient that depends on the shape of the abutment as listed in Table 10,  $K_2$  is a coefficient that depends on the angle between the abutment and the flow,  $L_a$  is the length of the flood-plain flow obstructed by the bridge abutment (in ft),  $y_a$  is the flow depth in the abutment (in ft) and  $Fr_a$  is the Froude number of the flow upstream from the embankment.

Table 10 Correction factor,  $K_1$  , for abutment shape (taken from Brunner 2010)

Abutment shape description	$K_1$
Vertical-wall abutment	1.00
Vertical-wall abutment with wing walls	.82
Spill-through abutment	.55

### 6.2.1 Bridge Pier Scour Estimation for I-55 Bridge

Figure 70 shows the simplified cross section of the I-55 Bridge. A picture of the circular bridge piers is also shown in the same figure. The bridge has piers with 8ft and 10ft diameter. The piers with the larger diameter are located in the main channel. To demonstrate the use of 2D model results, only the estimation of the local scour for the larger pier with a diameter of 10 ft will be considered. Since this is a transient flow case due to a dam-breach flood, the consideration of the contraction scour would require a more detailed study with long-term simulations, which is outside the scope of the present report.

The flow conditions at the I-55 Bridge are shown in Figure 71. As it can be seen, the flow overtops the bridge and the road embankment with a depth close to 3 m over the crown of the road. Using the values computed by the simulation with the 3m DEM, the following values are determined:

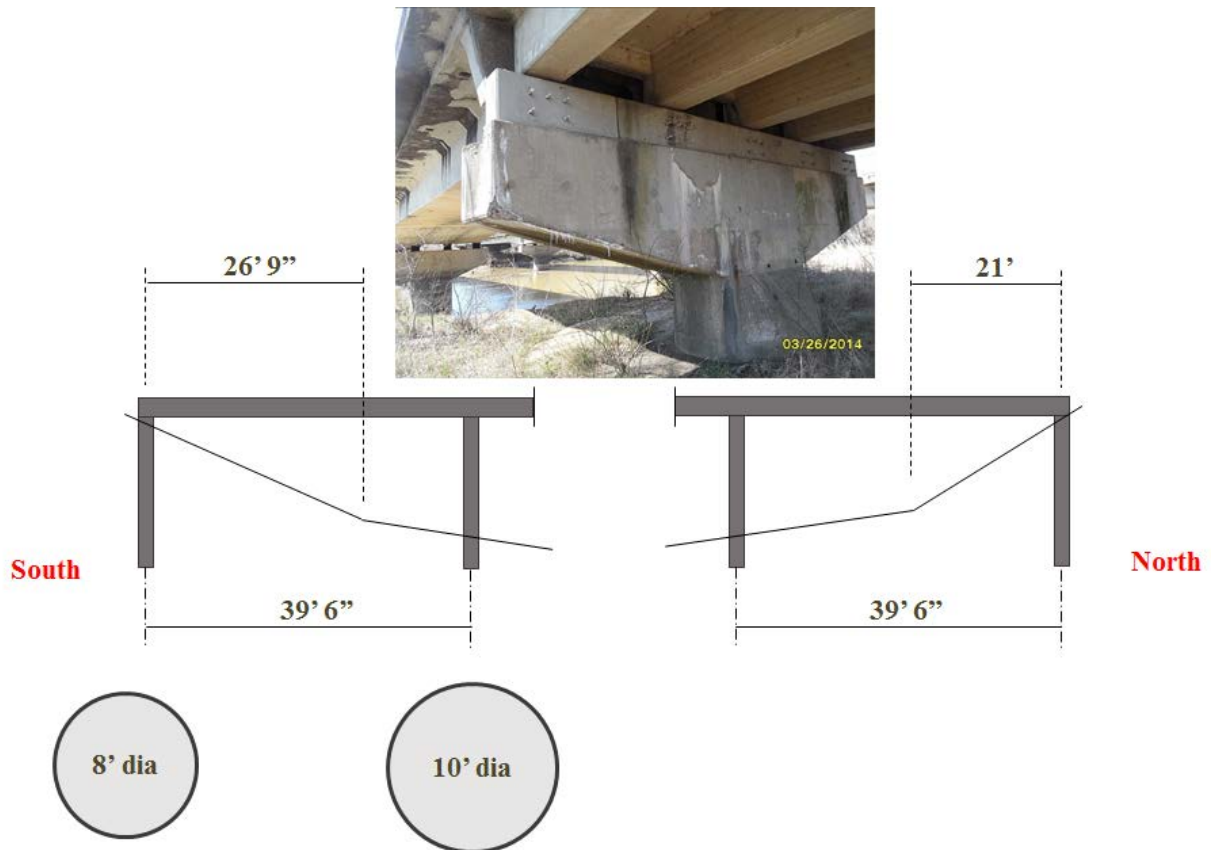


Figure 70 Simplified cross section of I-55 Bridge.

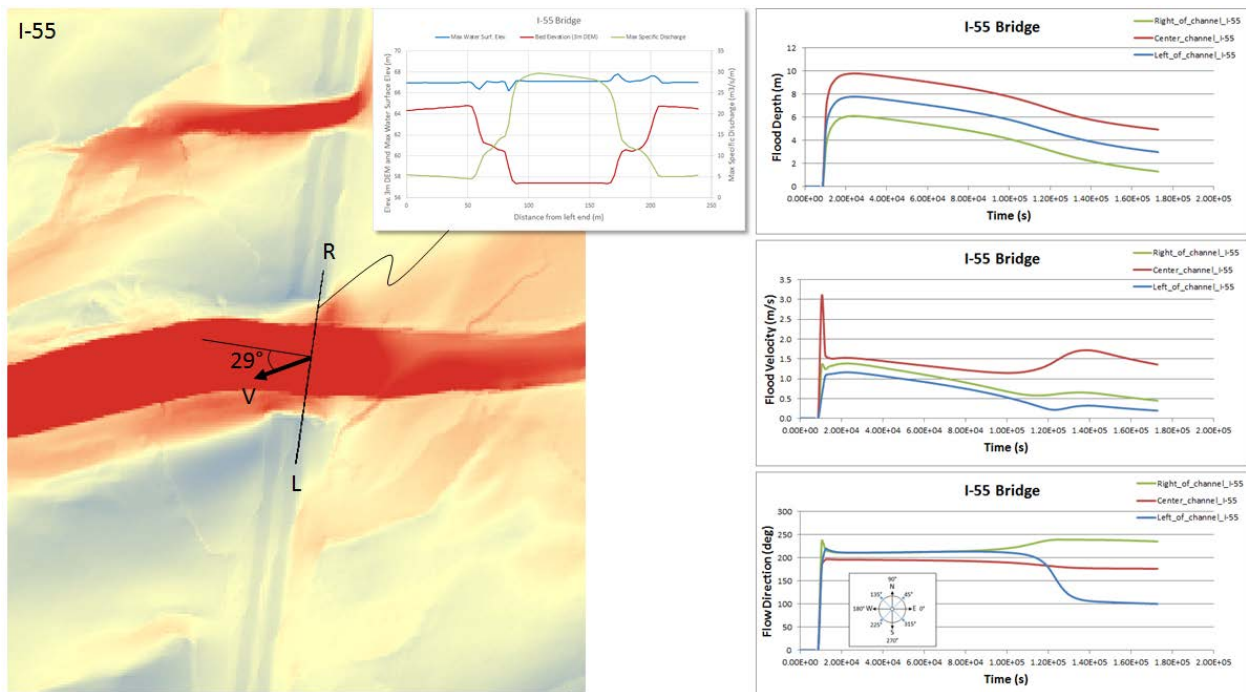


Figure 71 Flow conditions at the I-55 Bridge.

- $K_1 = 1$  (for circular cylinder from Table 8)
- $L_a = 10 \text{ ft} = 3.048 \text{ m}$
- $a = 10 \text{ ft} = 3.048 \text{ m}$
- $L_a/a = 1$
- $\theta = 29^\circ = 0.5061 \text{ rad}$  (based on the flow direction from Figure 71)
- $K_2 = 1.22$  (computed using Eq. (10))
- $K_3 = 1.1$  (from Table 9: clear-water value is assumed)
- $y_p = 9 \text{ m}$  (Figure 71 shows that the flow depth at the center observation point decreases from a peak value of 10m to 8m within the first 24 hours. Thus an average value of 9 m is assumed)
- $V_p = 1.3 \text{ m/s}$  (Figure 71 shows that after an initial sudden peak reaching 3m/s, the flow velocity at the center observation remains between 1.5 m/s and 1.3 m/s within the first 24 hours. Thus an average value of 1.4 m/s is assumed)
- $Fr_p = 0.15$  (computed using Eq. (11))

Based on these values and using Eq. (9), the local scour around the 10 ft-diameter piers in the main channel is estimated as  $y_{sp} = 5.27 \text{ m} = 17.30 \text{ ft}$ . This is a quite substantial scour depth and it does not take into account the contraction scour. Unless the pier foundations are sufficiently deep and/or appropriate local scour prevention measures are taken, the integrity of the bridge may be in danger due to excessive scour.

## 6.2.2 Bridge Pier Scour Estimation for Railroad Bridge

Unfortunately, no reliable information was available concerning the structural details of the Railroad Bridge. An attempt was made to estimate the location and dimensions of the bridge piers from Google Earth imagery as shown in Figure 72. Two different rectangular pier types could be identified. The piers in the main channel seem to be more slender with estimated dimensions of 2 m by 6 m. The piers on the floodplain are estimated to be 3 m by 10 m. The scour estimation will consider only the slender piers in the main channel. The contraction scour is not considered.

The flow conditions at Railroad Bridge are shown in Figure 73. As it can be seen, the flow overtops the bridge and the road embankment with a depth close to 3 m over the crown of the road. Using the values computed by the simulation with the 3m DEM, the following values are determined:

- $K_1 = 1.1$  (for square nose from Table 8)
- $L_a = 19.69 \text{ ft} = 6.0 \text{ m}$
- $a = 6.56 \text{ ft} = 2.0 \text{ m}$
- $L_a/a = 3$
- $\theta = 6^\circ = 0.1047 \text{ rad}$  (based on the flow direction from Figure 73)
- $K_2 = 1.22$  (computed using Eq. (10))
- $K_3 = 1.1$  (from Table 9: clear-water value is assumed)
- $y_p = 8.2 \text{ m}$  (Figure 73 shows that the flow depth at the center observation point decreases from a peak value of 9.2 m to 7.2 m within the first 24 hours. Thus an average value of 8.2 m is assumed)
- $V_p = 2.4 \text{ m/s}$  (Figure 73 shows that after an initial sudden peak reaching 3m/s, the flow velocity at the center observation remains between 2.5 m/s and 2.3 m/s within the first 24 hours. Thus an average value of 2.4 m/s is assumed)
- $Fr_p = 0.27$  (computed using Eq. (11))

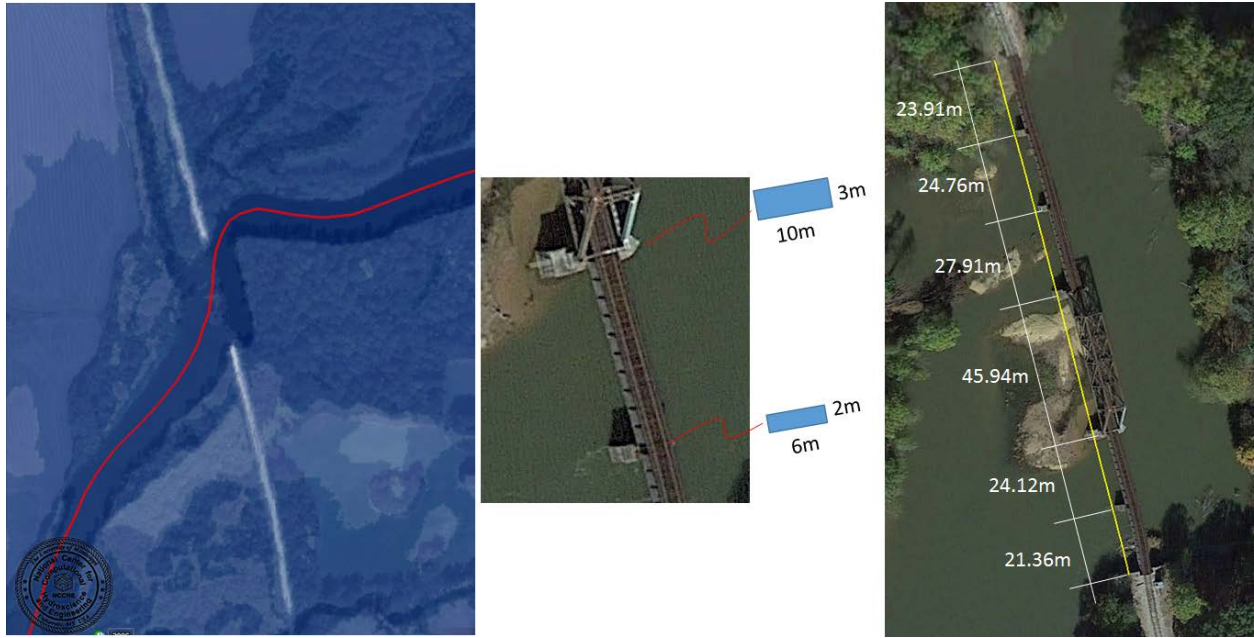


Figure 72 Left: Inundation around the Railroad Bridge. Right: Estimation of the structural characteristics of the Railroad Bridge from Google Earth imagery.

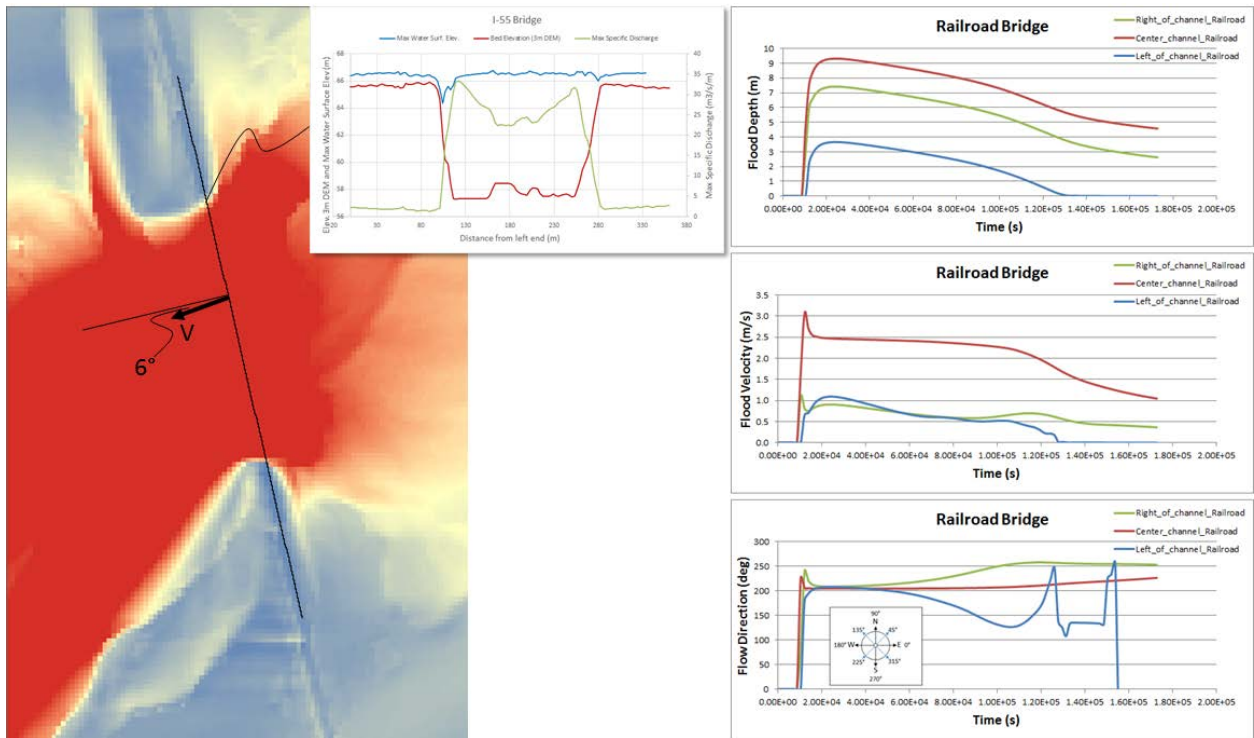


Figure 73 Flow conditions at the Railroad Bridge.

Based on these values and using Eq. (9), the local scour around the slender piers in the main channel is estimated as  $y_{sp} = 5.36 \text{ m} = 17.58 \text{ ft}$ . This is a quite substantial scour depth and it does not take into

account the contraction scour. Unless the pier foundations are sufficiently deep and/or appropriate local scour prevention measures are taken, the integrity of the bridge may be in danger due to excessive scour.

### 6.2.3 Bridge Pier Scour Estimation for US-51 Bridge

Figure 74 shows the simplified cross section of the US-51 Bridge. The bridge is supported by different types of bents with multiple slender rectangular piers. These rectangular piers exist in three sizes: 0.38m by 0.25m, 0.48 m by 0.28 m and 0.584 m by 0.26 m. To demonstrate the use of 2D model results, only the estimation of the local scour for the 0.584 m by 0.26 m will be considered. The contraction scour is not considered.

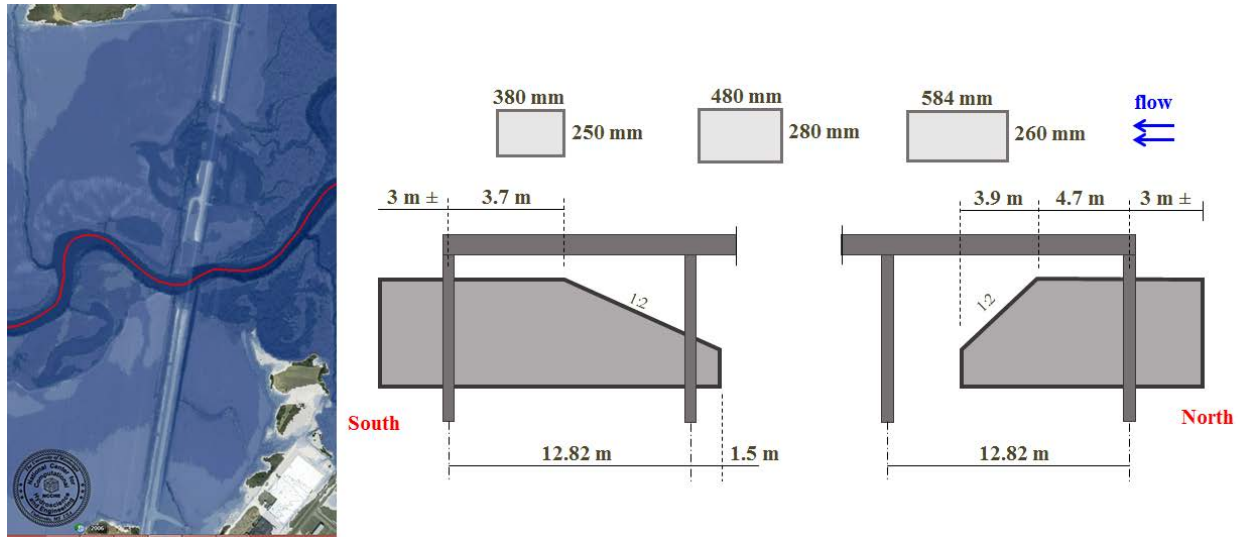


Figure 74 Left: Inundation around the US-51 Bridge. Right: Structural characteristics of the US-51 Bridge.

The flow conditions at the US-51 Bridge are shown in Figure 75. As it can be seen, the flow overtops the bridge and the road embankment with a depth of 1 to 2 m over the crown of the road. Using the values computed by the simulation with the 3m DEM, the following values are determined:

- $K_1 = 1.1$  (for square nose from Table 8)
- $L_a = 1.92 \text{ ft} = 0.584 \text{ m}$
- $a = 0.85 \text{ ft} = 0.26 \text{ m}$
- $L_a/a = 2.25$
- $\theta = 31^\circ = 0.541 \text{ rad}$  (based on the flow direction from Figure 75)
- $K_2 = 1.22$  (computed using Eq. (10))
- $K_3 = 1.1$  (from Table 9: clear-water value is assumed)
- $y_p = 8.4 \text{ m}$  (Figure 75 shows that the flow depth at the center observation point decreases from a peak value of 9.2 m to 7.5 m within the first 24 hours. Thus an average value of 8.4 m is assumed)
- $V_p = 2.75 \text{ m/s}$  (Figure 75 shows that after an initial sudden peak reaching 3m/s, the flow velocity at the center observation remains between 3.0 m/s and 2.5 m/s within the first 24 hours. Thus an average value of 2.75 m/s is assumed)
- $Fr_p = 0.30$  (computed using Eq. (11))

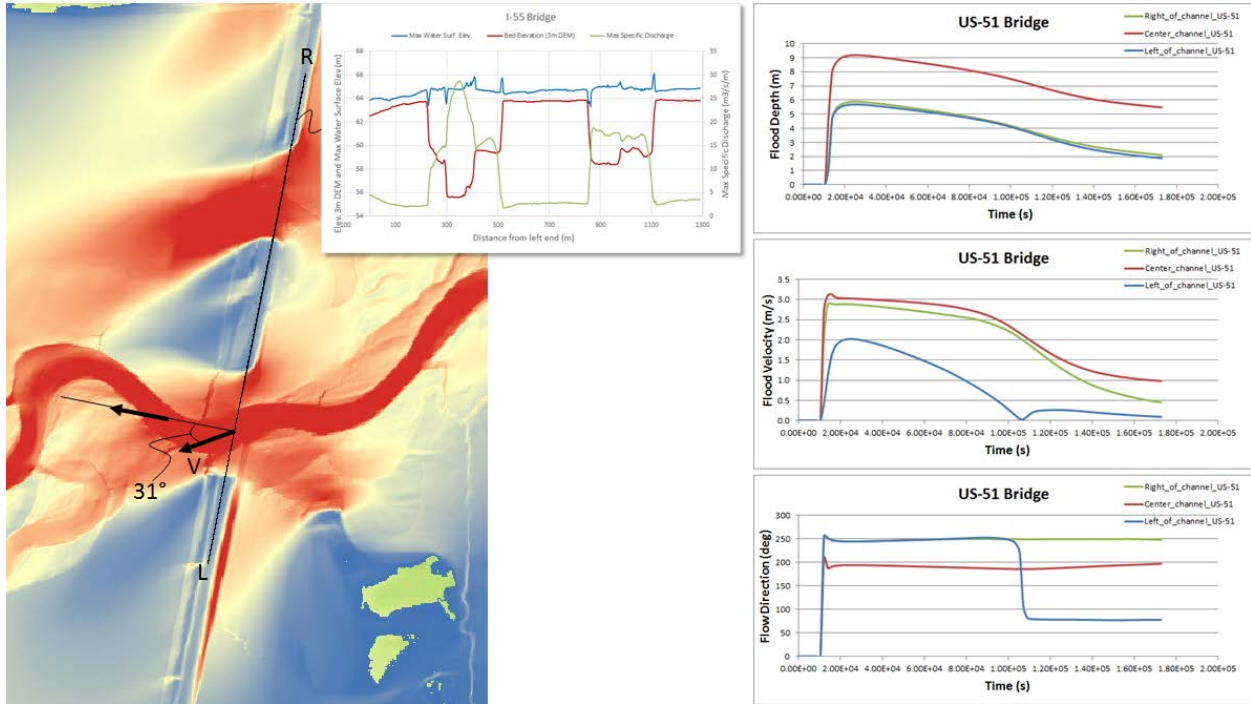


Figure 75 Flow conditions at the US-51 Bridge.

Based on these values and using Eq. (9), the local scour around the rectangular pier (0.584 m by 0.26 m) in the main channel is estimated as  $y_{sp} = 2.00 \text{ m} = 6.57 \text{ ft}$ . This is a reasonable scour depth. The piers reach deep into the ground. Thus, there is no significant danger to the structure.

## Chapter 7 REFERENCES

- Altinakar, M.S., M. Z. McGrath, E. K. Fijolek and E. Miglio (2008). Risk and Vulnerability Studies for Water Infrastructures Using a GIS-Based Decision Support System with 2D Numerical Flood Modeling. *International Conference on Computational Hydroscience and Engineering, ICHE-2008*, September 8-12, 2008, Nagoya, Japan
- Altinakar, M.S., M.Z. McGrath, and V.P. Ramalingam (2010a). An Enhanced Two-Dimensional Numerical Model for Simulating Floods Due to Dam and Levee Break/Breaching. *International Conference on Hydroscience and Engineering (ICHE-2010)*, August 2-5, Chennai, India
- Altinakar, M.S., M.Z. McGrath, V.P. Ramalingam, and Hamzeh Omari (2010b). 2D Modeling of Big Bay Dam Failure in Mississippi: Comparison with Field Data and 1D Model Results. *International Conference on Fluvial Hydraulics (River Flow 2010)*, September 8-10, Braunschweig, Germany
- Altinakar, M.S., McGrath, M.Z., Ramalingam, V.P. and Omari, H. (2010c). "2D Modeling of Big Bay Dam Failure in Mississippi: Comparison with Field Data and 1D Model Results"; *Proceedings of the International Conference on Fluvial Hydraulics (River Flow 2010)*, September 8-10, Braunschweig, Germany.
- Altinakar, M.S., McGrath, M.Z., Matheu, E.E., Ramalingam, V.P., Seda-Sanabria, Y., Breikreutz, W., Oktay, S., Zou, J., & Yeziarski, M. (2012a). Validation of Automated Dam-Break Flood Simulation Capabilities and Assessment of Computational Performance. *Proc. of Dam Safety 2012 Conf.*, ASDSO, Sep. 16-21, 2012, Denver, CO.
- Altinakar, M.S. and McGrath, M.Z. (2012b). "Parallelized Two-Dimensional Dam-Break Flood Analysis with Dynamic Data Structures," *ASCE-EWRI, 2012 World Environmental & Water Resources Congress*, Albuquerque, New Mexico, May 20–24, 2012.
- Brunner, G.W. (2010). HEC-RAS River Analysis System Hydraulic Reference Manual. Version 4.1. U.S. Army Corps of Engineers, Computer Program Documentation, CPD-69, January 2010, Chapter 10: *Estimating Scour at Bridges*.
- Dise, K.M. (2002). Estimating Potential for Life Loss Caused by Uncontrolled Release of Reservoir Water. *Risk Analysis Methodology Appendix O, U.S. Bureau of Reclamation*, Technical Service Center, Denver, CO.
- FEMA. (2000). Coastal Construction Manual, *FEMA 55 Report, Federal Emergency Management Agency*, Washington, D.C.
- FEMA/FIA. (Not Dated). Non-Residential Floodproofing – Requirements and Certification – for Buildings Located in Special Flood Hazard Areas. *Federal Emergency Management Agency (FEMA), Federal Insurance Administration*, Technical Bulletin 3-93 (FIA-TB-3), <http://www.fema.gov/pdf/fima/job6.pdf>
- Gesch, D.B., Oimoen, M.J., and Evans, G.A. (2014). Accuracy assessment of the U.S. Geological Survey National Elevation Dataset, and comparison with other large-area elevation datasets—SRTM and ASTER: *U.S. Geological Survey. Open-File Report 2014–1008*, 10 p. <http://dx.doi.org/10.3133/ofr20141008>
- Graf, W.H. and Altinakar, M.S. (2002). Fluvial Hydraulics: Flow and transport processes in channels of simple geometry. 3<sup>rd</sup> Edition, *John Wiley and Sons*, 692 pages.
- Graham, W.J. (1999). A Procedure for Estimating Loss of Life Caused by Dam Failure. *Report No. DSO-99-06, Dam Safety Office, US Bureau of Reclamation*, Denver, CO
- Godunov, S.K. (1959). A Difference Scheme for Numerical Solution of Discontinuous Solution of Hydrodynamic Equations. *Math. Sbornik*, 47, 271–306, transl. *US Joint Publ. Res. Service, JPRS 7226*, 1969.
- Godunov S.K., Zabrodine, A., and Ivanov, A. (1976). "Résolution numérique des problèmes multidimensionnels de la dynamique des gaz," *Editions MIR de Moscou*, 1976.
- Harten, A., Lax, P., and van Leer, D. (1983). "On Upstream Differencing and Godunov-type Methods for Hyperbolic Conservation Laws," *SIAM Review* 25, pp. 35–61.

- Holnbeck, S.R. and Parrett, C. (1997). Method for Rapid Estimation of Scour at Highway Bridges Based on Limited Site Data. *U.S. Geological Survey. Water Resources Investigations Report 96-4310 (prepared in collaboration with Montana Department of Transportation)*.
- Laursen, E.M. (1960). Scour at bridge crossings. *ASCE, Journal of Hydraulic Engineering*, v. 86, no. 2, p. 39-55.
- Laursen, E.M. (1963). Analysis of relief bridge scour. *ASCE, Journal of Hydraulic Engineering*, v. 89, no. HY3, p. 92-116.
- Neill, C.R. (1968). Note on initial movement of coarse uniform bed material. *Journal of Hydraulic Research*, vol. 17, no. 2, p. 247-249.
- NETSC Technical Note – Watersheds-16 Rev. 2 (1978). United States Department of Agriculture (USDA) Soil Conservation Services – Northeast Technical Service Center, Broomall, PA 19008;
- Qi, H., Altinakar, M.S., Ying, X, and Wang, S.S.Y. (2005a). Flood Management Decision Making Using Spatial Compromise Programming with Remote Sensing and Census Block Information. *XXXI International Association for Hydraulic Research (IAHR) Congress*, Seoul, Korea, Sept 2005.
- Qi, H., Altinakar, M.S., Ying, X., and Wang, S.S.Y. (2005b). Risk and Uncertainty Analysis in Flood Hazard Management Using GIS and Remote Sensing Technology. *American Water Resources Association (AWRA) Annual Conference*, Seattle, Nov 2005.
- Qi, H., M.S. Altinakar, Youngho Jeon (2006). A Decision Support Tool for Flood Management under Uncertainty Using GIS and Remote Sensing. *International Conference on Hydroscience and Engineering (ICHE 2006)*, Philadelphia, PA, Sept 2006.
- Qi, H. and Altinakar, M.S. (2011a). Simulation-based decision support system for flood damage assessment under uncertainty using remote sensing and census block information. *Natural Hazards*, Vol: 59, Issue: 2, pp. 1125-1143
- Qi, H. and Altinakar, M.S. (2011b). A GIS-based decision support system for integrated flood management under uncertainty with two dimensional numerical simulations. *Environmental Modelling and Software*, Vol: 26, Issue: 6, pp. 817-823.
- RESCDAM. (2000). The use of physical models in dam-break flood analysis. Rescue actions based on dam-break flood analysis. *Final report of Helsinki University of Technology*, Helsinki, Finland. 57 p.
- Richardson, E.V., Harrison, L.J., Richardson, J.R., and Davis, S.R. (1993). Evaluating scour at bridges (2<sup>nd</sup> ed.). *U.S. Department of Transportation Hydraulic Engineering Circular 18*, 132 p.
- Tkach, R.J. and Simonovic, S.P. (1997). A New Approach to Multi-criteria Decision Making in Water Resources. *Journal of Geographic Information and Decision Analysis*, vol. 1, no 1, 25-44
- Toro, E.F., Spruce, M., & Speares, W. (1992). Restoration of the Contact Surface in the HLL–Riemann Solver, *Technical Report CoA–9204, Department of Aerospace Science, College of Aeronautics, Cranfield Institute of Technology, UK*.
- Toro, E. F., Spruce, M., Speares, W. (1994). “Restoration of the contact surface in the HLL-Riemann Solver,” *Shock Waves*, 4(1), pp. 25–34.
- USACE. (1985). Business depth damage analysis procedure, *Engineer Institute for Water Resources. Research Report 85-R-5*. Portland, Oregon. 100 p.